EPA Radiogenic Cancer Risk Models and Projections for the U.S. Population

April 2011

Accessibility Statement

This document does not conform to current Section 508 Compliance standards. For assistance in accessing this document, please submit a request to radiation.questions@epa.gov and include the document link as part of your request.

EPA 402-R-11-001

EPA Radiogenic Cancer Risk Models and Projections for the U.S. Population

April 2011

U.S. Environmental Protection Agency
Office of Radiation and Indoor Air
1200 Pennsylvania Ave., NW
Washington, DC 20460

PREFACE

This document presents new U.S. Environmental Protection Agency (EPA) estimates of cancer incidence and mortality risks due to low doses of ionizing radiation for the U.S. population, as well as their scientific basis. It replaces the 1994 EPA report, *Estimating Radiogenic Cancer Risks*, often referred to as the "Blue Book." In 1999, the Agency applied the 1994 Blue Book contents, metabolic models, and usage patterns to publish *Federal Guidance Report 13 (*FGR-13), *Cancer Risk Coefficients for Environmental Exposure to Radionuclides.* FGR-13 includes coefficients for calculating estimates of cancer risk for over 800 radionuclides. It is anticipated that results presented here will be applied to update the radionuclide risk coefficients in the next revision of FGR-13.

For the most part, estimates of radiogenic risk in this document are calculated using models recommended in the National Academy of Sciences report: *Health Risks from Exposure to Low Levels of Ionizing Radiation, BEIR VII Phase 2* (NAS 2006). The NAS report, often referred to as BEIR VII, was sponsored by EPA and several other federal agencies. As in BEIR VII, models are provided here for estimating risk as a function of age at exposure, age at risk, gender, and cancer site, but a number of extensions and modifications to the BEIR VII approach have been implemented.

In response to requests by the Office of Radiation and Indoor Air (ORIA), the Radiation Advisory Committee (RAC) of the Science Advisory Board (SAB) has formally reviewed the scientific basis and methodology for this report. In 2008, the SAB completed an Advisory in response to the draft *White Paper: Modifying EPA Radiation Risk Models Based on BEIR VII.* In the "White Paper," ORIA proposed many of the methods for calculating risks which were eventually adopted for this report. Then in December, 2008, ORIA submitted for SAB review the draft *EPA Radiogenic Cancer Risk Models and Projections for the U.S. Population*. The RAC review was released on January 5, 2010. In the cover letter to Administrator Jackson, Dr. Deborah Swackhamer, Chair, SAB, and Dr. Bernd Kahn, Chair, RAC, wrote that the 2008 draft was "impressively researched [and] based on carefully considered concepts" and "scientifically defensible and appropriate." They also provided comments and suggestions. In her letter of March 3, 2010, Lisa P. Jackson provided responses to the RAC comments and suggestions.

This report was prepared by David J. Pawel and Jerome S. Puskin of EPA's Office of Radiation and Indoor Air (ORIA). The authors gratefully acknowledge reviews by: Owen Hoffman, Iulian Apostoaei, John Trabalka, and David Kocher of SENES Oak Ridge, Inc.; Mary Clark, Neal Nelson, and Lowell Ralston of ORIA.

Contact information for the authors is:

U.S. Environmental Protection Agency
Office of Radiation and Indoor Air (6608J)
Washington, DC 20460
Email address: pawel.david@epa.gov

ABSTRACT

Background. This document presents new U.S. Environmental Protection Agency (EPA) estimates of cancer incidence and mortality risks due to low doses of ionizing radiation for the U.S. population, as well as their scientific basis. It replaces the 1994 EPA report *Estimating Radiogenic Cancer Risks*, often referred to as the "Blue Book." In 1999, the Agency applied the 1994 Blue Book contents, metabolic models, and usage patterns to publish *Federal Guidance Report 13 (*FGR-13), *Cancer Risk Coefficients for Environmental Exposure to Radionuclides.* FGR-13 includes coefficients for calculating estimates of cancer risk for over 800 radionuclides. It is anticipated that results presented here will be applied to update the radionuclide risk coefficients in the next revision of FGR-13. For the most part, estimates of radiogenic risk in this document are calculated using models recommended in the National Academy of Sciences' report: *Health Risks from Exposure to Low Levels of Ionizing Radiation, BEIR VII Phase 2* (NAS 2006). The NAS report, often referred to as BEIR VII, was sponsored by EPA and several other federal agencies. As in BEIR VII, models are provided here for estimating risk as a function of age at exposure, age at risk, gender, and cancer site.

A number of extensions and modifications to the BEIR VII approach have been implemented. First, BEIR VII focused on the risk from low-LET radiation only, whereas risks from high-LET radiations are also addressed here. Second, this document goes beyond BEIR VII in providing estimates of risk for basal cell carcinomas, kidney cancer, bone sarcomas, and cancers from prenatal exposures. Third, a modified method is employed for estimating breast cancer mortality risk, which corrects for temporal changes in breast cancer incidence and survival. Fourth, an alternative model is employed for estimating thyroid cancer risk, based primarily on a report from the National Council on Radiation Protection and Measurements (NCRP). Fifth, EPA's central estimate of risk for many cancer sites is a weighted arithmetic mean of values obtained from the two preferred BEIR VII models for projecting risk in the U.S. population, rather than a weighted geometric mean, as employed in BEIR VII. Finally, this report provides a somewhat altered and expanded analysis of the uncertainties in the cancer risk estimates, focusing especially on estimates of risk for whole-body irradiation and for specific target organs.

Results. Summary risk coefficients are calculated for a stationary population (defined by 2000 U.S. vital statistics). Numerically, the same coefficients apply for a cohort exposed throughout life to a constant dose rate. For uniform whole-body exposures of low-dose gamma radiation to the entire population, the cancer incidence risk coefficient (Gy^{-1}) is 1.16×10^{-1} (5.6×10^{-2} to 2.1×10^{-1}), where the numbers in parentheses represent an estimated 90% confidence interval. The corresponding coefficient for cancer mortality (Gy^{-1}) is about one-half that for incidence: 5.8×10^{-2} (2.8×10^{-2} to 1.0×10^{-1}).

CONTENTS

Preface ii
Abstract iv
List of Tables vii
List of Figures ix
Acronyms and Abbreviations x
Executive Summary 1
1. Introduction 5
2. Scientific Basis for Cancer Risk Models 6
2.1 Biological Mechanisms 6
2.1.1 Biophysical interactions 6
2.1.2 Carcinogenesis 7
2.1.3 Radiogenic carcinogenesis 8
2.1.4 Extrapolation of low-LET risks to low doses and low dose rates 10
2.1.5 Low dose phenomena 11
2.2 Epidemiology 13

3. EPA Risk Projections for Low-LET Radiation 16
3.1 Introduction 16
3.2 BEIR VII Risk Models 16
3.3 Risk Models for Kidney, Central Nervous System, Skin, and Other “Residual Site” Cancers 24
3.4 Risk Model for Thyroid Cancer 31
3.5 Calculating Lifetime Attributable Risk 33
3.6 Dose and Dose Rate Effectiveness Factor 35
3.7 EAR and ERR LAR Projections for Cancer Incidence 35
3.8 ERR and EAR Projections for Cancer Mortality 36
3.9 Data on Baseline Rates for Cancer and All-Cause Mortality 38
3.10 Combining Results from ERR and EAR Models 40
3.10.1 BEIR VII approach 40
3.10.2 EPA approach 41
3.10.3 A justification for the weighted AM 42
3.11 Calculating Radiogenic Breast Cancer Mortality Risk 45
3.12 LAR by Age at Exposure 47
3.13 Summary of Main Results 58
3.14 Comparison with Risk Projections from ICRP and UNSCEAR 67
3.14.1 ICRP risk models 67
3.14.2 UNSCEAR risk models 69

4. Uncertainties in Projections of LAR for Low-LET Radiation 72
4.1 Introduction 72
4.2 Sources of Uncertainty Quantified in this Report 73
4.3 "One at a Time" Uncertainty Analysis 75
4.4 Monte Carlo Approach for Quantifying Uncertainties in LAR 85
4.4.1 Monte Carlo method 85
4.4.2 Non-sampling sources of uncertainty 86
4.4.3 Bayesian analysis for sampling variability 93
4.4.4 Approach for other cancers 96
4.5 Results 98
4.6 Comparison with BEIR VII 104
4.6.1 Quantitative uncertainty analysis in BEIR VII 104
4.6.2 Comparison of results 105
4.7 Conclusions 106

5. Risks from Higher LET Radiation 108
5.1 Alpha Particles 108
5.1.1 Laboratory studies 108
5.1.2 Human data 109
5.1.3 Nominal risk estimates for alpha radiation 119
5.1.4 Uncertainties in risk estimates for alpha radiation 120
5.2 Lower Energy Beta Particles and Photons 120

6. Risks from Prenatal Exposures 125

7. Radionuclide Risk Coefficients 127

8. Noncancer Effects at Low Doses 128

Appendix A: Baseline rates for Cancer and All-Cause Mortality and Computational Details for Approximating LAR 130

Appendix B: Details of Bayesian Analysis 135

References 142

Glossary 159

LIST OF TABLES

Table		Page
3-1	BEIR VII risk model cancer sites	18
3-2	Summary of BEIR VII preferred risk models	19
3-3	Parameter values for preferred risk models in BEIR VII	21
3-4	Projection of LAR (Gy^{-1}) for brain and CNS cancers for three alternative ERR models	31
3-5	Estimated ERR/Gy and effect modifiers for age at exposure and TSE.	32
3-6	Summary of SEER thyroid relative and period survival rates	33
3-7	EAR and ERR model projections of LAR for cancer incidence for a stationary population and a population based on 2000 census data	36
3-8	Age-averaged LAR for cancer mortality based on a stationary population	38
3-9	Changes in age-averaged cancer rates for the SEER 13 registries	40
3-10	Comparison of EPA and weighted GM method for combining EAR and ERR LAR projections for incidence	42
3-11	Female breast cancer cases and 5-y relative survival rates by age of diagnosis for 12 SEER areas, 1988-2001	46
3-12	LAR for cancer incidence by age at exposure	54
3-13	LAR for cancer mortality by age at exposure	56
3-14	LAR for cancer incidence for lifelong and childhood exposures rates	58
3-15	LAR projections for incidence	59
3-16	LAR projections for mortality	60
3-17	Comparison of EPA and FGR-13 LAR projections for incidence	62
3-18	Comparison of EPA and FGR-13 LAR projections for mortality	63
3-19	Sex-averaged LAR projections for incidence and mortality	64
3-20	Comparison of EPA and BEIR VII LAR calculations	65
3-21	LAR incidence and mortality projections for a population based on 2000 census data	66
3-22	Comparison of ICRP (2007) and EPA risk model parameter values for solid cancers	68
3-23	Comparison of EPA and ICRP (2007) sex-averaged projections of incidence for chronic exposures to the U.S. population	69

LIST OF TABLES, continued

Table		Page
3-24	Summary of UNSCEAR (2008) risk models for solid cancer incidence and leukemia mortality	70
3-25	EPA and UNSCEAR (2008) cancer incidence risk projections from chronic exposures to the U.S. population	71
4-1	Uncertainty factors for non-sampling sources of uncertainty	86
4-2	EPA projections and uncertainty distributions for cancer incidence LAR	99
4-3	Percentage of uncertainty in LAR for cancer incidence attributable to sampling, risk transport, and DDREF	102
4-4	EPA projection and uncertainty distributions for cancer incidence for childhood exposures for selected sites	103
4-5	EPA and BEIR VII uncertainty intervals for LAR of solid cancer Incidence	106
5-1	Lung cancer mortality and RBE	118
B-1	Prior distributions for ERR model parameters	136
B-2	Comparison of posterior distributions for ERR linear dose response parameter with estimates in BEIR VII	138

LIST OF FIGURES

Figure		Page
2-1	Dose response for low-LET γ-rays and high-LET neutrons or α-particles	9
3-1	Age-time patterns in radiation-associated risks for solid cancer incidence excluding thyroid and nonmelanoma skin cancer	20
3-2	ERR for leukemia for age-at-exposure = 20 and TSE = 10	23
3-3	ERR and EAR for exposures at low doses and/or dose rates by TSE for three different ages at exposure	24
3-4	Comparison of two ERR models for brain and CNS cancers with the residual site ERR model	30
3-5	Examples of distributions which might be used for the risk transport weight parameter.	44
3-6	LAR for incidence by age at exposure for solid cancer sites	49
3-7	LAR for mortality by age at exposure for solid cancer sites	51
3-8	LAR by age at exposure for leukemia for incidence and mortality	53
3-9	LAR for all cancers combined by age at exposure for exposures at low doses and/or dose rates for incidence and mortality	53
4-1	Dependence of LAR for selected cancer sites for both lifelong and childhood exposures (age < 15) on ERR model parameter values	78
4-2	Dependence of LAR for selected cancer sites for lifelong exposures on the linear dose response parameter (β), DDREF, and the ERR model weight parameter (w)	82
4-3	Subjective probability density function for DDREF	88
5-1	Cumulative fraction of total dose vs. secondary electron kinetic energies for a variety of low-LET radiations calculated using the method of Burch	123
5-2	Cumulative fraction of total dose vs. secondary electron energies for a variety of slow and fast initial electron energies calculated by the Monte Carlo track structure method	124
A-1	Baseline incidence and mortality rates for specific cancer sites	131
B-1	Posterior distributions for ERR for selected cancer sites	139
B-2	Posterior distributions for the age-at-exposure parameter	140
B-3	Posterior distributions for the attained age parameter	141

LIST OF ACRONYMS AND ABBREVIATIONS

ATB	At the Time of the Bombings
BCC	Basal Cell Carcinoma
BEIR VII	*Health Risks from Exposure to Low Levels of Ionizing Radiation BEIR VII Phase 2*
CI	Confidence Interval
DDREF	Dose and Dose Rate Effectiveness Factor
DEF	Dose Effectiveness Factor
DREF	Dose Rate Effectiveness Factor
DSB	Double Strand Break
EAR	Excess Absolute Risk
EPA	Environmental Protection Agency
ERR	Excess Relative Risk
eV	Electron Volt
FGR-13	Federal Guidance Report 13
GM	Geometric Mean
GSD	Geometric Standard Deviation
Gy	Gray
ICRP	International Commission on Radiological Protection
IREP	Interactive RadioEpidemiological Program
LAR	Lifetime Attributable Risk
LET	Linear Energy Transfer
LNT	Linear No -Threshold
LQ	Linear-Quadratic
LSS	Life Span Study
NAS	National Academy of Sciences
NCHS	National Center for Health Statistics
NCI	National Cancer Institute
NCRP	National Council on Radiation Protection and Measurements
NIOSH	National Institute for Occupational Safety and Health
ORIA	Office of Radiation and Indoor Air
RBE	Relative Biological Effectiveness
REF	Radiation Effectiveness Factor
RERF	Radiation Effects Research Foundation
RR	Relative Risk
SCC	Squamous Cell Carcinoma
SEER	Surveillance, Epidemiology, and End Results
Sv	Sievert
TSE	Time Since Exposure
UF	Uncertainty Factor
UI	Uncertainty Interval
UNSCEAR	United Nations Scientific Committee on the Effects of Atomic Radiation
WLM	Working Level Months

EXECUTIVE SUMMARY

The U.S. Environmental Protection Agency, as part of its responsibilities for regulating environmental exposures and its Federal Guidance role in radiation protection, develops estimates of risk from low-level ionizing radiation.[1]

This document presents new EPA estimates of cancer incidence and mortality risk coefficients pertaining to low dose exposures to ionizing radiation for the U.S. population, as well as their scientific basis. The "dose" refers to the amount of energy deposited by the radiation in a unit mass of tissue, expressed in units of gray (Gy). The "risk" is generally defined to be the probability of a health effect (*i.e.*, a cancer or a cancer death), and the risk per unit dose is called a "risk coefficient." Where there is no possible confusion, "risk coefficients" and "ionizing radiation" will usually be referred to here, simply, as "risks" and "radiation." For the most part, risk estimates are calculated using models recommended in the National Academy of Sciences' BEIR VII Report (NAS 2006), which was sponsored by EPA and several other federal agencies. The models and risk estimates presented here replace those published in a 1994 report, *Estimating Radiogenic Cancer Risks,* with some modifications in 1999 (EPA 1994, 1999a, 1999b).

As in BEIR VII, models are provided for estimating risk as a function of age at exposure, age at risk, gender, and cancer site, but a number of extensions and modifications to the BEIR VII approach have been implemented. First, BEIR VII focused on the risk from low-LET radiation only, whereas risks from high-LET radiations are also addressed here. Second, this document goes beyond BEIR VII in providing estimates of risk for basal cell carcinomas, kidney cancer, bone sarcomas, and cancers from prenatal exposures. Third, a modified method is employed for estimating breast cancer mortality risk, which corrects for temporal changes in breast cancer incidence and survival. Fourth, an alternative model is employed for estimating thyroid cancer risk, based primarily on a report from the National Council on Radiation Protection and Measurements (NCRP). Fifth, EPA's central estimate of risk for many cancer sites is a weighted arithmetic mean of values obtained from the two preferred BEIR VII models for projecting risk in the U.S. population, rather than a weighted geometric mean, as employed in BEIR VII. Finally, this report provides a somewhat altered and expanded analysis of the uncertainties in the cancer risk estimates, focusing especially on estimates of risk for whole-body irradiation and for specific target organs.

Underlying the risk models is a large body of epidemiological and radio-biological data. In general, results from both lines of research are consistent with a linear, no-threshold dose (LNT) response model in which the risk of inducing a

[1] See http://www.epa.gov/radiation for further information on EPA's radiation protection activities and Federal Guidance function.

cancer in an irradiated tissue by low doses of radiation is proportional to the dose to that tissue.

The most important source of epidemiological data is the Life Span Study (LSS) of the Japanese atomic bomb survivors, who received an acute dose of radiation, mostly in the form of γ-rays, with a small admixture of neutrons. The LSS study has important strengths, including: a nearly instantaneous exposure, which can be pinpointed in time; a large, relatively healthy exposed population encompassing both genders and all ages; a wide range of radiation doses to all organs of the body, which can be estimated reasonably accurately; and detailed epidemiological follow-up for about 50 years. The precision of the derived risk estimates is higher than all other studies for most cancer sites; nevertheless it is limited by errors in dosimetry and sampling errors. The sampling errors are often quite large for specific cancer types, and the uncertainties are even larger if one focuses on a specific gender, age at exposure, or time after exposure. Another important uncertainty is the transfer of site-specific cancer risk estimates to the U.S. population, based on results obtained on the LSS population, for sites with substantially different baseline incidence rates.

In addition to the LSS, other epidemiological studies provide important information about radiogenic cancer risks. These include studies of medically irradiated patients and groups receiving occupational or environmental exposures. For thyroid and breast cancers, risk estimates are based on pooled analyses of the LSS and medically irradiated cohorts. While studies on populations exposed occupationally or environmentally have, so far, been of limited use in quantifying radiation risks, they can provide valuable insight into the risks from chronic exposures.

Summary risk coefficients are calculated for a stationary population (defined by 2000 U.S. vital statistics) rather than a population with an age distribution of the actual U.S. population. Numerically, the same coefficients apply for a cohort exposed throughout life to a constant dose rate. This puts the radiation risk estimates derived here on a comparable basis to risk estimates for chemicals derived from lifetime animal exposure experiments. For uniform whole-body exposures of low-dose gamma radiation to the entire population, the cancer incidence risk coefficient (Gy^{-1}) is 1.16×10^{-1} (5.6×10^{-2} to 2.1×10^{-1}), where the numbers in parentheses represent an estimated 90% confidence interval. The corresponding coefficient for cancer mortality (Gy^{-1}) is about half that for incidence: 5.8×10^{-2} (2.8×10^{-2} to 1.0×10^{-1}). For perspective, the average individual receives about 1 mGy each year from low-LET natural background radiation, or about 75 mGy, lifetime. The average cancer incidence and mortality risks from natural background radiation are then estimated to be about 0.87% and 0.44%, respectively.

The estimated risks are significantly higher for females than for males: 1.35×10^{-1} Gy^{-1} vs. 9.55×10^{-2} Gy^{-1} (incidence) and 6.9×10^{-2} Gy^{-1} vs. 4.7×10^{-2} Gy^{-1}

(mortality), respectively. Estimates of risk per unit dose differ widely among cancer sites. For females, these are largest for lung and breast cancers, which together account for about 44% (incidence) and 50% (mortality) of the risk from uniform whole-body radiation. For males, risks per unit dose are largest for colon and lung cancers, accounting for about 29% (incidence) and 40% (mortality) of the risk for all cancer sites.

Radiogenic risks for childhood exposures are of special interest. Doses received from ingestion or inhalation are often larger for children than adults, and the risks per unit dose are substantially larger for exposures during childhood (here defined as the time period ending at the 15^{th} birthday) than from exposures later in life. For children, the estimated risks from uniform whole-body radiation for cancer incidence are 2.0×10^{-1} Gy^{-1} (males) and 3.3×10^{-1} Gy^{-1} (females) with 90% uncertainty intervals: 7.7×10^{-2} to 3.6×10^{-1} Gy^{-1} (males) and 1.2×10^{-1} to 5.5×10^{-1} Gy^{-1} (females). The corresponding estimated risks for mortality are 8.5×10^{-2} Gy^{-1} (males) and 1.5×10^{-1} Gy^{-1} (females). There is generally much more uncertainty in the estimated risks from childhood exposures than in the risks for the entire population. A-bomb survivors who were children at the time of the bombings (ATB) still have substantial years of life remaining in which cancers are to be expressed. Further follow-up will provide more statistical precision and greater clarity as to how these risks vary many decades after the exposure.

For ingestion or inhalation of radionuclides that concentrate in individual organs, the risk for those specific sites may predominate. In this context, it is important to recognize that the percent uncertainties for site-specific risk coefficients are generally greater than the coefficient for uniform, whole-body irradiation; this is largely due to the smaller number of cancers for specific sites in the LSS and to uncertainties in how radiogenic risks for specific cancer sites in the U.S. might differ from those in a Japanese population of A-bomb survivors.

Cancer sites with large relative changes in the calculated lifetime risk (about 2-fold or more) from EPA's previous estimates published in Federal Guidance Report 13 (FGR-13) (EPA 1999b) include: kidney, liver, female lung, and female bladder (increased); and female colon (decreased). For both males and females, the estimated risk for all cancers combined increased by about 35%. For mortality, there was a notable change in estimated risk for cancers of the female colon (decreased), and female lung (increased). In general, the new EPA mortality estimates do not differ greatly from those in FGR-13; remarkably, for all sites combined, the estimates changed by less than 2% for both males and females.

One issue in radiation risk assessment is how to extrapolate risk estimates derived from data on relatively high acute exposures in case of the LSS cohort to low dose, or chronic exposure situations, which are of greatest interest to EPA. Many subjects in the LSS cohort did receive very low doses, but there is inadequate statistical power to quantify risk below about 0.1 Gy. This is about 100 times the annual whole-body, low-LET dose to an average individual from

natural background. Thus, the question is how to extrapolate from an observed risk due to an instantaneous dose of 0.1 Gy or more to an extrapolated risk from a chronic exposure of ≈ 1 mGy per year.

Efforts have been made to integrate information gathered from radiation biology and epidemiology into a theoretical framework that would allow reliable risk projections at dose rates approaching natural background. Radiation is known to induce mutagenic damage to the cell's DNA. Due to clustering of ionizations produced by low-LET as well as high-LET radiation, this damage is often complex, involving two or more breaks with concomitant base damage all within a few nanometers in the DNA molecule. This argues against a threshold for radiation-induced carcinogenesis and in favor of a linear dose-response relationship at low doses. Experimental studies have uncovered novel low-dose phenomena, which may modulate the dose-response relationship at low doses. However, the relevance of these findings to human carcinogenesis remains unclear, and epidemiological studies of cancer induction in cohorts receiving fractionated or chronic exposures have so far been broadly consistent with LNT predictions. The BEIR VII Committee unequivocally recommended continuing adherence to the LNT approach. EPA also finds strong scientific support for LNT, while acknowledging that new research might conceivably lead to revisions in the future.

Aside from the case of radon (which is not in the scope of this report), human data on risks from high-LET radiation (α-particles) are much more limited than for low-LET. For most cancer sites, risk coefficients for α-particles are based on a relative biological effectiveness (RBE) factor of 20 estimated from laboratory experiments; *i.e.,* the organ-specific risk coefficients are set equal to 20 times that for γ-rays. Epidemiological results on patients injected with an α-emitting radionuclide are consistent with an RBE of 20 for liver cancer, relative to the LSS, but an RBE of only about 2 for leukemia. An analysis of data on plutonium workers at the Mayak plant in the former Soviet Union also yielded an estimated α-particle RBE of roughly 20 for lung cancer (relative to the LSS), but there is considerable uncertainty in the doses delivered to sensitive cells in the lung for the Mayak worker cohort. In the case of bone cancer, low-LET data on humans is very sparse, and the bone cancer risk model employed here is derived from data on patients injected with ^{224}Ra.

Radiation is known to induce mutations in animal germ cells, but hereditary effects in humans have not been demonstrated. Nevertheless, genetic risks from low dose radiation exposure can be estimated based on animal studies. These estimates are generally lower than for cancer induction. There is also evidence that radiation at moderate doses can induce health effects such as cataracts and cardiovascular disease, and these effects may not have a threshold. However, unlike the case of radiogenic cancer and hereditary effects, there is, at present, no direct evidence nor a strong theoretical basis for such effects at lower/chronic exposures.

1. Introduction

The 1994 report, *Estimating Radiogenic Cancer Risks* (EPA 1994), presented EPA estimates of site-specific risks cancer incidence and mortality associated with low doses of ionizing radiation. (For brevity, the modifier "ionizing" will usually be omitted in the remainder of this report.) Primarily, the calculated risks were derived from models recommended by the International Commission on Radiological Protection (Land and Sinclair 1991), based on analysis of epidemiological data on Japanese atomic bomb survivors. While focusing mainly on a quantitative assessment of uncertainties in these estimates, a subsequent report also made minor adjustments in EPA's cancer risk estimates, reflecting changes in U.S. vital statistics (EPA 1999a). Finally, the methodology developed in the above reports was used in Federal Guidance Report No. 13 (FGR-13) to derive cancer risk coefficients for low level internal and external exposures to a set of over 800 radionuclides (EPA 1999b).

In 2006, the National Research Council of the National Academy of Sciences (NAS) released the BEIR VII report (NAS 2006), which reviewed recent evidence pertaining to the health risks from low-level, low linear energy transfer (LET) radiation. The BEIR VII Committee developed models for calculating the risks of radiogenic cancers, based on updated information on the A-bomb survivors, as well as other data. In this report, we employ the BEIR VII models to arrive at revised estimates of radiogenic risks for most cancer sites. BEIR VII risk estimates were derived for low doses of γ-rays with typical energies between about 0.1 and 10 MeV, with a brief discussion of possible enhancement of risk for more densely ionizing electrons and photons. Although the main focus here is, as in BEIR VII, on low-LET risks, we extend the evaluation of cancer risks to high-LET radiation (α-particles) and outline a biophysical approach to estimating risks from low energy photons and electrons. We also present risk models and estimates for prenatal exposures, and for kidney, bone, and non-melanoma skin cancers, which are not covered in BEIR VII.

Deviations from the BEIR VII approach are made for averaging the two types of models used to project risk from the A-bomb survivors to the U.S. population and for generating estimates of the risks of thyroid cancer and breast cancer mortality. Finally, a quantitative uncertainty analysis is presented, which is based on a different approach from that in BEIR VII and which incorporates some additional sources of uncertainty.

This report is not intended to provide an exhaustive review of the scientific basis for our risk models. For the most part, the reader is referred to BEIR VII and other sources in the literature. We have attempted to highlight major sources of uncertainty and, where pertinent, to include recently published information not considered by the BEIR VII Committee.

2. Scientific Basis for Cancer Risk Models

2.1 Biological Mechanisms

2.1.1 Biophysical interactions. By definition, ionizing radiation passing through matter has sufficient energy to break chemical bonds and to remove electrons from molecules. When this chemical damage occurs in the DNA of a somatic cell, a mutation in the genetic material can result, ultimately leading to a malignancy. The damage can be produced directly, when an ionizing particle impacts the DNA, or indirectly, through the creation of free radicals in the cellular medium, which diffuse and interact with the genetic material.

Only a tiny fraction of the free radicals produced in cells each day arise from radiation; nevertheless, DNA damage by low-level radiation is not negligible. This is because energy deposition events are often produced in clusters, which can, in turn, produce double strand breaks (DSBs) and more complex damage in DNA, involving multiple breaks and chemical modifications within a very restricted portion of the double helix. Cellular repair processes are less capable of repairing DSBs and complex damage than the simpler types of damage almost always induced by isolated free radicals. This makes ionizing radiation unique among environmental carcinogens. Even a single track of the radiation is capable of producing complex damage sites, which, if misrepaired, can leave the cell with a mutated gene that can be passed on to the cell's progeny. Depending on the nature of the mutation, this may be one step in the formation of a malignancy. At reasonably low doses the number of DSBs and sites of complex damage is expected to be strictly proportional to dose (UNSCEAR 2000b, NCRP 2001, NAS 2006); this is the primary basis for the linear no-threshold (LNT) theory in which the probability of inducing a cancer by radiation is proportional to dose with no threshold below which there is no risk.

Some recent research has cast doubt on the LNT assumption, but the BEIR VII Report concluded that these results in no way constituted compelling evidence against LNT. Additional discussion of the issue will be found in sections below.

The degree of clustering of ionizations, and therefore of the DNA damage, depends on the type of radiation and its energy. This is reflected in the linear energy transfer of charged particle radiation (LET), which is a measure of the amount of energy deposited, per unit path length, as the particle passes through a medium. Alpha particles emitted by the decay of unstable atomic nuclei have a relatively high LET (≈ 100-200 keV/μm) in aqueous media, producing a high density of ionizations, leading to a high frequency of DSBs and clustered damage sites in the DNA. Since this type of damage is more likely to be misrepaired, high-LET radiation is more effective at causing mutations, cell transformation, and cell death (NCRP 2001). This higher effectiveness per unit dose, relative to some standard radiation (*e.g.*, ^{60}Co γ-rays), is expressed in terms of a factor

called the relative biological effectiveness[2] (RBE) (see Section 5). Initially, 200 kVp X-rays were used as the reference; however, since current radiogenic cancer risk estimates largely rest on studies of the Japanese atomic bomb survivors, whose predominant exposure was from γ-rays, it is now common to use ^{60}Co γ-rays as the reference radiation.

Compared to α-particles, β-particles and secondary electrons produced by incident γ-rays or medical X-rays typically have much lower linear energy transfer (0.1-10 keV/μm). The ionizations produced by energetic electrons are more widely spaced, on average, but their production is a stochastic process in which several ionizations can be created separated by a distance no greater than the characteristic distance between adjacent DNA bases or between DNA strands. Moreover, as electrons lose energy, the LET increases and closely spaced ionizations become more frequent. Hence, clustered DNA damage is more likely to be produced near the ends of the electron tracks.

X-rays and γ-rays can travel appreciable distances through matter without producing ionizations; however, they interact with atoms to produce energetic secondary electrons, which behave identically to incident electrons of the same energy. In aqueous media, over the incident photon energy range 0.1-10 MeV, the predominant photon interaction is Compton scattering, a process in which an incident photon transfers part of its energy to an atomic electron, creating a free electron and a lower energy photon. The energy of a Compton electron is positively correlated with the incident photon energy. Consequently, as the incident photon energy is reduced within this energy range, a higher fraction of the energy is dissipated in the form of lower energy (higher LET) electrons, resulting in more complex DNA damage and, therefore, perhaps an increased RBE. As the incident photon energy is reduced further, below 0.1 MeV, photoelectric absorption becomes increasingly important compared to Compton scattering, and the variation of LET with photon energy is no longer monotonic.

2.1.2 Carcinogenesis. Carcinogenesis is thought to be a multi-staged process "initiated" by a mutation in a single cell. Before a malignancy can result, however, additional mutations must accumulate. This process may be enhanced by enlarging the pool of initiated cells (clonal expansion), which might be triggered by the presence of a "promoter." After clonal expansion, more initiated cells are available to undergo additional mutations, a process referred to as "cancer progression." Particularly important may be those mutations that

[2] Kocher et al. (2005) have introduced a quantity called the "radiation effectiveness factor" (REF) to compare the cancer causing potency in humans of a specified type of radiation relative to some standard. According to their definition, the REF is to be distinguished from measured RBEs that may be used as a basis for estimating the REF, although the RBEs themselves may have been measured for a different end-point or in a different species. Although it is important to keep in mind that RBEs used for human risk estimation are generally extrapolated, and not directly measured, we follow common practice here in applying the term RBE more broadly to include the estimation of human radiogenic cancer risk.

increase the probability of further mutations – *e.g.*, those impairing DNA repair processes. Eventually, a set of mutations may remove the essential controls over cell division, resulting in a malignancy.

2.1.3 Radiogenic carcinogenesis. Over a period of decades, a conceptual model of radiation carcinogenesis was built up from numerous studies conducted at the molecular, cellular, tissue, and whole organism levels. In this picture an ionizing track produces DNA damage through direct interaction with the double helix or through the interaction of free radicals diffusing to the DNA damage site, after being produced nearby. Misrepair of the DNA damage can then lead to an initiated cell and, eventually, to a malignancy as outlined above. The dose response for radiation carcinogenesis is then expected to have the same mathematical form as that for radiation-induced mutations.

As shown in Figure 2-1, the dose response for the induction of mutations, cell transformation, or carcinogenesis by low-LET radiation appeared to be linear at low doses, curvilinear upward at higher doses until eventually becoming concave downward at still higher doses. Mathematically, the initial portions of the curve is expressed as a "linear-quadratic" (LQ) function of effect (E) vs dose (D).

$$E = \alpha_1 D + \alpha_2 D^2 \qquad (2\text{-}1)$$

At low dose rates, the effect was found to increase linearly, with the same slope, α_1, observed initially at high dose rates. The expected response at high doses is therefore reduced by lowering the dose rate, which effectively removes the quadratic term in Eq. 2-1.

As also shown in Figure 2-1, the dose-response for high-LET radiation, appeared to be linear and independent of dose rate, except at rather high doses, where the function flattens or even turns over. At the high doses, moreover, an "inverse dose rate effect" may be observed in which the response is increased when the dose rate is reduced.

Thus, at low doses and dose rates the dose-response for either low- or high-LET radiation appears to be linear with no evidence of a threshold.

In the case of low-LET radiation, it was inferred that the passage of two tracks close together in space and time increases the probability of misrepaired damage, either because the damage produced is more complex or because the repair machinery becomes partially saturated, reducing its effectiveness. It was presumed that, at either low doses or low dose rates, only the damage produced by single tracks is significant, and the response is simply proportional to dose. At high dose rates, however, repair efficiency will decrease with increasing dose, leading to the quadratic term in Eq. 2-1.

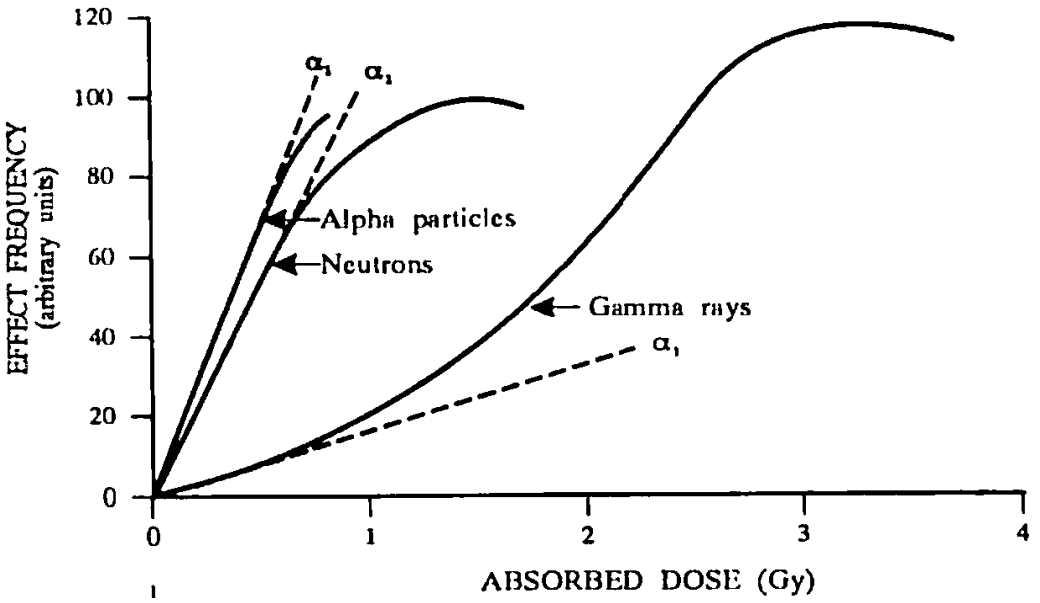

Figure 2-1: Solid curves depict the classical dose-response curves for low-LET γ-rays and high-LET neutrons or α-particles. The dashed lines show the expected response at low dose rates for each type of radiation. From UNSCEAR 1993, p. 698.

At low or moderate doses of high-LET radiation, the production of multiply-damaged sites in DNA is dominated by single track events. The flattening or downturn observed at high acute doses may reflect cell killing (NCRP 1980). An alternative explanation has been proposed in which at any given time a subpopulation of cells exists in a sensitive time window; spreading the dose out more in time allows more cells to be hit while they are in that time window, resulting in an enhanced response (Rossi and Kellerer 1986, Elkind 1994). Downward curvature and an inverse dose rate effect can also result from the "bystander effect" (Brenner and Sachs 2003), which will be discussed below.

Conclusions: Traversal of a cell nucleus by radiation can induce damage to the cell's DNA, initiating the carcinogenic process. Since the damage produced by even a single track of ionizing radiation can sometimes be misrepaired, a threshold for cancer induction would appear improbable unless there is a mechanism for eliminating essentially all dividing cells with damaged DNA (*e.g.*, through some kind of immune surveillance). A nearly foolproof screening mechanism of this sort would seem to be ruled out, however, by the significant rate of cancer incidence among people not exposed to high levels of radiation.

Under conditions of low doses or low dose rates, the effect of multiple tracks is expected to be negligible, so the probability of a cell becoming initiated is simply proportional to dose. This provides a mechanistic basis for the linear no-threshold (LNT) model of carcinogenesis in which the probability of radiation causing a cancer is proportional to dose, even at very low doses for which there

is insufficient statistical power to detect any excess incidence of the disease in a human population.

2.1.4 Extrapolation of low-LET risks to low doses and dose rates. As discussed above, radiobiological data suggest that the probability of mutational damage in a cell's DNA from an *acute* exposure to low-LET radiation can be expressed as a linear-quadratic (LQ) function of dose (D):

$$E = \alpha_1 D + \alpha_2 D^2 \tag{2-1}$$

The linear term is assumed to reflect the effect of single tracks, the quadratic term the added effect of two tracks traversing the cell close together in space and time, or perhaps the saturation of repair mechanisms at higher doses. If doses are delivered in a widely spaced temporal series of acute dose fractions, it is expected that each dose fraction, D_f , will produce an incremental effect,

$$E_f = \alpha_1 D_f + \alpha_2 D_f^2 \tag{2-2}$$

If each fraction is made very small, the quadratic terms will be negligible, and the overall summed effect will be linear with dose; *i.e.*, $E = \alpha_1 D$, where $D = \Sigma D_f$. A chronic exposure can be thought of as a sequence of very small fractionated exposures. It follows that if the dose rate from a chronic exposure is low enough so that the interaction of multiple tracks can be neglected, then the effect will again be simply given by $E = \alpha_1 D$, where D is the total dose.

The effect per unit dose will be reduced in going from a large acute dose, *D*, where the quadratic term is significant, to a low dose, where only the linear term contributes. Overall the effect will be reduced by a Dose Effectiveness Factor (DEF) = $(\alpha_1+\alpha_2 D)/\alpha_1 = 1+\theta D$, where $\theta = \alpha_2/\alpha_1$. Likewise the estimated effect per unit dose will be reduced by a Dose Rate Effectiveness Factor (DREF), when a large acute dose is delivered chronically. Since the slope is the same (α_1) at low doses or dose rates, the DREF and the DEF are equal. Thus, according to the LQ model, the extrapolation from a high acute dose to either a low dose or to a low dose rate can be embodied into a single correction factor, the Dose/Dose Rate Effectiveness Factor (DDREF).

It is presumed that the probability of carcinogenesis induced in an organism from an exposure to radiation is proportional to the number of induced mutations remaining after repair is complete. This has led scientists to model the excess risk as a LQ function of dose for a relatively high acute dose, with a reduction by a DDREF factor for low doses and dose rates. The DDREF for carcinogenesis would be equal to that for the underlying process of radiation-induced mutagenesis.

Based on its review of radiobiological and epidemiological data, the UNSCEAR Committee (UNSCEAR 1993; 2000b) concluded that any dose below 200 mGy, or any dose rate below 0.1 mGy/min (when averaged over about an hour), should be regarded as low. Thus, according to the linear-quadratic model, for these doses and dose rates, the risk per unit dose would be approximately equal to the linear coefficient, α_1.

2.1.5 Low dose phenomena. Much recent research in radiobiology has focused on several new phenomena relating to the effects of low dose radiation, including: (1) the adaptive response, (2) genomic instability, and (3) bystander effects. These phenomena have raised questions about the reliability of the LNT model for radiation carcinogenesis. They indicate that, at least under some conditions, radiation may induce DNA damage, *indirectly,* by affecting non-targeted cells, and that the processing of DNA damage by cells may be strongly dependent on dose, even at very low doses.

Adaptive response. Under some conditions, it has been found that pre-irradiating cells with an "adapting dose" of low-LET radiation (~10 mGy) reduces the effects (*e.g.*, chromosome damage, mutations, or cell transformation) of a subsequent "challenge dose" of ~1 Gy. This has provided some support for the suggestion that low-dose radiation may stimulate defense mechanisms, which could be beneficial in preventing cancer or other diseases. Supporting this view also have been studies in which the spontaneous transformation rates of certain cells in culture have been reduced by exposure to very low level radiation (Azzam *et al*. 1996, Redpath and Antoniono 1998). A subsequent study has, however, shown a threshold for this "beneficial effect": suppression of trans-formation disappeared when the dose rate was reduced below 1 mGy/day (Elmore *et al*. 2008). Thus, even if this phenomenon occurs *in vivo*, it may not be operative at environmental exposure levels.

Genomic instability. It has been found that irradiation of a cell can produce some kind of change in that cell, not yet characterized, which increases the probability of a mutation one or more cell divisions later (Morgan *et al*. 1996). The relatively high frequency of inducing genomic instability implies that the relevant target is much larger than a single gene, and there is evidence that, at least in some cases, the phenomenon is mediated by radiation-induced epigenetic changes rather than DNA damage (Kadhim *et al*. 1992, Morgan *et al*. 1996). The delayed mutations are typically simple point mutations, unlike other mutations caused by radiation, which are typically deletions or other types of chromosomal changes resulting from DSBs and more complex DNA damage (Little *et al*. 1997).

Bystander effects. Contrary to the conventional picture, DNA damage in a (bystander) cell can be induced by passage of an ionizing track through a neighboring cell. The bystander effect can apparently be triggered by passage of a signal through gap junctions (Azzam *et al*. 1998). Media transfer experiments

have demonstrated that it can also be induced – although probably less effectively (Mitchell *et al*. 2004) – by molecules leaking out into the extracellular fluid (Mothersill and Seymour 1998, Lehnert and Goodwin 1998). It also appears that the adaptive response and genomic instability may be induced in bystander cells under some conditions (Coates *et al*. 2004, Kadhim *et al*. 2004, Tapio and Jacob 2007). Recent evidence has also been found of bystander signals from irradiated cells inducing apoptosis in neighboring transformed cells (Portess *et al*. 2007).

The preponderance of data regarding these effects has been obtained from experiments on isolated cells. There is limited information on the occurrence of these effects *in vivo*, and no understanding of how they might modulate risks at low doses. At first sight, it would appear that the adaptive response should be protective, whereas bystander effects and genomic instability might increase risk. Interpretation may be complicated, however, by the possibility for triggering protective mechanisms in bystander cells, such as an adaptive response or apoptosis of precancerous cells (Lyng *et al*. 2000, Portess *et al*. 2007, Tapio and Jacob 2007).

The BEIR VII Committee was not convinced that these effects would operate *in vivo* in such a way as to significantly modify risks at low doses. It was a consensus of the Committee that:

> the balance of evidence from epidemiologic, animal and mechanistic studies tend to favor a simple proportionate relationship at low doses between radiation dose and cancer risk (BEIR VII, p. 14).

A similar conclusion was reached by another group of experts assembled by the International Commission on Radiological Protection (ICRP 2005).

In contrast, the French Academy of Sciences issued a report that strongly questioned the validity of the LNT hypothesis (Tubiana *et al*. 2005). The French Academy report cited a paper by Rothkamm and Löbrich (2003) showing that repair of DSBs, as measured by the disappearance of γ-H2AX foci, was absent or minimal at low doses, presumably leading to apoptosis of cells with DSBs. The French Academy report claimed that this finding indicated that risks were greatly overestimated at low doses. Recent studies have cast doubt on the significance of this finding, however (Lőbrich *et al*. 2005, Marková *et al*. 2007).

Conclusion. EPA accepts the recommendations in the BEIR VII and ICRP Reports to the effect that there is strong scientific support for LNT and that there is no plausible alternative at this point. However, research on low dose effects continues and the issue of low dose extrapolation remains unsettled.

2.2 Epidemiology

There is overwhelming evidence from epidemiological studies of irradiated human populations that radiation increases the risk of cancer. Most important from the standpoint of quantifying radiation risks is the Lifespan Study (LSS) of atomic bomb survivors in Hiroshima and Nagasaki, Japan. These survivors constitute a relatively healthy population at the time of exposure, including both genders and all ages, with detailed medical follow-up for about half a century. Extremely significant, also, is the wide range of fairly accurately known individual radiation doses.

The LSS cohort shows an excess in various types of cancer, with the rates increasing with increasing dose to the target organ. The data from the LSS are adequate to serve as a basis for developing detailed mathematical models for estimating risk as a function of cancer site, dose, age, and gender. However, due to limitations in statistical power, it has not been possible to demonstrate and quantify risk in the LSS at doses below about 100 mGy.

Epidemiological studies of medically irradiated cohorts provide strong confirmation for the carcinogenic effects of radiation and some additional information for generating risk estimates – in particular, for the bone, thyroid, liver, and breast. Radiation risks have also been extensively studied in occupationally exposed cohorts, but so far such studies – aside from those on radon-induced lung cancers in underground miners – have not proved very useful for actually quantifying risk. Major reasons for this failure have been: poor dosimetry; low doses, leading to low statistical power; and potential confounding by life-style factors or other occupational exposures. As discussed in a later section, however, recent data on workers at the Mayak plutonium production plant in the former Soviet Union may provide an improved basis for estimating risks from inhaled α-emitters.

Although the epidemiological data on radiation-induced carcinogenesis are extensive, calculated risks to members of the U.S. population from doses of radiation typically received environmentally, occupationally, or from diagnostic medical procedures suffer from significant sources of uncertainty. Among these sources are: (1) errors in the epidemiological data underlying the risk models, including sampling errors, errors in dosimetry, and errors in disease ascertainment; (2) uncertainties in how risks vary over times longer than the period of epidemiological follow-up; (3) uncertainties in “transporting” risk estimates to the U.S. population from a study population (*e.g.*, the LSS cohort), which may differ in its sensitivity to radiation; (4) differences in the type of radiation, or its energy, between the epidemiological cohort and the target U.S. population; and (5) uncertainty in how to extrapolate from moderate doses (> 0.1 Gy), for which there are good data upon which to quantify risk, to lower doses, and from acute to chronic exposure conditions.

Especially contentious is the extrapolation to low doses and dose rates. Generally speaking, epidemiology cannot be used to detect and quantify the carcinogenic effects of radiation at doses below about 100 mGy of low-LET radiation because of limitations on statistical power (Land 1980, Brenner *et al*. 2003). Most cells in the body receive a radiation dose of about 1 mGy/y – predominantly γ-rays from cosmic, terrestrial and internal sources. Given the typical energies of these background γ-rays (0.1-3 MeV) this corresponds to roughly 1 ionizing track traversing each cell nucleus, on average, annually. Thus, during the estimated typical time for DNA repair to be completed (a few hours), roughly 1 out of 1,000 cell nuclei will be hit, and the probability of multiple hits to the same nucleus will be very low. By way of comparison, at the lowest doses for which risk can be quantified in the A-bomb survivors, each nucleus was instantaneously impacted by ~ 100 tracks.

A notable exception to this 100-mGy limit on the sensitivity of epidemiological studies appears to be for studies of childhood cancers induced by prenatal exposure to diagnostic X-rays, where an excess risk has been observed at a dose level of about 6-10 mGy (see Section 6). In this case, statistical power is magnified by the apparent heightened sensitivity of the fetus, combined with a low background rate of childhood cancers. Typically, the X-rays employed in these examinations were 80 kVp, and the estimated mean dose was 6 mGy; this corresponds to only about 1 incident photon per cell nucleus (Brenner and Sachs 2006). Thus, this finding argues against a threshold for radiation carcinogenesis.

Although epidemiology otherwise lacks the power to detect risks from acute doses of radiation below about 100 mGy, it can provide information on risks from smaller doses through studies of populations receiving fractionated or chronic radiation doses that cumulatively add up to about 100 mGy or more. For example, it was found that multiple fluoroscopic examinations, each delivering an average dose of approximately 8 mGy, produced a similar increase in breast cancer, per unit dose, as a single acute dose to the breast (Howe and McLaughlin 1996). Likewise, female scoliosis patients under 20 years of age, who received repeated X-ray examinations, each with a mean breast dose of approximately 4 mGy, had a higher breast cancer mortality compared to controls and an increasing mortality with an increasing number of examinations (Doody *et al*. 2000). In both these studies, breast cell nuclei received at most a few nuclear hits from each dose fraction. Finally, based on a revised analysis of the Israeli tinea capitis study first published by Ron *et al*. (1989), but incorporating uncertainties in dosimetry, Lubin *et al*. (2004) found that children receiving a mean total thyroid dose of 75 mGy in 5 fractions had a statistically significant increase in thyroid cancer compared to unirradiated controls.

Epidemiological studies have also been conducted on cohorts of individuals who received cumulative doses of 100 mGy or more, but where the dose is spread out over months or years. Radiologists (Lewis 1963, Smith and Doll 1981, Berrington *et al*. 2001) and radiological technicians (Wang *et al*. 1988,

Doody *et al*. 2006), working before modern radiation protection standards had been implemented, show increased risks of leukemia and breast cancer, respectively. However, individual dose estimates are generally lacking in these studies, and they are not very useful for obtaining quantitative risk estimates. A number of cohort studies are underway, however, which may better demonstrate and quantify risks from protracted doses of low-LET radiation.

Among the most important of these studies are: nuclear workers in various countries (Cardis *et al*. 2005a, 2007, Muirhead *et al*. 2009); Chernobyl cleanup workers ("liquidators") (Hatch *et al*. 2005, Kesminiene *et al.* 2008, Romanenko *et al.* 2008); children exposed to radioiodine releases from the Chernobyl accident (Cardis *et al*. 2005b, Tronko *et al*. 2006); residents downriver from the Mayak nuclear plant in Russia (Ostroumova *et al*. 2006, Krestinina *et al*. 2005); residents downwind from the Semipalatinsk nuclear test site in Kazakhstan (Bauer *et al*. 2005); and inhabitants of Taiwanese apartments constructed with steel beams contaminated with ^{60}Co (Hwang *et al*. 2008). Studies on these populations are ongoing and suffer from various shortcomings, including incomplete follow-up, dosimetric uncertainties, limited statistical power and confounding. Nevertheless, results from several of them suggest that radiation risks can be detected and quantified, even in cases where the average dose rate is well below 1 mGy/day, corresponding to less than 1 ionizing track per cell nucleus per day (Puskin 2008).

Jacob et al. (2009) performed a meta-analysis on 12 epidemiological studies of cancer risks from moderate doses (50-500 mGy) of low dose rate, low-LET radiation. The ERR/Gy derived from the meta-analysis was a factor of 1.21 times that derived for the LSS cohort (90% CI: 0.51-1.90). This would correspond to a DREF of 0.83, with 90% CI of approximately 0.5 to 2.

3. EPA Risk Projections for Low-LET Radiation

3.1 Introduction

For cancer sites other than thyroid, bone, kidney, and skin cancers, the new EPA risk projections for low-LET radiation are based on the risk models recommended in BEIR VII and are described in the next section. As in BEIR VII, the risk models form the basis for calculating estimates of lifetime attributable risk (LAR), which approximate the premature probability of a cancer or cancer death that can be attributed to radiation exposure. Relatively minor modifications were made to the approach used in BEIR VII to the methodology for calculating LAR; details are given in Section 3.2 and subse-quent sections. Although the main results are the new EPA estimates of LAR associated with a constant lifetime dose rate, we also provide estimates to indicate how radiogenic risks might depend on age at exposure. A detailed discussion of the uncertainties associated with these risks is given in Section 4.

The main focus of the BEIR VII Report was to develop estimates of risk for low-dose, low-LET radiation. However, the BEIR VII models are predominantly based on analyses of the A-bomb survivor data, where the exposure included high-LET neutrons, as well as γ-rays. A recently completed reappraisal of the A-bomb dosimetry, referred to as DS02, was used as a basis for the BEIR VII analysis. In BEIR VII, it was assumed that neutrons had a constant RBE of 10 compared to γ-rays, implying a "dose equivalent," D, to each survivor (in Sv) given by:

$$D = D_\gamma + 10\, D_n ,$$

where D_γ and D_n are, respectively, the γ-ray and neutron absorbed doses (in Gy). The BEIR VII approach then yields models for calculating the risk per Sv, which can be directly applied to estimate the risk per Gy from a γ-ray exposure.

With a constant RBE of 10, the estimated contribution of neutrons is relatively minor, although not negligible. A recent publication (Sasaki *et al*. 2008) presented radiobiological data supporting an RBE for neutrons that was highly dose dependent, approaching a value of nearly 100 in the limit of low doses. The authors found that applying their estimates for the RBE brought about better agreement between Hiroshima and Nagasaki chromosome aberration data and reduced the estimate of γ-ray risk by about 30%.

3.2 BEIR VII Risk Models

The BEIR VII Committee used excess relative risk (ERR) and excess absolute risk (EAR) to project radiogenic cancer risks to the U.S. population for each of the cancer sites given in Table 3-1. ERR represents the ratio of the age-specific increase in cancer rate attributable to a radiation dose divided by the

baseline rate, *i.e.*, the rate associated with the background radiation level, whereas EAR is simply the difference in rates attributable to radiation. In the models preferred by the BEIR VII Committee for solid cancer sites, ERR and EAR are functions of age-at-exposure, attained age (the age at which a cancer might occur), and sex. For leukemia, the "BEIR VII models" also explicitly allow for dependence of ERR or EAR on time-since-exposure (TSE).

For each cancer site, the BEIR VII risk models were based, at least partly, on analyses of data from atomic bomb survivors. ERR and EAR models of the form given in Eq. 3-1 and 3-2 were fit to LSS data on incidence and mortality:

$$\text{ERR model: } \lambda(c,s,a,b,D) = \lambda_0(c,s,a,b)[1+ERR(s,e,a,D)]$$
$$= \lambda_0(c,s,a,b)[1+D\overline{ERR}(s,e,a,D)] \quad (3\text{-}1)$$
$$\text{EAR model: } \lambda(c,s,a,b,D) = \lambda_0(c,s,a,b) + EAR(s,e,a,D)$$
$$= \lambda_0(c,s,a,b) + D\overline{EAR}(s,e,a,D) \quad (3\text{-}2)$$

Here, $ERR(s,e,a,D)$ and $EAR(s,e,a,D)$ are, respectively, the ERR and EAR for a given sex (s), age at exposure (e), attained age (a), and absorbed dose (D). $\overline{ERR}(s,e,a,D)$ and $\overline{EAR}(s,e,a,D)$ denote the ERR and EAR per unit of dose expressed in Gy (for low-LET radiation), and $\lambda_0(c,s,a,b)$ is the baseline rate, which depends on city (c, Hiroshima or Nagasaki), sex, attained age, and year of birth (b). For all solid cancer sites, an LNT model was fit to the LSS data. In other words, increases in solid cancer rates were assumed to be approximately equal to the product of a linear-dose parameter that depends on sex, the absorbed dose, and a function that depends on age-at-exposure and attained-age, so that $\overline{ERR}$ and $\overline{EAR}$ does not depend on dose.

The BEIR VII committee used very similar models to project risks to the U.S. population. Their ERR and EAR preferred risk models are of the form,

$$\lambda(s,a,D) = \lambda_0(s,a)[1+D\overline{ERR}(s,e,a,D)] \quad (3\text{-}3)$$
$$\lambda(s,a,D) = \lambda_0(s,a) + D\overline{EAR}(s,e,a,D) \quad (3\text{-}4)$$

The only difference in the BEIR VII models for projecting risk to the U.S. compared to the models fit to the LSS data is that in Eq. 3-3 and 3-4, $\lambda_0(s,a)$ represents the baseline rate for the U.S. population, which depends only on sex and attained age. Otherwise, the two set of models are identical, *i.e.*, $\overline{ERR}(s,e,a,D)$ and $\overline{EAR}(s,e,a,D)$ represent the same function in Eq. 3-3 and 3-4 as in Eq. 3-1 and 3-2. For example, the BEIR VII committee found that the ERR decreased by about 25% per decade of age at exposure (for ages under 30) in the model that "best" fit the LSS data for most cancer sites; consequently, the

ERR decreases by the same 25% per decade in their models used to project risk to the U.S.

Table 3-1: BEIR VII risk model cancer sites

Cancer site(s)	ICD-O-2 codes
Stomach	C16/3
Colon	C18/3
Liver	C22/3
Lung	C33, 34/3
Breast (female only)	C50/3
Prostate	C61/3
Uterus	C53-54, C559/3
Ovary	C56, C57 (0,1,2,3,4,8)/3
Bladder	C67/3
Thyroid	C739/3
"Remainder category" Solid cancers of the oral cavity, esophagus, small intestine, rectum, gall bladder, pancreas, digestive system*, nasal cavity, larynx, other respiratory system*, thymus, kidney, and central nervous system. Also includes renal pelvis, ureter cancers, melanoma, bone, connective tissue, other genital cancers*, and other solid cancers*	C00-C15/3, C17/3, C19-21/3, C 23-25/3, C26/3, C422 / 3, C37-39/3, C379/3, C649/3, C70-72/(2,3), C40/3, C41/3, C47/3, C49/3, C44/3, M8270-8279, C659/3, C 669/3, C51/3, C52/3, C57(7,8,9)/3, C58/ 3, C60/3, C63/3, C42 (0,1,3,4)/3, C69/3, C74-76/3, C77/3, C809/3
Leukemia (other than chronic lymphatic leukemia)	Revised ICD 9: 204-208

* Refers to sites not specified elsewhere in this table. Does not include lymphoma.

Of the two types of risk models, ERR models are more appropriate for cancer sites for which the age-specific excess in cancer incidence rates attributable to radiation might be roughly proportional to the baseline rate – independent of the population. In contrast, EAR models are appropriate when the excess in cancer rates is independent of the baseline risks. The BEIR VII Committee used each type of risk model (EAR and ERR) to calculate site-specific risk projections for a U.S. population. For cancers for which the baseline rates are higher in the U.S. than in the LSS, the ERR models tend to yield larger projections of radiogenic risk than the projections from EAR models. For other cancer sites, the projections from EAR models tend to be larger.

A compromise between the two approaches was used for most cancer sites. Based on the assumption that, for most cancer sites, radiogenic risks for

the U.S. population are within the ranges defined by the ERR and EAR projections, a reasonable approach would be to calculate an "average" of the projections based on the two types of risk models, *e.g.*, a weighted arithmetic or geometric mean. This is the approach used by BEIR VII and other comprehensive reports on radiation risks and is described in more detail in Section 3.10.

Table 3-2 provides a summary of the BEIR VII ERR and EAR risk models. For all solid cancer sites except breast and thyroid, the BEIR VII models were based exclusively on analyses of the A-bomb survivor incidence data. This differs from EPA's previous risk models (EPA 1994), which for most cancer sites were derived from LSS mortality data. In general, the LSS incidence data is preferred as a basis for the risk models because "site-specific cancer incidence data are based on diagnostic information that is more detailed and accurate than death certificate data and because, for several sites, the number of incident cases is larger than the number of deaths (NAS 2006)." For breast and thyroid cancers, the BEIR VII models were based on previously conducted pooled analyses of both A-bomb survivor and medical cohort data (Preston *et al*. 2002b, Ron *et al*. 1995). The risk model for leukemia was based on an analysis of mortality within the LSS cohort. In contrast to some other cancer types, "the quality of diagnostic information for the non-type-specific leukemia mortality used in these analyses is thought to be high" (NAS 2006).

Table 3-2: Summary of BEIR VII preferred risk models

Cancer site	Description	Data sources
Solid cancers except breast, thyroid	ERR and EAR increase linearly with dose; depends also on sex(s), age at exposure (e), attained age (a)	1958-1998 LSS cancer incidence
Breast	EAR increases linearly with dose. Effect modifiers: (e , a). Based on analysis of pooled data (Preston *et al*. 2002b). ERR model not used.	1958-1993 LSS breast cancer incidence; Massachusetts TB fluoroscopy cohorts (Boice *et al*. 1991); Rochester infant thymic irradiation cohort (Hildreth *et al*.1989)
Thyroid	ERR increases linearly with dose. Effect modifiers (s ,e). Based on analysis of pooled data (Ron *et al*. 1995). EAR model not used.	1958-1987 LSS thyroid cancer incidence (Thompson *et al*. 1994). Medical cohort studies: Rochester thymus (Shore *et al*. 1993), Israel tinea capitis (Ron *et al*. 1989), Chicago tonsils (Schneider *et al*. 1993), Boston tonsils (Pottern *et al*. 1990).
Leukemia	ERR and EAR are linear-quadratic functions of dose. Effect modifiers: (s , e , a), time since exposure (t).	1950-2000 LSS cancer mortality (Preston *et al*. 2004).

Solid cancer sites other than breast and thyroid. For most solid cancer sites, the preferred BEIR VII EAR and ERR models are functions of sex, age at exposure, and attained age, and are of the following form:

$$EAR(D,s,e,a) \text{ or } ERR(D,s,e,a) = \beta_s D \exp(\gamma e^*)(a/60)^{\eta}, \quad (3\text{-}5)$$

$$\text{where } e^* = \frac{\min(e,30) - 30}{10}. \quad (3\text{-}6)$$

As seen in Table 3-3, the values for the parameters, β_s, γ, and η, depend on the type of model (EAR or ERR). For ERR models, for most sites:

β, the ERR per Sv at age-at-exposure 30 and attained age 60, tends to be larger for females than males;

γ = -0.3 implies the radiogenic risk of cancer at age e falls by about 25% for every decade increase in age-at-exposure up to age 30; and

η = -1.4 implies the ERR is almost 20% smaller at attained age 70 than at age 60.

As a consequence, ERR decreases with age-at-exposure (up to age 30) and attained age. In contrast, for EAR models, γ = -0.41 and η = 2.8 for most sites. Thus EAR decreases with age-at-exposure, but *increases* with attained age. These patterns are illustrated in Figure 3-1.

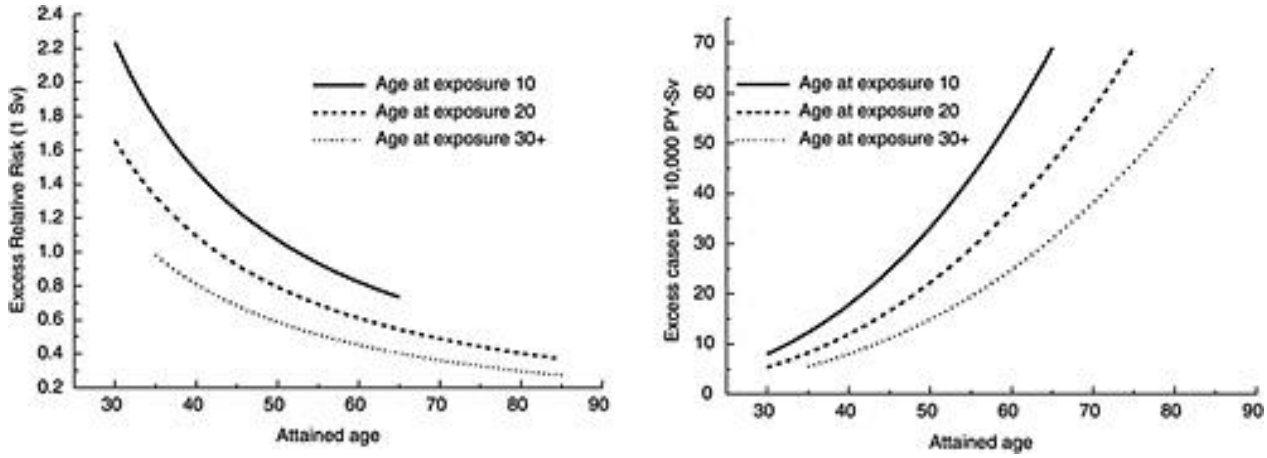

Figure 3-1: Age-time patterns in radiation-associated risks for solid cancer incidence excluding thyroid and nonmelanoma skin cancer. Curves are sex-averaged estimates of the risk at 1 Sv for people exposed at age 10 (solid lines), age 20 (dashed lines), and age 30 or more (dotted lines). (BEIR VII: Figure 12-1A, p. 270).

Thyroid. For thyroid cancer, the BEIR VII Committee used only an ERR model to quantify risk. It was of slightly different form than for other solid cancers in that ERR continues to decrease exponentially with age-at-exposure for ages greater than 30 y, and ERR is independent of attained age. The BEIR VII ERR model for thyroid cancer is given in Eq. 3-7:

$$ERR(D,s,e) = \beta_s D \exp[\gamma(e-30)/10](a/60)^{\eta}. \quad (3\text{-}7)$$

The BEIR VII thyroid model is a modified version of an ERR model for childhood exposures (ages < 15) from a pooled analysis of thyroid cancer incidence studies (Ron *et al*. 1995). NIH (2003) later extended the results to all ages of exposure. The NIH model is a stochastic model in which probability distributions are assigned to ERR, and the probability distributions depend only on dose and age-at-exposure. More speci-fically, the geometric means of these distributions are assumed to be linear with dose and decline in an exponential fashion with age-at-exposure. The BEIR VII model is very similar to the NIH model, except that it is not stochastic, and, consistent with findings of Ron *et al*., the ERR/Gy is assumed to be two times larger for females than males.

Neither model accounts for the dependency of ERR on TSE. Analyses of the pooled thyroid study data indicate that ERR peaks around 15-19 years after exposure but is still elevated for TSE > 40 (NCRP 2008).

Table 3-3: Parameter values for preferred risk models in BEIR VII[1]

Cancer	ERR model				EAR model			
	β_M	β_F	γ	η	β_M	β_F	γ	η
Stomach	0.21	0.48	-0.3	-1.4	4.9	4.9	-0.41	2.8
Colon	0.63	0.43	-0.3	-1.4	3.2	1.6	-0.41	2.8
Liver	0.32	0.32	-0.3	-1.4	2.2	1	-0.41	4.1
Lung	0.32	1.4	-0.3	-1.4	2.3	3.4	-0.41	5.2
Breast	Not used				See text			
Prostate	0.12		-0.3	-1.4	0.11		-0.41	2.8
Uterus		0.055	-0.3	-1.4		1.2	-0.41	2.8
Ovary		0.38	-0.3	-1.4		0.7	-0.41	2.8
Bladder	0.5	1.65	-0.3	-1.4	1.2	0.75	-0.41	6
Other solid	0.27	0.45	-0.3	-2.8	6.2	4.8	-0.41	2.8
Thyroid[2]	0.53	1.05	-0.83	0	Not used			
Leukemia	1.1 $\delta = -0.48$, θ = 0.87 Sv^{-1}, $\phi = 0.42$	1.2	-0.4	None	1.62 $\delta = 0$, θ = 0.88 Sv^{-1}, $\phi = 0.56$	0.93	0.29	None

[1] Adapted from Tables 12-2 and 12-3 of BEIR VII.

[2] Unlike for other sites, the dependence of ERR on age-at-exposure is not limited to ages<30.

Breast. For breast cancer, the BEIR VII Committee used only an EAR model to quantify risk. The model was based on a pooled analysis (Preston *et al*. 2002b) of eight cohorts: the LSS cohort, and seven cohorts in which subjects were given radiation treatment for various diseases and/or conditions – tuberculosis, an "enlarged" thymus, mastitis, benign breast disease, and skin hemangioma. The cohorts included Asians, Europeans, and North Americans, who received either single acute, fractionated, or protracted exposures. Although there was no simple unified ERR or EAR model that "adequately describes the excess risks in all cohorts," the BEIR VII EAR model provides a reasonable fit to data from four of the cohorts: the LSS, two cohorts of U.S. tuberculosis patients, and one of the "enlarged" thymus infant cohorts. No ERR model was found to provide an adequate fit to the LSS and tuberculosis cohorts because excess rates attributable to radiation after adjusting for age-at-exposure are similar in all the three cohorts, despite much larger baseline breast cancer rates in the U.S. than Japan. For two of the remaining cohorts – Swedish patients treated for benign breast disease and a N.Y. cohort of mastitis patients – the authors suggested that effects of predisposition may have accounted for differences in excess rates, *e.g.*, mastitis patients may be more sensitive to radiation than other women. The other two cohorts not used in fitting the BEIR VII model were the cohorts of hemangioma patients and were of limited size.

In the BEIR VII model, the EAR depends on both age at exposure and attained age (Eq. 3.8), where the parameter estimates are from Preston *et al.* (2002b, Table 12). Unlike for other cancers, the EAR continues to decrease exponentially with age-at-exposure throughout one's lifetime, and the EAR increases with attained age less rapidly after age 50 (about the time of menopause).

$$EAR(D,s,e,a) = \beta D \exp[\gamma(e-25)/10](a/50)^{\eta} \qquad (3\text{-}8)$$

where β = 9.9; γ = -0.51; η= 3.5 for $a < 50$ and 1.1 for $a \geq 50$.

Leukemia. BEIR VII provided both EAR and ERR risk models for leukemia (see Eq. 3-9). These differ from models for most other cancer sites. In the leukemia models, both the ERR and EAR depend on TSE (*t*), and risk is a linear-quadratic function of dose. As shown in Figure 3-2, the EAR and ERR per unit dose both increase with dose (the fitted value for θ in Eq. 3-9 is positive).

$EAR(D,e,t)$ or $ERR(D,e,t) = \beta_S D(1+\theta D)\exp[\gamma e^* + \delta \log(t/25) + \phi e^* \log(t/25)]$, for $t \geq 5$, and

$$EAR(D,e,t) = EAR(D,e,5), \text{ for } 2 < t \leq 5,$$
$$ERR(D,e,t) = ERR(D,e,5)\frac{\lambda_0(s,e+5)}{\lambda_0(s,e+2)}, \text{ for } 2 < t \leq 5, \text{ and}$$
$$EAR(D,e,t) = ERR(D,e,t) = 0 \text{ for } t \leq 2. \qquad (3\text{-}9a,b)$$

The dependence of EAR and ERR on age and TSE is illustrated in Figure 3-3. Both EAR and ERR decrease with TSE for $t > 5$, and the rate of decrease is larger for younger ages at exposure. For the time period 2 to 5 y after exposure, the EAR is constant. The EAR that would be calculated using the ERR model (note that excess absolute risk is equal to the product of the ERR and the baseline cancer rate) is also constant for this time period ($2 < t \leq 5$).

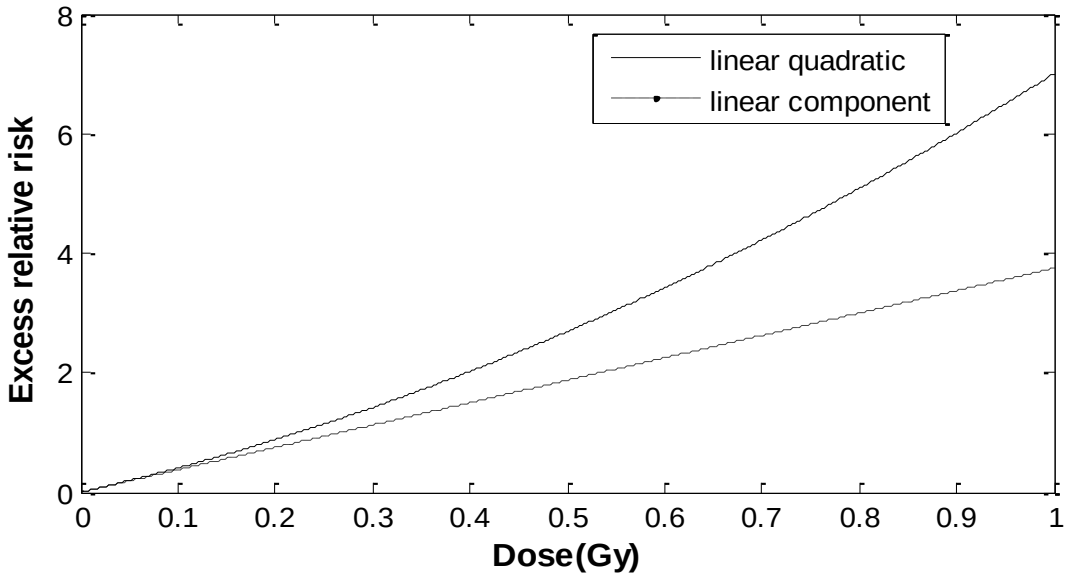

Figure 3-2: ERR for leukemia for age-at-exposure = 20 and TSE=10. The linear component of the dose-response is also shown.

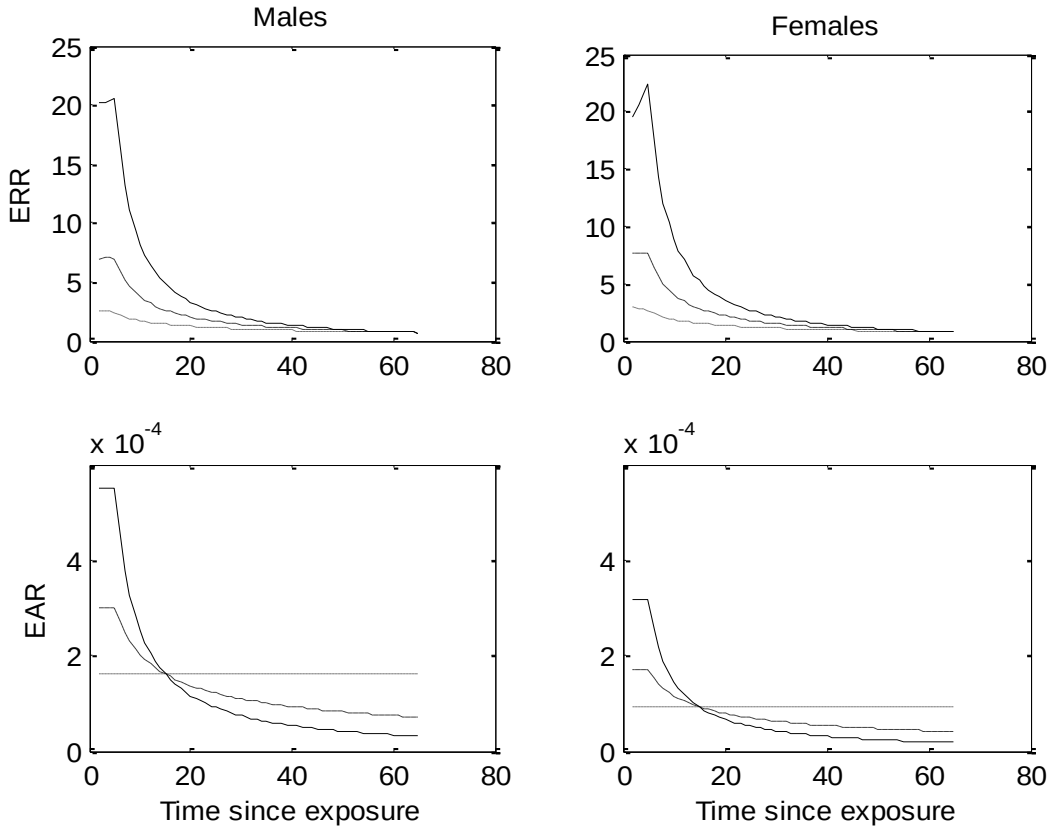

Figure 3-3: ERR (per person-Gy) and EAR (cases per person-Gy) for exposures at low doses and/or dose rates by TSE for three different ages at exposure: 10 (solid), 20 (long dashes), and 30 and above (short dashes).

3.3. Risk Models for Kidney, Central Nervous System, Skin, and Other "Residual Site" Cancers

BEIR VII's risk model for what are often termed "residual site" cancers deserves special mention. The residual category generally includes cancers for which there were insufficient data from the LSS cohort or other epidemiological studies to reliably quantify radiogenic site-specific risks. For these sites, results from the LSS cohort were pooled to obtain stable estimates of risk. With five exceptions (cancers of the esophagus, bone, kidney, prostate and uterus) the BEIR VII Report included the same cancers in this category as EPA did in its previous risk assessment (EPA 1994, 1999b). This section also describes risk models for cancers of the skin and of the brain and central nervous system (CNS).

Esophagus. EPA (1994, 1999b) employed a separate risk model for esophageal cancer, whereas in BEIR VII the esophagus is one of the "residual" sites. In part, this is because the risk models for the previous assessment were based on LSS mortality data, for which there was a significant dose-response for esophageal cancer. In contrast, the BEIR VII models are based on LSS

incidence data, for which there was insufficient evidence of a dose-response. Consistent with BEIR VII, we include esophageal cancer as one of the residual sites. This decision is expected to have only a minor impact on EPA's risk coefficients for intake of radionuclides.

Kidney. EPA (1999b) uses a separate model for cancer of the kidney, but BEIR VII includes kidney as one of the residual sites. In contrast to esophageal cancer, a separate risk model is needed for this cancer site because the kidney is an important target for several radionuclides, including isotopes of uranium. There is little direct evidence upon which to base an estimate for kidney cancer LAR. In a recent analysis of LSS incidence data (Preston *et al*. 2007), there were only 115 kidney cancers, 70% of which were renal cell cancers. The authors estimated only 6 excess renal cell cancers from radiation exposure. Furthermore, whatever the association might be between kidney cancer and radiation, it is complicated by the fact that the etiology for the various kidney cancer types differ. The estimated dose-response in the LSS appears to be sensitive to the type of model being fit. Within the LSS cohort, no indication of a positive dose response was found ($p > 0.5$) when a constant ERR model was fit, but results were significant when fit to a constant EAR model. Confidence intervals for linear dose response parameters are wide for both models, and there is insufficient evidence to conclude that the dose response in LSS is substantially different for kidney cancers than other residual site cancers. It was therefore concluded that a reasonable approach would be to use the BEIR VII residual site ERR model for kidney cancers. For the kidney EAR model, an adjustment factor was applied, equal to the ratio of the age-specific kidney cancer baseline rates divided by the rates for the residual site cancers. EPA's new kidney cancer EAR model is given in Eq. 3-10:

$$\overline{EAR}_{kidney}(s,e,a) = \frac{\lambda_{I,kidney}(s,a)}{\lambda_{I,residual}(s,a)} \overline{EAR}_{residual}(s,e,a) \qquad (3\text{-}10)$$

Bone. A new EPA model for α-particle-induced bone cancer risks is based on an analysis of data on radium dial painters exposed to ^{226}Ra and ^{228}Ra and patients injected with the shorter-lived isotope ^{224}Ra (Nekolla *et al*. 2000). The risk per Gy for low-LET radiation is assumed to be 1/10 that estimated for α-particle radiation. Details about the EPA bone cancer risk model and its derivation are provided in Section 5.1.2 (on human data on risks from higher-LET radiation).

The new risk projections for bone cancer incidence from low-LET radiation are 2.4×10^{-4} Gy^{-1} (males), 2.3×10^{-4} Gy^{-1} (females), and 2.4×10^{-4} Gy^{-1} (sex-averaged). About 35% of all bone cancers are fatal (SEER Fast Stats), and it is assumed here that the same lethality holds for radiogenic cases. The projected mortality risk estimates are then 8.6×10^{-5} Gy^{-1} (males), 8.2×10^{-5} Gy^{-1} (females), and 8.4×10^{-5} Gy^{-1} (sex-averaged).

Prostate and uterus. In contrast to EPA (1999b), BEIR VII provides separate risk models for these two cancer sites, and these BEIR VII models form the basis for new EPA projections. This is in contrast to EPA (1994, 1999b), in which these two cancer sites were included in the residual category. The A-bomb survivor data now provide sufficient information on radiogenic uterine cancer to formulate a risk projection of reasonable precision. BEIR VII cited the vastly differing baseline rates for the U.S. compared to Japan as a reason for providing a separate prostate estimate.

Skin. Previously, EPA risk estimates for radiation-induced skin cancer mortality (EPA 1994) were taken from ICRP Publication 59 (ICRP 1991). The one modification made by EPA was to apply a DDREF of 2 at low doses and dose rates. Recognizing that the great majority of nonmelanoma skin cancers are not life threatening or seriously disfiguring, EPA included only the fatal cases in its estimates of radiogenic skin cancer incidence. The contribution of skin cancers to the risk from whole-body irradiation was then minor: about 0.2% and 0.13% of the total mortality and incidence, respectively.

ICRP's calculation of skin cancer incidence risk employed an ERR of 55% per Sv, along with U.S. baseline skin cancer incidence rates from the 1970s. The ICRP mortality estimate was also based on conservative assumptions that: (1) 1/6 of radiogenic skin cancers would be squamous cell carcinomas (SCC), the remainder basal cell carcinomas (BCC) and (2) essentially all of the BCC would be curable, whereas about 1% of SCC would be fatal. Based on these considerations, ICRP Publication 59 estimated that 0.2% of the cases would be fatal.

The ICRP risk estimates closely mirror those previously published by Shore (1990), who also served on the committee that drafted ICRP Publication 59. Shore (2001) reviewed the subject again in light of additional information and concluded that essentially all of the radiation-induced skin cancers at low to moderate doses would be BCC. Therefore, it is assumed here that only BCC are radiogenic at low doses. He maintained that the fatality rate for BCC is "virtually nil" but cited a study indicating a rate of 0.05% (Weinstock 1994). Shore also noted that there was no persuasive evidence that radiation-induced BCC would be more fatal than sporadic cases.

At the same time, there is evidence that the baseline rates for BCC have increased dramatically since the 1970s, which might also result in a higher (absolute) risk per unit dose of inducing a radiogenic skin cancer.

There are 3 major cohort studies of radiation-induced skin cancer with thorough dosimetry and long-term follow-up (Shore 2001): (1) the LSS cohort, including both children and adults, exposed to a wide range of doses of γ-rays from the atomic bomb (Ron *et al*. 1998, Preston *et al*. 2007); (2) a cohort of 2,224 children in New York City treated for tinea capitis (ringworm of the scalp) with an

average dose of 4.75 Gy of 100 kVp X-rays (Shore *et al*. 2002); and (3) a cohort of 10,834 children in Israel treated for tinea capitis with an average dose of 6.8 Gy of 70-100 kVp X-rays (Ron *et al*. 1991).

The ERR/Gy for the two tinea capitis cohorts were found to be very similar: 0.6 Gy^{-1} (NY) and 0.7 Gy^{-1} (Israel). Both studies showed a decline in risk with age at exposure: 12% per y in the New York study, and 13% per y in the Israeli study (Shore 2001). The average age at exposure in the New York study was 7.8, compared to 7.1 in the Israeli. Overall, the results of the two studies then indicate a risk coefficient of ≈ 0.7 Gy^{-1} for exposure at age 7, with about a 12% per year decrease in risk with age at exposure. Both the LSS and the Israeli tinea capitis study appear to show some decline in the ERR at longer times since exposure, but the declines were not statistically significant; the New York tinea capitis study showed no indication of a decline, even after 45-50 years after irradiation (Shore 2001). Based on this information, the tinea capitis data can be reasonably described by the equation below:

$$ERR = 0.7D(0.88)^{e-7} \tag{3-11}$$

Where D is dose (Gy) and e is the age at exposure.

Skin cancer incidence exhibited a nonlinear dose response in the LSS (Preston *et al*. 2007). Fitted to a spline function with a knot at 1 Gy, the ERR/Gy for BCC was estimated to be about 5.5 times higher above 1 Gy than below (7 times for all nonmelanoma skin cancers). Similarly to the tinea capitis results, the risk was found to decrease by about 12.3% per year of age at exposure, the fall-off extending into adult age groups (Ron *et al*. 1998). Normalized to the same dose and age at exposure, the ERR was considerably higher in the Japanese A-bomb survivor population than in the mainly Caucasian populations irradiated for tinea capitis. In contrast to the tinea capitis cohorts, there was no evidence of a higher radiation risk to UV shielded parts of the body. This suggests that there may be a synergism between ionizing and ultraviolet radiation for Caucasians, but not for the Japanese. Quite possibly, this relates to differences in skin pigmentation (Ron *et al*. 1998). For this reason, we are primarily basing our skin cancer risk estimates on the tinea capitis data, which is probably more applicable to the U.S. population.

As discussed in Sections 2.14 and 3.6, the low-LET risk model in BEIR VII for all solid cancers is consistent with a LDEF of approximately 1+0.5*D*, where *D* is the dose in Gy. Assuming that this relationship holds for BCC induction, and given the magnitude of the average therapeutic doses received by the New York and Israeli tinea capitis patients, a LDEF of about 3.4 or 4.4 would be inferred for extrapolating the risks estimates derived from these studies to low doses, but this neglects the possible influence of cell killing at the high therapeutic doses administered to these patients, which may tend to flatten the dose-response and reduce the LDEF. On the other hand, a further reduction factor might be

appropriate for estimating risks from typical γ-rays with energies around 100 keV or higher (see Section 5.2). The LSS data on skin cancer suggest an even larger LDEF of about 5.5. The UNSCEAR 2006 Report (UNSCEAR 2008) fit various dose-response models to the LSS skin cancer incidence data and found a best fit for models in which either ERR or EAR are "quadratic-exponential" in dose and include an adjustment for attained age and age-at-exposure:

$$ERR \text{ or } EAR = \beta^2 D \exp(\alpha D) f(a,e) . \quad (3\text{-}12)$$

The UNSCEAR models project a negligible risk at very low doses.

Based on the above considerations, we adopt a low-dose/low-dose-rate γ-ray relative risk coefficient about one-third that inferred from a linear fit to the tinea capitis data:

$$ERR = 0.2\, D(0.88)^{e-7} \quad (3\text{-}13)$$

For life-table calculations, baseline incidence rates are needed, but SEER does not include nonmelanoma skin cancers in its database. BCC incidence rates have increased dramatically over the last 3 decades (Karagas *et al*. 1999), and it has been estimated that there are 900,000 incident cases of BCC annually in the U.S. (550,000 in men, 350,000 in women), the great majority of these in whites (Ramsey 2006). The estimated lifetime risk of BCC in the white population is very high: 33-39% in men and 23-28% in women. Overall, the age-adjusted incidence per 100,000 white individuals is 475 cases in men and 250 cases in women. To calculate age-specific baseline incidence rates, we applied these age-adjusted numbers and assumed that the rates increase with age to the power of 4.5, which is the roughly the pattern observed for many cancers (Breslow and Day 1987).

The age-adjusted fatality rate has recently been estimated to be 0.08 per 100,000 individuals, based on only 12 BCC deaths in the state of Rhode Island between 1988 and 2000 (Lewis and Weinstock 2004). The case fatality rate for BCC can then be roughly estimated to be: 0.08 / 0.5(475+250) ≈ 0.03%, which we have adopted for making skin cancer mortality projections.

The derived risk projections for skin cancer incidence are: 1.8×10^{-2} Gy^{-1} (males), 9.6×10^{-3} Gy^{-1} (females), and 1.4×10^{-2} Gy^{-1} (sex-averaged). The mortality risk projections are: 5.4×10^{-6} Gy^{-1} (males), 2.9×10^{-6} Gy^{-1} (females), and 4.1×10^{-6} Gy^{-1} (sex-averaged).

As noted above, the great majority of non-melanoma skin cancers are not serious, in the sense that they are not life threatening or significantly disfiguring. This is particularly true for BCC. We believe that it is reasonable to omit these cancers from our cancer incidence risk estimates rather than including them

along with much more serious types of cancers. Were we to include all the estimated radiogenic BCC cases, the numerical estimate of risk from uniform, whole-body radiation would be increased by about 9%. Serious cases of BCC, involving invasion of the cancer into underlying tissues can arise, however, if the problem is neglected for a long time. It would be reasonable to include all these cases in our whole-body risk estimates. Unfortunately, however, there appear to be no reliable data on the fraction of BCC cases that turn out to be significantly disfiguring or to require extensive surgery. For this reason, EPA is following its previous practice of including only the estimated radiogenic BCCs in its official estimates of radiogenic cancer incidence (Table 3-16). By way of illustration, if one were to assume that 5% of the radiogenic BCC cases are "serious" enough to be included in the cancer incidence estimates, the resulting average skin cancer risk coefficient would be $\approx 5 \times 10^{-4}$ per Gy, and the age-averaged whole-body risk coefficient for incidence would be increased by about 0.5%

Brain and central nervous system. As in BEIR VII, EPA has no formal separate risk model for brain and central nervous system (CNS) cancers. Instead, these cancers are included as part of the residual site category. Nevertheless, it is possible to compare BEIR VII's ERR model for residual site cancers to alternative ERR models that have been derived from LSS data on brain and CNS cancers. Preston *et al*. (2002a) found a nearly statistically significant ($p=0.06$) dose-related excess of CNS tumors other than schwannomas that were diagnosed between 1958 and 1995 among 80,160 A-bomb survivors. There was a "marked decrease" in excess risk with age at exposure, but no clear pattern associated with attained age. A model for ERR, based on their analysis, is given in Eq. 3-14. Based on essentially the same data, UNSCEAR (2008) obtained the model given in Eq. 3-15. As shown in Figure 3-4, the UNSCEAR model features an even steeper decrease in ERR with age-at-exposure (for ages < 10) than the model by Preston and others. It can be seen in the same Figure that a more gradual decrease in ERR with age-at-exposure is predicted by the BEIR VII risk model for residual cancers. However, in the BEIR VII model, the ERR is highly dependent on attained age; *e.g.*, for exposures before age 10, the ERR per Gy at attained age 15 ranges from about 15 to 22, whereas the ERR per Gy for attained age 60 is always less than 1.

$$ERR(D,e) = 0.15D\exp(-0.97(e-30)/10) \tag{3-14}$$

$$ERR(D,e) = 7.43145D\exp[-0.9897\log(e)] \tag{3-15}$$

Unfortunately, it is not clear which of the three alternative ERR models shown in Figure 3-4 is closer to the "truth." For example, it is not clear whether the ERR for CNS cancers depends on attained age. In the analysis by Preston *et al*., no decrease was found in ERR with attained age, but this may be due to the small number of excess CNS tumors that were associated with radiation (12, excluding schwannomas). Some evidence of an attained age effect is suggested in the Israeli tinea capitis (ringworm) study (Ron *et al*., 1988). The authors found

a significantly elevated risk for attained ages up to 35, “when the risk appeared to decline.” However, other studies provide no conclusive evidence of an attained age effect, and it is not clear why the age pattern in radiogenic risk for CNS should be similar to that for other “residual site” cancers.

Table 3-4 indicates that the projected LAR for CNS cancers based on the three alternative models are within a factor of about 2; sex-averaged LAR range from 0.0013 (Preston *et al*. model) to 0.0029 (UNSCEAR model) for lifelong exposures, and from about 0.005 (Preston *et al*.) to 0.010 (BEIR VII residual ERR model) for childhood exposures.

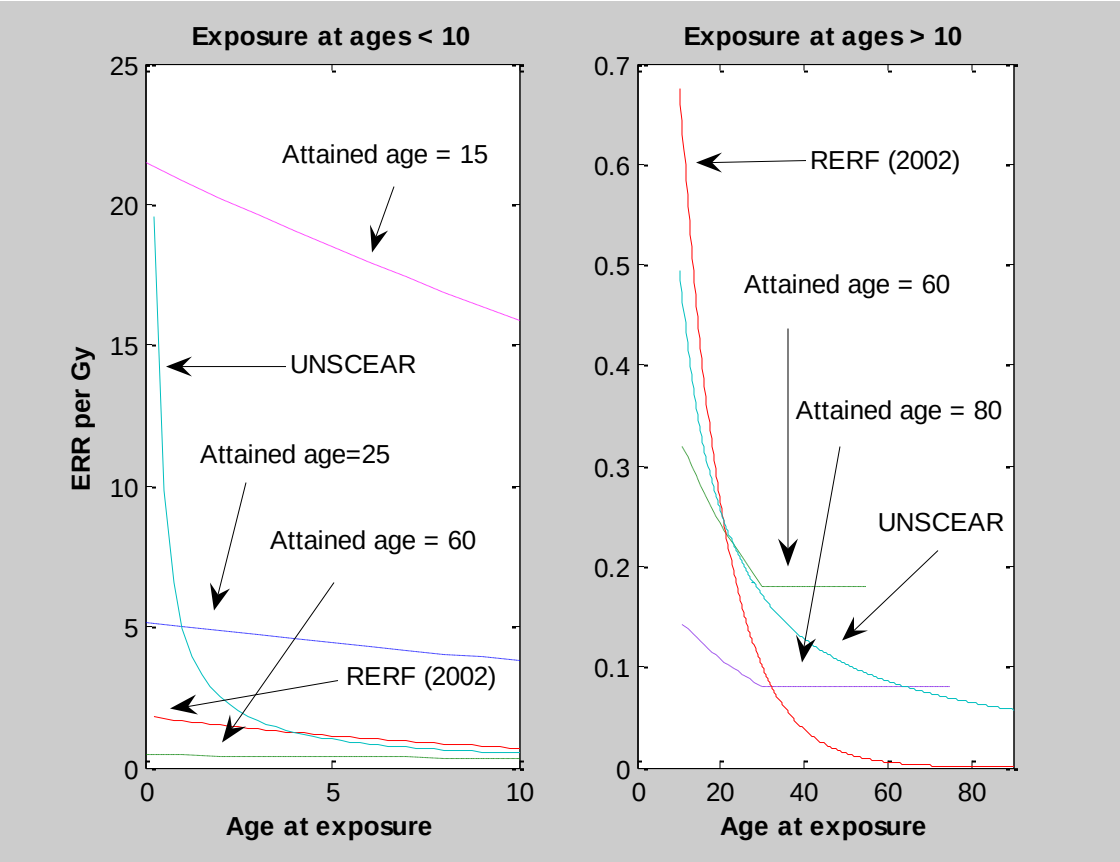

Figure 3-4: Comparison of two different ERR models for brain and CNS cancer with the residual site ERR model (dashed-and-dotted lines). For UNSCEAR (2006) and RERF (Preston *et al*. 2002a), ERR depends on age at exposure. ERR for the residual site cancer (shown here for males) depends on sex, age at exposure and attained age.

Table 3-4: Projection of LAR (Gy^{-1}) for brain and CNS cancers for three alternative ERR models

	Lifelong exposures[1]		Childhood exposures[2]	
ERR model	**Males**	**Females**	**Males**	**Females**
BEIR VII "Residual"	0.0023	0.0029	0.0085	0.0119
Preston *et al.* (2002a)	0.0014	0.0011	0.0056	0.0045
UNSCEAR (2008)	0.0017	0.0013	0.0061	0.0049

[1] Risks for exposures during the first year of life are omitted from these calculations; ERR for the UNSCEAR model approaches infinity for ages near zero.
[2] Risk from exposures between 1st and 15th birthday.

3.4 Risk Model for Thyroid Cancer

EPA's new risk model for thyroid cancer incidence is very similar to a model recommended by NCRP (2008), which explicitly accounts for the dependence of ERR on both age-at-exposure and time-since-exposure. Both the NCRP and new EPA thyroid risk models are primarily based on a model derived by Lubin and Ron (1998) from a subset of the pooled data of thyroid incidence studies described in previous section. The models are all of the form:

$$ERR(D,e,t) = \beta D A(e) T(t), \tag{3-16}$$

and the multiplicative factors for age-at-exposure, $A(e)$, and time-since-exposure, $T(t)$, are given in Table 3-5.

As is apparent in Table 3-5, the models are very similar. However, in contrast to the model derived by Lubin and Ron, EPA uses a single coefficient for TSE between 5 and 14, and TSE > 30. (There is insufficient data to detect differences in ERR for some of the subcategories for TSE used by Lubin and Ron). The Lubin and Ron model does not provide estimates of ERR for age-at-exposure > 15. For these "non-childhood" exposures, the EPA model borrows from the BEIR VII model, which stipulates an 8% y^{-1} decrease in ERR with age-at-exposure. We chose not to use the NCRP model because, although their model appears reasonable, the report did not provide an explanation for the minor discrepancies with Lubin and Ron (1998) or how results were extended for age-at-exposure > 15.

For calculating LAR for mortality, NCRP (2008) used the sex-averaged estimates of 5-y cancer fatality rates from the SEER program for the period 1998-2002 (see Table 3-6), and then doubled these to account for further mortality more than 5 y after diagnosis. Thus, 2(100–99.3)% = 1.4% of radiogenic cancers diagnosed before age 45 were assumed to be fatal, compared to 50% for cancers diagnosed after age 75.

Table 3-5: Estimated ERR/Gy and effect modifiers for age at exposure and time since exposure (TSE)

	Models		
	Lubin & Ron (1998)	**EPA[1]**	**NCRP (2008)**
ERR/Gy (*β*)	**10.7**	**10.7**	**11.7**
Age-at-exposure: *A*(*e*)			
<5	1.0	1.0	1.0
5-9	0.6	0.6	0.7
10-14	0.2	0.2	0.2
15-19	None given	0.2 exp[-0.083(e-15)]	0.2
20+	None given	0.2 exp[-0.083(e-15)]	0.09 ($e \leq 30$), 0.03 ($e > 30$)
TSE: *T*(*t*)			
<5	0	0	0
5-14	1.3 ($t \leq 10$); 1.0 ($t > 10$)	1.15	1
15-19	1.9	1.9	1.6
20-24	1.2	1.2	1
25-29	1.6	1.6	1.4
30-40	0.5 ($t \leq 35$); 0.2 ($t > 35$)	0.47	0.394
40+	0.7	0.47	0.394

[1] For age-at-exposure > 15, the ERR per Gy decreases 8% y^{-1}

Based on the EPA thyroid incidence model, and the NCRP approach for mortality, the LAR for mortality would be about 2.7×10^{-4} (males) and 5.7×10^{-4} (females). Dividing these by EPA projections for incidence (see Section 3.13) yields overall fatality rates of 13% (males) and 9% (females). However, 10-y relative survival rates for thyroid cancer have been about 95% since 1993 (see Table 3-6), and few deaths are found to occur more than 10 y after diagnosis. Furthermore, the fatality rate for radiogenic thyroid cancer is unlikely to be greater than for sporadic cancers (Bucci *et al.* 2001). Based on these considerations, EPA conservatively assumes a simple 5% fatality rate for all radiogenic thyroid cancers.

Table 3-6: Summary of SEER thyroid relative and period survival rates

Type of Statistic	Data	Sex	Age at diagnosis	Percent
5-year relative survival	1998-2002[1]	Both	<45	99.3
			45-54	98.1
			55-64	93.7
			65-74	90.2
			75+	75.0
5-year period survival	1999-2006[2]	Both	All	97.4
		Male	All	94.2
		Female	All	98.3
10-year relative survival	1999-2006[2]	Both	All	(95.1, 95.2, 96.3, 95.0, 95.7)[3]

[1] From NCRP (2009)
[2] From Altekruse *et al.* (2010)
[3] Year of diagnosis: 1993-1997

3.5 Calculating Lifetime Attributable Risk

As in BEIR VII, lifetime attributable risk (LAR) is our primary risk measure. As discussed in Section 3.2, separate evaluations of LAR were made for most cancer sites using both an excess absolute risk (EAR) model and an excess relative risk (ERR) model. For a person exposed to dose (D) at age (e), the LAR is:

$$LAR(D,e) = \int_{e+L}^{110} M(D,e,a) \cdot S(a)/S(e) da\,, \qquad (3\text{-}17)$$

where $M(D, e, a)$ is the excess absolute risk at attained age a from an exposure at age e, $S(a)$ is the probability of surviving to age a, and L is the minimum latency period (2 y for leukemia, 5 y for solid cancers). (Note: In Eq. 3-17 and subsequent equations, dependence of these quantities on sex is to be understood). The LAR approximates the probability of a premature cancer death from radiation exposure and can be most easily thought of as weighted sums (over attained ages up to 110) of the age-specific excess probabilities of radiation-induced cancer incidence or death, $M(D, e, a)$.

For any set of LAR calculations (Eq. 3-17), the quantities $M(D, e, a)$ were obtained using either an EAR or ERR model. For cancer incidence, these were calculated using either:

$$M_I(D,e,a) = EAR_I(D,e,a) \qquad \text{(EAR model)} \qquad (3\text{-}18)$$

or $$M_I(D,e,a) = ERR_I(D,e,a) \cdot \lambda_I(a) \qquad \text{(ERR model)} \qquad (3\text{-}19)$$

where $\lambda_I(a)$ is the U.S. baseline cancer incidence rate at age a. Datasets used to derive baseline incidence rates are described in Section 3.8.

For mortality, the approach is very similar, but adjustments needed to be made to the equations since both ERR and EAR models were derived using incidence data. In BEIR VII, it was assumed that the age-specific ERR is the same for both incidence and mortality, and the ERR model-based excess risks were calculated using:

$$M_M(D,e,a) = ERR_I(D,e,a) \cdot \lambda_M(a) \,. \tag{3-20}$$

i.e., the age- and sex-specific mortality risks is the excess relative incidence risk times the baseline mortality rate. For EAR models, BEIR VII used essentially the same approach by assuming:

$$M_M(D,e,a) = \frac{EAR_I(D,e,a)}{\lambda_I(a)} \lambda_M(a) \,. \tag{3-21}$$

Note that in Eq. 3-21, the ratio of the age-specific EAR to the incidence rate is the ERR for incidence that would be derived from the EAR model. Eq. 3-20 was used for all cancer sites other than skin and thyroid cancers, for which a constant fatality rate (0.03% for skin cancer and 5% for thyroid cancer) was applied to the projections for incidence. Eq. 3-21 was used for all sites except bone (fatality rate = 35%) and breast cancer. A description of the approach for estimating breast cancer mortality risk, and its rationale, is given in Section 3.11.

The LAR for a population is calculated as a weighted average of the age-at-exposure specific LAR. The weights are proportional to the number of people, $N(e)$, who would be exposed at age e. The population-averaged LAR is given by:

$$LAR(D, pop) = \frac{1}{N^*} \int_0^{110-L} N(e) \cdot LAR(D,e) \cdot de \,. \tag{3-22}$$

For the BEIR VII approach, $N(e)$ is the number of people, based on census data, in the U.S. population at age e for a reference year (1999 in BEIR VII), and N^* is the total number summed over all ages. In contrast, for our primary projection, we used a hypothetical stationary population for which $N(e)$ is proportional to $S(e)$, based on observed 2000 mortality rates. In this case,

$$LAR(D, stationary) = \frac{\int_0^{110-L} S(e) \cdot LAR(D,e) \cdot de}{\int_0^{110-L} S(e) de} \,. \tag{3-23}$$

Eq. 3-23 represents the radiogenic risk per person-Gy from a lifetime chronic exposure. Note that the equations above do not account for changes in future mortality rates. ***For a stationary population, Eq. 3-23 is equivalent to Eq. 3-22, so that the risk coefficient for a chronic exposure is equal to the (age-averaged) risk coefficient for an acute exposure.***

Computational details on how the integrals in Eq. 3-17, 3-22 and 3-23 were approximated are given in Appendix A.

3.6 Dose and Dose Rate Effectiveness Factor

To project risk at low or chronic doses of low-LET radiation, the BEIR VII Committee recommended the application of a Dose and Dose Rate Effectiveness Factor (DDREF), as described in Section 2.1.4. Effectively, this assumes that at high acute doses, the risk is given by a linear-quadratic (LQ) expression, $\alpha_1 D+\alpha_2 D^2$, whereas at low doses and dose rates, the risk is simply $\alpha_1 D$.

In the case of leukemia, LSS data shows upward curvature with increasing dose. The BEIR VII fit to the LQ model yielded a value of $\theta = \alpha_2/\alpha_1 = 0.88$ Sv^{-1}.

For solid tumors, the upward curvature in the LSS data appears to be lower and is not statistically significant (*i.e.*, θ is not significantly different from 0). While BEIR VII did not explicitly recommend a LQ model for solid cancer risk, it nevertheless concluded that some reduction in risk at low doses and dose rates was warranted. It adopted a Bayesian approach, developing separate estimates of the DDREF from radiobiological data and a statistical analysis of the LSS data. The estimate for the DDREF obtained in this way was 1.5, somewhat lower than values that had been commonly cited in the past. The BEIR VII Report notes that the discrepancy can largely be attributed to the fact that the DDREF is dependent on the reference acute dose from which one is extrapolating. According to BEIR VII, the appropriate dose should be about 1 Sv because data centered at about this value drives the LSS analysis. In contrast, much of the radiobiological data refers to effects observed at somewhat higher doses, for which the DDREF would be higher. Assuming that the extrapolation is indeed from an acute dose of 1 Sv, the DDREF of 1.5 corresponds to a LQ model in which $\theta = 0.5$ Sv^{-1}.

3.7 EAR and ERR LAR Projections for Cancer Incidence

EAR and ERR model-based LAR projections for a stationary population based on 2000 mortality data are given in bold typeface in Table 3-7. These are compared to EAR and ERR projections based on census data, with weights proportional to the number of people of each age in the year 2000. The results indicate that our primary risk projections are about 5-10% lower than they would be if based on a census population. Results in Table 3-7 reflect the DDREF adjustment of 1.5 for all cancer sites except leukemia, bone and skin.

Table 3-7: EAR and ERR model projections of LAR for cancer incidence[1,2] for a stationary population[3] and a population based on 2000 census data[4]

		Risk Model Population Weighting			
		ERR Projection		EAR Projection	
Cancer Site	**Sex**	**Stationary**	**Census**	**Stationary**	**Census**
Stomach	M	**15**	16	**171**	184
	F	**19**	21	**204**	217
Colon	M	**160**	171	**112**	120
	F	**103**	110	**67**	71
Liver	M	**17**	19	**92**	98
	F	**7.4**	8.0	**53**	56
Lung	M	**155**	166	**120**	126
	F	**485**	520	**233**	244
Breast	F	**Not Used**	Not Used	**289**	316
Prostate	M	**126**	135	**3.8**	4.1
Uterus	F	**11**	12	**50**	53
Ovary	F	**34**	37	**29**	31
Bladder	M	**107**	113	**75**	79
	F	**105**	111	**63**	66
Thyroid	M	**22**	24	**No model**	No model
	F	**65**	70	**No model**	No model
Residual	M	**275**	300	**196**	210
	F	**292**	315	**184**	196
Kidney	M	**26**	28	**21**	23
	F	**24**	26	**16**	17
Bone	M	**No model**	No model	**2.4**	2.7
	F	**No model**	No model	**2.3**	2.6
Leukemia	M	**109**	109	**53**	57
	F	**86**	87	**32**	34
Skin	M	**182**	199	**No model**	No model
	F	**96**	103	**No model**	No model

[1] Number of cases per 10,000 person-Gy.
[2] Uses DDREF of 1.5 for all sites except leukemia, bone, and skin
[3] Based on 2000 decennial life tables (Arias 2008)
[4] NCHS (2004)

3.8 ERR and EAR Projections for Cancer Mortality

We adopt the BEIR VII approach for ERR and EAR projections of LAR for mortality for all cancer sites except breast cancer. As noted previously, for its ERR model-based projection, BEIR VII used:

$$M_M(D,e,a) = ERR_I(D,e,a) \cdot \lambda_M(a) \ , \tag{3-24}$$

and for its EAR based projections,

$$M_M(D,e,a) = \left[\frac{EAR_I(D,e,a)}{\lambda_I(a)} \right] \lambda_M(a) \ . \tag{3-25}$$

In Eq. 3-25, the ratio in square brackets is equal to the ERR for incidence that would be calculated using the EAR model. In both Eq. 3-24 and 3-25, the BEIR VII approach assumes that the ERR for incidence and mortality are equal. However, this ignores the "lag" between incidence and mortality, which could lead to bias in the estimate of mortality risk in at least two different ways.

First, there would be a corresponding lag between the ERR for incidence and mortality, which might result in an underestimate of mortality risk. For purposes of illustration, suppose that: (a) a particular cancer is either cured without any potential life-shortening effects or results in death exactly 10 y after diagnosis and (b) survival does not depend on whether or not it was radiation-induced. Then,

$$ERR_M(e,a) = ERR_I(e,a-10) \geq ERR_I(e,a) \, . \tag{3-26}$$

The relationship would also hold for the EAR if the baseline cancer rate has the same age-dependence for A-bomb survivors as for the U.S. population.

Second, since current cancer deaths often occur because of cancers that developed years ago, application of the EAR-based ERR for incidence can result in a substantial bias due to birth cohort effects. If age-specific incidence rates increase (decrease) over time, the denominator in Eq. 3-25 would be too large (small). This could result in an underestimate (overestimate) of the LAR.

The BEIR VII approach is reasonable for most cancers, because the time between diagnosis and a resulting cancer death is typically short. An exception is breast cancer, for which our approach is presented in Section 3.11.

Results of LAR calculations using the BEIR VII approach are given in Table 3-8. Although not shown, LAR for mortality tends to be about 5% larger for census-based weights than for weights based on a stationary population. Mortality and incidence data used for the calculations are described in the next section.

Table 3-8: Age-averaged LAR[1,2,3] for cancer mortality based on a stationary population[4]

		Risk Model	
Cancer Site	**Sex**	**ERR**	**EAR**
Stomach	M	7.5	88
	F	11	111
Colon	M	74	51
	F	45	29
Liver	M	12	75
	F	6.1	46
Lung	M	140	111
	F	384	200
Breast	F	Not used	95[5]
Prostate	M	19	0.8
Uterus	F	2.5	16
Ovary	F	22	22
Bladder	M	21	19
	F	27	23
Thyroid	M	1.1	No model
	F	3.2	No model
Residual	M	112	103
	F	132	108
Kidney	M	8.4	8.0
	F	7.4	6.3
Bone	M	No model	0.9
	F	No model	0.8
Leukemia	M	80	31
	F	63	20
Skin	M	0.05	No model
	F	0.03	No model

[1] Cases per 10,000 person-Gy
[2] Except for skin, bone, kidney, and thyroid cancers, projections based on BEIR VII risk models.
[3] Based on DDREF of 1.5 except for leukemia, bone, and skin
[4] Arias (2008).
[5] See Section 3.11

3.9 Data on Baseline Rates for Cancer and All-Cause Mortality

Cancer specific incidence and mortality rates are based on data from the Surveillance, Epidemiology, and End Results (SEER) program of the National Cancer Institute (NCI). Begun in the early 1970s, SEER collects incidence and survival data from several, mostly statewide and metropolitan, cancer registries

within the U.S. The SEER program has expanded several times – most notably, from 9 registries (SEER 9) to 13 registries (SEER 13) in the early 1990s and, more recently, from 13 registries to 17 registries (SEER 17). The program also obtains mortality data from the National Center for Health Statistics (NCHS).

Cancer incidence (SEER 2009a,b) and mortality (SEER 2010) rates for this report were obtained using the software package SEER-Stat, available from the SEER website (http://seer.cancer.gov). For this report, the cancer and sex- and age-specific baseline incidence rates were obtained as a weighted average of the smoothed 1998-1999 rates based on data from the SEER 13 registries and 2000-2002 rates from SEER 17 registries. This contrasts with BEIR VII, which used (a previous version) of public-use SEER 13 data for the years 1995-99. Graphs of the baseline rates and details on how the data were smoothed are given in Appendix A.

SEER areas currently comprise about 26% of the U.S. population and are not a random sample of areas within the U.S. Nevertheless the cancer rates observed in the combined SEER areas are thought to be reasonably similar to rates for the U.S. population. Sampling errors for these baseline rates are relatively small, and contribute only negligibly to uncertainties in projections of (radiogenic) LAR. However, it is anticipated that risk projections might occasionally be updated to reflect changes in rates for both incidence and mortality.

Table 3-9 gives estimates of the annual rate of change in incidence rates for the SEER 13 registries for the years 1992-2007. During this time period, incidence rates for most cancers changed by less than 2% per year. Notable exceptions include liver cancer (> 6% per year increase from 1992-96), thyroid cancer (almost 6% per year increase from 1997-2007), and prostate cancer (about 11% per year decrease from 1992-1995). Thus, if these past trends are any indication, it is conceivable that after about 10 years, an update in baseline incidence rates alone could be responsible for a 50% or greater change in the LAR projection for one or more cancers. (It is beyond the scope of the report to speculate on changes in baseline mortality rates).

For calculating survival probabilities, 2000 decennial life tables (Arias 2008) were used instead of 1999 life tables as in BEIR VII.

Table 3-9: Changes in age-averaged cancer rates from 1992-2007 for the SEER 13 registries[1]

Cancer site	Average annual percent increase
Stomach	-1.4
Colon and Rectum	-2.2 (1992-95), 1.9 (1995-98), -2.6 (1998-2007)
Liver & Intrahepatic Bile Duct	6.4 (1992-96), 2.6 (1996-2007)
Lung (male)	-2.1
Lung (female)	0.6 (1992-98), -0.6 (1998-2007)
Bladder	0.1 (1992-2004), -1.5 (2004-2007)
Breast	1.1 (1992-99), -1.8 (1999-2007)
Prostate	-11.1 (1992-95), 2.0 (1995-2000), -2.3(2000-07)
Corpus and Uterus, NOS	0.6 (1992-97), -0.6 (1997-2007)
Cervix Uteri	-2.9
Ovary	-0.6 (1992-2001), -2.0 (2001-07)
Thyroid	3.0 (1992-97), 5.7 (1997-2007)
Leukemia	-0.1 (1992-2004), 2.1 (2004-2007)

[1] Abstracted from SEER Fast Stats (NCI 2011)

3.10 Combining Results from ERR and EAR Models

3.10.1 BEIR VII approach. BEIR VII calculates LAR values separately based on preferred EAR and ERR models and then combines results using a weighted geometric mean. More specifically,

$$LAR^{(B7)} = (LAR^{(R)})^{w*}(LAR^{(A)})^{1-w*} \quad (3\text{-}27)$$

where w* is the weight for the ERR model and depends on cancer site. If the weight (w*) equals 0.5, a simple GM would be calculated. Instead for most cancer sites, BEIR VII recommended a weight (w*) equal to 0.7 – placing somewhat more emphasis on results from ERR models. (A notable exception is lung cancer, for which the EAR model was given more weight. BEIR VII cited Pierce *et al.* (2003), who found a submultiplicative interaction between smoking and radiation in the A-bomb survivor data. Subsequently, Furukawa *et al.* (2010) reported that the submultiplicative interaction may be restricted to only heavy smokers.)

There are at least two problems with BEIR VII's use of the weighted GM. First, it is difficult to explain how a projection based on the GM should be interpreted. Second, the GM is not additive in the sense that: the GM of two risk projections for the combined effect of separate exposures is generally not equal

to the sum of the GM projections for the exposures. For these reasons, EPA has instead employed a weighted AM to combine ERR and EAR projections, which has a relatively straightforward interpretation and is additive.

3.10.2 EPA approach. We calculate the combined age-specific risk (at high dose rates) using a weighted arithmetic mean, so that:

$$M^{(EPA)}(D,e,a) = w^*[M^{(R)}(D,e,a)] + (1-w^*)[M^{(A)}(D,e,a)]\,, \tag{3-28}$$

and the LAR at exposure age e is calculated as before:

$$LAR(D,e) = \int_{e+L}^{110} M^{(EPA)}(D,e,a)\cdot S(a)/S(e)da\,. \tag{3-29}$$

In Eq. 3-28, $M^{(A)}$ and $M^{(R)}$ represent the age-specific EARs derived from the EAR and ERR models, respectively; *e.g.*, for incidence: $M_I^{(A)}(D,e,a) = EAR_I(e,a)D$, and $M_I^{(R)}(D,e,a) = ERR_I(e,a)D\cdot\lambda_I(a)$. It can be easily shown that:

$$LAR^{(EPA)}(D,e) = w^* LAR^{(R)}(D,e) + (1-w^*)LAR^{(A)}(D,e) \tag{3-30}$$

In general, the weighted arithmetic mean approach (Eq. 3-30) will always result in larger LAR projections than the BEIR VII approach based on the GM. However, as can be seen in Table 3-10, the difference is substantial only for sites such as stomach, liver, prostate, and uterine cancers, for which the LAR projection is sensitive to the model type (ERR vs. EAR). For all cancers combined (excluding nonfatal skin cancers), use of the weighted AM results in an LAR projection about 12% (males) or 6% (females) greater than the BEIR VII approach based on the GM.

Table 3-10: Comparison of EPA and weighted geometric mean (GM) method for combining EAR and ERR LAR projections for incidence[1,2]

Cancer Site	Sex	ERR Projection (A)	EAR Projection (B)	EPA Projection (C)	Weighted GM of A and B: (D)	Ratio: D/C
Stomach	M	15	171	62	31	2.01
	F	19	204	75	39	1.90
Colon	M	160	112	146	144	1.01
	F	103	67	92	91	1.02
Liver	M	17	92	40	28	1.40
	F	7.4	53	21	13	1.57
Lung	M	155	120	130	129	1.01
	F	485	233	308	290	1.06
Breast	F	Not used	289	289	289	1.00
Prostate	M	126	3.8	89	44	2.02
Uterus	F	11	50	23	18	1.30
Ovary	F	34	29	33	33	1.00
Bladder	M	107	75	97	96	1.01
	F	105	63	92	90	1.02
Thyroid	M	22	No model	22	22	1.00
	F	65	No model	65	65	1.00
Residual	M	275	196	251	248	1.01
	F	292	184	259	254	1.02
Kidney	M	26	21	24	24	1.00
	F	24	16	22	21	1.02
Leukemia	M	109	53	92	87	1.05
	F	86	32	69	63	1.09
Bone	M	No model	2.4	2.4	2.4	1.00
	F	No model	2.3	2.3	2.3	1.00
Total (excluding skin)	M			955	856	1.12
	F			1350	1270	1.06

[1] Cases per 10,000 person-Gy.
[2] Based on DDREF of 1.5 for sites other than leukemia and bone

3.10.3 A justification for the weighted AM. The weighted arithmetic mean approach can be justified by first expressing the age-specific lifetime excess risk for the U.S. as a weighted arithmetic mean of the relative risk and absolute risk model projections. One then assigns a subjective probability distribution to the weight (w), for which the expected value of the probability distribution is approximated by the BEIR VII nominal value ($\mathrm{E}[w] = w^*$). For any

such subjective distribution, the weighted arithmetic mean will be an unbiased estimate of the "true" excess risk.

More specifically, let w be an (unknown) parameter such that the (true) excess risk $M^{(true)}$ in the U.S. population is given by:

$$M^{(true)} = w\, M^{(R)} + (1- w)\, M^{(A)} \ . \tag{3-31}$$

It follows from Eq. 3-31 that:

$$w = \frac{M^{(true)} - M^{(A)}}{M^{(R)} - M^{(A)}}, \tag{3-32}$$

and if $0 \le w \le 1$, then $M^{(true)}$ is bounded by $M^{(A)}$ and $M^{(R)}$. A subjective probability distribution might be then assigned to the parameter (w) to reflect one's state of knowledge about the relationship between $M^{(true)}$, $M^{(A)}$ and $M^{(R)}$. For example, if one believes that either the ERR or EAR model is correct ***AND*** each model is equally plausible, then one would assign subjective probabilities of 0.5 to the corresponding values for w:

$$P(w=0) = 0.5;\ P(w=1) = 0.5$$

Alternatively, if the ERR model is more plausible than the EAR model, a larger probability would be assigned to the former: *e.g.,*

$$P(w=0) = 0.3;\ P(w=1) = 0.7.$$

On the other hand, $M^{(true)}$ may actually be intermediate between the excess rates calculated using the EAR and ERR models. If any such value is "equally likely," then the uniform distribution U(0,1) can be assigned to the parameter w. However, if the excess rates are more likely to be close to the rates predicted by, say, some type of average of the two risk models, then other choices, such as a trapezoidal distribution, Tr(a,b,c,d), might be more appropriate (see Figure 3-5). For both distributions shown in Figure 3-5, neither of the two risk models is "on average" closer to the truth, $E[w] = 0.5$, and the simple unweighted average ($w^* = 0.5$) would arguably still be the most reasonable approach.

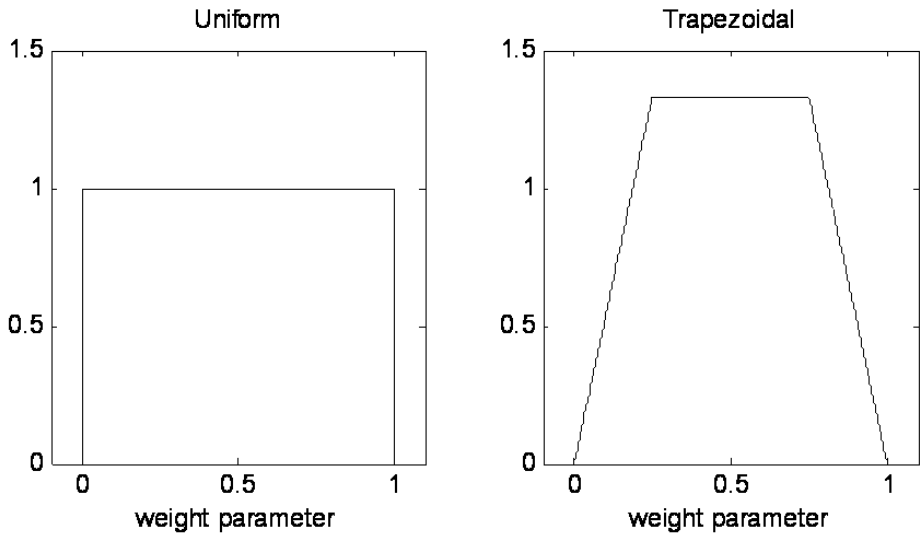

Figure 3-5: Examples of uniform [U(0,1)] and trapezoidal [Tr(0, 0.25, 0.75, 1.0)] distributions, which might be used for the risk transport weight parameter. Probabilities for the weight parameter are equal to areas under the curve.

The BEIR VII report stated that the choice of weight of 0.7, "which clearly involves subjective judgment, was made because mechanistic considerations… suggest somewhat greater support for relative risk transport projection, particularly for cancer sites (such as stomach, liver, and female breast) for which known risk factors act mainly on the promotion or progression of tumors." Although the BEIR VII committee did not explicitly specify a subjective distribution, any subjective distribution for the weight parameter for which E[w] is approximately 0.7 is arguably consistent with their conclusion. The simplest distribution with this property is the one for which:

$$P(w=0) = 0.3;\ P(w=1) = 0.7.$$

Another distribution for which $E[w] = 0.7$ is one that is U(0,1) with probability 0.5, $P(w=0) = 0.05$ and $P(w=1) = 0.45$. The latter distribution implies that there is a substantial probability (≈ 50%) that one of the two (ERR or EAR) methods for transport would yield a very close approximation to the truth, and, if so, the ERR is far more likely to be "correct." However, if neither model represents a good approximation, any LAR value within the interval bounded by the two projections would be equally plausible.

Note that for any subjective probability distribution for the parameter w,

$$E[M^{(true)}] = E[w]\, M^{(R)} + (1- E[w])\, M^{(A)}\ , \qquad (3\text{-}33)$$

and if $w^* = E[w]$, then the "true" value for excess risk will "on average" be equal to the weighted arithmetic mean. That is,

$$E[M^{(true)}] = w^*\, M^{(R)} + (1- w^*)\, M^{(A)}. \qquad (3\text{-}34)$$

3.11 Calculating Radiogenic Breast Cancer Mortality Risk

This section details our method for calculating radiogenic breast cancer mortality risk and compares results with calculations based on the BEIR VII method.

Let $M_I(D,e,a_I)$ denote the EAR for incidence at attained age a_I from an exposure at age e. If da represents an infinitesimally small age increment, the probability of a radiogenic cancer between ages a_I and (a_I + da) would be:

$$f_{D,e}(a_I)da = M_I(D,e,a_I)\,S(a_I)/S(e)da\,. \tag{3-35}$$

For the cancer to result in a death at age $a_M > a_I$, the patient would have to survive the interval (a_I, a_M), and then die from the cancer at age a_M. This and the concept of the relative survival rate form the basis for the method. The relative survival rate for a breast cancer patient would be the ratio of the survival rate for the patient divided by the expected survival rate (without breast cancer). Assume the relative survival depends only on the length of the time interval and the age of diagnosis. Let $t = a_M - a_I$, and let $R(t,a_I)$ be the relative survival function. Then the probability of survival with breast cancer for the interval (a_I, a_M) is $S(a_M)/S(a_I)R(t,a_I)$.

Suppose the breast cancer mortality rate (h) among those with breast cancer depends on the age of diagnosis but does not depend on other factors, such as whether the cancer is radiogenic, or on attained age. Then the probability of a radiogenic breast cancer death between ages a_M and (a_M + da) can be shown to equal:

$$f_{D,e}(a_M)da = \left(\frac{1}{S(e)} \int_{e+L}^{a_M} h(a_M)\,M_I(D,e,a_I)\,S(a_M)R(t,a_I)\,da_I \right) da\,. \tag{3-36}$$

The LAR for breast cancer mortality for an exposure at age e is:

$$LAR(D,e) = \int_{e+L}^{110} f_{D,e}(a_M)da_M\,, \tag{3-37}$$

and Eq. 3-38 is applied as before to calculate the LAR for the U.S. population.

$$LAR(D, stationary) = \frac{\int_0^{110-L} S(e) \cdot LAR(D,e) \cdot de}{\int_0^{110-L} S(e) de} \quad (3\text{-}38)$$

For these calculations, we used the 5-y relative survival rates given in Table 3-11 (Ries and Eisner, 2003) and assumed that breast cancer mortality rates (for those with breast cancer) depend only on age at diagnosis and are equal to:

$$h(a_I) = -(0.2) \log R(5, a_I) \quad (3\text{-}39)$$

It should be noted that results from several studies indicate that, for most stages, breast cancer mortality rates are not highly dependent on time since diagnosis – at least for the first 10 years (Bland *et al*. 1998, Cronin *et al*. 2003). Thus, for these calculations, we assumed that relative survival rates depend on time since diagnosis as in Eq. 3-40.

$$R(t, a_I) = \exp[-t \cdot h(a_I)] \quad (3\text{-}40)$$

Table 3-11: Female breast cancer cases and 5-y relative survival rates by age of diagnosis for 12 SEER areas, 1988-2001[1]

Age (y)	Cases	Relative Survival Rates (%)
20-34[2]	6,802	77.8
35-39	12,827	83.5
40-44	24,914	88.0
45-49	33,784	89.5
50-54	34,868	89.5
55-59	32,701	89.6
60-64	32,680	90.1
65-69	34,435	91.0
70-74	32,686	91.8
75-79	27,134	91.4
80-84	17,475	90.7
85+	12,457	86.6
Total	302,763	89.3

[1]Adapted from Table 13.2 in Ries and Eisner (2003)
[2]For ages of exposure < 20, 5-y relative survival rate of 77.8% was assumed.

Based on the method just outlined, the LAR for breast cancer mortality is 0.95×10^{-2} Gy^{-1}. This is about 30% larger than in BEIR VII. Much of the discrepancy between the two sets of results can be attributed to observed increases in breast cancer incidence rates and declines in mortality rates. From 1980 to 2000, age-averaged breast cancer incidence rates (per 100,000 women) increased by about 35% (102.2 to 136.0), whereas the mortality rates declined by about 15% (31.7 to 26.6) (Ries *et al*. 2008).

To understand the effect these trends in incidence and mortality have on the BEIR VII LAR projection for mortality, recall the BEIR VII formula:

$$M(D,e,a) = EAR(D,e,a)\frac{\lambda_M(a)}{\lambda_I(a)} \ . \qquad (3\text{-}41)$$

The underlying assumptions are that: a) the absolute risk of radiogenic cancer death from an exposure at age e is equal to the absolute risk of a radiation-induced cancer multiplied by a lethality ratio (that depends on attained age) and b) lethality ratios can be approximated by current mortality to incidence rate ratios. However, since the time between breast cancer diagnosis and death is relatively long, lethality rates might be better approximated by comparing current mortality rates to incidence rates observed for (much) earlier time periods. If, as data indicate, current incidence rates are considerably higher than in the past, the BEIR VII denominator is too large, and the estimated lethality ratio is too small. This would result in a downward bias in the BEIR VII projection for mortality.

Our projection has limitations which must be noted. First, its validity depends on the extent to which estimates of relative survival functions can be used to approximate mortality rates from breast cancer for people with breast cancer. Long-term survival rates for breast cancer patients are desirable for constructing valid estimates for this approach, but since these survival rates can change rapidly, there is considerable uncertainty in extrapolating rates for periods beyond 5-10 y. Finally, reduced expected survival among breast cancer patients may be partly attributable to causes other than breast cancer. For example, if some breast cancers are related to obesity, breast cancer patients as a group may be at greater risk of dying from cardiovascular disease.

3.12 LAR by Age at Exposure

Sex-averaged LAR for incidence and mortality by age-at-exposure are plotted in Figures 3-6 to 3-8 for selected cancer sites. More specifically, for both males and females, LAR is calculated as described in previously according to:

$$LAR(D,e) = \int_{e+L}^{110} M^{(EPA)}(D,e,a) \cdot S(a)/S(e)da \ , \qquad (3\text{-}42)$$

where

$$M^{(EPA)}(D,e,a) = w^*[M^{(R)}(D,e,a)] + (1-w^*)[M^{(A)}(D,e,a)]\ , \qquad (3\text{-}43)$$

and sex-averaged LAR were calculated using Eq. 3-44:

$$LAR_{AVG}(D,e) = \frac{1.048 S_{MALE}(e) LAR_{MALE}(D,e) + S_{FEMALE}(e) LAR_{FEMALE}(D,e)}{1.048 S_{MALE}(e) + S_{FEMALE}(e)}\ , \qquad (3\text{-}44)$$

where 1.048 is the ratio of the male to female births. Figures 3-6 to 3-8 show that, for most cancer sites, the probability of premature cancer (or cancer death) attributable to an acute exposure decreases with age-at-exposure. The notable exception is leukemia mortality, for which the projected LAR increases slightly from birth to about age 60.

For most cancers, the decrease in LAR with age-at-exposure is assumed to be similar to the pattern shown for colon, lung, and bladder cancers: the LAR decreases by a factor of about 2 or more from birth to age 30; it then levels off until about age 50 and then gradually decreases towards 0. The same type of relationship between LAR and age-at-exposure can be seen in Figure 3-9 for all cancers combined. During the first 30 y, the decrease in LAR is almost entirely attributable to the exponential decline in modeled age-specific ERR and EAR (in the risk models, $\gamma <$ -0.3), whereas the decrease in LAR after age 50 is largely attributable to competing risks – as people age, they have an ever-decreasing chance of living long enough to contract a radiation-induced cancer. For breast and thyroid cancers, the modeled age-specific ERR or EAR continue to decrease after age 30, and the LARs do not level off after age 30. In general, the LAR decreases more rapidly for breast, bone, thyroid, and residual cancers than for other sites. For thyroid cancer, the modest discontinuities evident in LAR at ages 5, 10, and 15 are an artifact of the categorization used for age-at-exposure in the thyroid risk model. Tables 3-12(a-c) and 3-13(a-c) provide sex- and age-at-exposure-specific LAR values by cancer site.

Risks for childhood exposures are often of special interest. As shown in Figures 3-6 through 3-8, for most cancer sites, the LAR per unit dose is substantially larger for exposures during childhood (here defined as the time period ending at the 15th birthday) than later on in life. In addition, doses received from ingestion or from inhalation are often larger for children than adults. Table 3-14 compares the average LAR per Gy for cancer incidence for exposures before age 15 to the average LAR for all ages. For uniform, whole-body radiation, the cancer risk coefficient (Gy^{-1}) is 1.16×10^{-1} for people of all ages. This compares to 2.60×10^{-1} for exposures before age 15. The corresponding risk coefficients for cancer mortality are 5.80×10^{-2} (all ages) and 1.15×10^{-1} (before age 15). Risks from childhood exposures, like those for adults, are generally greater for females

(3.29x10^{-1}, incidence; 1.47x10^{-1}, mortality) than for males (1.95x10^{-1}, incidence; 8.51x10^{-2}, mortality).

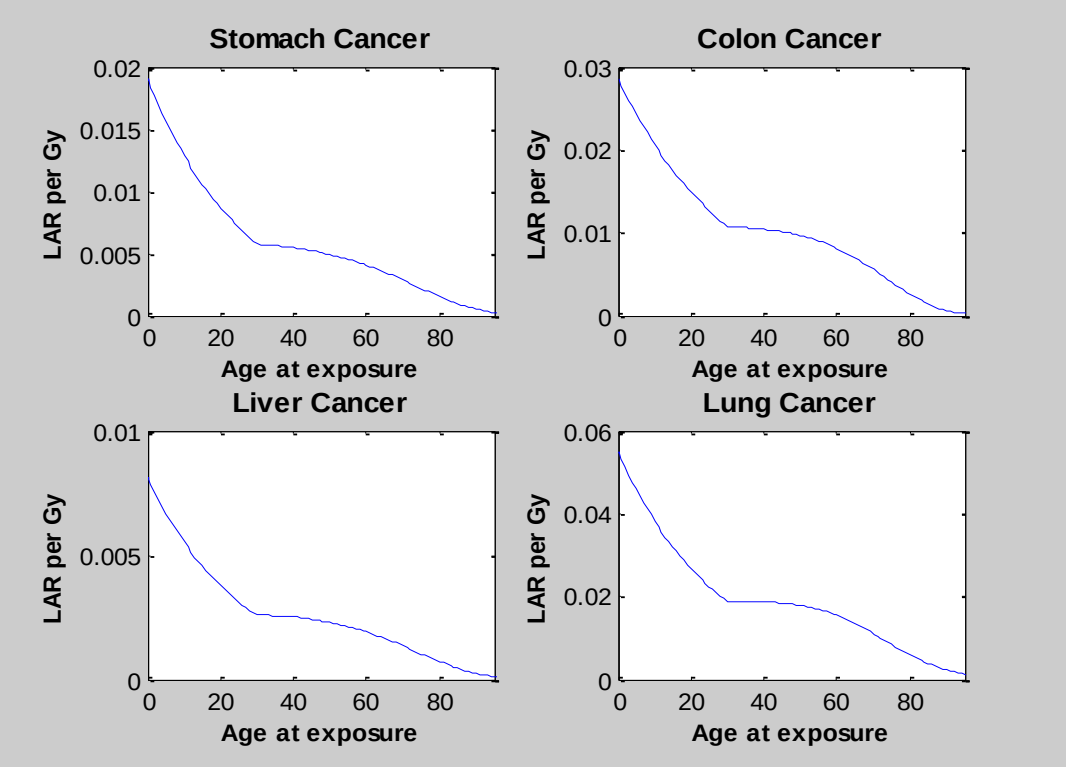

Figure 3-6(a): Sex-averaged LAR for incidence by age at exposure using a DDREF of 1.5

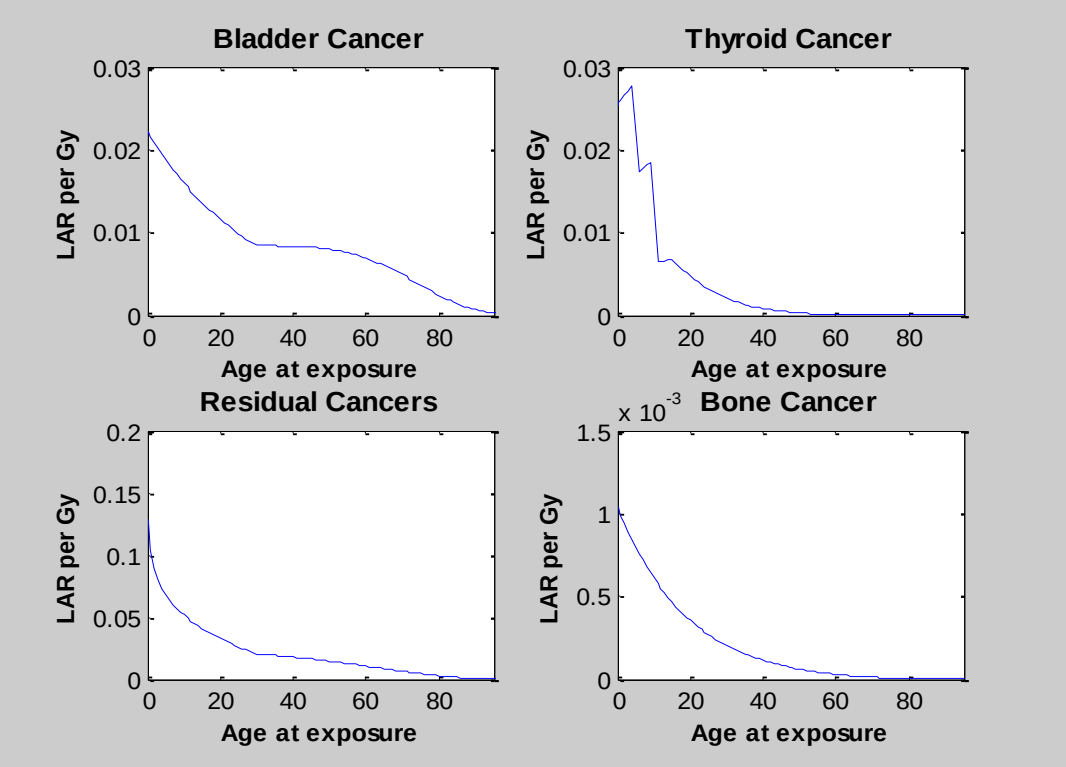

Figure 3-6(b): Sex-averaged LAR for incidence by age at exposure: DDREF = 1.5 except for bone cancer

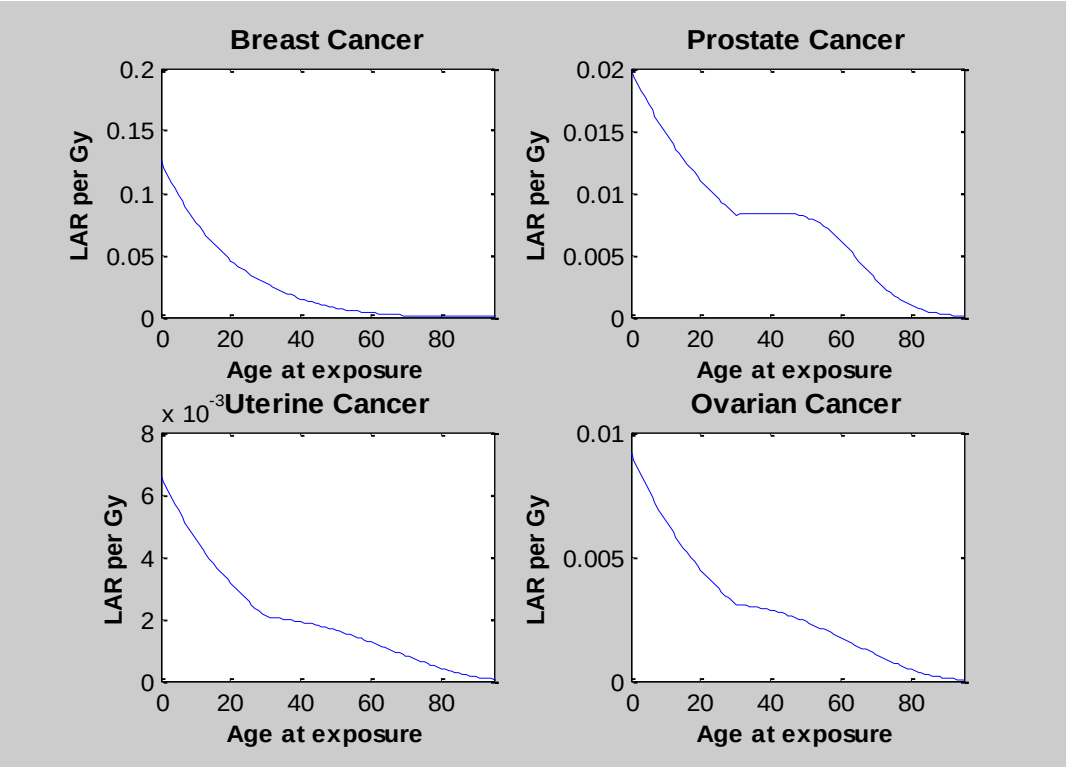

Figure 3-6(c): LAR for incidence by age at exposure using a DDREF = 1.5

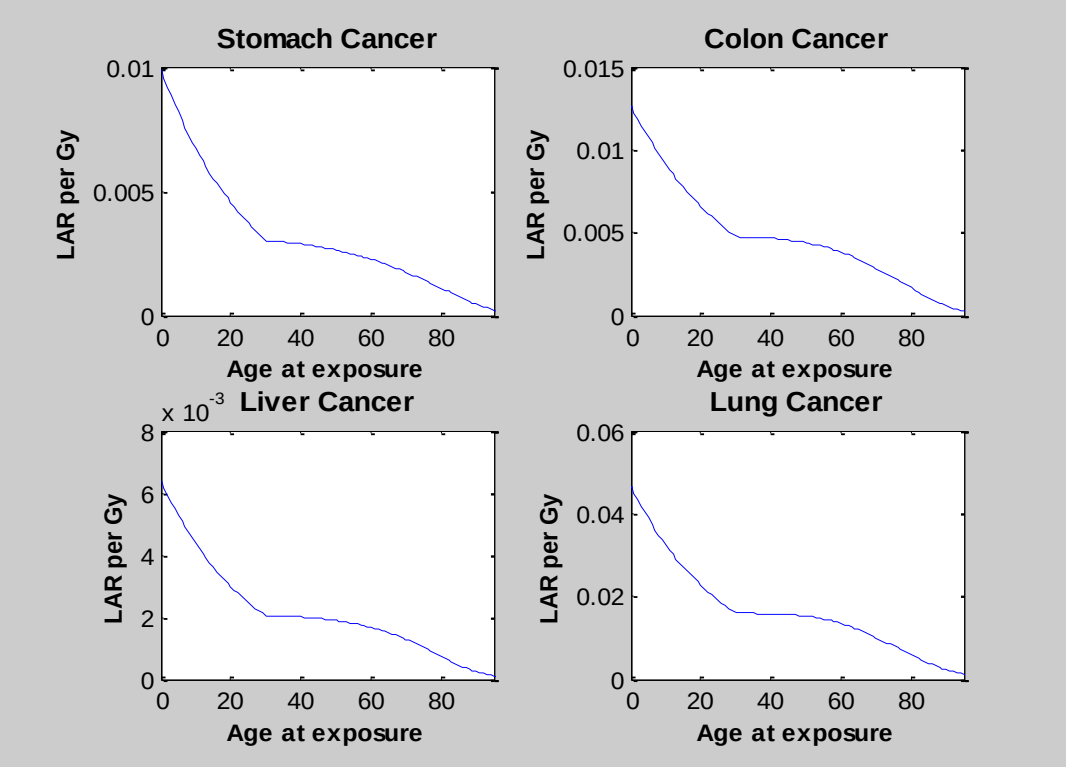

Figure 3-7(a): Sex-averaged LAR for mortality by age at exposure using a DDREF of 1.5

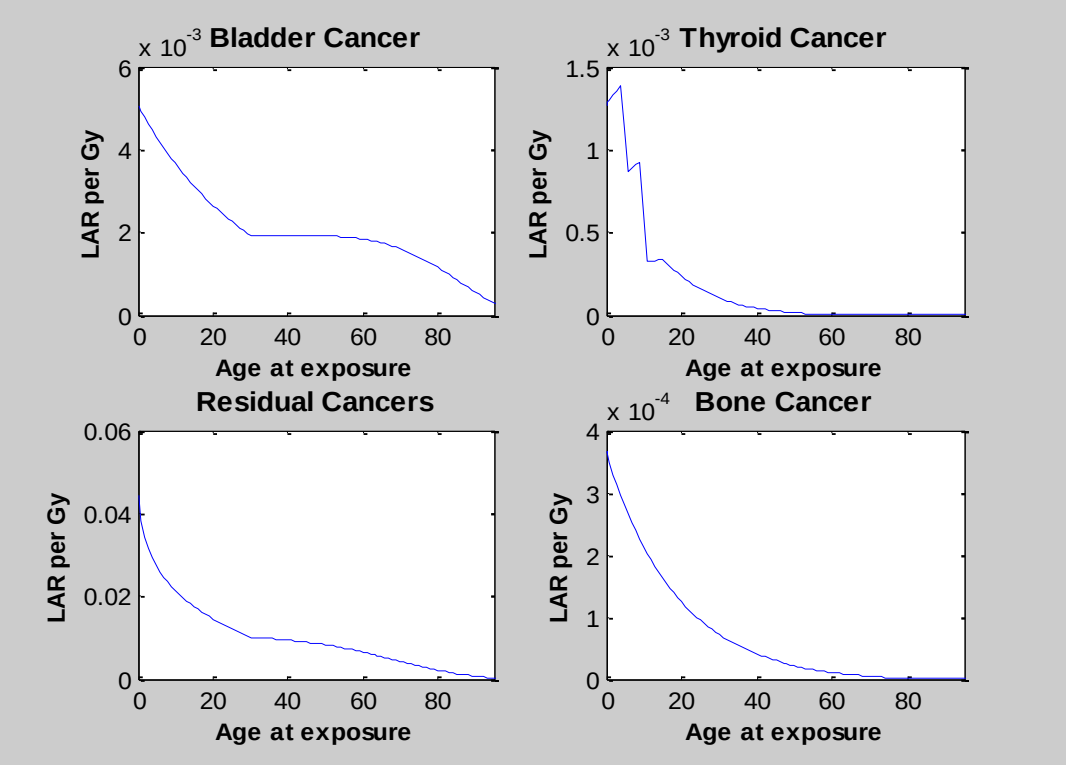

Figure 3-7(b): Sex-averaged LAR for mortality by age at exposure: DDREF=1.5 except for bone cancer

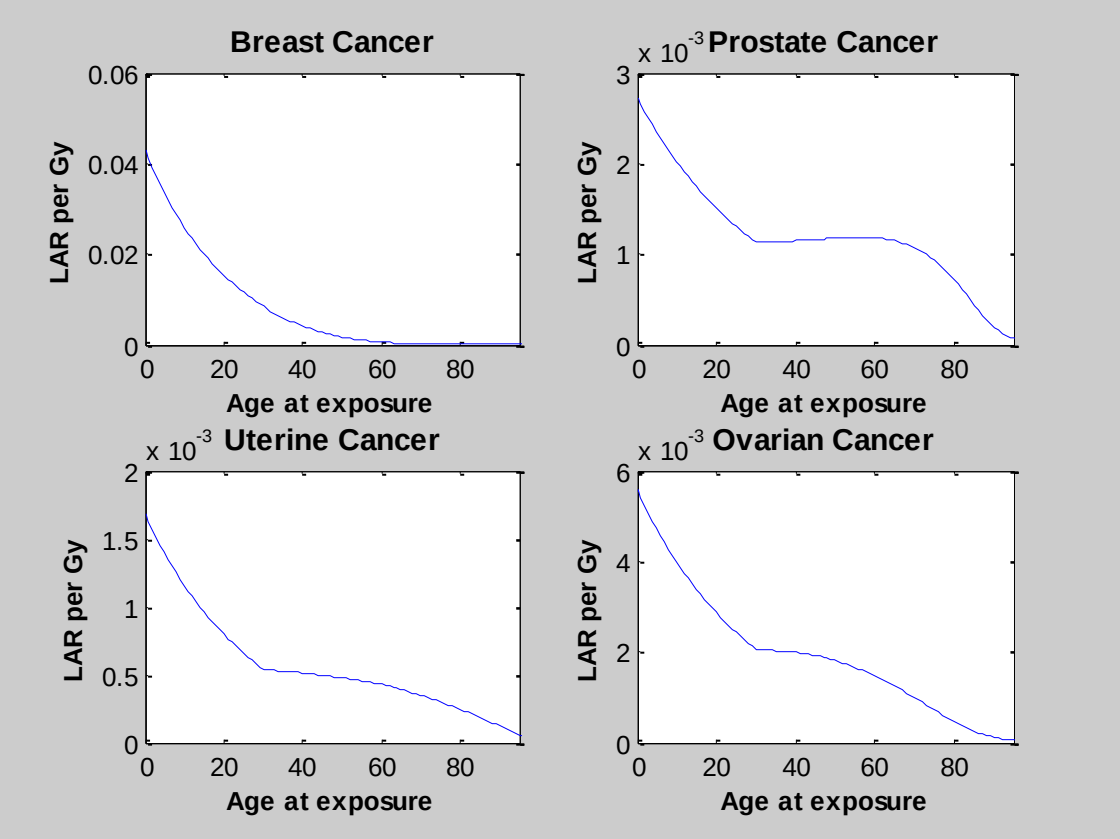

Figure 3-7(c): LAR for mortality by age at exposure using a DDREF of 1.5

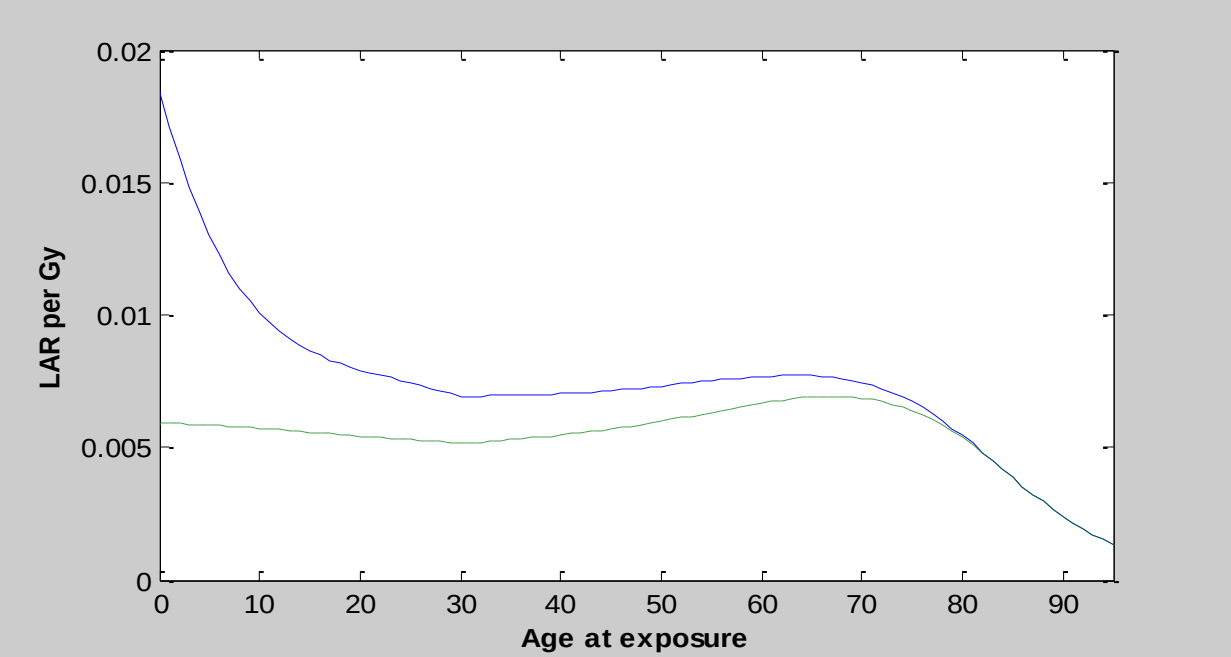

Figure 3-8: LAR by age at exposure for leukemia for incidence (solid) and mortality (dashed) using a DDREF of 1.5

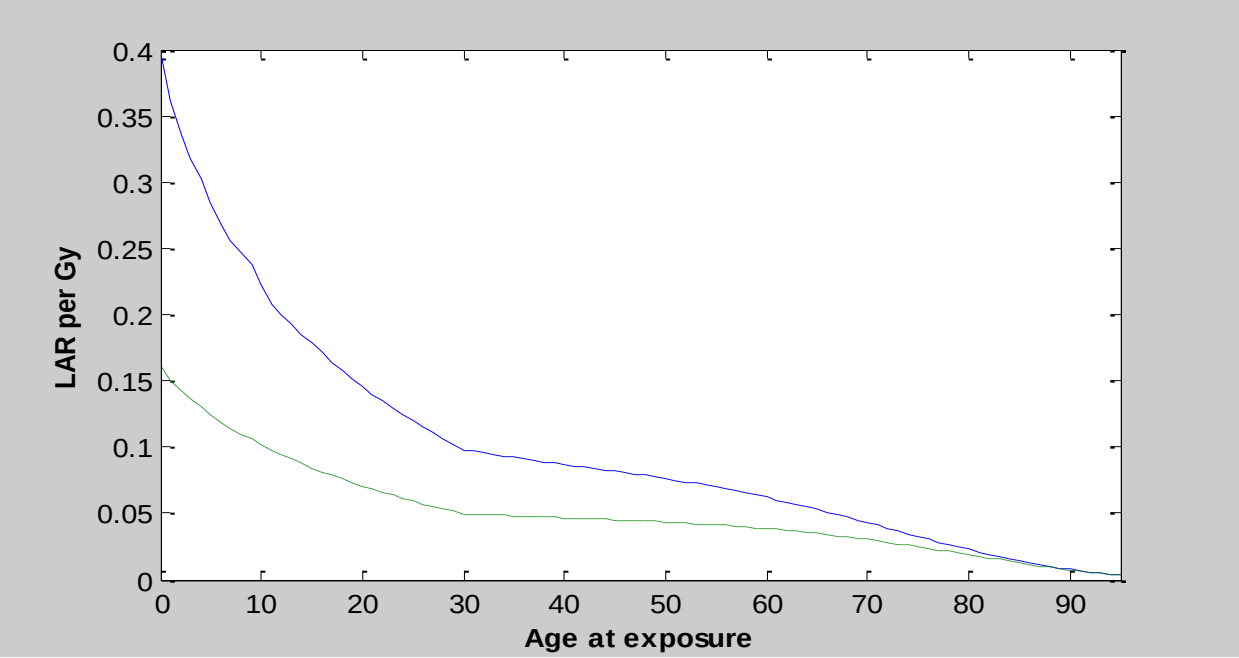

Figure 3-9: LAR for all cancers combined by age at exposure for exposures at low doses and/or dose rates for incidence (solid) and mortality (dashed)

Table 3-12a: LAR for cancer incidence[1,2] by age at exposure for males

	Age at exposure										
Cancer site	**0**	**5**	**10**	**15**	**20**	**30**	**40**	**50**	**60**	**70**	**80**
Stomach	168	139	114	94	77	51	48	43	35	24	12
Colon	342	292	248	210	179	129	126	117	97	65	29
Liver	103	86	71	59	49	34	33	29	24	17	9
Lung	320	268	222	185	154	108	107	104	90	65	35
Prostate	198	172	148	127	110	82	83	80	61	30	9
Bladder	219	188	159	135	116	84	84	81	71	50	24
Thyroid	123	107	58	32	23	11	5	2	1	0	0
Residual	1180	653	498	394	313	199	174	142	101	58	24
Kidney	102	55	44	37	31	22	20	16	11	6	2
Bone	10.4	8.0	6.1	4.6	3.5	2.0	1.1	0.6	0.3	0.1	0.0
Skin	1720	917	484	256	136	38	10	3	1	0	0
Solid[3]	2760	1970	1570	1280	1050	722	682	616	492	314	144
Leukemia	193	142	112	97	89	78	79	83	88	87	64
Total[3]	2950	2110	1680	1370	1140	801	761	699	580	402	208

[1] Cases per 10,000 person-Gy.
[2] DDREF of 1.5 for sites other than leukemia, bone, and skin
[3] Excludes nonfatal skin cancers

Table 3-12b: LAR for cancer incidence by age at exposure[1,2] for females

	Age at exposure										
Cancer site	**0**	**5**	**10**	**15**	**20**	**30**	**40**	**50**	**60**	**70**	**80**
Stomach	212	175	144	118	97	64	61	55	46	33	18
Colon	225	193	164	139	118	84	82	76	65	46	23
Liver	57	47	39	32	26	18	18	16	14	10	6
Lung	785	660	552	462	387	272	269	255	217	150	79
Breast	1260	982	761	588	454	265	146	72	32	12	4
Uterus	66	55	46	38	31	21	19	16	12	8	4
Ovary	91	77	64	53	45	31	28	24	17	11	5
Bladder	221	189	161	137	116	84	83	78	67	48	24
Thyroid	386	352	196	106	73	30	12	4	1	0	0
Residual	1410	707	534	422	336	213	184	151	112	69	31
Kidney	133	53	41	34	28	20	17	14	10	5	2
Bone	10.4	8.0	6.1	4.7	3.6	2.1	1.2	0.6	0.3	0.1	0.0
Skin	972	517	273	144	76	21	6	2	0	0	0
Solid[3]	4850	3500	2710	2130	1720	1100	920	764	594	393	195
Leukemia	173	117	88	75	69	60	61	63	65	63	47
Total[3]	5020	3620	2800	2210	1780	1160	981	827	659	456	242

[1] Cases per 10,000 person-Gy.
[2] DDREF of 1.5 for sites other than leukemia, bone, and skin
[3] Excludes nonfatal skin cancers

Table 3-12c: Sex-averaged LAR for cancer incidence[1,2] by age at exposure

	Age at exposure										
Cancer site	**0**	**5**	**10**	**15**	**20**	**30**	**40**	**50**	**60**	**70**	**80**
Stomach	190	157	129	106	87	58	55	49	41	29	15
Colon	285	244	207	175	149	107	104	97	81	55	26
Liver	81	67	55	46	38	26	25	23	19	13	7
Lung	547	459	383	320	268	188	187	179	154	110	60
Breast	614	480	372	288	222	130	72	36	16	6	2
Prostate	101	88	75	65	56	42	42	40	30	14	4
Uterus	32	27	22	18	15	10	9	8	6	4	2
Ovary	44	38	31	26	22	15	14	12	9	6	3
Bladder	220	188	160	136	116	84	83	80	69	49	24
Thyroid	252	227	126	68	47	21	8	3	1	0	0
Residual	1290	680	515	408	324	206	179	146	106	64	28
Kidney	117	54	43	36	30	21	19	15	10	6	2
Bone	10.4	8.0	6.1	4.7	3.5	2.0	1.1	0.6	0.3	0.1	0.0
Skin[3]	1360	722	381	201	106	30	8	2	1	0	0
Solid	3780	2720	2130	1700	1380	910	799	690	543	356	173
Leukemia	183	130	101	86	79	69	70	73	77	75	54
Total[3]	3970	2850	2230	1780	1460	979	870	763	620	430	227

[1] Cases per 10,000 person-Gy.
[2] DDREF of 1.5 for sites other than leukemia, bone, and skin
[3] Excludes nonfatal skin cancers

Table 3-13a: LAR for cancer mortality[1,2] by age at exposure for males

	Age at exposure										
Cancer site	**0**	**5**	**10**	**15**	**20**	**30**	**40**	**50**	**60**	**70**	**80**
Stomach	85	71	58	48	39	26	25	22	19	14	8
Colon	154	131	112	95	81	58	57	54	47	34	19
Liver	79	65	54	45	37	26	25	24	21	16	9
Lung	293	245	203	169	141	99	98	95	84	63	35
Prostate	27	24	20	17	15	11	11	12	12	11	7
Bladder	43	37	31	27	23	17	17	17	16	14	10
Thyroid	6.2	5.4	2.9	1.6	1.1	0.6	0.3	0.1	0.0	0.0	0.0
Residual	388	248	195	160	134	93	88	77	59	38	18
Kidney	26	18	15	12	10	7	7	6	5	3	1
Bone	3.6	2.8	2.1	1.6	1.2	0.7	0.4	0.2	0.1	0.0	0.0
Skin	0.5	0.3	0.1	0.1	0.0	0.0	0.0	0.0	0.0	0.0	0.0
Solid[3]	1110	847	693	576	482	338	329	307	262	192	108
Leukemia	65	65	65	63	61	58	61	67	76	80	63
Total[3]	1170	912	758	638	542	396	390	375	339	272	170

[1] Deaths per 10,000 person-Gy.
[2] DDREF of 1.5 for sites other than leukemia, bone, and skin

Table 3-13b: LAR for cancer mortality[1,2] by age at exposure for females

	Age at exposure										
Cancer site	**0**	**5**	**10**	**15**	**20**	**30**	**40**	**50**	**60**	**70**	**80**
Stomach	113	93	77	63	52	34	33	30	26	20	13
Colon	96	82	70	59	50	36	35	33	30	23	15
Liver	48	40	33	27	22	15	15	14	13	10	6
Lung	642	539	450	376	315	221	219	210	183	135	77
Breast	431	336	260	200	153	85	42	17	6	2	0
Uterus	17	14	12	10	8	5	5	5	4	3	2
Ovary	56	47	40	34	29	20	20	18	15	10	5
Bladder	58	50	42	36	30	22	22	22	21	18	13
Thyroid	19	18	10	5	4	2	1	0	0	0	0
Residual	498	301	233	190	157	108	100	88	70	48	24
Kidney	29	16	13	10	9	6	6	5	4	3	1
Bone	3.6	2.8	2.1	1.6	1.3	0.7	0.4	0.2	0.1	0.0	0.0
Skin	0.3	0.2	0.1	0.0	0.0	0.0	0.0	0.0	0.0	0.0	0.0
Solid	2010	1540	1240	1010	831	556	499	444	372	273	156
Leukemia	53	51	50	49	48	45	48	52	57	58	47
Total	2060	1590	1290	1060	878	601	547	496	429	331	203

[1] Deaths per 10,000 person-Gy.
[2] DDREF of 1.5 for sites other than leukemia, bone, and skin

Table 3-13c: Sex-averaged LAR for cancer mortality[1,2] by age at exposure

	Age at exposure										
Cancer site	**0**	**5**	**10**	**15**	**20**	**30**	**40**	**50**	**60**	**70**	**80**
Stomach	99	82	67	55	45	30	29	26	23	17	11
Colon	126	107	91	77	66	47	47	44	38	29	17
Liver	64	53	44	36	30	20	20	19	17	13	7
Lung	463	389	324	270	226	159	158	153	134	100	59
Breast	210	164	127	98	75	42	21	9	3	1	0
Prostate	14	12	10	9	8	6	6	6	6	5	3
Uterus	8	7	6	5	4	3	3	2	2	2	1
Ovary	27	23	20	17	14	10	10	9	7	5	3
Bladder	51	43	37	31	26	19	19	19	18	16	11
Thyroid	13	11	6	3	2	1	0	0	0	0	0
Residual	442	274	214	175	145	101	94	83	65	43	22
Kidney	27	17	14	11	10	7	6	6	4	3	1
Bone	3.6	2.8	2.1	1.6	1.2	0.7	0.4	0.2	0.1	0.0	0.0
Skin	0.4	0.2	0.1	0.1	0.0	0.0	0.0	0.0	0.0	0.0	0.0
Solid	1550	1190	961	789	652	445	413	375	318	234	135
Leukemia	59	58	57	56	54	52	55	60	67	69	54
Total	1610	1240	1020	845	707	497	468	435	384	303	189

[1] Deaths per 10,000 person-Gy.
[2] DDREF of 1.5 for sites other than leukemia, bone, and skin

Table 3-14: LAR for cancer incidence[1,2] for lifelong and childhood exposures

	Lifelong exposure			Exposures before age 15		
Cancer site	Males	Females	Sex-averaged	Males	Females	Sex-averaged
Stomach	62	75	68	128	161	144
Colon	146	92	119	272	179	227
Liver	40	21	30	79	43	62
Lung	130	308	220	247	611	425
Breast	—	289	146	—	885	433
Prostate	89	—	44	161	—	82
Uterus	—	23	12	—	51	25
Ovary	—	33	17	—	71	35
Bladder	97	92	95	175	176	175
Thyroid	22	65	44	81	265	171
Residual	251	259	255	616	675	645
Kidney	24	22	23	53	53	53
Bone	2.4	2.3	2.39	7.2	7.2	7.2
Skin	182	96	138	773	436	608
Solid[3]	863	1280	1080	1820	3180	2480
Leukemia	92	69	80	132	108	120
Total[3]	955	1350	1160	1950	3290	2600

[1] Cases per 10,000 person-Gy for a stationary population.
[2] DDREFof 1.5 for sites other than leukemia, bone, and skin
[3] Excludes nonfatal skin cancers

3.13 Summary of Main Results

New EPA LAR projections for incidence and mortality are given in Tables 3-15 and 3-16. The tables also provide 90% uncertainty intervals for the LAR. As described in Section 4, a 90% uncertainty interval would be any interval which contains the parameter of interest, *e.g.,* the LAR, with a probability of 0.90 – based on all that is known about the LAR from analyses of epidemiologic data and additional sources of information on how radiogenic risk depends on dose rate and other factors. The uncertainty intervals were calculated using Bayesian methods, which involved a somewhat complex (Markov Chain) Monte Carlo method for simulating site-specific LAR values. This approach allowed for the quantification of uncertainties associated with sources such as: 1) sampling variability, 2) transport of risk estimates from the Japanese A-bomb survivor population, 3) uncertainty associated with the DDREF, and 4) dosimetry errors.

Table 3-15: LAR projections for incidence[1,2]

	Males		Females		Sex-averaged	
Cancer Site	**LAR**	**90% UI**	**LAR**	**90% UI**	**LAR**	**90% UI**
Stomach	62	(8, 220)	75	(9, 220)	68	(9, 220)
Colon	146	(40, 230)	92	(37, 210)	119	(42, 220)
Liver	40	(6, 110)	21	(4, 88)	30	(6, 94)
Lung	130	(58, 320)	308	(95, 540)	220	(83, 420)
Breast	—	—	289	(140, 570)	146	(70, 290)
Prostate	89	(0, 410)	0	—	44	(0, 200)
Uterus	—	—	23	(0, 130)	12	(0, 65)
Ovary	—	—	33	(11, 82)	17	(5, 42)
Bladder	97	(27, 230)	92	(14, 130)	95	(24, 170)
Thyroid	22	(5, 54)	65	(21, 240)	44	(15, 140)
Residual	251		259		255	
Kidney	24	(99, 610)[3]	22	(120, 700)[3]	23	(120, 630)[3]
Bone	2.4		2.3		2.4	
(Skin)	182	—	96	—	138	—
Solid[4]	863	—	1280	—	1080	—
Leukemia	92	(27, 210)	69	(18, 160)	80	(29, 160)
Total[4]	955	(430, 1810)	1350	(650, 2520)	1160	(560, 2130)

[1] Cases per 10,000 person-Gy.
[2] DDREFof 1.5 for sites other than leukemia, bone, and skin
[3] Interval for residual, kidney and bone cancer cases combined
[4] Excludes skin cancers

Table 3-16: LAR projections for mortality[1,2]

	Males		Females		Sex-averaged	
Cancer site	**LAR**	**90% UI**	**LAR**	**90% UI**	**LAR**	**90% UI**
Stomach	32	(4, 110)	41	(5, 120)	36	(5, 120)
Colon	67	(18, 110)	41	(16, 94)	54	(19, 97)
Liver	31	(5, 83)	18	(4, 76)	25	(5, 77)
Lung	120	(54, 290)	255	(78, 450)	188	(72, 360)
Breast	0	—	95	(45, 190)	48	(23, 95)
Prostate	14	(0, 62)	0.0	—	6.8	(0, 31)
Uterus	—	—	6.4	(0, 36)	3.2	(0, 18)
Ovary	—	—	22	(7, 56)	11	(4, 28)
Bladder	20	(6, 48)	26	(4, 37)	23	(6, 40)
Thyroid	1.1	(0.3, 3)	3.2	(1, 12)	2.2	(0.7, 7)
Residual	110		125		117	
Kidney	8.3	(42, 260)[3]	7.0	(57, 330)[3]	7.7	(55, 280)[3]
Bone	0.9		0.8		0.8	
Skin	0.05	—	0.03	—	0.04	—
Solid[4]	404	—	639	—	523	—
Leukemia	65	(19, 150)	50	(13, 110)	57	(20, 110)
Total[4]	469	(230, 880)	689	(320, 1230)	580	(280, 1040)

[1] Deaths per 10,000 person-Gy.
[2] DDREFof 1.5 for sites other than leukemia, bone, and skin
[3] Interval for residual, kidney and bone cancer deaths combined
[4] Excludes skin cancers

For most cancer sites, BEIR VII derived parameter estimates for ERR and EAR models based on a statistical analysis of LSS data that was cross-classified by city, sex, dose, and intervals based on age-at-exposure, attained age, and follow-up time. Sampling variability refers to the uncertainty in parameter estimates associated with the variation in the observed numbers of cancer cases or deaths within each of these subgroups. In contrast to BEIR VII, our uncertainty analysis at least partially accounted for the sampling variability associated with the site-specific risk model parameters for age-at-exposure and attained age. Transport of risk estimate uncertainty refers to uncertainty associated with how to apply the results from the analysis of the Japanese LSS cohort data to the U.S. The ratio of LAR projections based on the EAR model divided by the projection based on the ERR model is a crude indicator of the magnitude of this uncertainty. It follows that “transport” uncertainty is greatest for sites such as stomach and prostate cancer, for which Japanese and U.S. baseline rates are vastly different.

A dominant source of uncertainty for all cancers combined is that associated with the value of the DDREF. This includes some of the uncertainty associated with the shape of the dose-response function at very low doses. As discussed in Section 4, it does not incorporate uncertainty associated with the validity of the assumption that the linear portion of the dose-response function fitted to the LSS data can be equated to the response that would be observed at lower doses or for chronic exposures. Additional sources of uncertainty, including dosimetry errors, were also incorporated into the uncertainty analysis. Details are provided in Section 4.

The new EPA risk projection is 955 cancer cases per 10,000 person-Gy for males, and 1350 cancer cases for females. The 90% uncertainty intervals suggest these projections are accurate to within a factor of about 2 or 3. Uncertainties, as measured by the ratio of the upper to lower uncertainty bounds, are greatest for stomach, prostate, uterine, bladder, liver, and thyroid cancers.

In the first four columns in Table 3-17, the new EPA risk projections for incidence are compared to risk projections in the current (1999) version of FGR-13. For all cancers other than esophagus, uterus, prostate, and residual site cancers (which are defined differently for the two sets of projections), the EPA risk projection for both males and females is about 35% higher than in FGR-13. Cancer sites for which the relative change from the projected LAR in FGR-13 is greatest include: female colon (↓), female lung (↑), female bladder (↑), kidney (↑), and liver (↑).

For the current version of FGR-13, the risk models were applied to 1989-1991 mortality data to first derive projections for radiogenic cancer mortality. For risk projections for cancer morbidity, the risk projections were then multiplied by the inverse of cancer specific lethality ratios. For example, for ovarian cancers, it was assumed that 70% of the radiogenic cancers would be fatal. The last two columns of Table 3-17 show what the new EPA risk projections would be if the new risk models were applied to baseline incidence rates derived from the same 1999-2001 mortality data used for FGR-13. These calculations indicate that the overall increase in LAR for incidence is due to both changes in the risk models (predominantly due to a reduction in the nominal DDREF for most cancer sites from 2 to 1.5) and, for most cancers, increases in the baseline rates (and survival probabilities) to which these models were applied. It is important to realize that the data on baseline rates are not strictly comparable, in that the data were derived from different sources (incidence data from SEER registries versus U.S. mortality data and lethality ratios), and that it is not appropriate to conclude that incidence rates actually increased for each of the cancers shown in Table 3-17.

Table 3-17: Comparison of EPA and FGR-13 LAR projections for incidence[1]

	New EPA		FGR-13 (1999)		New risk models applied to 1989-1991 mortality & lethality data	
Cancer site	**Males**	**Females**	**Males**	**Females**	**Males**	**Females**
Stomach	62	75	36	54	56	72
Colon	146	92	152	225	140	88
Liver	40	21	19	12	32	20
Lung	130	308	81	126	126	267
Breast	Not provided	289	Not provided	198	Not provided	287
Ovary	—	33	—	42	—	32
Bladder	97	92	66	30	49	59
Thyroid	22	65	21	44	19	29
Kidney	24	22	10	6	12	11
Bone	2.4	2.3	1.3	1.4	2	2
Leukemia	92	69	65	48	71	56
Sum of cancers listed above[2]	***615***	***1070***	***451***	***786***	***507***	***923***
Esophagus	Not provided	Not provided	7.7	17	No direct comparison for these sites	
Prostate	89	—	Not provided	—		
Uterus	—	23	—	Not provided		
Residual[3]	251	259	191	229		
Total[4]	***955***	***1350***	***651***	***1030***		

[1] Cases per 10,000 person-Gy for low dose and/or chronic exposures
[2] Excludes esophagus, prostate, uterine, and other "residual-site" cancers not specified here, and skin cancer. FGR-13 did not provide an LAR projection for nonfatal skin cancer incidence.
[3] Defined differently for new EPA projections and FGR-13.
[4] Excludes nonfatal skin

Table 3-18 gives the LAR projections for mortality. From the first four columns of results, the largest relative changes in LAR compared to the projections in FGR-13 were for female colon (↓), female lung (↑) and skin (↓) cancers. A comparison of results in the last four columns – derived using the same (1989-1991) mortality data – indicates that the effect of changes in the risk models, mostly associated with the DDREF, was to increase risk projections by about 20%. However, since the new EPA projections were based on mortality rates that tended to be smaller by almost the same percentage, the LAR for all

sites combined barely changed, *i.e.*, from 462 to 469 per 10,000 person-Gy for males and 683 to 689 for females.

Table 3-18 Comparison of EPA and FGR-13 LAR projections for mortality[1]

	New EPA		FGR-13		New risk models applied to 1989-1991 mortality data	
Cancer site	**Males**	**Females**	**Males**	**Females**	**Males**	**Females**
Stomach	32	41	33	49	50	64
Colon	67	41	84	124	77	49
Liver	31	18	18	12	31	19
Lung	120	255	77	119	120	254
Breast	Not provided	95	Not provided	99	Not provided	94
Ovary	—	22	—	29	—	22
Bladder	20	26	33	15	24	30
Thyroid	1.1	3.2	2.1	4.4	1.9	2.9
Kidney	8.3	7.0	6.4	3.9	8.0	7.3
Bone	0.9	0.8	0.9	1.0	0.9	0.8
Leukemia	65	50	65	47	69	55
Sum of cancers listed above[2]	***346***	***558***	***319***	***503***	***382***	***598***
Esophagus	Not provided	Not provided	7.3	16	No direct comparison for these sites	
Prostate	14	—	Not provided	—		
Uterus	—	6.4	—	Not provided		
Residual	109	125	135	163		
Skin	0.05	0.03	1.0	1.1		
Total	***469***	***689***	***462***	***683***		

[1] Deaths per 10,000 person-Gy for low dose and/or chronic exposures
[2] Excludes esophagus, prostate, uterine, skin, and "residual-site" cancers not specified here.
[3] Defined differently for new EPA projections and FGR-13.

Table 3-19 summarizes the sex-averaged LAR projections for cancer incidence and mortality. Table 3-20 compares the new EPA LAR projections with projections in BEIR VII. For some sites such as stomach, liver and prostate cancers, which have very different baseline rates in U.S. compared to Japan, the new EPA projections are substantially larger. This is due to EPA's adoption of the weighted arithmetic mean for combining results derived from ERR and EAR

models. For some other sites, in part because of our use of a stationary population, EPA's projections tended to be slightly smaller.

Finally, Table 3-21 provides estimates of LAR for a (non-stationary) population, in which the number of males and females at each age is based on the 2000 Census. Results given in this table are appropriate for assessing risks for certain types of exposures to mixed populations with demographics similar to the one targeted by the 2000 Census. Compared to the stationary population, the census population contains a somewhat larger proportion of younger people. Since projected radiogenic risks decrease with age-at-exposure, the LARs given in Table 3-21 are slightly larger than LARs given in other tables of this report for stationary populations. For example, the sex-averaged LAR for uniform whole-body dose is 1.24×10^{-2} Gy^{-1} for the census population as compared to the corresponding LAR of 1.16×10^{-2} Gy^{-1} given in Table 3-19.

Table 3-19: Sex-averaged LAR projections for incidence and mortality[1]

	Incidence		Mortality	
Cancer site	**Projection**	**90% UI**	**Projection**	**90% UI**
Stomach	68	(9, 220)	36	(5, 120)
Colon	119	(42, 220)	54	(19, 97)
Liver	30	(6, 94)	25	(5, 77)
Lung	220	(83, 420)	188	(72, 360)
Breast	146	(70, 290)	48	(23, 95)
Prostate	44	(0, 200)	6.8	(0, 31)
Uterus	12	(0, 65)	3.2	(0, 18)
Ovary	17	(5, 42)	11	(4, 28)
Bladder	95	(24, 170)	23	(6, 40)
Thyroid	44	(15, 140)	2.2	0.7, 7)
Residual	255		117	
Kidney	23	(120, 630)[2]	7.7	(55, 280)[2]
Bone	2.4		0.8	
Skin	138		0.04	
Solid	1080		523	
Leukemia	80	(29, 160)	57	(20, 110)
Total[3]	1160	(560, 2130)	580	(280, 1040)

[1] Cases or deaths per 10,000 person-Gy
[2] Interval for residual, kidney and bone cancer deaths combined
[3] Excludes nonfatal skin cancers

Table 3-20: Comparison of EPA and BEIR VII LAR calculations

		Incidence[1,2]		Mortality[1,2]	
Cancer site	**Sex**	**EPA**	**BEIR VII**	**EPA**	**BEIR VII**
Stomach	M	62	34	32	19
	F	75	43	41	25
Colon	M	146	160	67	76
	F	92	96	41	46
Liver	M	40	27	31	20
	F	21	12	18	11
Lung	M	130	140	120	140
	F	308	300	255	270
Breast	F	289	310	95	73
Prostate	M	89	44	14	9
Uterus	F	23	20	6.4	5
Ovary	F	33	40	22	24
Bladder	M	97	98	20	22
	F	92	94	26	28
Thyroid	M	22	21	1.1	None
	F	65	100	3.3	None
Residual	M	251	290	109	120
	F	259	290	124	132
Kidney	M	24	None	8.3	None
	F	22	None	7.0	None
Bone	M	2.5	None	0.9	None
	F	2.3	None	0.8	None
Solid cancers	M	863	800	404	410
	F	1280	1310	639	610
Leukemia	M	92	100	65	69
	F	69	72	50	52
Total	M	955	900	469	479
	F	1350	1382	689	662

[1] Cases or deaths per 10,000 person-Gy
[2] DDREF of 1.5 for sites other than leukemia

Table 3-21: LAR incidence and mortality projections for a population based on 2000 census data[1,2]

	Males		Females		Sex-averaged	
Cancer site	**Incidence**	**Mortality**	**Incidence**	**Mortality**	**Incidence**	**Mortality**
Stomach	66	34	80	43	73	39
Colon	156	71	98	43	127	57
Liver	42	33	22	19	32	26
Lung	138	127	327	269	234	199
Breast	0	0	316	104	160	53
Prostate	96	14	0	0	47	7.0
Uterus	0	0	25	6.7	12	3.4
Ovary	0	0	35	24	18	12
Bladder	103	21	98	27	100	24
Thyroid	24	1.2	70	3.5	48	2.4
Residual	273	118	279	133	276	126
Kidney	27	9.0	23	7.5	25	8.2
Bone	2.7	0.9	2.6	0.9	2.6	0.9
Skin	199	0	103	0	150	0
Solid[3]	928	429	1380	680	1150	556
Leukemia	93	64	71	50	82	57
Total[3]	1020	494	1450	730	1240	613

[1] Cases or deaths per 10,000 person-Gy.
[2] DDREFof 1.5 for sites other than leukemia, bone, and skin
[3] Excludes skin cancers

3.14 Comparison with Risk Projections from ICRP and UNSCEAR

This section compares the new EPA risk models to the risk models used in recent reports of the ICRP (2007) and UNSCEAR (2008). For most cancer sites, UNSCEAR and ICRP ERR and EAR risk models were derived from analyses of recent A-bomb survivor data with DS02 doses. As in BEIR VII, most ICRP models were based on 1958-1998 incidence data, whereas the UNSCEAR models were based on 1950-2000 mortality data. ICRP models were applied to a mix of Euro-American and Asian populations; the UNSCEAR models were applied to 5 populations (China, Japan, Puerto Rico, U.S., and United Kingdom).

3.14.1 ICRP risk models. For most cancer sites, the ICRP risk projections are based on an approach very similar to that used by both EPA and BEIR VII. For all three, an approximate LNT dose-response is assumed at very low doses and dose rates. ICRP projections were based on a weighted average of ERR and EAR risk model projections and a DDREF (of 2 instead of 1.5). For most sites, ICRP used a weight (w) of 0.5 for the ERR model; exceptions include breast, bone, and leukemia cancers (w=0), thyroid cancer (w=1), and lung cancer (w=0.3). In the ICRP risk models, the dose-response for most solid cancer sites is modified according to functions of age-at-exposure and attained age, which are of similar or identical form to those used here and in BEIR VII. In ICRP, the ERR and EAR for most solid cancer sites decrease with age-at-exposure by about 17% (ERR) or 24% (EAR) per decade (even beyond age 30); in BEIR VII, the per decade decrease for exposures before age 30 was somewhat steeper, typically 26% (ERR) or 34% (EAR), but there is no decrease in risk with age-at-exposure after age 30. A more detailed comparison of risk model parameter values for solid cancers is given in Table 3-22. ICRP has separate risk models for the most of the cancers with risk projections in this report. However, there is an ICRP model for esophageal cancer and none for kidney, prostate, or uterine cancers.

Table 3-23 compares LAR projections for the U.S. population – calculated using ICRP and EPA risk models and 1998-2002 incidence data. The EPA projections tend to be somewhat larger, although much of the difference can be attributed to the EPA's smaller nominal value for the DDREF (1.5 vs. 2). For the vast majority of sites, the ICRP and EPA risk projections are well within a factor of 2 of each other. Some of the largest differences are for lung, "other" solid (not directly comparable), kidney, and leukemia, but even these differences are small when compared to uncertainties associated with these risks. For leukemia, EPA's risk projection is larger because EPA assigns a larger weight (0.7 vs. 0.5) to its ERR model and baseline rates are higher in the U.S. than in Japan. ICRP risk projection for skin cancer (see Section 3.3) is much larger than EPA's.

Table 3-22: Comparison of ICRP (2007) and EPA risk model parameter values for solid cancers

	ERR Model				EAR Model			
	ICRP		EPA		ICRP		EPA	
	Linear Dose Response Parameter							
Cancer Site	β_M	β_F	β_M	β_F	β_M	β_F	β_M	β_F
Esophagus	0.52	0.84	None		0.33	0.46	None	
Stomach	0.30	0.49	0.21	0.48	4.6	6.4	4.9	4.9
Colon	0.88	0.43	0.63	0.43	4.0	1.7	3.2	1.6
Liver	0.32	0.52	0.32	0.32	2.9	0.9	2.2	1
Lung	0.37	1.8	0.32	1.4	3.4	4.7	2.3	3.4
Breast[1]	Not used				—	10	—	9.9
Prostate	None		0.12		None		0.11	
Uterus	None			0.055	None			1.2
Ovary		0.41		0.38		1.0		0.7
Bladder	0.86	1.42	0.5	1.65	0.75	1.0	1.2	0.75
Thyroid	0.53	1.05	See text		Not used			
Other solid	0.28	0.22	0.27	0.45	5.2	7.2	6.2	4.8
	Age-at-exposure: per decade % change in ERR or EAR 100(1-exp(γ))							
All but Esophagus, Breast, Bladder, Thyroid, Other solid	-17		-26 for age<30; 0 otherwise		-24		-34 for age < 30; 0 age ≥ 30	
Esophagus	-17		None		64		None	
Lung	17		-26 for age < 30; 0 otherwise		1		-34 for age < 30; 0 age ≥ 30	
Breast	Not used				-39		-40	
Bladder	-17		-26 for age <30; 0 otherwise		-11		-34 for age < 30; 0 age ≥ 30	
Thyroid	-56		See text		Not used			
Other Solid	-34		-26 for age < 30; 0 otherwise		-24		-26 for age < 30 0 age ≥ 30	
	Power of attained age by which EAR varies (η)							
All but Liver, Lung, Breast, Bladder, Thyroid, Other Solid	-1.65		-1.4		2.38		2.8	
Liver	-1.65		-1.4		2.38		4.1	
Lung	-1.65		-1.4		4.25		5.2	
Breast[1]	Not used				See text		See text	
Thyroid	0		0		Not used			
Bladder	-1.65		-1.4		6.39		6.0	
Other Solid	-1.65		-2.8		2.38		2.8	

[1] ICRP and EPA use essentially the same model for female breast cancer (see Section 3.2).

Table 3-23: Comparison of EPA and ICRP (2007) risk models: Projections of incidence for chronic exposures to the U.S. population[1,2]

	Males		Females	
Cancer	**ICRP**	**EPA**	**ICRP**	**EPA**
Esophagus	15[3]	No model	16[3]	No model
Stomach	48	62	74	75
Colon	100	146	46	92
Liver	32	40	13	21
Lung	87	130	207	308
Breast	—	—	230	289
Prostate	No model	89	—	—
Uterus	—	—	No model	23
Ovary	—	—	22	33
Bladder	65	97	50	92
Thyroid	16	22	83	65
Other Solid	157[3]	251	131[3]	259
Kidney	13	24	10	22
Bone	2.0	2.4	2.0	2.3
Leukemia	48[3]	93	36[3]	71
Skin	1000[3]	182	1000[3]	96

[1] Number of cases per 10,000 person-Gy
[2] "ICRP" projections for sites other than esophagus, leukemia and skin calculated using models summarized in Table 3-18, a DDREF of 2, 1998-2002 SEER incidence data, and 1999-2001 U.S. life table data
[3] ICRP projections for Euro-Asian population (ICRP 2007, Table A.4.14, p. 209)

3.14.2 UNCSCEAR risk models. Comparisons with the models used by UNSCEAR (2008) are somewhat more complicated than for ICRP. The form of the UNSCEAR ERR and EAR models depends on cancer site. For most cancer sites, the models found to best fit the A-bomb survivor cancer incidence data were LNT models for which radiogenic risk is modified only by attained age. For many other cancer sites, the slope of the dose-response is also modified by sex and/or TSE. In contrast to the BEIR VII models, age-at-exposure is seldom used as a dose effect modifier – exceptions are the EAR and ERR models for thyroid cancer and the ERR model for brain/CNS cancers. A summary of the UNSCEAR risk models is given in Table 3-24. For the risk transport problem, UNSCEAR did not recommend a method for combining site-specific ERR and EAR risk projections. Although a value for the DDREF was not formally adopted, it was noted that "values of DDREF of about 2, recommended by others *[e.g.*, ICRP], are consistent with…a large body of epidemiological and experimental data." UNSCEAR provided separate risk models for cancers of the esophagus, brain/CNS, bone, skin (nonmelanoma), and for all other BEIR VII cancer sites except prostate, uterus and ovary.

Table 3-24: Summary of UNSCEAR (2008) risk models for solid cancer incidence and leukemia mortality

Cancer	Dose Response	Effect Modifiers
Esophagus	Linear	None
Stomach	Linear	Attained age
Colon	Linear	ERR: Attained age EAR: TSE
Liver	Linear	ERR: None EAR: Attained age
Lung	Linear	ERR: Sex EAR: Sex, Attained age
Female Breast	Linear	ERR: Attained age EAR: TSE
Bladder	Linear	ERR: None EAR: Attained age
Brain and CNS	Linear	ERR: Age-at-exposure EAR: None
Thyroid	Linear	ERR: Age-at-exposure, Attained age EAR: Sex, Age-at-exposure
Leukemia	ERR Linear-quadratic[1] (Fit using Bayesian methods)	ERR: Attained age EAR: Sex, TSE
Bone	(Pure) quadratic	ERR: Attained age EAR: None
Skin	Quadratic-exponential[2]	ERR: TSE, Attained age EAR: TSE

[1] One of several alternative models for leukemia fit using Bayesian methods
[2] Product of quadratic and exponential functions of dose

Table 3-25 compares LAR projections for chronic exposures to the U.S. population – calculated using UNSCEAR and EPA risk models. The UNSCEAR ERR-model projection for all solid cancers combined is almost twice as large as the corresponding EPA projection. However, much of this difference is due to the much larger UNSCEAR projection for breast cancer, which in contrast to EPA's projection, was based entirely on an analysis of A-bomb survivor data. Although the models are often of quite different form, the UNSCEAR and EPA EAR risk projections are often remarkably consistent, with almost identical projections for all solid cancers combined: 1.17×10^{-1} (UNSCEAR) vs. 1.04×10^{-1} (EPA). However, this last observation may be a bit misleading, since for the UNSCEAR projections there was no explicit DDREF adjustment, and EPA applies a DDREF of 1.5 for most cancer sites. Finally, we note that EPA's projections for skin cancer risk are larger than UNSCEAR's (see Section 3.3).

Table 3-25: EPA and UNSCEAR (2008) sex-averaged cancer incidence risk projections from chronic exposures to the U.S. population[1,2]

Cancer site	ERR		EAR	
	UNSCEAR	EPA	UNSCEAR	EPA
Esophagus	23	No model	5	No model
Stomach	20	17	249	188
Colon	174	132	152	89
Liver	18	12	73	72
Lung	441	322	202	177
Breast	638	No model	141	146
Prostate	No model	62	No model	1.9
Uterus	No model	6	No model	25
Ovary	No model	17	No model	15
Bladder	184	106	81	69
Thyroid	118	44	86	No model
Other Solid	408	283	165	190
Kidney	No model	25	No model	18
Bone	2	2.4	0	2.4
Brain/CNS	32	No model	17	No model
Skin	36	138	1	No model
Solid Total[3]	2095	1180[4]	1171	1040[5]
Leukemia	55[6]	97	Not used	42
Total[3]	2150	1280[4]		1080[5]

[1] Number of cases per 10,000 person-Gy
[2] UNSCEAR (2008) solid cancer projections (Table 70, p. 254) for test doses of 0.01 Sv
[3] Does not include skin cancer
[4] Based on EAR projections for bone and breast cancer and ERR projections for all other sites
[5] Based on ERR projection for thyroid cancer and EAR projections for all other sites
[6] Mortality risk (deaths per 10,000 person-Gy) from Table 66 in UNSCEAR (2008) for a test dose of 0.01 Gy, and based on a model fit using Bayesian methods. UNSCEAR did not provide risk projections for leukemia incidence.

4. Uncertainties in Projections of LAR for Low-LET Radiation

4.1 Introduction

This chapter describes uncertainties relating to the LAR projections given in Section 3. After a brief description of sources of uncertainty (Section 4.2), a simple analysis is presented to gain insight as to how large the uncertainties might be for three of the most important sources: sampling errors in the epidemiological data underlying the risk models, the DDREF, and risk transport of the radiogenic risks estimated from the cohort of Japanese A-bomb survivors to the U.S. population. In this initial examination of uncertainties, the LAR is calculated for ranges of "plausible" values for parameters in the ERR model, the DDREF, and the weight assigned to the ERR model. Each parameter is varied in sequence (one-at-a-time), while other parameters are set to nominal values, and the corresponding range of LAR values is examined using graphical methods. (In this Section, the term *nominal* value refers to the value for a parameter used in Section 3 for calculating projections of radiogenic risk: *e.g.,* for most cancer sites, the nominal values are -0.3 for the age-at-exposure parameter and 1.5 for the DDREF).

As discussed in Section 4.3, results indicate that for some cancers (*e.g.,* bladder cancer) the (sampling) uncertainty associated with the linear dose-response parameter dominates, whereas for others (*e.g.,* stomach cancer, for which baseline rates are much larger in Japan than in the U.S.) uncertainty associated with risk transport is greatest. Colon cancer is an example for which the DDREF is one of the most important sources of uncertainty, whereas for prostate cancer, the uncertainty associated with both risk transport and sampling errors are especially large. A problem with the simple approach is that it does not adequately account for the combined effect of uncertainties associated with several parameters.

In Section 4.4, a more sophisticated Monte Carlo approach is introduced, which generates 90% uncertainty bounds associated with the sex- and cancer site-specific LARs. The approach is similar to those used elsewhere, *e.g.,* for the Interactive RadioEpidemiological Program (IREP, see Kocher *et al.* 2008). Probability distributions are assigned to parameter values associated with each of several relevant sources of uncertainty, and Monte Carlo methods are used to generate uncertainty bounds for quantities of interest. In our application of Monte Carlo, the joint probability distribution of parameter values associated with the ERR model and non-sampling sources of uncertainty are simulated through repeated random sampling. Then, sex- and site-specific LAR values are calculated for each set of simulated parameter values, and 90% uncertainty bounds are equal to the 5^{th} and 95^{th} percentile values of the simulated LAR values.

The fundamental difference between this approach and IREP's is that a formal Bayesian analysis is used here to approximate probability distributions

associated with sampling variability. First, initial (prior) subjective probability distributions were assigned to each parameter in the risk models, *i.e.,* the linear dose-response parameter (β), age-at-exposure parameter (γ), and attained-age parameter (η). Then, information on radiogenic risks from the LSS data was applied to update these distributions. The Bayesian analysis of the LSS data is described in Section 4.4 and in more detail in Appendix B. A Bayesian approach for evaluating uncertainties in risk projections has also been used for the UNSCEAR 2006 report (Little 2008).

For most cancer sites, the risk models used for this uncertainty analysis are the same ERR models that BEIR VII fit to the LSS data. However, there are two important differences between the two approaches. First, BEIR VII used classical statistical methods to derive "best" estimates for the parameters which describe how ERR depends on dose, age-at-exposure and attained age. In contrast, we assigned (prior) probability distributions to these parameters and then applied information gleaned from the LSS to update these distributions. Second, for most sites, our Bayesian analysis placed fewer restrictions than BEIR VII on the parameters for age-at-exposure and attained age.

Section 4.5 presents the main results of the quantitative uncertainty analysis – uncertainty bounds summarizing the distributions for LAR, which reflect both sampling and non-sampling sources of uncertainty. A comparison with BEIR VII's quantitative uncertainty analysis is given in Section 4.6. BEIR VII used a non-Bayesian approach, which for most cancer sites produced results not unlike ours. Although the BEIR VII uncertainty analysis has many desirable features, it has several limitations which prompted us to consider an alternative approach. Most notably, only uncertainties associated with sampling variation, DDREF, and risk transport were quantified, and the non-Bayesian approach does not ensure that results will be internally consistent; *e.g.,* BEIR VII's upper bound for prostate cancer LAR is almost as large as the upper bound for all male cancers combined.

Conclusions are given in Section 4.7. Foremost among them is that the results of the analysis – the uncertainty distributions for the LAR summarized in Section 4.5 – should not be over-interpreted. Results may be sensitive to distributions which are subjectively assigned to sources of uncertainty (*e.g.*, risk transport), and not all sources of uncertainty can be quantified. Results of the uncertainty analysis are meant primarily as guidance as to the extent to which "true" site-specific risks for a hypothetical stationary U.S. population might differ from the central estimates derived in Section 3.

4.2 Sources of Uncertainty Quantified in this Report

We quantified uncertainties associated with sampling variability, DDREF, risk transport, errors in dosimetry, risk model misspecification, selection bias, and errors in disease detection and diagnosis.

Sampling variability. BEIR VII derived parameter estimates for most of its ERR and EAR models from a statistical analysis of LSS solid cancer cases and leukemia deaths, which were cross-classified by city, sex, dose, and intervals based on age-at-exposure, attained age, and follow-up time. Here, sampling variability refers to the uncertainty in parameter estimates associated with the variation in the observed numbers of cancer cases or deaths in each of the subcategories. For solid cancers, this includes uncertainties in parameters for the linear dose-response (β), and its modification by age-at-exposure (γ) and attained-age (η), but it does not include uncertainty relating to the shape (curvature) of the dose-response.

DDREF. The dose and dose rate effectiveness factor was described in Section 3.6. The uncertainty in the DDREF refers to problems associated with extrapolating results on risks from studies of acute exposures and relatively large doses to risks at low dose and dose rates. We adopted the BEIR VII nominal value of 1.5, which was based on the curvature in the dose response observed in data from the LSS and animal carcinogenesis studies. Uncertainty in the BEIR VII DDREF estimate is due, in part, to the effect of sampling errors on estimates of curvature.

***Risk transport*.** This refers to the uncertainty in projecting risks to the U.S. population using risk models derived from the Japanese A-bomb survivor data. The uncertainty is due to lack of knowledge as to how radiogenic risks in the Japanese cohort and the U.S. may differ.

The BEIR VII ERR models would be appropriate if radiogenic risks are proportional to baseline rates. Likewise, the EAR model may be a reasonable alternative if radiogenic risks are unrelated to baseline rates. For most sites, it is plausible that projections based on some combination of the two models would yield better approximations of risk. EPA's nominal risk projections are weighted averages of ERR and EAR model-based projections. Here, risk transport uncertainty is confined to the problem of assigning site-specific weights (among competing plausible values) to the ERR risk model projections.

Incomplete follow-up. This uncertainty refers to the lack of any direct information on risks for TSE outside the period of follow-up. For most solid cancer sites, risk estimates were derived from data on cancers in the A-bomb survivor cohort that occurred between 1958 and 1998. Thus, estimates of solid cancer risks for TSE outside the interval (13y, 53y) must necessarily be based on extrapolation. Models are fit to the data that best describe how ERR and EAR depend on factors such as age-at-exposure and attained-age within the period of follow-up. One then assumes that these age-related patterns hold for TSE beyond the follow-up. Incomplete follow-up uncertainty is the uncertainty in risk projections associated with these underlying assumptions.

***Errors in dosimetry*.** This refers to uncertainty in estimates of ERR and EAR, and ultimately projections of risk, that result from errors in doses assigned to the A-bomb survivors in the LSS cohort. The RERF report on DS02 (Kaul *et al.* 2005) divides such dosimetry uncertainties into two broad categories: systematic and random. "Systematic" refers to "the likelihood that doses to all individuals at a given city will increase or decrease together [from imperfectly or unknown effects]," whereas "random" refers to effects on individual survivor doses that act more or less independently. Examples of systematic uncertainties are those relating to the yields, neutron outputs, and burst heights, as well as the air transport calculation method. Examples of random uncertainties are those relating to survivor location and inputs needed to estimate shielding for individual survivors. Both systematic and random uncertainties in dose estimates can lead to bias in parameter estimates in the ERR and EAR models. Random errors will tend to decrease the precision of estimates and can also have an effect on the shape of the dose-response.

Errors in disease detection and diagnosis. Types of diagnostic misclassification that can occur include classification of cancers as non-cancers (detection error) and erroneous classification of non-cancer cases as cancer (confirmation error). The former leads to an underestimate of the EAR but does not affect the estimated ERR. Conversely, the latter leads to an underestimate of the ERR but does not affect the EAR (EPA 1999a). Errors can also occur in the misclassification of sites where cancers originate.

Selection bias in the LSS cohort. This refers to the possibility that risk estimates derived from the LSS are biased downward because members of the cohort, by being able to survive the bombings, demonstrated a relative insensitivity to radiation.

4.3 "One-at-a-Time" Uncertainty Analysis

In this section, the LAR is calculated for ranges of "plausible" values (95% CI) for parameters in the ERR models, the DDREF, and the weight assigned to the ERR model. (A more sophisticated uncertainty analysis, which accounts for additional sources of uncertainty is presented in Section 4.4). Each parameter is varied in sequence (one-at-a-time), while other parameters are set to nominal values, and the corresponding range of LAR values is examined using graphical methods. We start by examining how LAR for a solid cancer site (using stomach cancer as an example) depends on sampling variability associated with parameters for linear dose-response (β), age-at-exposure (γ), and attained age (η) in the ERR model:

$$ERR(D,e,a) = \beta D \exp(\gamma e^*)(a/70)^{\eta} \quad . \tag{4-1}$$

It is helpful to note that in Equation 4-1, β is the ERR per Gy for age-at-exposure 30 and attained-age 70, and $\exp(\gamma)$ is the increase in ERR per decade increase in age-at-exposure (for e < 30). LAR projections for plausible values of each parameter are then calculated using the methods described in Section 3, as is shown next.

First, for any value of the linear dose-response parameter (β), and nominal values for the other parameters (γ_0 = -0.3 and η_0 = -1.4), the estimate of the LAR from an exposure (D) at age e is:

$$LAR^{(R)}(D,e,\beta) = \int_{e+L}^{110} M(D,e,a,\beta)\cdot S(a)/S(e)da$$

$$= \int_{e+L}^{110} \beta D \exp(-0.3e^*)(a/70)^{(-1.4)}\cdot S(a)/S(e)da \qquad (4\text{-}2)$$

Using the nominal DDREF value of 1.5, the corresponding estimate of risk for a lifelong chronic exposure is:

$$LAR^{(R)}(D,\beta,stationary) = \frac{\int_0^{110-L} S(e)\cdot LAR^{(R)}(D,e,\beta)\cdot de}{1.5\int_0^{110-L} S(e)de} \qquad (4\text{-}3)$$

The projection given in Equation 4-3 is based on the ERR model only. As described in Section 3, EPA's (final) risk projections are weighted averages of ERR *and* EAR risk projections. Analogously, we scale the ERR model-based projection by a constant, which depends on EPA's nominal EAR and ERR model-based projections and the weight assigned to the ERR model. For male stomach cancer these are (per 10,000 person-Gy): 15 (ERR model) and 171 (EAR model), so that for the nominal weight of 0.7, EPA's risk projection is 0.7(15) + 0.3(171) = 62. Thus, for stomach cancer, a reasonable scaling parameter would be 4.1 (=62/15). (Note that this scaling factor is larger for stomach cancer than for other cancers because, unlike most other cancers, baseline stomach cancer rates are much greater in Japan than in the U.S.). Thus for any value of the ERR weight parameter (w), the LAR is approximated as:

$$K(w,sex,site)\times LAR^{(R)}(D,\beta,stationary), \text{ with}$$
$$K(w,male,stomach) = \frac{w(15)+(1-w)(171)}{15} \qquad (4\text{-}4)$$

The top-left panel in Figure 4-1(a) shows how values for the LAR (based on Equation 4-4) for both male and female stomach cancer depend on the linear

dose-response parameter (β). For males, plausible values of β are between 0.1 to 0.25, and the LAR ranges from about 15 to 60 (cancers per 10,000 person-Gy). The corresponding range for females is somewhat narrower (about 25 to 60); there are more females than males in the LSS, and thus, for many sites, less sampling variation.

The top-middle panel shows how values for LAR depend on parameters for age-at-exposure (γ). First, note that for stomach cancer, γ is likely between about 0 and -0.5, *i.e.*, ERR may be independent of age-at-exposure or, alternatively, decrease by as much as 40% per decade (at γ=-0.5) with age-at-exposure < 30. (At γ near -0.5, radiogenic risk would be almost 3 times as large at age 0 as at age 30). In Figure 4-1(a), it is seen that the LAR for male stomach cancer risk can vary from about 80 (γ about -0.5) to less than 50 ($\gamma \approx 0$). For females, the corresponding range is from about 90 to less than 60. These are about half the width of the ranges for LAR associated with the linear dose-response variable (β), which suggests that there may be more uncertainty in LAR associated with β than there is with γ.

The rightmost panel shows ranges of LAR values for the attained age parameter. A comparison with results from the other panels (for β and γ) indicates that uncertainty in LAR associated with attained age is relatively small.

The bottom panels in Figure 4-1(a) provide results on how LAR for childhood (ages < 15) exposures depend on the same three ERR parameters. (The results were generated in exactly the same manner as above, except that in Eq. 4-3 the integration is from age 0 to 15). Here, the uncertainty associated with the age-at-exposure parameter (γ) is much greater than seen before (for lifelong exposures), and is comparable to the uncertainty associated with β.

Figures 4-1(b)-(d) show the dependence of LAR on the ERR parameters for three other sites: liver, lung, and bladder. The graphs for these sites share many of the characteristics already noted. In general, for lifelong exposures, uncertainty appears greatest for the linear dose-response parameter; for childhood exposures uncertainty in LAR associated with age-at-exposure is also large. A comparison of figures for the four cancer sites indicates that the variation in LAR is much larger for bladder cancer than for the other cancers. This is not surprising since in the LSS dataset there were only 342 bladder cancers as compared to 1146 liver, 1344 lung, and 3602 stomach cancers. For bladder cancer, the LSS provides very little information on how ERR depends on age-at-exposure or attained age, and the uncertainty in LAR associated with all three ERR parameters is large.

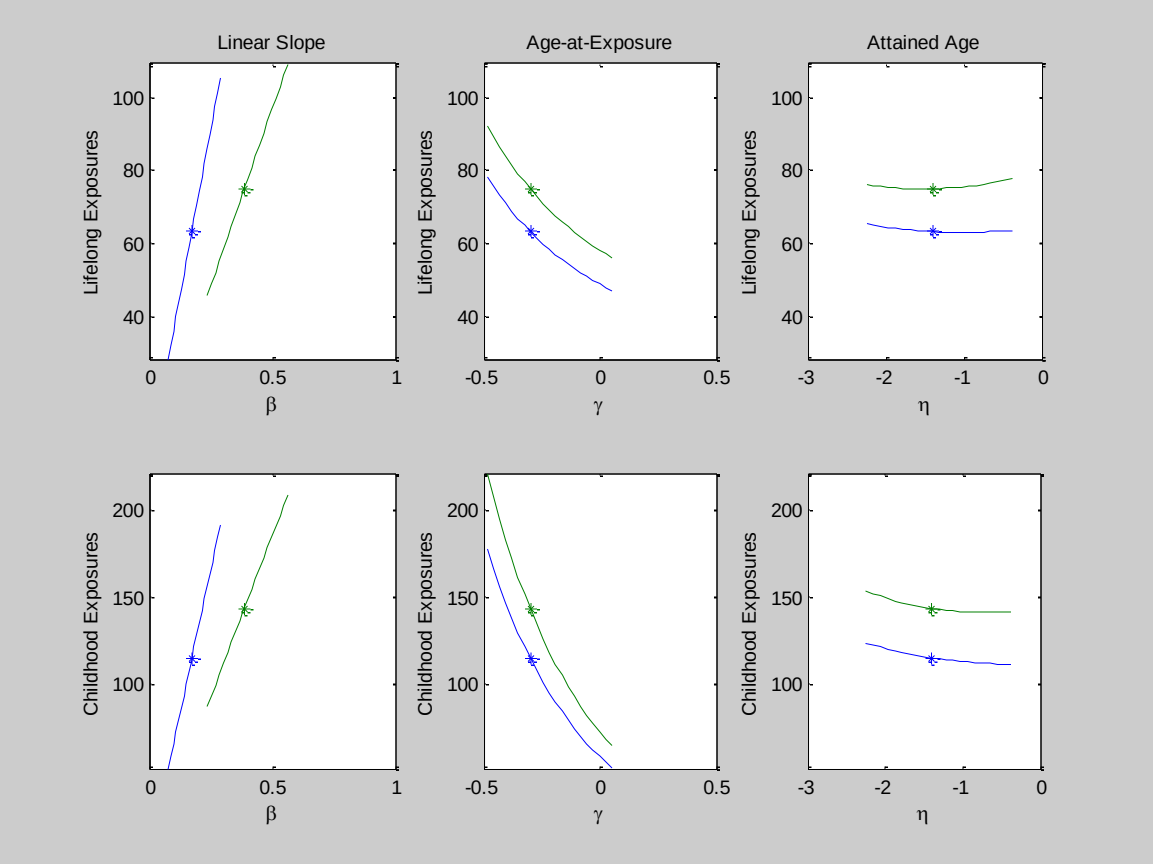

Figure 4-1(a): Dependence of stomach cancer LAR, for both lifelong and childhood exposures (age < 15) on ERR model parameter values within 95% CI's. LAR (per 10^4 person-Gy) is graphed along the y-axis. The 95% CI's were obtained using standard Poisson regression methods to fit the ERR model to the A-bomb survivor cohort data using Epicure software (Preston *et al.* 1993). For each parameter, the 95% CI's were conditioned on nominal values for the remaining parameters: *e.g.*, the CI for linear dose response parameter was conditioned on the assumption that γ = -0.3 and η = - 1.4. The nominal ERR model weight was used (w = 0.7). Nominal values for parameters and risk projections are also indicated (*).

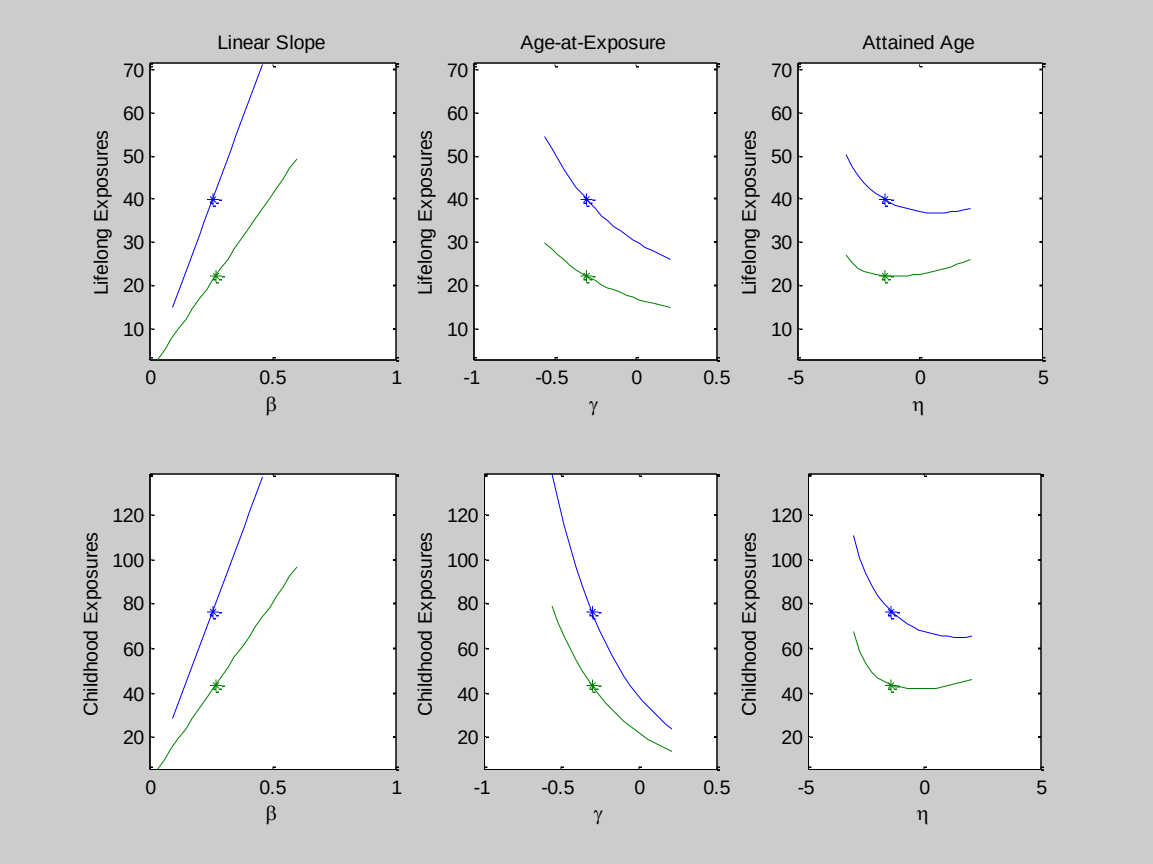

Figure 4-1(b): Dependence of liver cancer LAR, for both lifelong and childhood exposures (age < 15) on ERR model parameters associated with the linear dose response (β), age-at-exposure (γ), and attained-age (η).

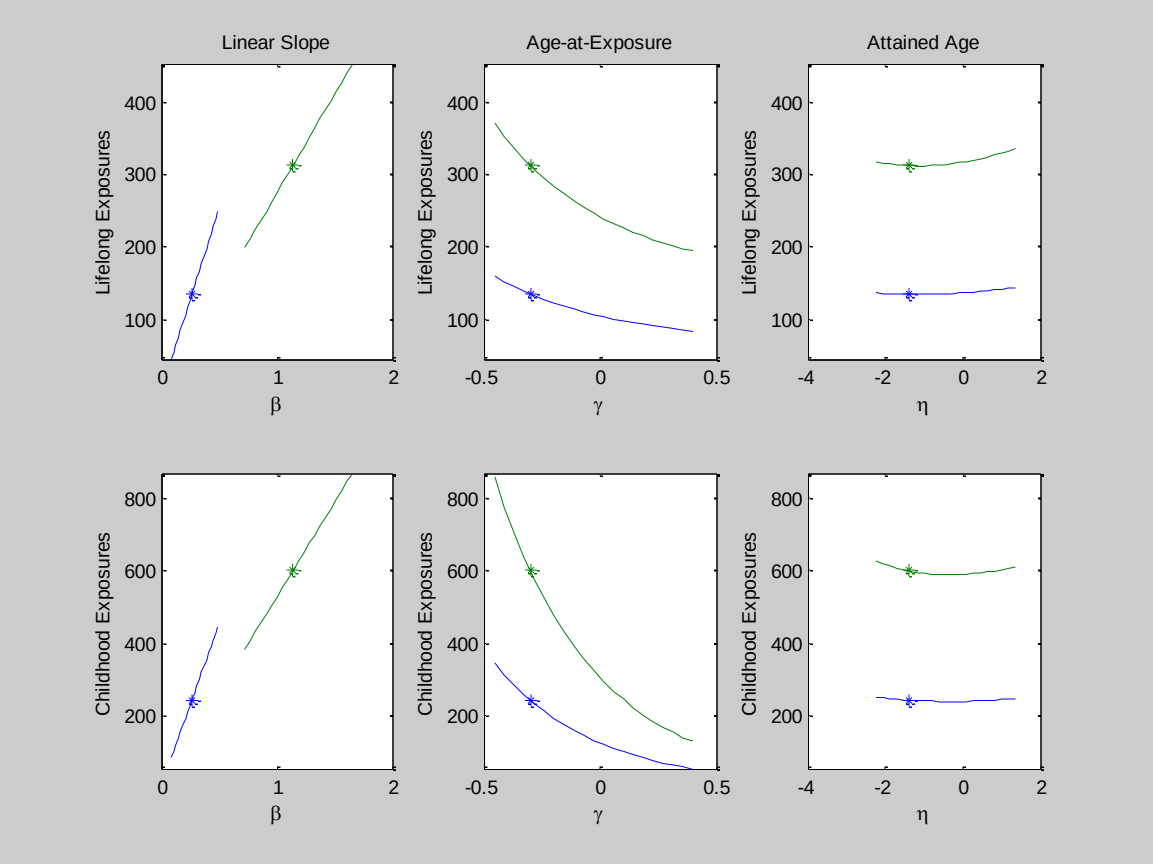

Figure 4-1(c): Dependence of lung cancer LAR, for both lifelong and childhood exposures (age < 15) on ERR model parameters associated with the linear dose response (β), age-at-exposure (γ), and attained-age(η).

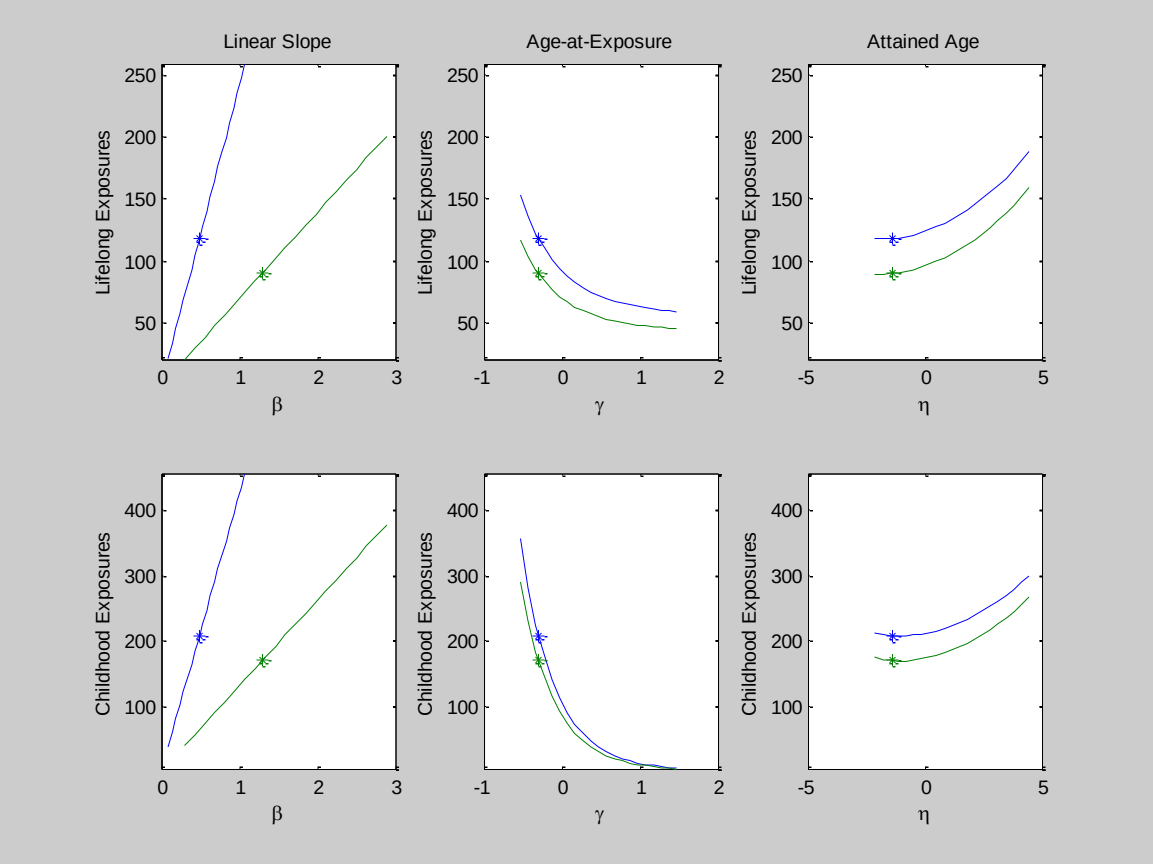

Figure 4-1(d): Dependence of bladder cancer LAR, for both lifelong and childhood exposures (age < 15) on ERR model parameters associated with the linear dose response (β), age-at-exposure (γ), and attained-age (η).

The graphs in Figures 4-2(a)-(c) compare "uncertainties" associated with the linear dose response parameter to those associated with both risk transport and the DDREF. Here, risk transport is evaluated by observing the dependence of LAR on the ERR-model weight parameter ($0 \leq w \leq 1$). For DDREF, plausible values of 0.8 to 2.7 were chosen to be consistent with the treatment of uncertainties associated with the DDREF in BEIR VII (see Section 4.4.2).

Figures 4-2(a)-(c) only account for part of the uncertainty associated with sampling variation (the portion associated with β) because for many sites, uncertainty associated with the age-at-exposure and even the attained-age parameters can be sizeable. Nevertheless, these graphs illustrate that the dominant source of uncertainty (among sampling variation, DDREF, and risk transport) depends on cancer site. The uncertainty in LAR associated with sampling variation appears largest for bladder cancer, and LAR depends most on DDREF for residual site cancers. The uncertainty associated with risk transport appears greatest for stomach and liver cancers, but, for colon and male lung cancer, none of these three sources of uncertainty appears predominant.

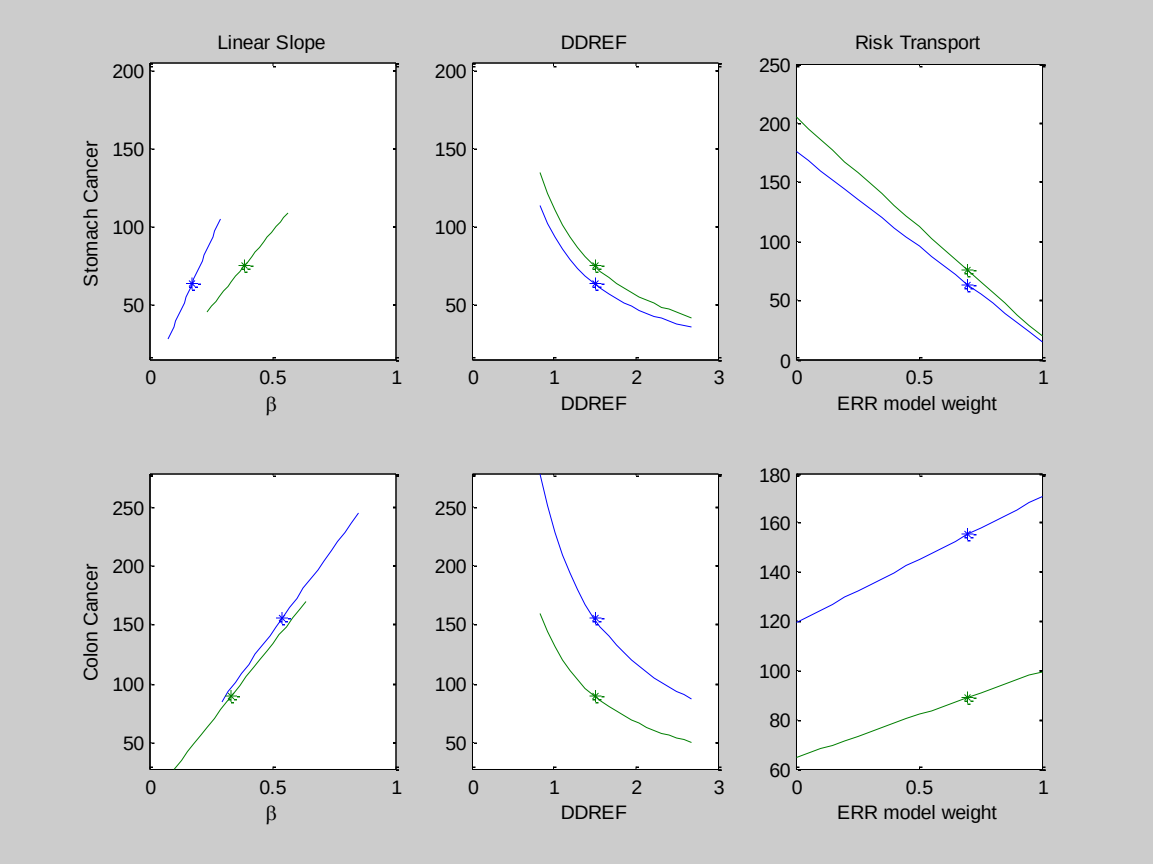

Figure 4-2(a): Dependence of LAR (for lifelong exposures), for stomach and colon cancers on the linear dose response parameter (β), DDREF, and the ERR model weight parameter (w).

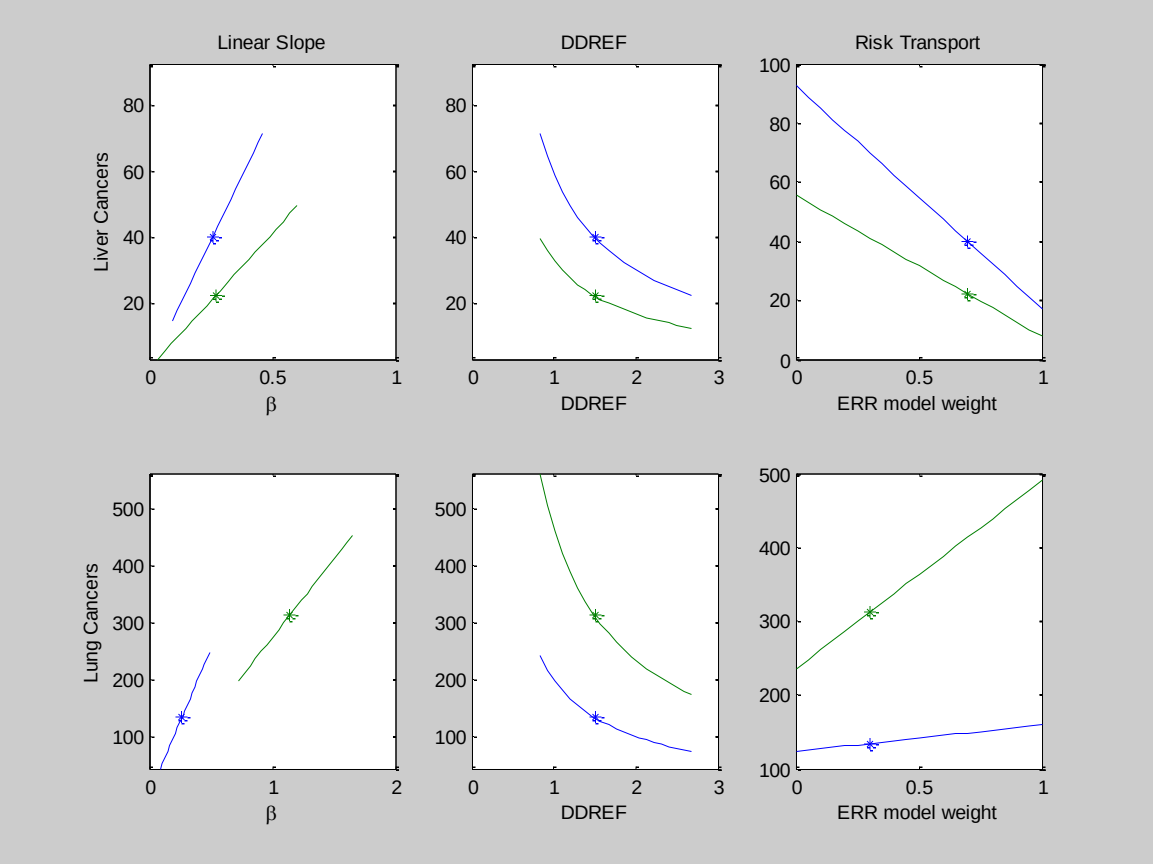

Figure 4-2(b): Dependence of LAR (for lifelong exposures), for liver and lung cancers, on the linear dose response parameter (β), DDREF, and the ERR model weight parameter (w).

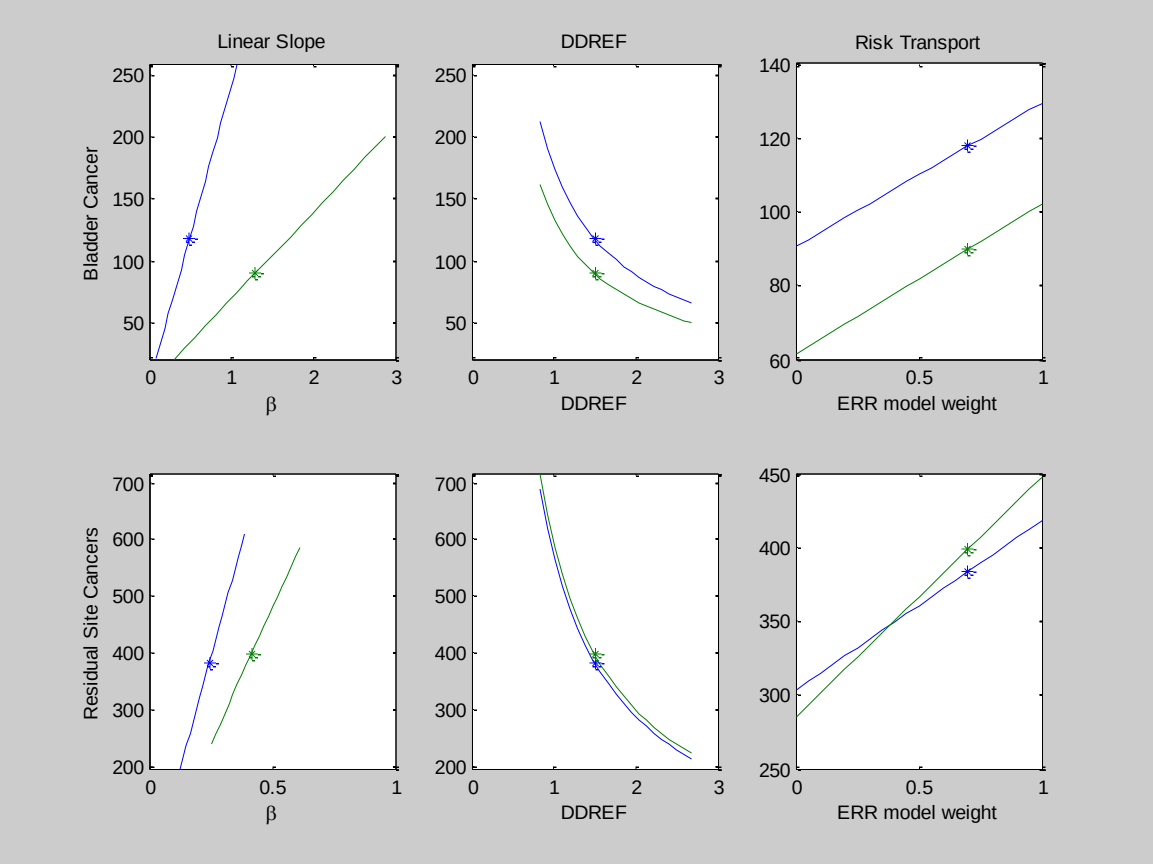

Figure 4-2(c): Dependence of LAR (for lifelong exposures), for bladder and residual site cancers, on the linear dose response parameter (β), DDREF, and the ERR model weight parameter (w).

4.4 Monte Carlo Approach for Quantifying Uncertainties in LAR

For each cancer site: a multivariate probability distribution was assigned to ERR model parameters, independent probability distributions were assigned to parameters associated with non-sampling uncertainties, and Monte Carlo methods were used to simulate the distribution of LAR for the U.S. population. Bayesian methods used to generate the ERR model parameters are outlined in the next section. Section 4.4.1 outlines the Monte Carlo method for simulating the distribution for LAR. Section 4.4.2 describes how distributions were assigned to non-sampling uncertainties, Section 4.4.3 describes the Bayesian method for sampling variation, and Section 4.4.4 describes our Monte Carlo approach for specific sites for which the Bayesian approach was used.

4.4.1 Monte Carlo method. The method is based on repeated random sampling of all the parameters associated with uncertainty. In many important aspects, the handling of sampling variation is identical to the approach described in Section 4.3. For each iteration of the Monte Carlo process, a set of random values for the ERR model parameters are generated, using Bayesian methods described in the next Section, and a value for LAR is calculated based on Equation 4-3. Then, to incorporate non-sampling uncertainties, the simulated values of LAR are modified by randomly generated multiplicative "uncertainty factors" (EPA 1999a), which are described next using the example of DDREF.

In Section 3, the LAR for low dose chronic exposures was calculated as the ratio of the LAR for acute exposures divided by a nominal value of 1.5 for the DDREF. For quantifying uncertainties, a subjective distribution is assigned to the DDREF, which is lognormal with GM = 1.5 and GSD 1.35, corresponding to 2.5 and 97.5 percentile values of 0.8 and 2.7. Thus, if the only source of uncertainty in our projections is uncertainty in the DDREF, the "true" LAR projection would – with subjective probability of 95% – deviate from EPA's projection by a multiplicative factor from (1.5/2.7) to (1.5/0.8). In general, an uncertainty factor (UF) is the random factor by which a projection deviates from the "true" LAR due to a specific source of uncertainty such as DDREF or risk transport. For uncertainty associated with DDREF, the uncertainty factor is the ratio of 1.5 divided by the lognormal random variable with GM = 1.5 and GSD = 1.35. Then, the Monte Carlo approach for simulating LAR is as follows:

1. Simulate N sets of ERR model parameters values using Bayesian methods;
2. For each set of ERR model parameters, use Equation 4-4 to calculate an initial value for LAR;
3. Assign a distribution for uncertainty factors associated with each non-sampling source of uncertainty;
4. Generate N random values for each uncertainty factor;

5. Multiply, element by element, the N initial values of the LAR generated in Step 2 by the corresponding product of uncertainty factors generated in Step 4.

4.4.2 Non-sampling sources of uncertainty. A summary of how each source of uncertainty was treated is given in Table 4-1, with more detailed discussions on each in the text below.

Table 4-1: Uncertainty factors for non-sampling sources of uncertainty

Source	Uncertainty Factor Distribution[1,2]
Risk transport (quantified in BEIR VII)	See this Section
DDREF (quantified in BEIR VII)	1.5 / LN(1.0, 1.35)
Incomplete follow-up[3]	LN(GSD = 1.2)
Errors in dosimetry	LN(GSD = 1.16)
Random: linear dose response	LN(GSD = 1.05)
Random: DDREF	LN(GSD = 1.1)
Systematic	LN(GSD = 1.1)
Nominal neutron RBE	LN(GSD = 1.05)
Errors in disease detection/diagnosis	LN(GSD = 1.05)
Selection bias	LN(GSD = 1.1)
Relative effectiveness of X-rays	Not quantified
Model misspecification for dose response	Not quantified
Total for sources not quantified in BEIR VII[4]	LN(GSD = 1.3): solid cancers LN(GSD = 1.2); leukemia

[1]LN stands for lognormal. LN(a,b) is the distribution with GM = a and GSD = b.
[2]Mean of distributions other than for DDREF is set to 1
[3]For solid cancers only
[4]Includes incomplete follow-up, dosimetry, disease detection/diagnosis, selection bias

Risk transport. The uncertainty factor for risk transport is defined here as the random factor by which the projection of LAR based on the ERR model, derived from data on the Japanese A-bomb survivors, deviates from the "true" LAR because radiogenic risk may not be proportional to baseline rates. For sites other than thyroid, breast, bone, and lung, independent subjective probability distributions were assigned to $LAR^{(true)}$ as follows:

$$P[LAR^{(true)} = LAR^{(R)}] = 0.45;\ P[LAR^{(true)} = LAR^{(A)}] = 0.05;$$
$$(LAR^{(true)} \sim \text{Uniform between } LAR^{(R)} \text{ and } LAR^{(A)}) \text{ with probability } 0.5$$

This distribution assigns: with 50% probability, either the EAR or the ERR model-based projection, or with 50% probability, a uniform distribution between the two "extremes." For some sites, the LAR may not be bounded by the ERR and EAR projections; however, in the absence of additional information, there is no way to determine how far the probability distribution should be extended to account for this.

For lung cancer, the only difference is that $P[LAR^{(true)} = LAR^{(R)}]$ =0.05, and $P[LAR^{(true)} = LAR^{(A)}]$ = 0.45. For bone, thyroid, and breast cancer, no risk transport uncertainty was assumed. For the latter two cancer sites, note that the BEIR VII projections were based on analyses of data from non-Japanese populations, as well as from the LSS cohort.

The uncertainty factor for risk transport is the ratio: $\frac{LAR^{(true)}}{LAR^{(R)}}$. It can also be defined with respect to a random ERR model weight parameter as $\frac{wLAR^{(R)} + (1-w)LAR^{(A)}}{LAR^{(R)}}$, where *w* is U(0,1) with probability 0.5, equal to 1 with probability 0.45, and equal to 0 with probability 0.05.

DDREF. A lognormal uncertainty factor with GM=1 and GSD=1.35 was assigned to the DDREF for solid cancers (Figure 4-3). This is consistent with the distributional assumptions made by BEIR VII, *i.e.,* the variance associated with the log-transformed DDREF is 0.09.

BEIR VII's quantification of uncertainty in DDREF was primarily based on a Bayesian analysis of the LSS data and animal carcinogenesis studies. The main objective of their analysis was to estimate the curvature of the dose-response, which, as described in Section 2.1.4, translates directly into an estimate for DDREF. The analysis resulted in a posterior distribution for the DDREF with GM=1.5 and GSD=1.28. The latter is equivalent to $Var(\log(DDREF))$ = 0.06. However, the BEIR VII Committee opined that: "the [Bayesian] DDREF analysis is necessarily rough and the variance of the uncertainty distribution is …, if anything, misleadingly small." Accordingly, they inflated the variance for the $\log(\text{DDREF})$ by 50% and set its variance equal to 0.09.

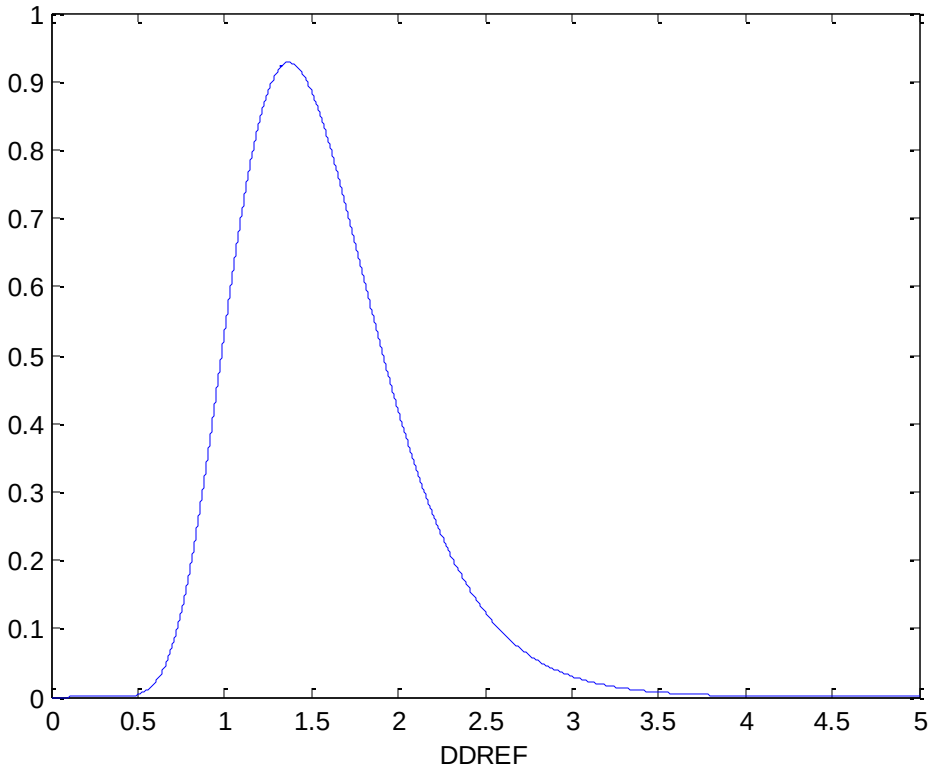

Figure 4-3: Subjective probability density function for DDREF

Other non-sampling sources of uncertainty. Sources of uncertainty considered here include uncertainties from: incomplete follow-up in the LSS, dosimetry errors, and diagnostic misclassification. ***For cancers other than leukemia, we assigned a single (encompassing) lognormal uncertainty factor with GSD = 1.3.*** (For leukemia the GSD is 1.2, for reasons described in the section on incomplete follow-up). The GMs for the component sources of uncertainty considered in this subsection would range from about -0.9 to 1.1, with about half of them greater than 1. The expected value (mean) of the overall distribution was set to 1, since to use any other value would suggest a "precision" in the stated uncertainties that is not warranted.

Incomplete follow-up*.* A-bomb survivors who were children at the time of the bombings (ATB) still have substantial years of life remaining in which cancers are to be expressed. Thus, uncertainty associated with incomplete follow-up is greatest for childhood exposures, which accounts for about 40-45% of EPA's projected cancer incidence radiation risk. For a crude indication of the relative precision of the LAR for childhood exposures, we note that, for the BEIR VII analysis of the LSS cohort, fewer than 2100 survivors with cancers were exposed before age 15, compared to more than 3400 for age-at-exposure 15-30. Furthermore, approximately 90% of children < 10 ATB were still alive in the year 2000 (Little *et al*. 2008). More generally, about 45% of all survivors in the LSS were still

alive in 2000, so that uncertainties in LAR projections from the incomplete follow-up, especially for cancers that tend to develop relatively late in life, merit careful consideration.

Combined with the potential for model misspecification of temporal and age dependence, incomplete follow-up can lead to bias in projections of LAR. In the UNSCEAR models described by Little *et al*. (2008), ERR and EAR for solid cancer mortality depend on TSE. The UNSCEAR risk projections differ from those used here and in BEIR VII, in part, because different models are used for extrapolating risks for cancers that might occur more than 53 y after exposure. The uncertainty of projections based upon the parametric representations in BEIR VII depend on the extent to which ERR and EAR for incidence and mortality depend on TSE and other factors not accounted for in their risk models.

For EPA's previous assessment of radiogenic cancer risks, based primarily on analysis of the LSS mortality data for follow-up until 1985, site-specific uniform distributions were assigned to uncertainty factors to account for sampling errors and possible model misspecification associated with temporal dependence (1999a). For stomach, colon, lung, breast, thyroid and residual site cancers, it was thought that these uncertainties might lead to an overestimate of population risk. For these sites, a relative risk model was used that depended on age-at-exposure but not attained age, and most of the projected risk was associated with exposures before age 20. It was determined that "the contribution of childhood exposures was highly uncertain in view of statistical limitations [*i.e.*, sampling error] and possible decreases in relative risk with time after exposure [*i.e*, modeling misspecification]." For most of these sites, the uniform distribution, U(0.5, 1), was assigned to the uncertainty factor. In other words, the ratio of the "true" population risks to the EPA projection was thought to range between 0.5 and 1. For other solid cancer sites (except bone), the distribution for the uncertainty factor was 0.8 to 1.5. Due to the extended follow-up period and more flexible and appropriate modeling of age dependence in BEIR VII, uncertainties associated with incomplete follow-up should be greatly reduced.

To update the uncertainty analysis to account for incomplete follow-up, the new EPA risk models (see Section 3) were used to calculate the LAR for time-since-exposure restricted to between 13 and 53 y, the period of follow-up for the LSS incidence data. Slightly more than 50% of the projected LAR is associated with this time period. Thus, unless the temporal dependence differs substantially for time-since-exposure from what has been observed for the period of follow-up in the LSS, it is unlikely to be a major source of uncertainty, with the possible exception of childhood exposures. ***A common lognormal uncertainty factor with GSD = 1.2 was used for solid cancers.***

Leukemia deserves special mention. To paraphrase Little *et al*. (2008), uncertainties in risk projections for leukemia would have more to do with risks for times soon after exposure than for times extending beyond the current LSS

follow-up. This is because the mortality follow-up in the LSS began in October, 1950, about 5 y after the bombings in Hiroshima and Nagasaki, and there is evidence of risk for TSE < 5 y from other studies. In particular, a substantial number of leukemia cases reportedly occurred in the LSS before 1951, with an apparent subsequent decline; a significant increase in leukemia within 5 y of radiotherapy was observed in the International Cervical Cancer study; and in an analysis of the Mayak worker study (Shilnikova *et al*. 2003), the ERR/Gy for leukemia mortality was significantly higher for external doses received 3-5 y prior to death than for doses received more than 5 y earlier. We did not quantify uncertainty associated with time-since-exposures < 5 y because, although it might be larger than for most solid cancers, it is judged to be small compared to sampling uncertainties for leukemia (see Section 4.4.4). For leukemia an UF was not assigned for incomplete follow-up.

Errors in dosimetry. In 2003, RERF implemented a revised dosimetry system called DS02, which is the culmination of efforts stemming from concerns about the previous (DS86) system for assigning doses to the A-bomb survivors. Chief among these concerns were discrepancies between DS86 calculations and measured thermal neutron activation values (Roesch 1987). These measurements indicated that DS86 might have seriously underestimated neutron doses for Hiroshima survivors, and, as a result, γ-ray risk estimates for solid cancers could possibly be underestimated by more than 20% (Preston *et al*. 1993, EPA 1999a). However, the magnitude of this bias would depend on factors such as the RBE for neutrons. Other factors motivating development of the new system included improved computer models for radiation transport and biodosimetric and cancer data indicating overestimation of doses for Nagasaki factory workers (Preston *et al*. 2004).

A comprehensive review adequately resolved issues relating to the discrepancies with neutron activation measurements (Preston *et al*. 2004). As summarized in Preston *et al*. 2004 and detailed elsewhere (Cullings *et al*. 2006, Young and Hasai 2005), major changes in DS02 include: 1) changes in the burst height and yield for the Hiroshima bomb; 2) changes in the gamma radiation released by the Nagasaki bomb; 3) use of new data on neutron scattering, etc., to improve calculations for radiation transport; 4) more detailed information and better methods to account for in-home and terrain shielding; 5) more detailed information for computing free-in-air fluences; and 6) new weighting factors for fluence-to-kerma and fluence-to-dose calculations.

The RERF report on DS02 (Kaul *et al*. 2005) divides uncertainties associated with the dosimetry system into two broad categories: systematic and random. Systematic uncertainties include those relating to the yields, neutron outputs and burst heights, and the air transport calculation method. Random uncertainties include those relating to survivor location and inputs needed to estimate shielding for individual survivors. In Kaul *et al*. (pp. 989, 991), a

coefficient of variation (CV) of 12-13% (corresponding to a GSD of about 1.12) was associated with systematic uncertainties.

For assessing the effects of random dose errors on risk projections, we refer to the recent contribution by Pierce *et al.* (2008). As they note, "RERF has for more than 15 years made adjustments to individual (DS86 and DS02) dose estimates to reduce the effects of imprecision" on estimates of risk. Without adjustment, it is well-established that random dose errors would cause a downward bias in risk estimates if a linear dose-response is assumed. They may also introduce a bias in the estimate of curvature, which is used for evaluating the DDREF. RERF adjustments are currently based on the assumption that the random errors are independent and lognormal with GSD = 1.42.

Pierce *et al*. argue for adjustments based on more sophisticated treatment of the random errors that account for effects of "the use of smoothing formulae in the DS02 treatment of location and shielding." Results in Pierce *et al*. (Table 1, p. 123) indicate that the more realistic and sophisticated modeling of random dose errors would result in a change of about 2% in the estimated linear dose-response estimate of ERR and about a 15-20% change in the estimate of curvature, compared to estimates based on current methods and assumptions. The effect on the estimate of DDREF would be somewhat less than this, in part because it depends also on data from animal carcinogenesis studies. Perhaps, somewhat conservatively, ***we assign lognormal uncertainty factors with a GSD equal to 1.05 (effects of random errors on the linear dose parameter estimate) and 1.1 (effects on the estimate for the DDREF).***

Finally, we quantify uncertainties relating to the use of a nominal neutron RBE of 10. The use of this nominal weight assigned to the neutron component of dose has already been discussed in Section 3.1. Calculations in Preston *et al*. (2004) indicate that the use of an RBE of 20 would result in a relative decrease in ERR estimates for solid cancers by about 5%. Radiobiological data (Sasaki *et al*.) indicate an RBE of 20 or greater cannot be ruled out. A lognormal uncertainty factor with GSD of 1.05 is assigned to this source.

Errors in disease detection and diagnosis. The BEIR VII Committee concluded that "this is unlikely a serious source of bias in risk estimates." As stated earlier, both detection and confirmation error can occur. Detection error leads to an underestimate of the EAR, but does not affect the estimated ERR, whereas confirmation error leads to an underestimate of the ERR but does not affect the EAR (EPA 1999a).

Analyses of LSS mortality data formed the basis for EPA's previous risk assessment. For that assessment, results from studies of Sposto *et al*. (1992) and Pierce *et al*. (1996) were used to estimate the bias in risk estimates due to diagnostic misclassification in the LSS mortality data. Conclusions from these studies were that the ERR estimate for solid cancers in the LSS should be

adjusted upward by about 12% and that the EAR estimate should be adjusted upward by about 16%. Based on these results and results from the uncertainty analysis by the NCRP 126 Committee (NCRP 1997), EPA assigned an uncertainty factor of N(1.15, SD=0.06) for diagnostic misclassification. Here N(a, SD=b) refers to a normal distribution with mean a and standard deviation b.

Misdiagnosis is likely to lead to a somewhat smaller bias in the BEIR VII projections than in EPA's 1994 projections because the former were based on the LSS incidence data. As noted in the BEIR VII report, "cancer incidence data are probably much less subject to bias from under-ascertainment or from misclassification, and this was an important reason for the committee's decision to base models for site-specific cancers on incidence data. However, incidence data are not available for survivors who migrated from Hiroshima to Nagasaki. Adjustments are likely to account for this (Sposto *et al*. 1992), but there is likely to be some uncertainty in the adequacy of these adjustments." ***We have assigned a lognormal uncertainty factor with GSD = 1.05 to diagnostic misclassification.*** Admittedly, this understates the uncertainty for some cancers since the uncertainty factor does not account for misclassification among different cancer types.

Relative effectiveness of medical X-rays. For breast and thyroid cancers, the BEIR VII risk models were based on pooled analyses of data from the LSS and several medical studies. These medical studies were generally based on data from patients who had received therapeutic or diagnostic X-rays, which are of lower energy than the bulk of the photons irradiating the A-bomb survivors. If the risk per unit dose for lower energy photons is >1 (see Section 5.2), there may be an upward bias in risk estimates from the pooled studies. However, in many of the medical studies the doses were fractionated, so the DDREF of 1.5 would not be applicable. Thus, any upward bias due to the higher effectiveness of lower energy photons may be somewhat offset by the difference in DDREF.

We did not incorporate any uncertainty associated with a higher effectiveness in inducing cancer for medical X-rays compared with the photons from the atomic bombs. It should be relatively small compared to the uncertainties associated with sampling variability – especially for thyroid cancer.

Selection bias in the LSS cohort. The question as to whether there is a serious selection bias has been a subject of considerable controversy. For example, Little (2002) cited several papers by Stewart and Kneale from 1973 to 2000 which argued that the selection bias may be substantial. In a recent analysis, Pierce et al. (2007) argue that the magnitude of the bias on the ERR estimate for solid cancer is unlikely to be greater than 15-20%. (The bias might be greater for non-cancer effects). ***We assign a lognormal distribution with GSD 1.1 to the uncertainty factor for selection bias.***

Shape of the dose response. As described in Section 3.5, BEIR VII models explicitly (leukemia) or implicitly (solid cancers) assume a linear-quadratic (LQ) dose response for cancer induction by radiation. Although epidemiological data are generally consistent with linearity at low doses (Section 2.2), recent mechanistic studies have revealed complex phenomena (Section 2.1) that could conceivably modulate risks at very low doses and dose rates, either up or down, from what would be projected based on a LQ model. The BEIR VII Committee did not attempt a quantification of this source of uncertainty. Attempting to assign a probability distribution to the dose-response model would necessarily be highly speculative and subjective; consequently, EPA has not included this source of uncertainty in its quantitative uncertainty analysis. However, it is acknowledged that a breakdown in the model at low doses, leading to substantial errors in our risk projections, cannot be ruled out.

4.4.3 Bayesian analysis for sampling variability. This section describes a Bayesian analysis of LSS incidence data, which we used to derive uncertainty distributions for LAR for sampling variability. Distributions were derived for all solid cancer sites except breast and thyroid. (Our treatment of sampling variability for the latter two sites and leukemia is given in Section 4.4.4). Uncertainties for bone and kidney cancers, which for this analysis were added into the residual category, were not explicitly calculated.

The Bayesian analysis is in many respects similar to BEIR VII's analysis of LSS data (see also Preston *et al.* 2007). In BEIR VII, confidence intervals were derived for parameter values in ERR risk models by fitting these models to the LSS data. The fitting of the models was based on their likelihood (defined next), and the LSS data includes observed rates for solid cancer incidence and leukemia deaths for subgroups defined by city, sex, dose, and intervals based on age-at-exposure, attained age, and follow-up time. The likelihood refers to the probability of a set of observations given values for a set of parameters (Everitt 1995). In essence, the confidence intervals derived in BEIR VII contain values for parameters (β, γ, and η) for which the probabilities of observed cancer rates are largest.

The fundamental difference between EPA's Bayesian analysis and the analyses in BEIR VII is that the Bayesian analysis formally accounts for subjective information about parameter values using prior distributions. Prior distributions are probability distributions that summarize information about a parameter that is known or assumed, prior to obtaining further information from empirical data (Everitt 1995). For EPA's analysis of LSS data, the most important prior distributions were the ones assigned to parameters in the ERR model. An example is the prior distribution assigned to the age-at-exposure parameter for most cancer sites. Under the assumption that for most sites, ERR decreases with age-at-exposure, but that for most cancer sites the per decade decrease in ERR (before age 30) would not be much greater than 3 (for which γ < -1.1), a prior of

N(-0.3, SD=0.5) was assigned to γ. For this prior distribution, $P(\gamma < 0) \approx 0.7$ and $P(\gamma < -1.1) \approx 0.05$.

In any Bayesian analysis, distributions of the parameter values are updated using the likelihood (which incorporates all the information from the LSS about the parameters), yielding what is referred to as the posterior distribution. The posterior distribution incorporates all that is known about parameter values, and it can be used directly to calculate uncertainty intervals (often referred to as credible intervals). A 90% uncertainty interval would be any interval for which the quantity of interest, *e.g.,* the linear dose response parameter or the LAR, is included with posterior probability 0.90.

The relationship between the likelihood (the basis for the BEIR VII analysis) and the posterior distribution (the basis for the EPA uncertainty analysis) is that the posterior distribution is proportional to the product of the prior distribution and the likelihood. If, for example, a constant prior is used, as is often the case when there is very little prior information about a parameter value, the likelihood and posterior distributions will be (outside of a multiplicative constant) identical to each other, and the two types of approaches will yield similar, if not identical, results. However, if there is information from another epidemiological study about one or more parameters, then the prior can have a substantial influence on the posterior distribution. For example, suppose it is "known" that the linear dose-response parameter (β) for a particular cancer site cannot be greater than 0.5. The prior probability would be 0 for values above 0.5, and the corresponding posterior probability would also be 0 – regardless of the likelihood. Here, the confidence interval might contain values above 0.5, but the Bayesian uncertainty interval would not.

From the previous example, it should be clear that Bayesian posterior distributions and uncertainty intervals depend on the prior distributions assigned to parameter values. In general, posterior distributions are more sensitive to the choice of prior distributions when there is only limited data for updating them. At the end of this Section, we describe the underlying prior distributions and their rationale for our Bayesian analysis of the LSS data.

Although it is true that a different set of priors would have led to different results than presented in Section 4.5, *non*-Bayesian analyses also depend on assumptions made about parameter values. Unfortunately, it is often not obvious what these assumptions are. For example, many may be unaware of the implicit assumption in BEIR VII that the per decade decrease in ERR with age-at-exposure may be the same or similar for most solid cancer sites. In contrast, Bayesian analyses, through the use of prior distributions, provide a relatively straightforward and flexible approach for incorporating what might be assumed about parameter values.

The main task in Bayesian analyses is to calculate the posterior distribution – upon which inferences are based – from the data and prior distributions for the parameters. It is usually very difficult, or impossible, to calculate it using analytical means, so, instead, one typically simulates the posterior distribution using complex sampling techniques such as Markov Chain Monte Carlo (MCMC) – see for example, Gelman *et al.* (2003) for a description of Bayesian methods and computational methods such as MCMC. To simulate the posterior distribution for ERR model parameters, we applied MCMC to the LSS incidence data and the prior distributions for those parameters, as described next. This was accomplished using the software program WinBUGS (Lunn *et al*. 2000). Further details are given in Appendix B.

Prior distributions for ERR model parameters. An important feature of our uncertainty analysis is that the age-at-exposure and attained-age parameter values are allowed to depend on site. Separate sets of these two parameters were used for almost all cancer sites; exceptions are cancers of the prostate, ovary, and uterus. For these 3 sites, BEIR VII nominal values were used for age-at-exposure ($\gamma = -0.3$) and attained age ($\eta = -1.4$) because of insufficient data on these cancers to provide stable estimates for these parameters or their uncertainties. It should be noted that the uncertainty intervals for these sites are not meant to account for uncertainties relating to age and temporal dependence in risk.

Age-at-exposure parameter: Under the assumption that, for most cancer sites, the ERR decreases with age-at-exposure, but the per decade decrease in the ERR (before age 30) would not be > 3 (implying that γ < -1.1), a prior distribution of N(-0.3, 0.25) was assigned to γ. This allows the ERR to be up to ≈ 20 times larger at birth than at age 30. For this prior distribution, P(γ < 0) ≈ 0.7, and there is a 95% probability for the interval (-1.3, 0.7). As seems appropriate, this interval for any site-specific parameter is considerably wider than BEIR VII's 95% CI for the age-at-exposure parameter for all solid cancers: (-0.51, -0.10).

Attained age parameter: The attained age parameter represents the power to which the ERR increases (η > 0) or decreases (η < 0) with attained age. For cancers other than prostate, uterine, or ovarian, independent N(-1.4, 2) distributions were used. The distribution was chosen to be centered at the BEIR VII nominal value for solid cancers and to have a lower limit of around -4. At this lower limit, excess *absolute* risks for many cancers would not depend on attained age because baseline rates typically increase by a power of about 4 with age. The prior distribution assigns about a 95% probability to the interval (-4.2, 1.4).

Linear dose dose-response parameter: A lognormal prior distribution was used for each of the linear dose-response parameters. Log-transformed parameters for each cancer site were assumed to have prior distributions with a common (unknown) mean and variance (τ^2). Lognormal priors were chosen, in part, to ensure that ERR values cannot be negative. Details are given in

Appendix B. In essence, the method represents a flexible approach of sharing information on radiogenic risks among cancer sites. Such sharing of information is desirable – especially for cancer sites for which ERR estimates are less precise than for other sites. The variance (τ^2) determines how much information is shared among sites. For example, if the variance is set to zero, the linear dose-response parameter would be forced to be equal to the same value for each site. In contrast, if the variance is (essentially) infinite, posterior distributions for the site-specific dose-response parameters would be independent. In general, the site-specific posterior distributions are "shrunk together" by an amount dependent on τ^2. However, instead of specifying a value for τ^2 in advance, we assigned it a prior distribution, so that the data also has a role in deciding how similar values for the linear-dose-response parameter might be. The rationale for this type of approach is further discussed in Pawel *et al*. (2008).

There are two main reasons for choosing more complicated prior distributions for the linear dose-response parameters than for the age-related parameters. First, for most cancers, the LAR is more sensitive to the linear dose-response parameter than the other parameters, which warranted consideration of a more sophisticated approach. Second, "extreme" values for the distributions of the age-response parameters could be more easily determined and justified; *e.g.,* it is reasonable to assume for the purposes of this analysis that attained-age parameters would not be much less than -4 (for which EAR is constant with attained age) and not much greater than 0.

4.4.4 Approach for other cancers. Cancer sites included here are leukemia, breast, thyroid, and bone. EPA risk models for the latter three are not based exclusively on analyses of the LSS data. We also discuss the approach for uniform whole-body radiation.

Leukemia. The uncertainty from sampling variability was assumed to be lognormal with GM equal to the nominal sex-specific estimates presented in Section 3. The GSD was derived from the 95% CI in Table 12-7 of BEIR VII for the LAR associated with an exposure of 1 mGy per year throughout life. For example, for males, the CI is (19, 230) per 10^4 PY-Sv, which corresponds to a GSD ≈ 1.9. The BEIR VII confidence intervals account for uncertainties relating to the linear and quadratic components in the dose response. Values for other parameters were set to nominal values.

Breast and thyroid cancers. The EPA nominal estimates for these cancer sites were based on risk models derived from a pooled analysis of data from medical cohorts as well as the LSS. It would thus be inappropriate to calculate sampling variability uncertainties from an analysis of only the LSS data (as we did for almost all other cancer sites).

For ***breast*** cancer, the uncertainty from sampling variability was assumed to be lognormal with GM equal to nominal EPA estimates presented in Section 3.

The GSD was derived from the 95% CI in Table 12-2 of BEIR VII for the EAR linear dose-response parameter, *i.e.* (6.7, 13.3) per 10^4 PY-Sv (GSD = 1.2). Results from Preston *et al.* (2002) indicate that the data from the LSS was extremely influential in the derivation of the BEIR VII risk model. The BEIR VII risk model is quite similar to an EAR model that would have been derived from LSS data alone. Among the cohorts used for the final BEIR VII model, the LSS cohort had by far the greatest number of breast cancers and the largest number of excess cases among those exposed to 0.02 Gy or more (see Preston *et al.*, Tables 6, 10, and 12). It is thus reasonable to assume that uncertainties relating to DS02 dosimetry errors, selection bias, and other sources specific to the LSS would have a similar impact on the BEIR VII breast cancer as for other cancer sites.

For ***thyroid*** cancer, there is considerable uncertainty as to how risks may depend on TSE. The pooled analysis of epidemiological studies by Lubin and Ron (1998) indicates that radiogenic thyroid cancer risk decreases with time for TSE greater than about 30 y. Recent results on data on children treated for an enlarged thymus (Adams *et al.*, 2010) and tinea capitis in Israel (Sadetzki *et al.* 2006) are consistent with these findings. However, it is unclear whether radiogenic risk might reach a peak at TSE about 15-20 y, and at what TSE the decline in risks might be most precipitous. To account for uncertainty in risks associated with TSE, uncertainty intervals were derived using the two ERR models recommended by NCRP (Models 3 and 4, NCRP 2008, pp. 291-292) and the BEIR VII model (see Section 3-2, Eq. 3-7). For both of the NCRP models, the ERR is a categorical function of age-at-exposure and TSE. In the BEIR VII model, ERR does not depend on TSE. In one of these NCRP models (Model 3), ERR declines precipitously at TSE around 30 y and then remains flat. In the other (Model 4), the ERR is the same as in Model 3 for TSE up to 50 y, and then halved for TSE > 50 y.

A 25% probability was subjectively assigned to each of the NCRP models and a 50% probability to the BEIR VII model. For the NCRP models, a lognormal distribution was assigned to the linear dose-response parameter with a GM equal to the NCRP nominal value for this parameter (11.7) and a GSD = 1.6. The GSD was derived using the 95% CI (5.4, 24.9) given in the NCRP report (NCRP 2008, Table 5.11), but adjusted upward to account for possible differences in the ERR for males and females. For the BEIR VII model, lognormal distributions were assigned to the linear dose-response parameters with GSD chosen to coincide with 95% CI of (0.14, 2.0) for males and (0.28, 3.9) for females (see NAS 2006, Table 12-2). Although the thyroid risk models depended on data from medical cohorts, it is unlikely that uncertainties associated with sources such as dosimetry error (for both the LSS and the medical cohorts) would be smaller than for most other cancer sites. For thyroid cancer, an UF with GSD = 1.3 – the same as for other solid cancers – was assigned to sources of uncertainty not quantified in BEIR VII.

Bone cancer. The nominal EPA risk model was derived from data on radium dial painters exposed to ^{226}Ra and ^{228}Ra and patients injected with the shorter-lived isotope ^{224}Ra. The risk of bone cancer is a relatively small component of the risk for all cancers from uniform whole-body radiation. Uncertainties for bone cancer are not quantified here, but EPA plans to address this issue when it revises FGR-13.

Uniform whole-body radiation. To quantify uncertainties for the LAR for all cancers from uniform whole-body radiation the simulated site-specific LAR values were summed (over all cancer sites) at each iteration. For the Monte Carlo simulation, uncertainties in transfer weightings for different cancer sites were assumed to be independent. Transfer weightings for males and females for the same cancer site were assumed to be fully correlated. To avoid under-estimating the uncertainty for the LAR for all cancers combined, the DDREF was assumed to be fully correlated for different cancer types: *i.e.*, the DDREF was assumed to be identical for all cancers other than bone and leukemia. Similarly, the UFs associated with sources not quantified in BEIR VII were assumed to be identical for each solid cancer type. For leukemia (as mentioned earlier) the UF associated with incomplete follow-up was set to zero.

4.5 Results

The mean, median, and 90% uncertainty intervals for male and female cancer incidence LARs are given in Tables 4-2a and b. Sex-averaged uncertainty intervals are given in Table 4-2c. The lower bounds of 0 for prostate and uterine cancers coincide with analyses of LSS incidence data, which provides insufficient evidence to indicate a positive dose-response (Preston *et al*. 2007, NAS 2006). In general, it is important not to over-interpret the lower bounds for other sites, because they can be sensitive to prior distributional assumptions, *e.g*., whether a lognormal or normal distribution is used. Except for thyroid and breast cancers, the uncertainty bounds do not account for information about radiogenic risks gained from studies other than the LSS. These include the Techa River study, which, for example, showed a statistically significant effect of chronic radiation on leukemia incidence (Krestinina *et al.* 2010).

The tables also include the EPA nominal projections described in Section 3. For almost all cancer sites, differences between the mean of the uncertainty distribution and the EPA nominal projections are extremely small when compared to the range of plausible values for LAR indicated by the uncertainty bounds. When one also accounts for the different assumptions used for the uncertainty analysis – compared to those used for deriving the nominal estimates – results are remarkably consistent. For almost all individual cancers, and for all cancers combined, the mean of the uncertainty distributions and the nominal estimates are within 25% of each other. An exception is female bladder cancer, for which the LSS data provides relatively little information on radiogenic risk. EPA's projections are based the BEIR VII risk models, which were derived from LSS

data specific to those sites, whereas the uncertainty distribution is based, in part, on information on ERR "borrowed" from other sites. LSS data, although sparse, indicate that relative risk for female bladder cancer may be somewhat larger than for other sites. The mean of the uncertainty distribution for female bladder cancer is greater than the EPA estimate because it "averages" observed risks for prostate cancer with the larger observed risks for other cancer sites. In this way, the uncertainty analysis takes into account that some of the difference in estimates of site-specific ERRs may be due to sampling variation.

Table 4-2a: EPA projection and uncertainty distribution for the LAR for male cancer incidence[1,2]

		Uncertainty Distribution			
Cancer Site	**EPA Projection**	**Mean**	**Lower (5%) Limit (L)**	**Median**	**Upper (95%) Limit (U)**
Stomach	62	67	8	32	220
Colon	146	110	39	99	230
Liver	40	36	6	24	110
Lung	130	160	58	140	320
Prostate	89	89[2]	0[2]	0[2]	410
Bladder	97	100	28	86	230
Thyroid	22	22	5	17	54
Residual[3]	278	290	99	250	610
Leukemia	92	93	27	77	210
Total[4]	955	970	430	880	1800

[1] Cases per 10,000 person-Gy for exposures at low dose and/or dose rates.
[2] Dose response for prostate cancer is not significant at 0.05 level. Posterior mean equated to EPA projection. See Appendix B for further details.
[3] Includes kidney and other cancers not here specified.
[4] Excludes skin cancer

Table 4-2b: EPA projection and uncertainty distribution for the LAR for female cancer incidence[1]

Cancer Site	EPA Projection	Uncertainty Distribution			
		Mean	Lower (5%) Limit (L)	Median	Upper (95%) Limit (U)
Stomach	75	70	9	36	220
Colon	92	100	37	91	210
Liver	21	28	4	16	88
Lung	308	260	95	220	540
Breast	289	310	140	280	570
Uterus	23	23	0[2]	0[2]	130
Ovary	33	37	11	32	82
Bladder	92	57	14	47	130
Thyroid	65	91	21	67	240
Residual[3]	283	340	120	290	700
Leukemia	69	69	18	57	160
Total[4]	1350	1380	650	1270	2520

[1] Cases per 10,000 person-Gy for exposures at low dose and/or dose rates.
[2] Dose response for uterine cancer is not significant at 0.05 level. Posterior mean equated to EPA projection. See Appendix B for further details.
[3] Includes kidney and other cancers not specified here.
[4] Excludes skin cancer

Table 4-2c: EPA projections and uncertainty distributions for the sex-averaged LAR for cancer incidence[1]

		Uncertainty Distribution			
Cancer Site	EPA Projection	Mean	Lower (5%) Limit (L)	Median	Upper (95%) Limit (U)
Stomach	68	69	9	34	220
Colon	119	110	42	97	220
Liver	30	32	6	20	94
Lung	220	210	83	180	420
Breast	146	160	70	140	290
Prostate	44	44	0[2]	0[2]	200
Uterus	12	12	0[2]	0[2]	65
Ovary	17	19	5	16	42
Bladder	95	79	24	68	170
Thyroid	44	57	15	44	140
Residual[3]	281	310	120	270	630
Leukemia	80	81	29	72	160
Total[4]	1160	1180	560	1090	2130

[1] Cases per 10,000 person-Gy for exposures at low dose and/or dose rates
[2] Dose response for these cancers is not significant at 0.05 level. Posterior mean equated to EPA projection. See Appendix B for further details.
[3] Includes kidney and other cancers not specified here.
[4] Excludes skin cancer

A comparison of EPA's nominal estimates to the 90% uncertainty bounds indicates that, for some cancer sites, the nominal site-specific estimate may differ from the LAR by a factor as large as 5 or more (stomach, prostate, liver, uterus). For other sites (*e.g.*, ovary or bladder) results suggest the EPA projection underestimates the LAR by a factor of only about 2 and may overestimate risk by a factor of about 4. Estimates may be accurate to within a factor of 3 or less for lung, breast, colon, and residual site cancers, and to within a factor of about 2 for all cancers combined. The sex-averaged 90% uncertainty interval for uniform whole-body radiation, excluding skin cancer, is 5.6×10^{-2} to 2.1×10^{-1} Gy^{-1}.

The contribution to uncertainties associated with sampling variability, risk transport, DDREF, and other non-sampling sources of uncertainty are compared in Tables 4-3a and b. Sampling variability is the dominant source of uncertainty for bladder, thyroid, ovarian, leukemia, and residual site cancers. Risk transport uncertainty is dominant for stomach, liver, and uterine cancers. For prostate cancer, both sampling and risk transport uncertainties are large. DDREF is an important contributor of uncertainty (but accountable for < 50% of the total uncertainty) for many cancer sites. It is also an important source of uncertainty for risk relating to uniform whole-body radiation.

Table 4-3a: Percentage of uncertainty in LAR for male cancer incidence attributable to sampling, risk transport, and DDREF[1]

	Source of Uncertainty			
Cancer Site	**Sampling**	**Risk Transport**	**DDREF**	**Other**
Stomach	8	76	9	7
Colon	39	5	32	24
Liver	18	60	12	10
Lung	34	3	35	27
Prostate	82	11	4	3
Bladder	54	3	24	18
Thyroid	72	0	16	12
Residual	50	3	26	20
Leukemia	84	12	0	4

[1]Based on relative variance associated with each source of uncertainty

Table 4-3b: Percentage of uncertainty in LAR for female cancer incidence attributable to sampling, risk transport, and DDREF[1]

	Source of Uncertainty			
Cancer Site	**Sampling**	**Transport**	**DDREF**	**Other**
Stomach	7	77	9	7
Colon	36	7	32	25
Liver	18	64	10	8
Lung	19	27	31	24
Breast	16	0	47	37
Uterus	83	11	3	2
Ovary	55	1	25	19
Bladder	56	6	21	17
Thyroid	78	0	12	10
Residual	53	5	23	18
Leukemia	77	18	0	5

[1]Based on relative variance associated with each source of uncertainty

Results in Tables 4-2(a)-(c) were used to calculate uncertainty intervals for radiation-induced cancer mortality. This was accomplished by applying crude estimates of radiogenic cancer fatality rates, equal to the ratio of the nominal EPA projection for mortality divided by the corresponding projection for incidence to the lower and upper bounds for cancer incidence. For uniform whole-body radiation, 90% UIs for cancer mortality (Gy^{-1}) are $2.4x10^{-2}$ to $1.0x10^{-1}$ for males, $3.4x10^{-2}$ to $1.3x10^{-1}$ for females, and $2.9x10^{-2}$ to $1.1x10^{-1}$ when sex-averaged. These intervals do not account for uncertainties associated with the fractions of cancers that are fatal.

Tables 4-4a,b provide uncertainty intervals for the LAR for incidence associated with childhood exposures for selected sites. Results for most cancers are reasonably consistent with the estimates of radiogenic risk from childhood exposures, which were given in Section 3. However, for female bladder and lung cancers, the means of the posterior distributions are noticeably different than the central estimates derived using the BEIR VII models. As described above, the difference can be partially attributed to the sharing of information among cancer sites for the uncertainty analysis.

Another reason relates to BEIR VII assumptions relating to trends in the dose-response with age-at-exposure. In BEIR VII, the age-at-exposure parameters for these two sites were set to the same value as for most other cancer sites. This is because, when models without this restriction were fitted to the LSS data, differences among the age-at-exposure parameters for cancer sites other than the thyroid were not statistically significant. However, this only means that the LSS provides insufficient information to show that trends with age-at-exposure are different for these two sites. In fact, for lung cancer, data from the LSS suggests that radiogenic risks might not be as dependent on age-at-exposure as for other cancer sites. In contrast, the Bayesian uncertainty analysis allowed for different values for site-specific age-at-exposure parameters.

For all cancers combined, the 90% UI for LAR (Gy^{-1}) associated with childhood exposures is $7.7x10^{-2}$ to $3.6x10^{-1}$ for males and $1.2x10^{-1}$ to $5.5x10^{-1}$ for females. These uncertainties for childhood exposures may be somewhat understated because it is difficult to fully account for uncertainties relating to incomplete follow-up in the LSS. Also, for some cancer sites – not listed but included in the total, such as prostate and ovarian cancers – the analysis does not account for age and time-related uncertainties.

Table 4-4a: EPA projection and uncertainty distributions for male cancer incidence for childhood exposures for selected sites[1,2]

		Uncertainty Distribution			
Cancer Site	EPA Projection	Mean	Lower (5%) Limit (L)	Median	Upper (95%) Limit (U)
Stomach	128	110	11	52	370
Colon	272	200	63	170	440
Liver	79	68	11	44	200
Lung	247	200	50	160	480
Bladder	175	120	21	88	330
Residual[3]	676	790	240	630	1780
All[4]	1950	1860	770	1640	3620

[1] Cases per 10,000 person-Gy for exposures at low dose and/or dose rates.
[2] Risks for exposures before the 15th birthday.
[3] Includes kidney and other cancers not specified here.
[4] Excludes skin cancer

Table 4-4b: EPA projection and uncertainty distributions for female cancer incidence for childhood exposures for selected sites[1,2]

		Uncertainty Distribution			
Cancer Site	EPA Projection	Mean	Lower (5%) Limit (L)	Median	Upper (95%) Limit (U)
Stomach	161	120	13	59	400
Colon	179	200	59	170	450
Liver	44	57	7	31	190
Lung	611	350	86	280	880
Bladder	176	71	12	51	200
Residual[3]	736	1010	300	780	2340
All[4]	3290	2870	1230	2550	5490

[1] Cases per 10,000 person-Gy for exposures at low dose and/or dose rates.
[2] Risks for exposures before the 15th birthday.
[3] Includes kidney and other cancers not specified here.
[4] Excludes skin cancer

4.6 Comparison with BEIR VII

4.6.1 Quantitative uncertainty analysis in BEIR VII. The BEIR VII Report includes a quantitative uncertainty analysis with 95% subjective CIs for each site-specific risk estimate of LAR for low-LET radiation. The analysis focused on three sources of uncertainty thought to be most important: sampling variability in the LSS data, the uncertainty in transporting risk from the LSS to the U.S. population, and the uncertainty associated with values for the DDREF for projecting risk at low doses and dose rates from the LSS data. The BEIR VII Committee did not assign specific distributions (*e.g.,* normal or lognormal) to sources of uncertainty. Instead, the quantification was based on variances for log-transformed random variables (uncertainty factors) for each source of uncertainty. Their treatment of specific sources of uncertainty is outlined next.

Sampling variability. For most cancer sites, BEIR VII derived parameter estimates for ERR and EAR models based on a statistical analysis of LSS cancer cases and deaths, cross-classified by city, sex, dose, and intervals based on age-at-exposure, attained age, and follow-up time. For all solid cancer sites except breast and thyroid, the BEIR VII uncertainty analysis accounted for only the sampling variability associated with the linear dose parameter (β). The uncertainty analysis made use of an approximation for the variance of the $\log(LAR)$ associated with sampling variability:

$$Var_{SAMPLING}[\log(LAR(D,e))] \approx Var[\log(\hat{\beta})]. \quad (4\text{-}6)$$

Risk transport. To quantify uncertainties from risk transport, BEIR VII essentially assumed that either the EAR or ERR model is "correct" for risk

transport, and that a weight parameter (w) equals the probability the ERR model is correct. BEIR VII approximated $Var[\log(LAR)]$ as follows:

$$Var_{TRANSPORT}[\log(LAR)] \approx \log[LAR^{(R)}(\hat{\theta}^{(R)}) / LAR^{(A)}(\hat{\theta}^{(A)})]^2 \, w(1-w). \qquad (4\text{-}7)$$

Here, $\hat{\theta}^{(R)}$ denotes the vector of estimated and nominal parameter values for β, γ, η, and DDREF for the ERR model, and $LAR^{(R)}(\hat{\theta}^{(R)})$ represents the corresponding nominal LAR estimate. Likewise, $\hat{\theta}^{(A)}$ and $LAR^{(A)}(\hat{\theta}^{(A)})$ represent the estimated parameter values and nominal LAR values for the EAR model.

EPA's use of a subjective probability distribution for risk transport represents a significant departure from BEIR VII's approach. The BEIR VII method tends to yield larger estimates of uncertainty for risk transport, particularly for cancer sites such as the prostate, for which U.S. and the A-bomb survivor cohort have very different baseline rates.

DDREF. As detailed in Section 4.4.2, BEIR VII assumed that the variance of the log-transformed DDREF equals 0.09. EPA assigned a normal distribution to log(DDREF), also with variance = 0.09.

Combining sources of uncertainties. To calculate the var(log(LAR)), the BEIR VII Committee simply summed the variances for log(LAR) associated with sampling error, risk transport, and DDREF. To calculate 95% subjective confidence intervals, they further assumed that the combined uncertainty for LAR follows a lognormal distribution.

Unquantified sources of uncertainty. BEIR VII noted several other sources of uncertainty but did not quantify them, arguing instead that uncertainties for many of these other sources are relatively small. These other sources of uncertainty include: 1) uncertainty in the age and temporal pattern of risk, especially for individual sites, which was usually taken to be the same as that derived for all solid tumors; 2) errors in dosimetry; 3) errors in disease detection and diagnosis; and 4) unmeasured factors in epidemiological experiments.

4.6.2 Comparison of results. Results from EPA's quantitative uncertainty analysis are compared with BEIR VII uncertainty intervals for LAR cancer incidence (Table 4-5). For purposes of comparison, 95% uncertainty intervals were used. For most sites, results are reasonably consistent. Exceptions include prostate cancer (BEIR VII upper bound appears to be too large), ovarian cancer (BEIR VII upper bound much larger than EPA's), and female thyroid cancer (for which we considered different risk models than in BEIR VII).

Table 4-5: EPA and BEIR VII 95% uncertainty intervals for LAR of solid cancer Incidence[1]

	Males		Females	
Cancer Site	**EPA**	**BEIR VII**	**EPA**	**BEIR VII**
Stomach	(6, 270)	(3, 350)	(8, 270)	(5, 390)
Colon	(32, 280)	(66, 360)	(30, 250)	(34, 270)
Liver	(5, 130)	(4, 180)	(3, 110)	(1, 130)
Lung	(49, 360)	(50, 380)	(80, 650)	(120, 780)
Prostate	(0, 520)	(<0, 1860)	—	—
Breast	None	None	(120, 650)	(160, 610)
Uterus	—	—	(0, 180)	(<0, 131)
Ovary	—	—	(8, 99)	(9, 170)
Bladder	(22, 270)	(29, 330)	(11, 160)	(30, 290)
Remainder	(82, 740)	(120, 680)	(100, 860)	(120, 680)
Thyroid	(4, 69)	(5, 90)	(17, 310)	(25, 440)
Solid cancers	(320, 1970)	(490, 1920)	(520, 2800)	(740, 2690)

[1] Cases per 10,000 person-Gy for exposures at low dose and/or dose rates

4.7 Conclusions

The main results given in Section 4.6 suggest that the EPA risk projections for uniform whole-body radiation (total for all cancer sites) are likely to be within a factor of 2 or 3 of the "true" risk for the U.S. population. For many individual cancer sites, the projections and actual risks might differ by a factor of roughly 3 to 5, and even more for cancers of the stomach, prostate, liver, and uterus. For childhood exposures, the uncertainties are somewhat larger. An important caveat is that the analysis did not fully account for important uncertainties associated with the shape of the dose response at low doses and dose rates.

The quantitative uncertainty analysis did allow for sources of uncertainty, such as dosimetry errors and some cancer misdiagnosis, which were not quantified in BEIR VII. For sources of uncertainty quantified in BEIR VII, results from this analysis and BEIR VII are consistent for most sites.

Results from the EPA uncertainty analysis should not be over-interpreted. The results presented in Section 4.6 are meant solely as rough guidance on the (relative) extent to which "true" site-specific risks for a hypothetical stationary U.S. population might differ from the central estimates derived in Section 3. Distributions for uncertainty factors rely on subjective judgment, and it is not always possible to satisfactorily evaluate "biases" associated with sources of uncertainty such as risk transport. Modeling uncertainties, *e.g.*, the uncertainty associated with BEIR VII model assumptions on how ERR depends on attained

age, age-at-exposure, and TSE, are often especially difficult to quantify. Uncertainties in mortality risk projections associated with changes in cancer fatality rates were not evaluated.

5. Risks from Higher LET Radiation

5.1 Alpha Particles

Assessing the risks from ingested or inhaled α-emitting radionuclides is problematic from two standpoints. First, it is often difficult to accurately estimate the dose to target cells, given the short range of α-particles in aqueous media (typically < 100 μm) and what is often a highly non-uniform distribution of a deposited radionuclide within an organ or tissue. Second, for most cancer sites, there are very limited human data on risk from α-particles. For most tissues, the risk from a given dose of alpha radiation must be calculated based on the estimated risk from an equal absorbed dose of γ-rays multiplied by an "RBE" factor that accounts for different carcinogenic potencies of the two types of radiation, derived from what are thought to be relevant comparisons in experimental systems.

The high density of ionizations associated with tracks of α-particles produces DNA damage which is less likely to be faithfully repaired than damage produced by low-LET tracks. Consequently, for a given absorbed dose, the probability of inducing a mutation is higher for alphas, but so is the probability of cell killing. The effectiveness of α-particle radiation relative to some reference low-LET radiation (*e.g.*, 250 kVp X- rays or ^{60}Co γ-rays) in producing a particular biological end-point is referred to as the α-particle relative biological effectiveness (RBE). The RBE may depend not only on the observed end-point (induction of chromosome aberrations, cancer, etc.), but on the species and type of tissue or cell being irradiated, as well as on the dose and dose rate.

In most experimental systems, the RBE increases with decreasing dose and dose rate, apparently approaching a limiting value. This mainly reflects reduced effectiveness of low-LET radiation as dose and dose rate are decreased — presumably because of more effective repair. In contrast, the effectiveness of high-LET radiation in producing residual DNA damage, transformations, cancer, etc. may actually decrease at high doses and dose rates, at least in part due to the competing effects of cell killing. For both low- and high-LET radiations, it is posited that, at low enough doses, the probability of a stochastic effect is proportional to dose and independent of dose rate. Under these conditions, the RBE is maximal and equal to a constant RBE_M. In order to estimate site-specific cancer risks for low dose alpha radiation, we need a low-dose, low-LET risk estimate for that site and an estimate of the RBE_M.

5.1.1 Laboratory Studies. The experimental data on the RBE for α-particles and other types of high-LET radiation have been reviewed by the NCRP (NCRP 1990) and the ICRP (ICRP 2003). From laboratory studies, the NCRP concluded that: "The effectiveness of α-emitters is high, relative to β-emitters, being in the range of 15 to 50 times as effective for the induction of bone

sarcomas, liver chromosome aberrations, and lung cancers." The NCRP made no specific recommendations on a radiation weighting factor for alpha radiation.

The ICRP has reiterated its general recommendation of a radiation weighting factor of 20 for α-particles (ICRP 2003, 2005). However, ICRP Publication 92 further states (ICRP 2003):

> Internal emitters must be treated as a separate case because their RBE depends not merely on radiation quality, but also, and particularly for α-rays with their short ranges, on their distribution within the tissues or organs. It is, accordingly, unlikely that a single w_R should adequately represent the RBE_M for different α emitters and for different organs. The current w_R of 20 for α-rays can thus serve as a guideline, while for specific situations, such as the exposure to radon and its progeny, or the incorporation of ^{224}Ra, ^{226}Ra, thorium, and uranium, more meaningful weighting factors need to be derived.

Another set of recommendations for α-particle RBE is contained in the NIOSH-Interactive RadioEpidemiological Program (NIOSH-IREP) Technical Documentation intended for use in adjudicating claims for compensation of radiogenic cancers (NIOSH 2002, Kocher *et al*. 2005). For α-particle caused solid cancers (other than radon-progeny-induced lung cancer), IREP posits a lognormal uncertainty distribution for its radiation effectiveness factor (REF, equivalent to RBE_M) with a median of 18 and a 95% CI [3.4, 101]. For leukemia, IREP employs a hybrid distribution: REF = 1.0 (25%); LN with UI[1,15] (50%); LN with UI [2,60] (25%).

Studies comparing groups of animals inhaling insoluble particles with attached α- or β-emitters have been performed to assess RBE for lung cancer. In a large long-term study of beagle dogs, Hahn *et al*. (1999) reported that the RBE was at least 20. An RBE of about 20 was also found in F344 rats for inhaled α-emitting $^{239}PuO_2$ particles, relative to β-particles from inhaled $^{144}CeO_2$ or fractionated X-irradiation (Hahn *et al*. 2010). An analogous study of lung cancer induction in CBA/Ca mice found that, in the limit of low doses, ^{242}Cm α-particles were 9.4 times (90% CI: 5,23) as effective in producing adenocarcinomas as ^{45}Ca β-particles; however, the apparent RBE_M was only 1.5 (90% CI: 0.7,9) for adenomas (Priest *et al.* 2006).

5.1.2 Human Data. Results from epidemiological studies of groups with intakes of α-emitting radionuclides can be used directly to develop site-specific cancer risk coefficients for alpha radiation; they can also be used in conjunction with low-LET studies to estimate RBE; finally, these results can be used in combination with estimates of RBE to derive low-LET risk estimates where none can be obtained from low-LET studies.

There are 4 cancer sites for which there are direct epidemiological data on the risks from alpha irradiation: bone, bone marrow, liver, and lung. Not coincidentally, these are sites for which we are particularly interested in obtaining high-LET risk estimates because they are ones which tend to receive higher than

average doses of alpha radiation from certain classes of internally deposited radionuclides. For each of these sites except bone, we also have risk estimates for low-LET radiation derived from the LSS.

Bone cancer. Although new data are being obtained from research on Mayak plutonium workers (Koshurnikova *et al*. 2000, Sokolnikov *et al*. 2008), the most extensive sources of information on radiogenic bone cancer in humans continue to be from: (1) radium dial painters ingesting ^{226}Ra and ^{228}Ra and (2) patients injected with the shorter-lived isotope ^{224}Ra.

Given their long radioactive half-lives, the radionuclides ingested by the dial painters had time to redistribute throughout the mineral bone before decaying. It is estimated that the average α-dose to target endosteal cells is about 50% of the average skeletal dose (Marshall *et al*. 1978). The shorter-lived ^{224}Ra, however, is largely confined to the bone surface so the endosteal dose is higher than the average skeletal dose. Speiss and Mays (1970) estimated that the endosteal dose was higher by a factor of 9, but a subsequent determination of the surface-to-volume ratio in bone reduced the estimated factor to 7.5 (Lloyd and Hodges 1971, NAS 1980).

EPA has taken its estimates of risk of α-particle induced bone sarcoma from the BEIR IV analysis of the ^{224}Ra data, which is consistent with a linear, no-threshold dose response (NAS 1988, EPA 1994). The corresponding low-LET risk estimate (per Gy) was assumed to be a factor of 20 lower than that based on the assumed α-particle RBE_M of 20.

Subsequent to BEIR IV, improvements have been made in the dosimetry for the ^{224}Ra patients, especially those treated as children. Some additional epidemiological data have also become available. The updated data set has been analyzed by Nekolla *et al*. (2000) and found to be well-described by an absolute risk model, which for small acute doses reduces to the form:

$$\Delta r = \alpha D g(e) h(t),$$

where Δr is the increment in bone cancer incidence from an endosteal dose, D, of α-particle radiation; $g(e)$ reflects the variation in risk with age at exposure (e); and $h(t)$ represents the variation with time after exposure (t). A good statistical fit was found for $g(e)$ as an exponentially decreasing function of age at exposure, and for $h(t)$ as a lognormal function of time after exposure.

Normalizing the time integral of $h(t)$ to unity, a maximum likelihood calculation yielded:

$$\alpha = 1.782 \times 10^{-3}\ \mathrm{Gy}^{-1},$$

$$g(e) = \exp[-0.0532\,(e-30)],$$

$$h(t) = (2\pi\sigma^2)^{-1/2} \times \exp\left[-\frac{(\ln(t)-\ln(t_0))^2}{2\sigma^2}\right] \times \frac{1}{t},$$

where t_0 is 12.72 y and σ is 0.612. Thus, the temporal response, *h(t)*, has a GM = 12.72 y and a GSD = e^{σ} = 1.844.

For estimates of bone cancer risk from alpha radiation, we adopt the model and calculational methods of Nekolla *et al*., with two modifications. First, those authors assumed, for simplicity, a fixed life-span of 75 y; our lifetime estimates are derived using their derived mathematical models, but, as with our other risk estimates, applied in conjunction with gender-specific survival functions determined from U.S. vital statistics. Second, Nekolla *et al*. adopted the ratio of 9 for endosteal to skeletal dose published by Speiss and Mays; we employ the updated estimate of 7.5. The effect of this change is to increase the coefficient α in the model above by a factor of 1.2 (= 9/7.5). With these modifications, the calculated average lifetime risk of bone cancer incidence is 2.5×10^{-3} Gy^{-1} for males and 2.3×10^{-3} Gy^{-1} for females. The population average of 2.4×10^{-3} Gy^{-1} is close to the FGR-13 estimate of 2.72×10^{-3} Gy^{-1} (EPA 1999b). About 35% of all bone cancers are fatal (SEER Fast Stats), and it is assumed here that the same lethality holds for radiogenic cases – half that previously assigned (EPA 1994). Thus, the mortality risk projections for α-particle induced bone cancer are: 8.6×10^{-4} Gy^{-1} (males), 8.2×10^{-4} Gy^{-1} (females), and 8.4×10^{-4} Gy^{-1} (sex-averaged).

There has been a great deal of discussion in the scientific literature concerning a possible threshold for induction of bone sarcoma (NAS 1988). Often cited is a plot of bone cancer risk versus dose in radium dial painter data, which appears to show a rather abrupt threshold at about 10 Gy. However, it has been pointed out that such an apparent threshold may be an artifact of presenting the data on a semi-log plot (incidence vs. log dose); Mays and Lloyd found that a conventional plot of incidence vs. dose is consistent with linearity (Mays and Lloyd 1972, NAS 1988). In laboratory studies, Raabe *et al*. (1983) found that the mean time to tumor increases with decreasing dose rate, suggestive of a "practical threshold" in dose rate below which the latency period would exceed the lifespan of the animal. However, interpretation of this finding remains controversial (NAS 1988), and Rowland has noted that – contrary to the practical threshold hypothesis – bone sarcomas sometimes appeared in dial painters at short times after low intakes of radium (Rowland 1994). It has also been postulated that a sub-linear dose response relationship, resulting in a practical threshold below which the risk is negligible, might be produced by a requirement for two radiation-induced initiation steps (Marshall and Groer 1977, NAS 1988) or by the need for radiation-induced stimulation of cell division (Brenner *et al*. 2003).

A more recent statistical analysis of bone sarcomas in the dial painters concluded that the data could be fit with a linear model having a threshold at about 9 Gy but was inconsistent with a linear no-threshold model, even when a cell killing term was included (Carnes *et al*. 1997, Hoel and Carnes 2005). In contrast, the incidence of bone cancer among the ^{224}Ra patients was consistent with a linear no-threshold dose-response (BEIR IV, Nekolla *et al*. 2000), and there was evidence of an excess of bone cancers among a group of ankylosing spondylitis patients who received an estimated average endosteal dose of about 6 Gy – somewhat below the "threshold" dose estimated from the dial painter data.

One possible explanation for the discrepancy is that the differences in temporal and spatial pattern of the doses for two sets of nuclides give rise to a threshold in the case of ^{226}Ra and ^{228}Ra, but not ^{224}Ra. However, no plausible mechanism has been put forth for a linear, threshold model, and it is very hard to reconcile it with the standard paradigm for radiation-induced cancer in which cancer risk is enhanced by radiation-induced mutations in target cells, here presumably those contained in the endosteal cell layer.

Hoel and Carnes fit the radium dial painter data to a number of different dose response functions. Of these, the linear-threshold model provided the best fit. However, that model is only one example of a simple 2-component spline function (one in which there is zero slope up to an estimated threshold at 9 Gy and a positive slope at higher doses). Alternatively, the data could be fit to other 2-component spline functions having a positive (non-zero) slope up to some break point, above which the slope is increased. A range of such models would also be consistent with the dial painter data and are arguably as biologically plausible as the linear-threshold model. In particular, as shown below, the lack of observed bone cancers in the dial painters between 0 and 10 Gy is not inconsistent with the slope inferred from the patients injected with ^{224}Ra. In addition, an important limitation to the analysis of Hoel and Carnes is that it does not factor in the uncertainties in dosimetry, which could distort the shape of the dose-response in a way that produces an apparent threshold.

For many of the dial painters, there were possible complicating effects of tissue damage (fibrosis) associated with very high doses (10-200 Gy) of alpha radiation in the bone (Lloyd and Henning 1983). The usefulness of the dial painter data for low dose risk estimation also suffers from several other problems: the intake of radium was estimated many years after the event and may be inaccurate; the distribution of radium in the bone is nonuniform and "hot spots" capable of extensive cell killing may have occurred; the continuous receipt of dose makes it difficult to separate out the fraction of dose associated with cancer induction; the contributions from α-emitters and other radiations accompanying radium decay cannot be separated; and the fraction of the total dose to the endosteal cells cannot be specified precisely (Boice 2006).

Although no bone sarcomas were observed in dial painters who received an estimated dose of less than 10 Gy, this is not inconsistent with the linear projection based on the ^{224}Ra patients. Overall, 449 dial painters were classified as receiving an average skeletal dose > 0 but < 10 Gy. The estimated collective skeletal dose for this group was 738 person-Gy (Hoel and Carnes 2005). As noted above, the endosteal dose has been estimated to be ≈ 50% of the average skeletal dose, so the collective endosteal dose among these dial painters is calculated to be about 370 person-Gy. The risk coefficient derived from the ^{224}Ra patients is ≈ 2.4×10^{-3} Gy^{-1} (see above); hence, < 1 radiogenic bone cancer would be projected among the dial painters whose doses were below the posited threshold. On this basis, the dial painter data does not have the power to reject the low-dose risk estimate derived from the ^{224}Ra patients.

On the other hand, only 4 bone cancers were observed among the low-dose ^{224}Ra-treated spondylitis patients, whereas 7.8 radiogenic cases would be projected from the linear model, and 1.3 spontaneous cases would be expected. Moreover, none of the 4 cases were osteosarcomas, even though the majority of cases at higher doses were of that type. According to Nekolla *et al*. (2000), these findings suggest that the model projection based on the ^{224}Ra patient data may be conservative. These authors further note that a zero initial slope could not be rejected based on a linear-quadratic fit to the ^{224}Ra patient data.

Bijwaard *et al*. (2004) have carried out a biologically based modeling study of radiation-induced bone cancer incidence in beagles and in radium dial painters in which it was assumed that: (1) mutation of a stem cell produces an altered “intermediate” cell; (2) clonal expansion creates a pool of the intermediate cells; (3) mutation in an intermediate cell produces a malignant cell; and (4) the single malignant cell repeatedly divides to form a tumor. In earlier work, where the 2-mutation model was applied to data on radon-induced lung cancer in rats, it was found that the process was dominated by a linear increase in the first mutation rate with dose, leading to a linear increase in cancer risk with dose (Bijwaard *et al*. 2001). However, in the case of bone cancer induction in beagles, it appeared that the radiation had affected both mutational steps, leading to a linear-quadratic dose-response at lower doses, where cell-killing effects could be neglected. The data on radium dial painters showed a similar dependence (Leenhouts and Brugmans 2000, Bijwaard *et al*. 2004).

Sokolnikov *et al*. (2008) found an excess of bone cancer in plutonium exposed workers at the Mayak nuclear plant in Russia. The evidence for a bone cancer dose-response rests on only 3 deaths, all occurring in individuals with an estimated bone surface dose exceeding 10 Gy. Nevertheless, the data were not inconsistent with a linear dose-response relationship.

Studies of patients receiving radiotherapy for childhood cancers indicate that low-LET radiation exposure also increases the risk of bone cancer (Tucker *et al*. 1987, Hawkins *et al*. 1996, Vu *et al*. 1998). Also noteworthy, especially in view

of the presumed lower biological effectiveness of low-LET radiation, is that Vu *et al*. (1998) found an excess risk among patients receiving a localized bone dose of 1-10 Gy, with a mean dose of approximately 3 Gy, substantially lower than the threshold absorbed dose for α-particles suggested by the spline fit to radium dial painter data discussed above (Hoel and Carnes 2005). Hawkins *et al*. (1996), on the other hand, reported no observed risk below 10 Gy; however, in their study the median dose among irradiated patients receiving < 10 Gy was only about 0.1 Gy. The data are sparse, and the authors did not derive quantitative risk coefficients. Nevertheless a rough estimate of the ERR/Sv based on the data in Hawkins *et al*. is in reasonable agreement with that derived from the ^{224}Ra data, but with wide uncertainty bounds (unpublished calculations).

An RBE for bone cancer induction can be derived from a comparative analysis of data on beagles injected with the α-emitter ^{226}Ra or the β-emitter ^{90}Sr, both of which are distributed fairly uniformly throughout the volume of calcified bone (Mays and Finkel 1980, Bijwaard *et al*. 2004) . Employing a two-mutation model for bone cancer induction, Bijwaard *et al.* found that the dose-response relationships for both these radionuclides were approximately linear-quadratic at low doses, and that the linear coefficient was approximately 9.4 times higher for radium than for strontium. Based on this finding, EPA is adopting a revised RBE value of 10 for bone cancer; *i.e.*, the risk per Gy for low-LET radiation is assumed to be 1/10 that estimated for α-particle radiation.

Uncertainty. Based on a consideration of sampling error alone, Nekolla *et al*. derived a standard error of only ±33% on the slope of the linear dose-response relationship derived from the ^{224}Ra patient data, but a zero initial slope could not be excluded. A linear-quadratic fit to that data yielded about a 20% reduction in the best estimate of the linear coefficient. As discussed above, the ^{226}Ra data in both animals and humans are suggestive of a sublinear dose-response relationship for bone cancer, but the case for a threshold is unconvincing.

Recognizing that the estimate may be conservative, EPA has adopted the model for bone cancer risk due to alpha radiation derived by Nekolla *et al*. from the ^{224}Ra patient data. The uncertainty distribution is taken to be triangular with the vertex at the nominal estimate and the lower and upper bounds at zero and twice the nominal estimate, respectively. For low-LET radiation, the nominal estimate of risk per Gy is 10 times lower but the upper bound is taken to be 4 times the low-LET nominal estimate, reflecting additional uncertainty associated with the difference in biological effectiveness between low-LET radiation and α-particles.

Leukemia. Excess leukemia cases have not been observed in studies of radium dial painters or patients injected with high levels of ^{224}Ra, although in some cases there was evidence of blood disorders that may have been undiagnosed leukemias (NAS 1988). It appears from these studies that bone

sarcoma is a more common result of internally deposited radium, and that the radium leukemia risk is much lower than that calculated using ICRP dosimetry models together with a leukemia risk coefficient derived from the LSS weighted by an RBE of 20 (Mays *et al*. 1985, NAS 1988, Harrison and Muirhead 2003, Cerrie 2004). More recently, however, an excess of myeloid leukemia has been found in ankylosing spondylitis patients receiving lower doses of ^{224}Ra (Wick *et al*. 1999, 2008). Supported also by data on ^{224}Ra injected mice (Humphreys *et al*. 1993), it was hypothesized that at high doses the bone cancer risk is predominant, but at low doses the bone cancer risk is diminished and replaced by a leukemia risk (Wick *et al*. 2008).

In part, the anomalously low risk of leukemia from α-particles might be attributed to microdosimetry: *i.e.*, target cells may be non-uniformly distributed in the bone marrow in such a way that the dose to these cells is considerably lower than the average marrow dose. Evidence suggests, however, that microdosimetric considerations do not fully account for the lower risk, and that high-LET radiation is only weakly leukemogenic. Thorotrast patients, who are expected to have a more even distribution of α-particle energy, do show an excess of leukemia, but only about twice the risk per Gy as seen in the LSS (ICRP 2003). Moreover, an RBE of only about 2.5 has been found for neutron-induced leukemia in mice (Ullrich and Preston 1987), a situation in which the high-LET radiation dose would have been nearly uniform throughout the marrow.

The BEIR VII low-LET risk estimate for leukemia incidence is roughly 50% higher than that of UNSCEAR (2000b) or EPA (1994). Using a Bayesian approach, Grogan *et al*. (2001) estimated the α-particle leukemia risk to be 2.3×10^{-2} per Gy. If one adopts the BEIR VII low-LET leukemia (incidence) risk estimate, this would correspond to an RBE of approximately 2.9. Through a comparison of Thorotrast and A-bomb survivor data, Harrison and Muirhead (2003) also estimated the RBE to be 2-3. However, the authors noted that the Thorotrast doses were likely to be underestimated by a factor of 2-3 (Ishikawa *et al*. 1999), and that the RBE was perhaps very close to 1.

Ankylosing spondylitis patients (mostly young adult males) injected with relatively low amounts of ^{224}Ra had a higher rate of leukemia than that projected from the general population or that observed in a group of unirradiated control patients (Wick *et al*. 1999, 2008). After 26 y of average follow up, the exposed group of 1471 patients had 19 leukemias compared to 6.8 expected based on age- and gender-specific population rates; after 25 y of average follow up, the 1324 control patients had 12 leukemias (7.5 expected). The average dose to bone surface was estimated at 5 Gy in these patients. According to ICRP dosimetry models, the average marrow dose is about 10% of the bone surface dose for internally deposited ^{224}Ra (ICRP 1993). Thus, the estimated average marrow dose is ≈ 0.5 Gy, and the excess risk, calculated using the population projected rate is ≈ 1.7×10^{-2} Gy^{-1}. This is about twice the leukemia risk projection for 30-y old males derived in BEIR VII from the LSS data (NAS 2006, p. 281). Thus, these radium-injection data are also roughly consistent with an RBE of

about 2. Alternatively, if the unirradiated control patients are used as the comparison group, the estimated risk per Gy and RBE are roughly halved. Hence, these data also support an RBE for leukemia induction of about 1-2. It should be noted, however, that the temporal variation of excess leukemias appeared different in this study from that observed in the LSS (Wick *et al*. 1999).

EPA has been employing an RBE of 1 for α-particle induced leukemia (EPA 1994). Based on the information discussed above, the RBE is being adjusted upward to a value of 2, with a confidence interval of 1-3.

Liver cancer. The LSS shows a statistically significant excess of liver cancer. The uncertainty bounds derived by BEIR VII are wide, both because of the large sampling error and the uncertainty in the population transport (liver cancer rates are about an order of magnitude lower here than in the LSS cohort). The BEIR VII central estimate for gamma radiation is ≈ $2x10^{-3}$ Gy^{-1}; the EPA central estimate based on the weighted AM rather than the weighted GM of the two methods for transferring risk from the LSS to the U.S. population is ≈ 3 $x10^{-3}$ Gy^{-1}. For comparison, updated analyses of data on Thorotrast patients from Denmark (Andersson *et al*.1994) and Germany (van Kaick *et al*. 1999) yielded estimates of $7x10^{-2}$ and $8x10^{-2}$ excess liver cancers per Gy, respectively. Assuming an RBE of 20 for the α-particle RBE, these values are about 20% higher than what would be projected from the EPA liver cancer model – quite reasonable agreement given the large uncertainties and difference in age and temporal distribution. However, Leenhouts *et al*. (2002) has reanalyzed the Danish Thorotrast data, employing a biologically based, two-mutation model of carcinogenesis, and derived a lifetime liver cancer risk estimate of $2x10^{-2}$ Sv^{-1} (4 $x10^{-1}$ Gy^{-1}), an order of magnitude higher than the BEIR VII central estimate, but consistent with the BEIR VII upper bound. One reason given by Leenhouts *et al*. for the higher risk estimate is that the model projects risk over a whole lifetime, whereas the original analysis by Andersson *et al*. addressed only the risk over the period of epidemiological follow-up. The increase may also partly stem from a correction for downward curvature in the dose-response function at high doses.

An excess of liver cancer has been found among workers at the Mayak nuclear facility in the Russian Federation, especially among workers with plutonium body burdens and among female workers (Gilbert *et al*. 2000). Averaged over attained age, the ERR per Gy for plutonium exposures was 2.6 for males and 29 for females. (Sokolnikov *et al*. 2008). For comparison, the BEIR VII risk model for γ-ray induced liver cancer derived from the LSS yields an ERR per Gy of 0.32 for males and females, calculated for exposure age 30 and attained age 60. Thus, the RBEs that would be derived from the LSS and Mayak worker study would be roughly 8 for males and 90 for females.

In conclusion, the Danish and German Thorotrast results are in good agreement with one another, and the risk projections derived from them are in quite reasonable agreement with what would be projected from the LSS,

assuming a plausible RBE of about 20. There is considerable uncertainty in the estimates, relating to uncertainty in the dose estimates, the fraction of the dose "wasted" because it was delivered after the cancer was initiated, and the extrapolation from high doses (several Gy) to low environmental doses. In addition, as seen from the Leenhouts *et al*. modeling exercise, there is considerable uncertainty in projecting risk over a whole lifetime, especially the contribution from childhood exposures. The results from the Mayak worker study appear to be in only fair agreement with those from the Thorotrast studies. Based on its review of the available information, EPA adopts a model for calculating α-particle induced liver cancer, which is a scaled version of the BEIR VII model, equivalent to multiplying the corresponding BEIR VII low-LET risk estimates, on an age- and gender-specific basis, by an RBE of 20. The population average risk is then $6x10^{-2}$ Gy^{-1}.

Lung cancer. Excess lung cancers have been associated with the inhalation of α-emitting radionuclides in numerous epidemiological studies. Cohort studies of underground miners have shown a strong association between lung cancer and exposure to airborne radon progeny. This association has also now been found in residential case-control studies. In addition, a cohort study of workers at the Mayak nuclear plant has also shown an association with inhaled plutonium (Gilbert *et al*. 2004). The miner studies serve as the primary basis for BEIR VI and EPA estimates of risk from radon exposure (NAS 1999, EPA 2003), and results from the residential studies are in reasonable agreement with those risk estimates (Darby *et al*. 2005, Krewski *et al*. 2005). The Agency has no plans at this time to reassess its estimates of risk from exposure to radon progeny, but it is the intent here to reassess estimates of risk from inhaled plutonium and other α-emitters, along with the lung cancer risk associated with low-LET exposures.

Table 5-1 compares summary measures of risk per unit dose for the U.S. population derived from the LSS in BEIR VII and from the pooled underground miner studies in BEIR VI. For radon, the estimation of lung dose requires a conversion from radon progeny exposure, measured in working level months (WLM). Estimating this conversion factor involves a model calculation of the deposition of radon progeny in the airways, the distribution of α-particle energy on a microdosimetric scale, and the relative weights attached to different tissues in the lung (NAS 1999, EPA 2003, James *et al*. 2004). Results are presented for the dose conversion factor of ≈ 12 mGy per WLM derived by James *et al*. (2004) and for the estimate of 6 mGy per WLM recommended in UNSCEAR 2000a.

When compared to results from animal studies, the inferred α-particle RBEs in Table 5-1 may appear to be unreasonably low – especially for females. It should be recognized, however, that the risk model used to derive risk estimates for radon are in certain ways incompatible with the models for low-LET lung cancer risk in BEIR VII. They differ not only with respect to their functional dependence on age, gender, and temporal factors, but also with respect to the interaction with smoking. In contrast to the BEIR VII models, the radon risk

models do not incorporate a higher risk coefficient for females or for children. The miner cohorts from which the radon models were derived consisted essentially entirely of adult males, and it is possible that radon risks are underestimated for children and females. The radon risk appears to be almost multiplicative with smoking risk (or the baseline lung cancer rate), whereas the LSS data suggests an additive interaction. It is unclear whether these apparent differences with respect to gender and smoking reflect a real mechanistic difference in carcinogenesis by the two types of radiation exposure (chronic alpha vs. acute gamma) or unexplained errors inherent in the various studies.

Table 5-1: Lung cancer mortality and RBE

Data Source	Gender	Risk per 10^6 Person-WLM	Risk per 10^4 Person-Gy		RBE	
A-bomb mortality	Male	—	140		1.0	
	Female	—	270		1.0	
	Combined	—	210		1.0	
EPA radon risk model	Male	640	800[1]	1600[2]	5.7[1]	11.4[2]
	Female	440	550[1]	1100[2]	2.0[1]	4.1[2]
	Combined	540	675[1]	1350[2]	3.2[1]	6.4[2]

[1] Risk per Gy to the whole lung or RBE calculated assuming: (1) 12 mGy/WLM, on average, to sensitive cells in the bronchial epithelium (James *et al*. 2004) and (2) lung risk partitioned 1/3 (bronchi): 1/3 (bronchioles): 1/3 (alveoli).

[2] Calculated assuming 6 mGy/WLM, on average, to sensitive cells in the bronchial epithelium (UNSCEAR 2000a).

Lung cancer results from the LSS cohort can also be compared with those on Mayak workers, whose lungs were irradiated by α-particles emitted by inhaled plutonium (Gilbert *et al*. 2004), but the results of such an analysis must be viewed critically. The dose from inhaled Pu is highly uncertain, as is the relative sensitivity of different target cells to radiation. Information on smoking in both cohorts is limited. The populations are quite different with respect to gender and age profile. Males account for about 75% of the PY and over 90% of the lung cancers among the internally exposed Mayak workers, but for only about 30% and 55% of the PY and lung cancers, respectively, among the LSS cohort. Another issue is that the dependence of the risk on attained age appears to be quite different in the two studies – a monotonically increasing EAR for the LSS, but a sharp decrease in the EAR above age 75 for the Mayak workers. There are, however, very few data on these older Mayak workers. Focusing just on lung

cancers appearing between ages 55 and 75, one finds that the central estimates of risk per Sv in the two studies are comparable, consistent with an RBE for α-particles of 10 or more.

A more recent analysis of the Mayak plutonium worker data, based on improved dosimetry, has been published (Sokolnikov *et al*. 2008). From a statistical modeling of the lung cancer data, it was estimated that the ERRs per Gy at age 60 were 7.1 for males and 15 for females. For comparison, the LSS study yielded an ERR per Gy of 0.32 and 1.4, respectively, for males and females, for exposure age 30 and attained age 60. Thus, the two sets of data together would suggest an RBE of roughly 20 for males and 10 for females.

The risk per unit dose estimate from the plutonium exposed Mayak workers appears to be considerably higher than that from the radon studies despite the fact that the lung dose from radon progeny is projected to be almost entirely to the epithelial lining of the airways, whereas the inhaled plutonium dose is expected to be concentrated in the alveoli, which is generally thought to be a much less sensitive region for cancer induction.

There seems to be no fully satisfactory way to reconcile all the results from the LSS, miner, and Mayak worker studies with what one would expect from the dosimetry and experimental determinations of α-particle RBE, even taking into account the sampling errors in the various epidemiological studies. The Mayak study is ongoing, with possible improvements in the dosimetry still to be made; the LSS risk estimates are also somewhat suspect, especially their dependence on gender and age at exposure (see Section 3.2). In particular, it is odd that the risk among the A-bomb survivors is higher in females than males, despite the much lower lung cancer incidence among Japanese women than men. Also, the BEIR VII lung cancer model reflects the negative trend with age at exposure obtained from the analysis of ***all solid tumors***, but there is very little evidence to directly support a higher ***lung cancer*** risk for childhood exposures.

5.1.3 Nominal risk estimates for alpha radiation. Information on α-particle RBE_M (relative to γ-rays) for induction of cancer is sketchy, especially in humans. Laboratory studies are mostly indicative of a value of about 20, but with likely variability depending on cancer type and animal species or strain. There is also evidence in both animals and humans that the RBE_M is much lower for induction of leukemia. Comparisons of data on lung cancer induction by inhaled radon progeny or plutonium with data on the A-bomb survivors yields somewhat conflicting results, suggesting possible errors in the data or in the underlying assumptions regarding the form of the models, internal dosimetry, or the sensitivity of different parts of the lung. At this point, comparisons between the radon data and the LSS data suggest an RBE << 20 for lung cancer induction, but the Mayak results so far fail to substantiate this. Further follow-up of the LSS cohort and additional information on the Mayak workers may help to resolve this issue.

EPA's site-specific α-particle risk estimates will be obtained by applying an RBE of 20 to our γ-ray risk estimates, with two exceptions: 1) an RBE = 2 for leukemia and 2) continued use of models derived from BEIR VI to estimate lung cancer risk from inhaled radon progeny (NAS 1999, EPA 2003). The low-dose, γ-ray risk estimate for bone cancer is obtained by dividing the risk per Gy for α-particles – estimated from patients injected with ^{224}Ra – by an RBE of 10.

Aside from those revisions pertaining to leukemia, liver cancer, and bone cancer described above, this approach is consistent with previous EPA practice except in the case of breast cancer, where previously an RBE of 10 was employed rather than 20 (EPA 1994). The justification for the lower RBE was that the estimated (γ-ray) DDREF was 1 for breast cancer but 2 for other solid tumors. The evidence for such a difference in DDREF appears weaker now, and, for simplicity, we are now applying the same nominal DDREF (1.5) and RBE (20) for most solid tumors, including breast.

5.1.4 Uncertainties in risk estimates for alpha radiation. For most cancer sites, the uncertainty in α-particle risk can be calculated from the combined uncertainties in γ-ray risk, as presented in Section 4, and in α-particle RBE. For solid cancers, EPA previously assigned a lognormal uncertainty distribution to the α-particle RBE, with a 90% CI from 5 to 40. The median value is thus ≈ 14.1 and the GSD ≈ 1.88 (EPA 1999a). This distribution still appears reasonable for solid tumors other than bone cancers. The uncertainty distribution for leukemia induced by α-emitters deposited in the bone was previously taken to be uniform over the interval [0,1] (EPA 1999a). Based on the more current information discussed above, a lognormal distribution is now assumed, with GM = 2 and GSD = 1.4.

In the case of α-particle induced liver cancer, EPA is basing its 95% upper confidence limit on the risk estimate derived from the modeling approach of Leenhouts *et al*. (4×10^{-1} Gy^{-1}). This upper bound value is consistent with a log-normal distribution with a GM equal to EPA's nominal central estimate of 8×10^{-2} Gy^{-1} and a GSD of 2.66. The lower 95% confidence limit on the distribution is then 1.6×10^{-2} per Gy, which corresponds to what would be inferred from the LSS liver cancer risk estimate in conjunction with an assumed α-particle RBE of 8.

Risk projections for bone cancer are only important when considering internally deposited "bone-seekers." Given the difficulties in estimating the dose to target cells in bone, EPA is deferring the quantification of uncertainty in bone cancer risks until the Agency reevaluates the risks from specific internal emitters.

5.2 Lower Energy Beta Particles and Photons

As energetic electrons lose energy in passing through matter, they become more densely ionizing: *i.e.*, the average distance between ionization

events shrinks, and more energy is deposited in ionization clusters. As discussed earlier, such clusters produce DSBs and complex DNA damage that are more difficult for the cell to repair. Indeed it has been suggested that a large fraction of the residual damage caused by low-LET radiation may stem from such clusters produced at the ends of electron tracks (Nikjoo and Goodhead 1991). For this reason, it might be expected that lower energy β-particles would be more biologically damaging than higher energy betas. Furthermore, since the energy distribution of secondary Compton electrons is shifted downward as incident photon energy is reduced, the biological effectiveness of photons might also be expected to rise with decreasing energy, implying that lower energy photons, including medical X-rays, which typically have energies below 150 keV, might be more damaging than the γ-rays to which the LSS cohort was exposed.

Results from many studies tend to confirm these predictions for low-LET radiations, including measurements of chromosome aberrations, mutations, cell transformation and cancer induction. The most extensive source of data on the subject consists of comparative studies of X- and γ-ray induction of dicentrics in human lymphocytes. In these studies, 220-250 kVp X-rays generally produced 2-3 times as many dicentrics as ^{60}Co γ-rays (NCRP 1990, NAS 2006). The relevance of such findings for cancer induction is unclear; in particular, a dicentric will render a cell incapable of cell division. Other laboratory studies directed at ascertaining the RBE for various types of radiation, relative to X- or γ-rays, provide additional indirect information, suggesting again that the orthovoltage X-rays often used in radiobiology may be a factor of 2-3 times more hazardous than γ-rays with energies above about 250 keV (Kocher *et al*. 2005, NCRP 1990, NAS 2006). Kocher *et al*. further conclude that X-rays with energies < 30 keV, such as those used in mammography, may have a slightly higher RBE than those in the range 30-250 keV.

Kocher *et al*. also consider what RBEs should be applied to β-particles. Noting that the average energy of a Compton electron produced by an incident 250 keV photon is 60 keV, they conclude that β-particles above ≈ 60 keV should have about the same RBE as > 250 keV photons – *i.e.*, ≈ 1.0. One important radionuclide that emits a substantial fraction of its decay energy in the form of a lower energy beta is ^{3}H, for which the mean β-energy is 5.7 keV and the maximum is 18.6 keV. For ^{3}H and other betas with average energy below 15 keV, the authors recommend a lognormal uncertainty distribution with a GM = 2.4 and a GSD = 1.4, corresponding to a 95% CI of (1.2, 5.0). The reference radiation is again chronic γ-rays. In addition, they assign the same probability distribution to the RBE for internal conversion or Auger electrons with energy < 15 keV as for ^{3}H. This uncertainty range is comparable to what was recommended for < 30 keV photons and is generally consistent with experiments in which investigators compared ^{3}H with γ-rays in the induction of various end-points.

Kocher *et al*. also state that electrons of energy 15-60 keV would be expected to have about the same RBE as 30-250 keV photons but that direct biological data are lacking.

A review of tritium risks has recently been conducted by an independent advisory group for the Health Protection Agency of the UK (HPA 2007). The authors found that, in a wide variety of cellular and genetic studies, the RBE values for tritiated water (HTO) were generally in the range of 1-2 when compared with low dose-rate orthovoltage X-rays and 2-3 when compared with chronic γ-rays. The HPA Report also surveyed several laboratory studies comparing animal carcinogenesis by HTO and by chronic X-rays or γ-rays. Derived RBEs from those studies were generally consistent with those obtained *in vitro*, but it was pointed out that the carcinogenesis studies all suffered from methodological problems. Overall, the HPA Report concluded that "an RBE of two compared with high energy gamma radiation would be a sensible value to assume." Although much of the experimental evidence suggested a value between two and three, fractional values were "not considered appropriate."

The conclusions of the HPA report were supported by experimental and theoretical evidence (Nikjoo and Goodhead 1991, Goodhead 2006) that the biological effects of low-dose, low-LET radiation predominantly reflect complex DNA damage generated by ionization and excitation events produced by low energy electrons near the ends of their tracks with energies > 100 eV but no more than about 5 keV. Figure 5-1 shows a plot, for various incident radiations, of *F*, the cumulative fraction of the total dose deposited in an aqueous medium by electrons of energy *T* (> 100 eV). These fractions were estimated by Nikjoo & Goodhead (1991) using track-structure simulation codes, and results were found to be similar to those of a numerical approximation method developed by Burch (1957). Assuming that the amount of critical damage is proportional to *F*(5 keV), the estimated RBE is ≈ 2.3 for ^{3}H β-particles and ≈ 1.4 for 220 kVp X-rays, both relative to ^{60}Co γ-rays or 1 MeV electrons. Alternatively, if the critical damage is taken to be proportional to *F*(1 keV), the estimated RBEs would be ≈ 1.6 for ^{3}H and ≈ 1.2 for the X-rays.

Through a more accurate Monte Carlo procedure, Nikjoo and Goodhead calculated, for each of several initial electron energies, the cumulative fraction of the total dose deposited by electrons with energies between 100 eV and a specified energy. Those results are shown in Figure 5-2. From the figure, it is estimated that the contribution of low-energy (0.1-5 keV) electrons to the total dose from an electron with initial energy 10 keV would be ≈ 63%, compared to ≈51% for an incident 100 keV electron. The authors did not calculate the distribution for higher energy incident electrons, but assuming that the fractional increase in *F* obtained in applying the Monte Carlo method in place of the Burch approximation is about the same as for 100 keV electrons (≈10%), the result would be ≈37% for the higher energy electrons or ^{60}Co γ-rays. Using this approach, it should be possible to estimate average RBEs for a whole range of

low-energy β-emitters. Furthermore, from spectral information on the secondary electrons produced by a photon source of a given energy, RBEs could also be estimated for γ-ray emitters.

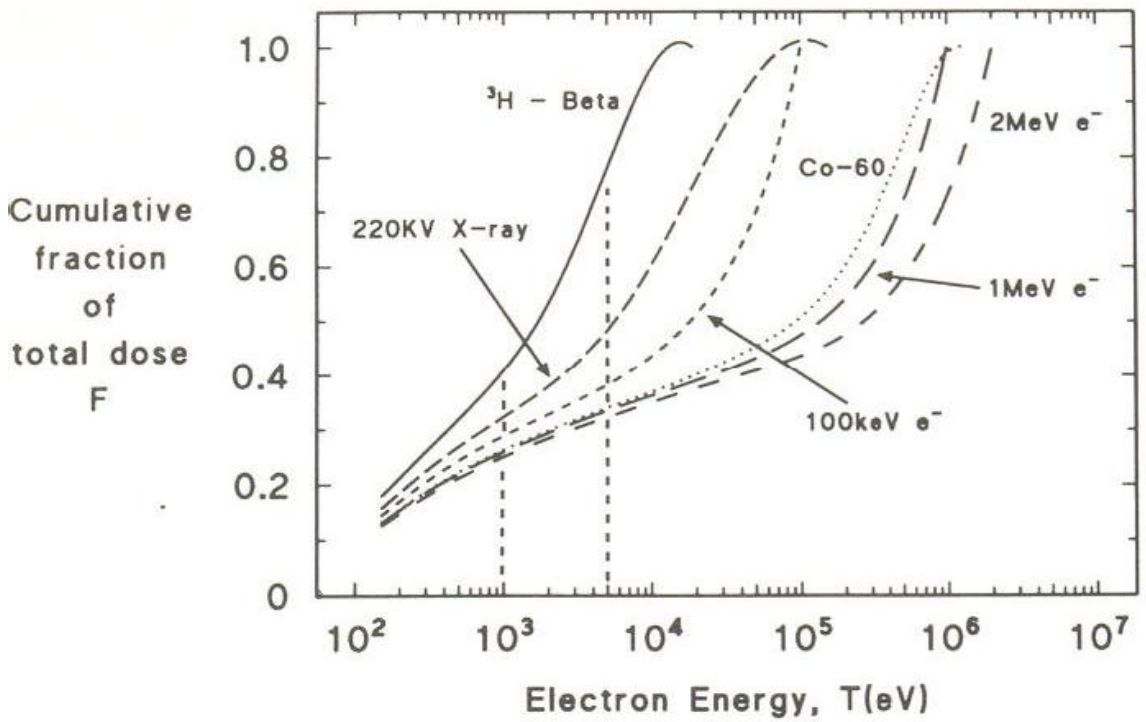

Figure 5-1: Cumulative fraction of the total dose, *F*, plotted against secondary electron kinetic energies, *T*, for a variety of low-LET radiations calculated by Nikjoo & Goodhead (1991) using the method of Burch (1957)

.

A comprehensive review on the subject of low energy electron and photon RBEs has recently been published (Nikjoo and Lindborg 2010). The authors tabulated results from experimental data on cell inactivation, chromosome aberrations, cell transformation, micronucleus formation, and DSBs and found a wide range of values, dependent on electron and photon energies, but apparently also on irradiation conditions, cell type, and experimental conditions. They also summarized results from biophysical modeling of DSB formation. Again there was a considerable spread in the estimated RBEs, presumably due to differences in the underlying assumptions and details of the calculations.

No firm conclusions can be drawn from human epidemiological data on the RBE for lower energy photons and electrons. Risk coefficients derived from studies of cohorts medically irradiated with X-rays are in some cases lower than what has been observed for the A-bomb survivors. Nevertheless, given the various uncertainties, such as those relating to dosimetry, sampling error, population differences, and possible confounders, it is still possible that medical X-rays are significantly more carcinogenic, per unit dose, than γ-rays (ICRP 2003, NAS 2006).

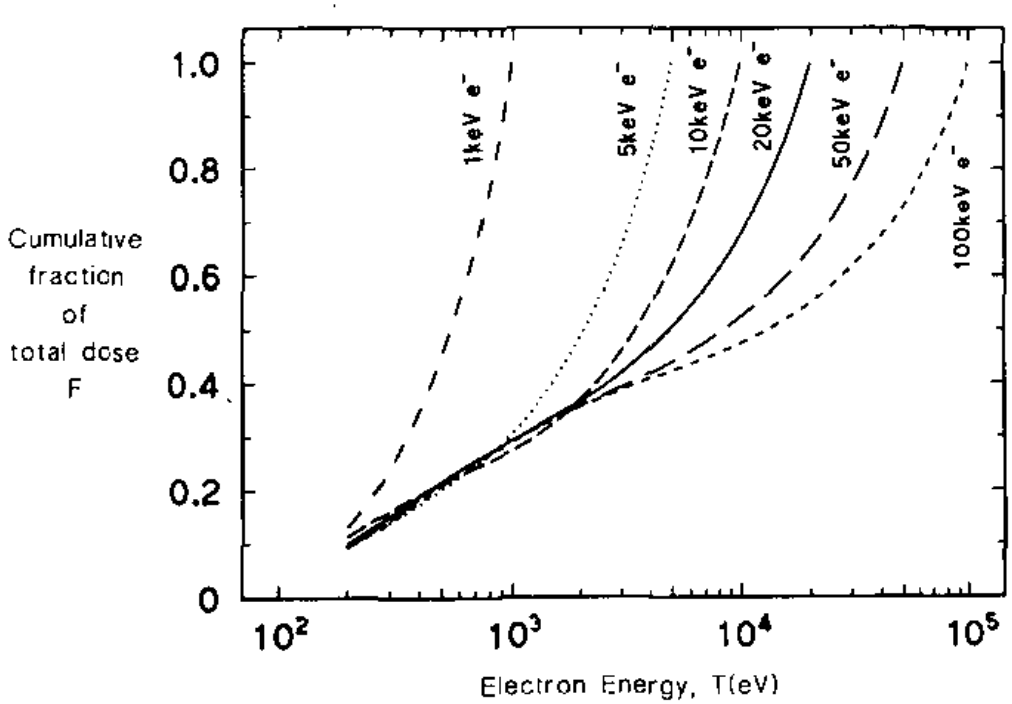

Figure 5-2: Cumulative fraction of total dose, *F*, plotted against secondary electron kinetic energies, *T*, for a variety of slow and fast initial electron energies calculated by the Monte Carlo track structure method (Nikjoo and Goodhead 1991).

In conclusion, there is strong experimental and theoretical support for the contention that low energy photons and electrons are more biologically effective than the γ-rays from a ^{60}Co source or those accounting for most of the dose received by the atomic bomb survivors in Hiroshima and Nagasaki (NAS 2006). However, this issue can only be fully resolved through experiment and a better understanding of the dependence of DNA damage and carcinogenesis on micro-dosimetric parameters. EPA is sponsoring a project aimed at deriving RBE values for low-LET emissions by specific radionuclides based on calculations of energy deposition and DNA damage events produced by low-energy electrons. The NCRP has also convened a committee to address the issue of RBEs for low energy, low-LET radiation. It is anticipated that these efforts can advance to the point where adjustments to the risk estimates for tritium, and possibly for other radionuclides, can be incorporated into the next version of FGR-13.

6. Risks from Prenatal Exposures

First carried out by Stewart and coworkers (Stewart *et al*. 1958, Bithell and Stewart 1975), case-control studies of childhood cancer have shown about a 40% increase in risk associated with exposure to diagnostic X-rays *in utero*. Typically, the X-rays employed in Stewart's "Oxford series" were 80 kVp and the mean dose was 6-10 mGy; this corresponds to only about 1 photon per cell nucleus. Hence this finding argues against the likelihood of a threshold for radiation carcinogenesis.

The estimate of risk for childhood cancer derived from the Oxford survey is about 0.06 per Gy (95% CI 0.01-0.126) for all cancers and about 0.025 per Gy for leukemia (Mole 1990, Doll and Wakeford 1997). Although numerous other case-control studies have shown a similar radiation-related risk as the Oxford survey (Doll and Wakeford 1997), the evidence from cohort studies is equivocal (Boice and Miller 1999). Children exposed *in utero* to radiation from the atomic bomb explosions have not experienced any detectable increase in cancer, and the derived upper bound is lower than the estimate derived from the case-control studies (Doll and Wakeford 1997). Results from a large cohort study did show an increase in leukemia of about the same magnitude as the Oxford series, but the observed increase in childhood solid tumors was much lower and not statistically significant (Monson and MacMahon 1984). Another question regarding the risk of solid tumors has been that the excess relative risk seen in the case-control studies is about the same, regardless of the type of tumor. This may suggest that the increase is due to some unaccounted for source of confounding (Boice and Miller 1999).

On balance, the evidence from the epidemiological studies indicates that the fetus is at risk of childhood cancer from ionizing radiation (Doll and Wakeford 1997). Following the recommendations of Doll and Wakeford (1997) and the ICRP (2000), EPA adopts the estimate of 0.06 Gy^{-1} for prenatal exposures to diagnostic X-rays. Since the individual radiation doses in the Oxford study were generally quite low, no DDREF adjustment is required to project risks at low doses or dose rates. However, as discussed in Section 5.2, an RBE > 1 should perhaps be assigned to X-rays commonly used in medicine. It would then be appropriate to divide the above estimate by the X-ray RBE to obtain the estimate of risk for higher energy γ-rays and electrons.

It can be inferred from recent SEER data (Altekruse *et al*. 2010: Tables 28.10 and 29.6) that long-term survival rates for childhood leukemias and solid cancers are approximately 70-80% (although this may not adequately account for delayed mortality due to second cancers resulting from the treatment). Based on those survival rates, the estimated childhood cancer mortality risk coefficient for prenatal exposures would be 20-30% of the incidence estimate.

The studies of medically irradiated fetuses only address the induction of childhood cancers. Epidemiological follow-up of the A-bomb survivors has indicated that individuals irradiated *in utero* may have a *lower* risk of adult cancers than those irradiated as young children, but the difference is not statistically significant (Preston *et al*. 2008). Based on this finding, we adopt the same set of models employed for calculating risk for exposure to young children to assess the risk of adult cancers due to an *in utero* exposure. More specifically, we directly applied the risk models of Section 3 with age-at-exposure set to 0. The sex-averaged projected risk for adult cancers (attained age > 15) is 0.29 Gy^{-1} for incidence and 0.12 Gy^{-1} for mortality. This risk is 2 or 3 times higher than that for the general U.S. population. It is also about 5 times the estimated risk of a radiogenic childhood cancer from prenatal exposures. Nevertheless it constitutes only a small fraction (< 3%) of the risk from a uniform whole-body exposure to the U.S. population.

7. Radionuclide Risk Coefficients

Subsequent to publication of this report, EPA plans to use its revised radiation risk models and ICRP's latest dosimetric models to update the radionuclide risk coefficients in Federal Guidance Report 13 (EPA 1999b). Radionuclide risk coefficients are EPA's best estimates of the lifetime excess mortality or morbidity risk per unit intake of a given radionuclide by ingestion or inhalation, or per unit exposure for external irradiation. The current version of FGR-13 contains risk coefficients for environmental exposure to over 800 radionuclides.

Based on the values in Tables 3-17 and 3-18, EPA expects that updated mortality risk coefficients for those radionuclides that irradiate the body uniformly will be similar to currently published values, whereas corresponding morbidity risk coefficients will likely increase by about 35%. For radionuclides irradiating the body nonuniformly, both increases and decreases are anticipated, depending on the target organ. For example, updated risk coefficients for inhaled radionuclides retained in the lung may be larger than present estimates because the population-averaged lung cancer risk has increased substantially over time. Conversely, updated risk coefficients for radionuclides that are poorly absorbed from the intestines into the bloodstream and that emit short-range radiation, especially α-particles, should be smaller than current values because of a reduced colon cancer risk coefficient and the adoption of new ICRP alimentary tract models (ICRP 2006) that place the location of target cells in the intestinal wall out of range of α-particles emitted from the contents of the colon.

8. Noncancer Effects at Low Doses

Hereditary effects. Ionizing radiation can produce mutations in the DNA of reproductive cells, which may be expressed as harmful hereditary effects in subsequent generations. Radiation-induced hereditary effects have been demonstrated in a number of species and have been extensively studied in laboratory mice. However, a statistically significant excess of these effects has not been detected in irradiated human populations, including the Japanese atomic bomb survivors. Epidemiological data can, therefore, only provide an upper bound on the magnitude of the genetic risk of radiation to humans.

Based on a careful consideration of the data on mice and known differences in the genetic make-up of mice and humans, the BEIR VII Committee arrived at a quantitative estimate of the genetic risk to humans. The total risk for all classes of genetic diseases was estimated to be about 3,000-4,700 cases per million first-generation progeny per Gy of low dose rate low-LET radiation (NAS 2006). This numerical estimate is defined relative to the "genetically significant dose," *i.e.*, the combined dose received by both parents prior to conception. The average parental age at the time of conception is roughly 30. So, for example, in a population receiving 1 mGy annually, the average genetically significant dose for each newborn will be approximately 30×2 mGy, or 60 mGy, and the estimated risk of an adverse genetic effect in the progeny will be $(180\text{-}280)\times10^{-6}$. For comparison, the estimated average lifetime risk of an incident cancer from a 1-mGy/y exposure is: $(1.1\times10^{-1}\ \text{Gy}^{-1})\ (75\times10^{-3}\ \text{Gy/lifetime}) \approx 8{,}000\times10^{-6}$. Thus, the estimated number of hereditary effects is low compared to the number of projected cancers.

Cardiovascular Disease. It is well established that high radiation doses (> 5 Gy), such as those sometimes administered therapeutically, can produce cardiovascular disease through direct damage to the structures of the heart and the coronary arteries (NAS 2000, UNSCEAR 2006, Little *et al*. 2008b). In addition, there is evidence of an increase in cardiovascular disease associated with much lower doses in the LSS cohort (Preston *et al*. 2003, Little *et al*. 2008b, Shimizu *et al*. 2010) and a few other groups (Little *et al*. 2008b) but the association in the LSS is not statistically significant at doses under 0.5 Sv (Shimizu *et al*. 2010), and the other studies, which focus on occupational cohorts, may suffer from bias.

Various biological mechanisms have been proposed that might increase the risk of cardiovascular disease at low doses: *e.g.*, mutational events in dividing epithelial cells of blood vessels, generating abnormal clones, which can, in turn, serve as sites for plaque formation. Although such mechanisms cannot be ruled out, the evidence for a low dose (< 0.5 Gy) risk of cardiovascular disease is not persuasive, and further research is required to understand the nature of the association between cardiovascular risk and radiation dose observed at moderate doses in epidemiological studies (Little *et al*. 2008b).

Cataracts. It is well established that exposure to ionizing radiation leads to the formation of cataracts (Ainsbury *et al*. 2009). The suggested mechanism involves radiation damage to dividing cells in the lens and their subsequent differentiation and migration, leading to the occurrence of opacities. Cataracts have been classified as a deterministic effect with a threshold of approximately 2 Gy, but recent data suggest a threshold of no more than about 0.5 Gy. There is, moreover, evidence of opacity formation in people exposed to chronic low-dose rate gamma radiation (Chen *et al*. 2001). Based on current data, it is possible that cataract induction is a linear, non-threshold phenomenon with a doubling dose of the order of 2 Gy (Ainsbury *et al*. 2009).

APPENDIX A: Baseline Rates for Cancer and All-Cause Mortality and Computational Details for Approximating LAR

Baseline rates. Age, gender and cancer site-specific cancer rates were obtained from NCI using the software packages SEER-Stat (for single ages from 0 to 84) and DevCan (for age categories 85-89, 90-94, and > 95). DevCan, which is available from the NCI's Surveillance Research Program's website (http://surveillance.cancer.gov), is software for calculating probabilities for developing and dying from cancer. Cancer rates in DevCan are conditioned on being alive and cancer free (at the beginning of each age interval), and were adjusted upward – usually by no more than about 1% – to account for individuals with two or more cancers.

For ages 0-84, SEER 13 data were used for 1998-1999 cancer rates, and SEER 17 data for 2000-2002 cancer rates. Generalized additive models were applied to the combined cancer rate data (from both SEER and DevCan), using the software package mcgv (version 1.6-1) in R (Wood 2006). Essentially, cancer rates were modeled as the sum of smooth (spline) functions of age with terms that allowed dependence on sex, and dataset (SEER 13 or SEER 17). The R program used to fit the cancer rate data is available on request.

Cancer rates for both incidence and mortality are graphed in Figure A-1.

Computational details. In Section 3.5, the integrals in Eq. 3-17 and 3-23 for calculating LAR were approximated using monotonic spline functions (Fritsch and Carlson 1980). However, before applying the spline functions, discontinuities in inte-grands were removed using a simple smoothly varying function. For almost all solid cancer sites, these discontinuities occur at the time of minimum latency (5 y), at which point the BEIR VII models specify that the ERR and EAR suddenly jump from 0 to some positive value.

The LAR for an exposure at age e is:

$$LAR(D,e) = \int_0^{110} M(D,e,a) \cdot S(a)/S(e) da \,.$$

Here, $M(D,e,a)$ is the excess risk at attained age a that, for most sites, would be calculated using a BEIR VII ERR or EAR model. For all solid cancer sites other than bone, $M(D,e,a)$ would be discontinuous at a-e = TSE = 5. In part, because such discontinuities are not biologically plausible, we replaced values of M with M*, where

$$M^*(D,e,a) = 0, \quad TSE < 4$$

$$M^*(D,e,a) = \frac{(TSE-4)^2}{(TSE-4)^2 + (TSE-6)^2} M(D,e,a), \quad 4 \le TSE \le 6$$

$$M^*(D,e,a) = M(D,e,a), \quad TSE > 6.$$

Spline functions were then used to approximate the integral

$$LAR(D,e) = \int_0^{110} M^*(D,e,a) \cdot S(a)/S(e) da \,.$$

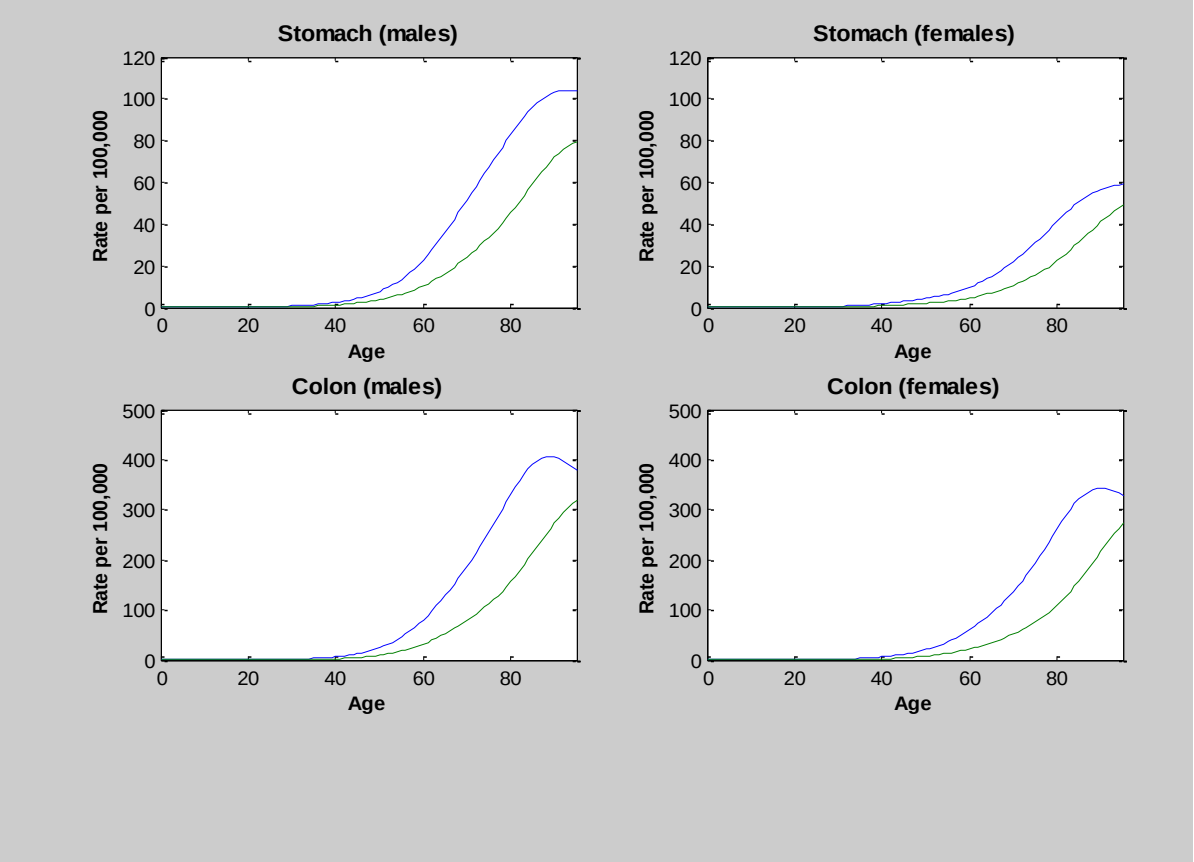

Figure A-1: The upper (blue) and the lower (green) curves show baseline incidence and mortality rates, respectively.

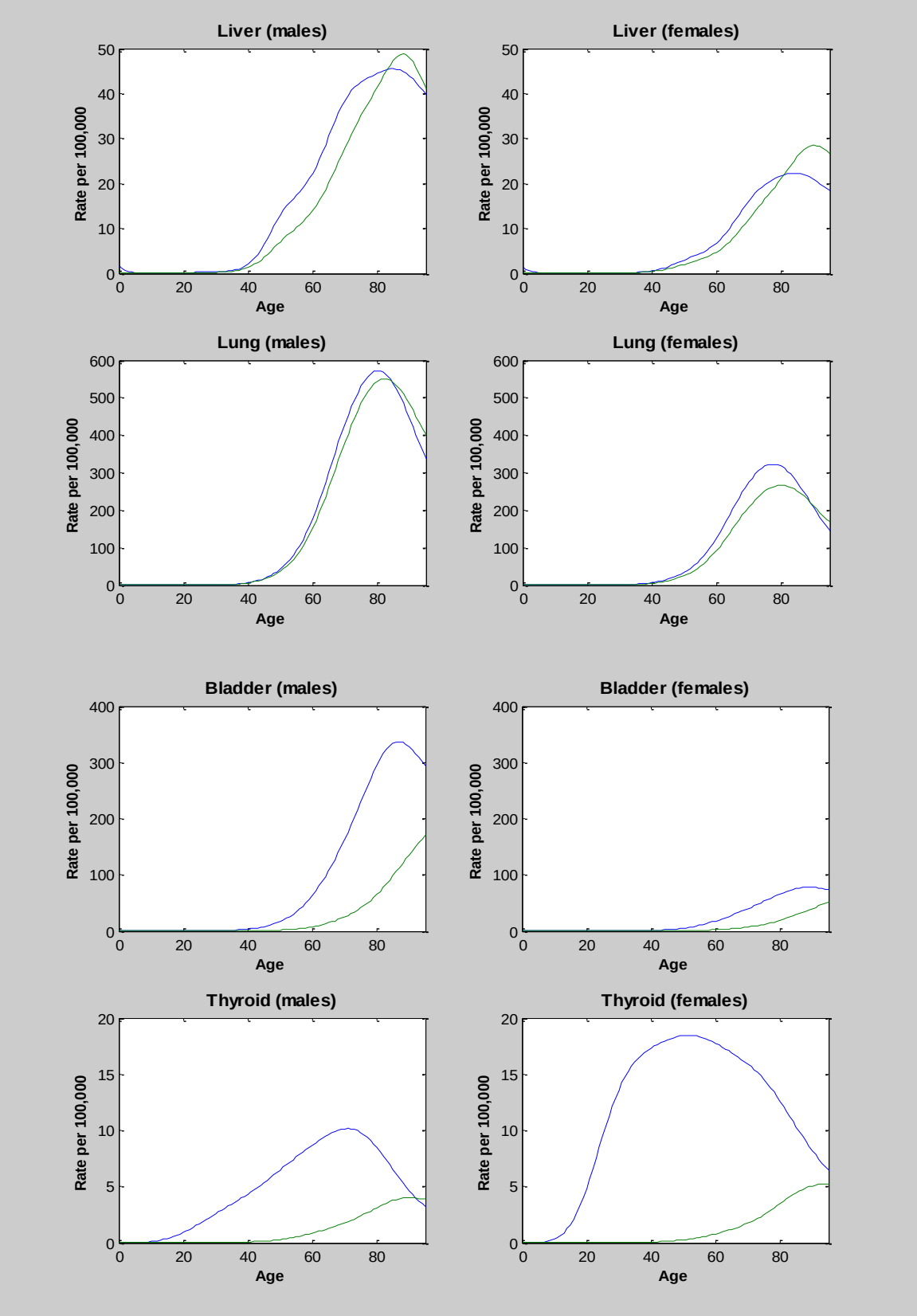

Figure A-1 (continued)

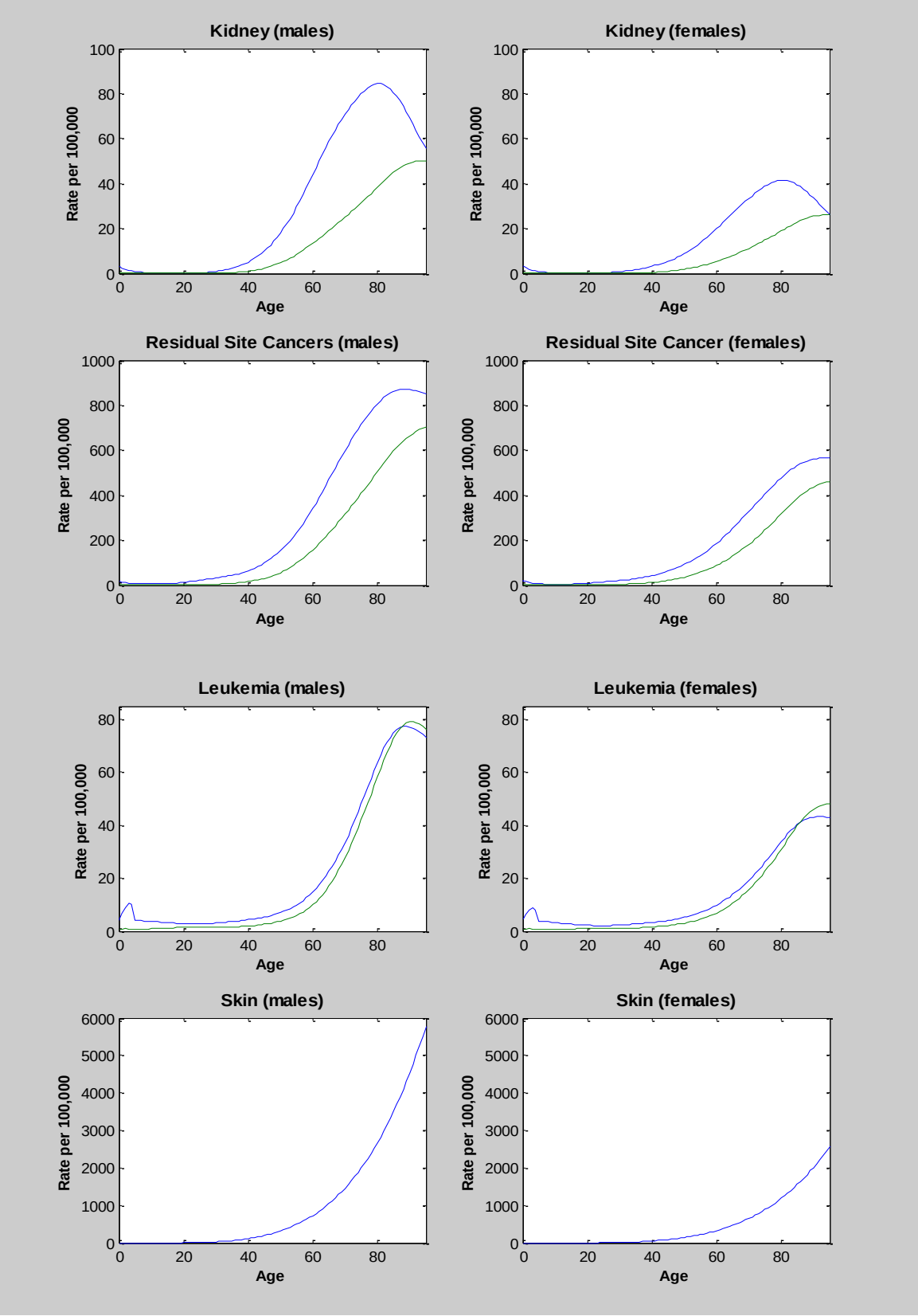

Figure A-1 (continued)

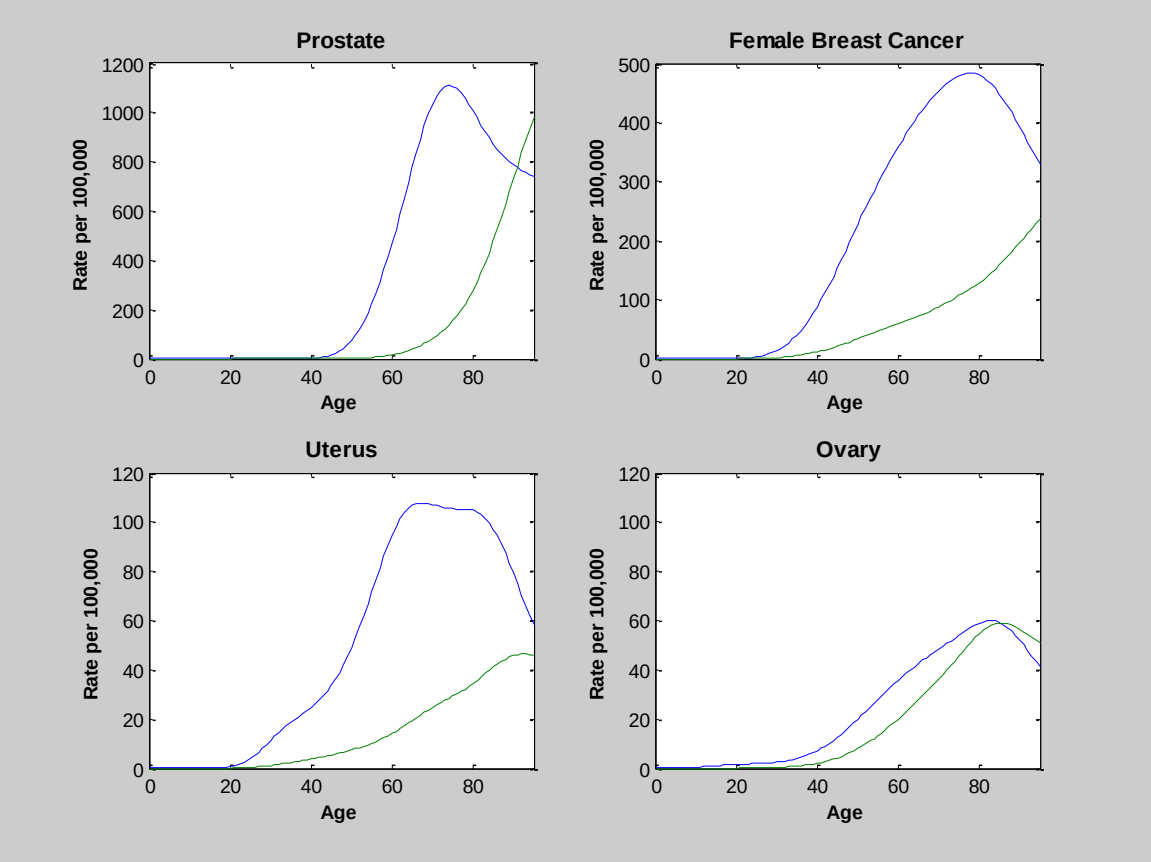

Figure A-1 (continued)

APPENDIX B: Details of Bayesian Analysis

Data. The dataset is a subset of the incidence data for the follow-up period 1958-1998, which was analyzed by Preston *et al*. (2007). The data can be downloaded from RERF at http://www.rerf.or.jp/library/dle/lssinc07.html (file lssinc07.csv). The dataset incorporates the latest (DS02) dosimetry and is otherwise essentially the same as the one used for the BEIR VII analysis, in that it excludes the "not-in-city" group (see Preston *et al*. 2007 for details). The data is in the form of an event-time table, which includes the number of cancer cases and person-years for subgroups defined by city, sex, and intervals based on dose, age-at-exposure, attained age, and follow-up time.

Risk models. For most solid cancer sites, BEIR VII ERR models were used. That is, for a specific cancer site, the ERR for an atomic bomb survivor is:

$$ERR(D,s,e,a) = \beta_s D \exp(\gamma e^*)(a/70)^{\eta},$$

where a and e denote attained age and age-at-exposure, and e^* is the age-at-exposure function, which is set to 0 for ages > 30. The corresponding cancer rate is:

$$\lambda(d,s,a,b,c) = \lambda_0(s,a,b,c)[1+ERR(D,s,e,a)]$$

Here, $\lambda_0(s,a,b,c)$ denotes the baseline rate, which depends on sex (s), attained age (a), year of birth (b), and city (c).

Baseline cancer rate models. For each cancer site, the same sex-specific parametric models as in Preston *et al*. are used for the baseline rates $\lambda_0(\cdot)$: "In the most general models, for each sex, the log rate was described using city and exposure status effects together with piecewise quadratic functions of log *age* joining smoothly at ages 40 and 70 and piecewise quadratic functions of birth year joining smoothly at 1915 (age at exposure 30) and 1895 (age at exposure 50). A smooth piecewise quadratic function of x with join points at x_1 and x_2 can be written as $\beta_0+\beta_1 x+\beta_2 x^2+\beta_3 \max(x-x_1,0)^2+\beta_4 \max(x-x_2,0)^2$. This parameterization provides flexible but relatively parsimonious descriptions of the rates."

Prior distributions for baseline cancer rates. For baseline cancer rate para-meters, the priors were normal distributions with mean 0 and extremely large variances. This is an example of what are sometimes referred to as non-informative priors. Use of non-informative priors will often yield results similar to what would be obtained from more traditional statistical methods, *e.g.*, maximum likelihood.

Prior distributions for ERR model parameters. Lognormal prior distributions were assigned to linear dose-response parameters for age-at-exposure 20 and attained age 70. The younger age-at-exposure is chosen for technical reasons to increase the speed of the Monte Carlo algorithm. Normal distributions were assigned to the age-at-exposure and attained-age parameters. Prior distributions are detailed in Table B-1.

Table B-1: Prior distributions for ERR model parameters[1]

	Parameter			
	Log(ERR) at age-at-exposure 20 and attained age 70		Age-at-exposure	Attained age
	Males	Females		
Cancer Site (*j*)	$\gamma_j^{-1}\log(\beta_{M,j})$	$\gamma_j^{-1}\log(\beta_{F,j})$	**(γ_j)**	**(η_j)**
Stomach Colon Liver Lung Bladder	$N(\mu_{M,j},\tau^2)$	$N(\mu_{F,j},\tau^2)$	N(-0.3,0.25)	N(-1.4,2)
Prostate	$N(\mu_M,\tau^2)$	—	-0.3	-1.4
Uterus	—	$N(\mu_{F,j},\tau^2)$	-0.3	-1.4
Ovary	—		-0.3	-1.4
Other solid	N(-0.5,10)	$N(\mu_{F,j},\tau^2)$	N(-0.3,0.25)	N(-1.4,2)
All sites	$\mu \sim N(-0.5,10),\ \mu_{F,j}=\mu+\delta_j,\ \mu_{M,j}=\mu-\delta_j$ $\delta_j \sim N(\mu_d,\tau_d^2),\ \mu_d \sim N(0,1)$ $1/\tau^2 \sim Gamma(3.5,1)$, $1/\tau_d^2 \sim Gamma(5.5,1)$			

[1]Linear dose response parameter (β) in Preston *et al*. (2007) represents the ERR for age-at-exposure 30 and attained-age 70. Here a prior distribution is assigned to the ERR for age-at-exposure 20 and attained age 70. The younger age-at-exposure (20 instead of 30) is chosen to reduce correlations that can increase run times for the MCMC algorithm.

Likelihood. The likelihood is based on the assumption that the hazard function for each cancer can be approximated as a piecewise-linear function of time. It can then be shown that the likelihood is identical to that for a Poisson model in which, for each cell within the event time table, the number of expected cases is equal to the product of the hazard rate and the total person-years. For a set of several cancers, the likelihood is the product of Poisson likelihoods associated with each cancer type (Larson 1984).

Simulation of posterior distributions using MCMC. The software package, WinBUGS, was used to simulate three independent "chains" of 25,000 sets of ERR and baseline rate parameter values. In MCMC, burn-in time refers to the time during which the chains of simulated values have not yet converged to the target distributions, and it is common practice not to use values simulated during burn-in. For this analysis, the first 12,500 sets of parameters of each chain were discarded. To save computer time, the sequences were then "thinned" by using every third value. The final analysis was based on 12,500 sets of parameter values.

Considerable care was taken to make sure that the results generated from MCMC would converge to the target (posterior) distribution. For example, an initial analysis – based on the assumption that maximum likelihood estimates of parameter values follow a multivariate normal distribution – was used to generate starting values, and modified Gelman-Rubin statistics (Brooks and Gelman 1998) were used to determine whether convergence had been achieved.

The WinBUGS program for simulating the parameter values – together with starting values used – is available upon request.

Prostate and uterine cancers. A lognormal prior distribution for a linear dose response parameter (β) assures that simulated values from the posterior distribution for that parameter will be positive. However, for both prostate and uterine cancers, the evidence for a positive dose-response is not statistically significant. For these two cancers, a set of the simulated values for the linear dose response parameter (β), generated using WinBUGS, were randomly chosen and set to zero. For each site, the percentage of values set to zero was determined so that the mean of the posterior distribution for LAR would equal the nominal value for the LAR given in Section 3.

Posterior distributions for ERR parameters. Table B-2 compares posterior distributions for the linear dose-response parameters (ERR Gy^{-1} for age-at-exposure 30 and attained age 70) to the corresponding estimates in BEIR VII. Except for bladder and colon cancer, the mean and uncertainty interval bounds for the posterior distributions are remarkably similar to the corresponding confidence intervals in BEIR VII. The 95% uncertainty interval calculated in this report for stomach cancer is (0.09, 0.33), whereas the 95% confidence interval reported in BEIR VII is (0.09, 0.32). In contrast, for female bladder cancer, the upper 95% uncertainty bound calculated here is only 2.2, versus the upper 95% CI bound of 3.2 in BEIR VII. Histograms of posterior distributions for ERR parameters are given in Figures B-1, B-2 and B-3. We note that, for specific cancer sites, parameter values are correlated; *e.g.*, the age-at-exposure parameter and the linear dose response parameter for bladder cancer are positively correlated.

Table B-2: Comparison of posterior distributions for ERR linear dose response parameter[1] with estimates in BEIR VII

	Males		Females	
Cancer	**Posterior Distribution[2]**	**BEIR VII[3]**	**Posterior Distribution[2]**	**BEIR VII[3]**
Stomach	0.19 (0.09, 0.33)	0.17 (0.09, 0.32)	0.38 (0.20, 0.60)	0.39 (0.25, 0.59)
Colon	0.38 (0.12 ,0.79)	0.51 (0.30, 0.89)	0.38 (0.14, 0.73)	0.35 (0.15, 0.77)
Liver	0.23 (0.07, 0.48)	0.26 (0.13, 0.52)	0.32 (0.10, 0.65)	0.26 (0.08, 0.81)
Lung	0.37 (0.17, 0.62)	0.26 (0.12, 0.56)	1.12 (0.63, 1.7)	1.13 (0.76, 1.7)
Bladder	0.50 (0.13 ,1.1)	0.40 (0.15, 1.13)	0.97 (0.24, 2.2)	1.33 (0.56, 3.2)
Remainder	0.16 (0.05, 0.32)	0.18 (0.10, 0.32)	0.29 (0.12, 0.52)	0.29 (0.18, 0.49)
Prostate	0.09 (0, 0.42)	0.10 (0, 0.56)		
Uterus			0.04 (0, 0.21)	0.04 (0, 0.18)
Ovary			0.34 (0.11, 0.69)	0.31 (0.08, 1.13)

[1]ERR Gy^{-1} for age-at-exposure 30 and attained age 70
[2]Mean and 95% uncertainty bounds
[3]Maximum likelihood estimate and 95% confidence interval

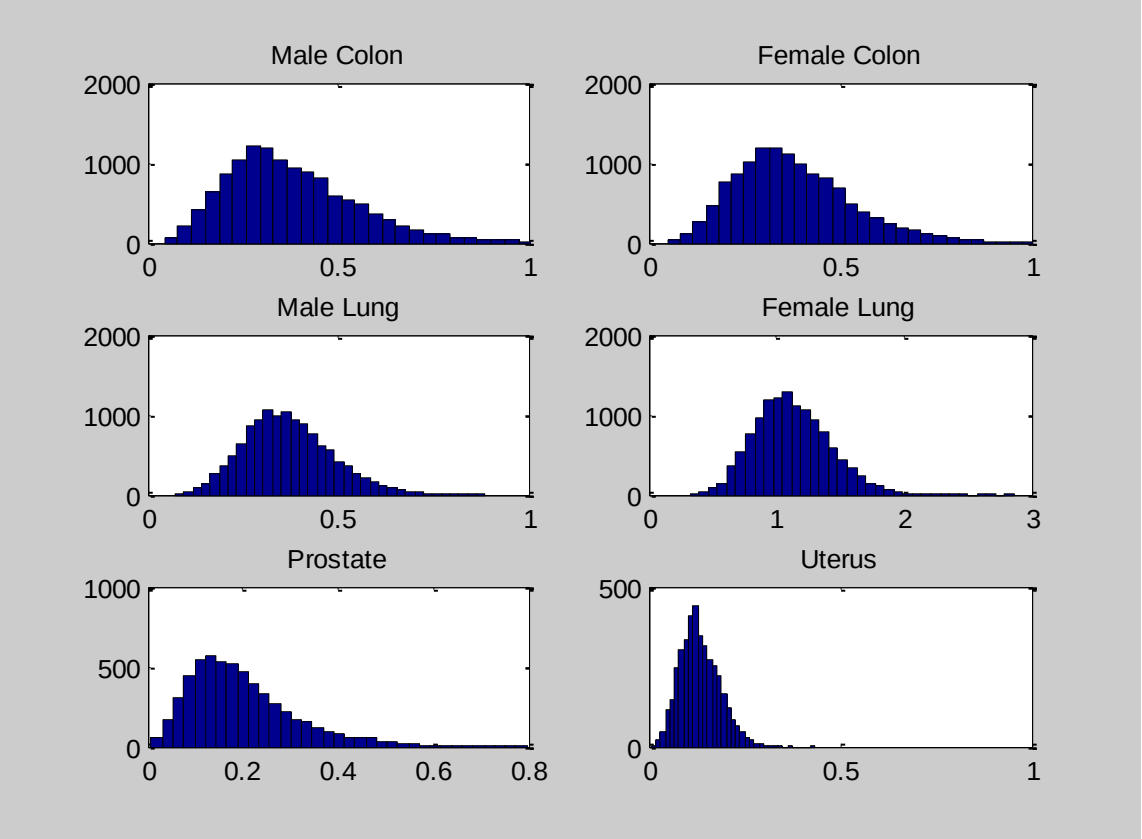

Figure B-1: Posterior distributions for ERR at age-at-exposure 30 and attained-age 70 for selected cancer sites. For prostate and uterine cancer, only positive values for ERR are shown.

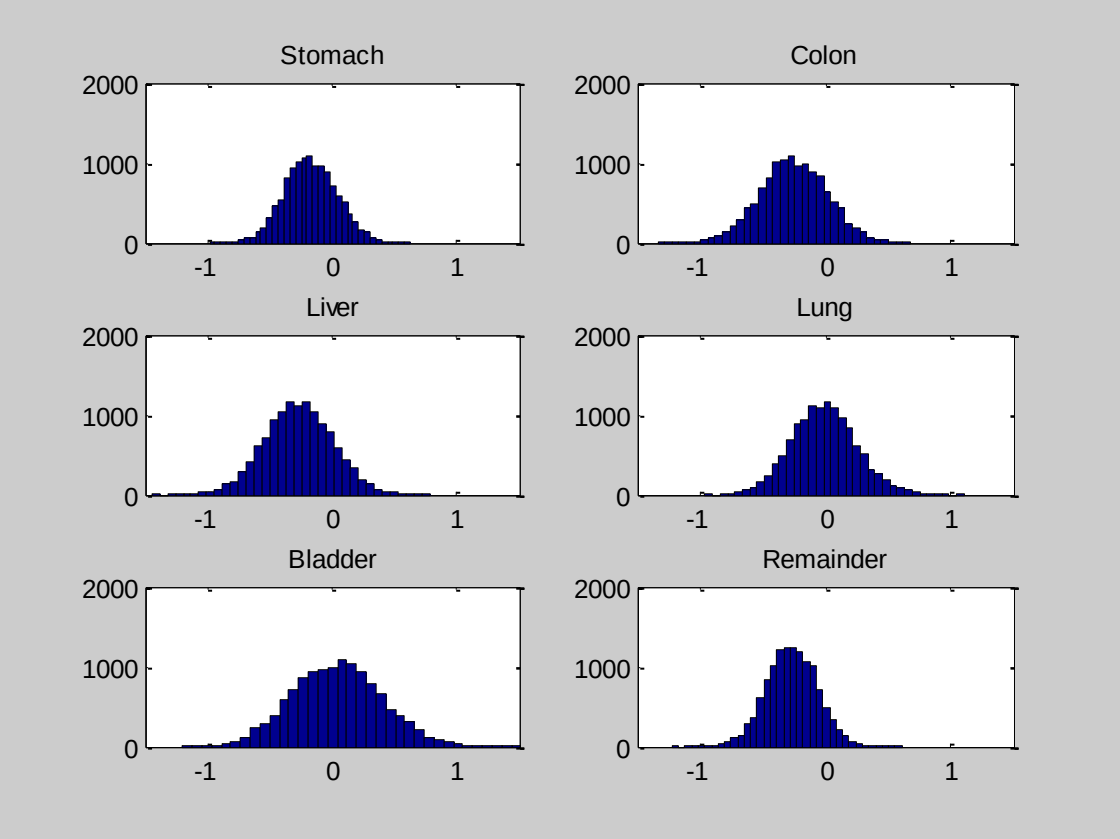

Figure B-2: Posterior distributions for the age-at-exposure parameter for selected sites

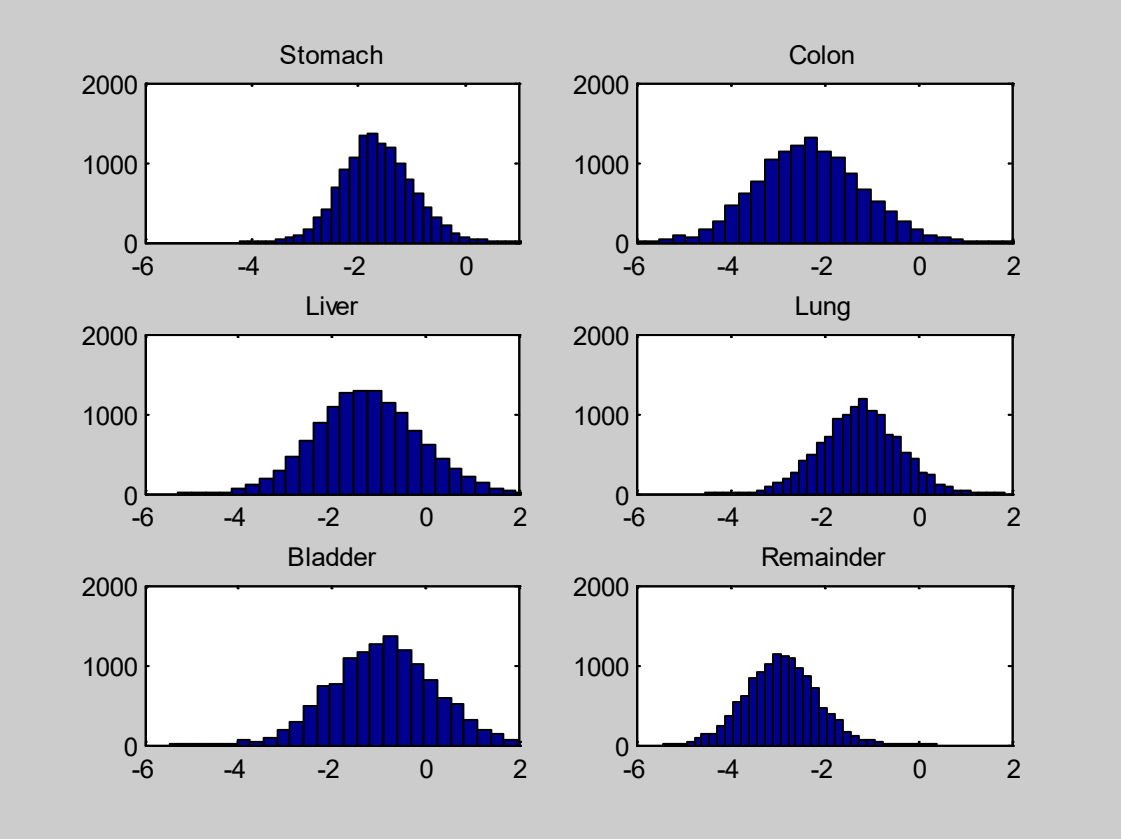

Figure B-3: Posterior distributions for the attained age parameter for selected sites

REFERENCES

Adams MJ, RE Shore, A Dozier, SE Lipshultz, RG Schwartz, LS Constine *et al. t*hyroid cancer risk 40+ years after irradiation for an enlarged thymus: an update of the Hempelman cohort. 2010. Radiat Res **174:** 753-762.

Ainsbury EA, SD Bouffler, W Dörr, J Graw, CR Muirhead, AA Edwards, J Cooper. 2009. Radiation cataractogenesis: A review of recent studies. Radiat Res **172:** 1-9.

Altekruse SF, CL Kosary, M Krapcho, N Neyman, R Aminou, W Waldron *et al.* (eds). 2010. *SEER Cancer Statistics Review, 1975-2007*, National Cancer Institute. Bethesda, MD, http://seer.cancer.gov/csr/1975_2007/, based on Nov. 2009 SEER data submission, posted to the SEER website, 2010.

Andersson M, M Vyberg, J Visfeldt, B Carstensen, HH Storm. 1994. Primary liver tumours among Danish patients exposed to Thorotrast. Radiat Res **137:** 262-273.

Arias E, LR Curtin, RW Wei, RN Anderson. 2008. *U.S. Decennial Life Tables for 1999-2001, United States Life Tables. National Vital Statistics Reports, Vol 57 No 1*. Hyattsville, Maryland: National Center for Health Statistics. Accessed 10/31/08 at CDC website: http://www.cdc.gov/nchs/data/nvsr/nvsr57/nvsr57_01.pdf

Azzam EI, SM de Toledo, GP Raaphorst, REJ Mitchel. 1996. Low-dose ionizing radiation decreases the frequency of neoplastic transformation to a level below the spontaneous rate in C3H 10T1/2 cells. Radiat Res **146:** 369-373.

Azzam EI, SM de Toledo, T Gooding, JB Little. 1998. Intercellular communication is involved in the bystander regulation of gene expression in human cells exposed to very low fluences of alpha particles. Radiat Res **150:** 497-504.

Bauer S, BI Gusev, LM Pivina, KN Apsalikov, B Grösche. 2005. Radiation exposure to local fallout from Soviet atmospheric nuclear weapons testing in Kazakhstan: solid cancer mortality in the Semipalatinsk historical cohort, 1960-1999. Radiat Res **164:** 409-419.

Berrington A, SC Darby, HA Weiss, R Doll. 2001. 100 years of observation on British radiologists: mortality from cancer and other causes 1897-1997. Br J Radiol **74:** 507-519.

Bijwaard H, MJP Brugmans, HP Leenhouts. 2004. Two-mutation model for bone cancer due to radium, strontium and plutonium. Radiat Res **162:** 171-184.

Bland KI, HR Menck, CEH Scott-Conner, M Morrow, DJ Winchester, DP Winchester. 1998. The national cancer data base 10-year survey of breast carcinoma treatment at hospitals in the United States. Cancer **83:** 1262-1273.

Boice JD, Jr. 2006. Ionizing Radiation, pp 259-293, in: *Cancer Epidemiology and Prevention. Third Edition.* D Schottenfeld and JF Fraumeni (eds). Oxford: Oxford University Press.

Boice JD, Jr., D Preston, FG Davis, RR Monson. 1988. Frequent chest X-ray fluoroscopy and breast cancer incidence among tuberculosis patients in Massachusetts. Radiat Res **125:** 214-222.

Boice JD, Jr., RW Miller. 1999. Childhood and adult cancer after intrauterine exposure to ionizing radiation. Teratol **59:** 227-233.

Boice JD, Jr., JH Hendry, N Nakamura, O Niwa, S Nakamura, K Yoshida. 2010. Low-dose-rate epidemiology of high background radiation areas. Radiat Res **171:** 849-854.

Brenner DJ, R Doll, DT Goodhead, EJ Hall, CE Land, JB Little *et al.* 2003. Cancer risks attributable to low doses of ionizing radiation: Assessing what we really know. PNAS **100:** 13761-13766.

Brenner DJ, RK Sachs. 2003. Domestic radon risks may be dominated by bystander effects–but the risks are unlikely to be greater than we thought. Health Phys **85:** 103-108.

Brenner AV, D Mykola, MD Tronko, M Hatch, TI Bogdanova, VA Oliynik *et al.* I-131 dose-response for incident thyroid cancers in Ukraine related to the Chornobyl accident. Environ Health Perspect 2011 Mar 14. [Epub ahead of print].

Brenner DJ, RK Sachs. 2006. Estimating radiation-induced cancer risks at very low doses: rationale for using the linear no-threshold approach. Radiat Environ Biophys **44:** 253-256.

Breslow NE, NE Day. 1987. *Statistical Methods in Cancer Research. Volume II: The Design and Analysis of Cohort Studies*. International Agency for Research on Cancer. Lyon.

Brooks SP, A Gelman. 1998. General methods for monitoring convergence of iterative simulations. J Comput Graph Stat **7:** 434-455.

Bucci A, E Shore-Freedman, T Gierlowski, D Mihailescu, E Ron, AB Schneider. 2001. Behavior of small thyroid cancers found by screening radiation-exposed individuals. J Clin Endocrinol Metab. **86:** 3711–3716.

Burch PRJ. 1957. Some physical aspects of relative biological efficiency. Br J Radiol **30:** 524-529.

Cardis E, M Vrijheid, M Blettner, E Gilbert, M Hakama, C Hill *et al*. 2005a. Risk of cancer after low doses of ionising radiation: retrospective cohort study in 15 countries. BMJ **331**: 77 doi:10.1136/bmj.38499.599861.E0 (published 29 June 2005).

Cardis E, A Kesminiene, V Ivanov, I Malakhova, Y Shibata, V Khrouch *et al.* 2005b. Risk of thyroid cancer after exposure to ^{131}I in childhood. JNCI **97:** 724-732.

Cardis E, M Vrijheid, M Blettner, E Gilbert, M Hakama, C Hill *et al*. 2007. The 15-country collaborative study of cancer risk among radiation workers in the nuclear industry: Estimates of radiation-related cancer risks. Radiat Res **167:** 396-416.

CDC (Centers for Disease Control) and NCI (National Cancer Institute). U.S. Cancer Statistics Working Group. 2005. *United States Cancer Statistics: 2002 Incidence and Mortality.* Atlanta: U.S. Department of Health and Human Services, Centers for Disease Control and Prevention and National Cancer Institute. Accessed at: http://www.cdc.gov/cancer/npcr/uscs/pdf/2002_uscs.pdf (7/24/06).

Chen W-L, J-S Hwang, T-H Hu, M-S Chen, WF Chang. 2001. Lenticular opacities in populations exposed to chronic low-dose-rate gamma radiation from radiocontaminated buildings in Taiwan. Radiat Res **156:** 71-77.

Coates PJ, SA Lorimore, EG Wright. 2004. Damaging and protective cell signalling in the untargeted effects of ionizing radiation. Mutat Res **568:** 5-20.

Cornforth MN, SM Bailey, EH Goodwin. 2002. Dose responses for chromosome aberrations produced in noncycling primary human fibroblasts by alpha particles, and gamma rays delivered at sublimiting low dose rates. Radiat Res **158:** 43-53.

Cronin K, E Feuer, M Wesley, A Mariotto, S Scoppa, D Green. 2003. *Current Estimates for 5 and 10 Year Relative Survival.* Statistical Research and Applications Branch, National Cancer Institute. Technical Report #2003-04. Accessed 10/17/08 at: http://srab.cancer.gov/reports/tech2003.04.pdf

Darby S, D Hill, A Auvinen, JM Barros-Dios, H Baysson, F Bochicchio, H Deo *et al*. 2005. Radon in homes and risk of lung cancer: collaborative analysis of individual data from 13 European case-control studies. BMJ **330:** 223.

Delongchamp RR, K Mabuchi, Y Yoshimoto, DL Preston. 1997. Cancer mortality among atomic bomb survivors exposed to *in utero* or as young children, October 1950-May 1992. Radiat Res **147:** 385-395.

Doll R, R Wakeford. 1997. Risk of childhood cancer from fetal irradiation. Brit J Radiol **70:** 130-139.

Doody MM, JE Lonstein, M Stovall, DG Hacker, N Luckyanov, CE Land. 2000. Breast cancer mortality after diagnostic radiography: Findings from the U.S. Scoliosis Cohort Study. Spine **25:** 2052-2063.

Edwards AA. 1999. Neutron RBE values and their relationship to judgements in radiological protection. J Radiol Prot **19:** 93-105.

El Ghissassi F, R Baan, K Straif, Y Grosse, B Secretan, V Bouvard *et al.,* on behalf of the WHO International Agency for Research on Cancer Monograph Working Group. 2009. A review of human carcinogens – Part D: Radiation. Lancet Oncol. 1**0:** 751-752.

Elkind MM. 1994. Radon-induced cancer: a cell-based model of tumorigenesis due to protracted exposures. Int J Radiat Biol **66:** 649-653.

Elmore E, X-Y Lao, R Kapadia, E Gedzinski, C Limoli, JL Redpath. 2008. Low doses of very low-dose-rate low-LET radiation suppress radiation-induced neoplastic trans-formation in vitro and induce an adaptive response. Radiat Res **169:** 311-318.

EPA (Environmental Protection Agency). 1994. *Estimating Radiogenic Cancer Risks*. EPA Report 402-R-93-076, Washington, DC: U.S. EPA.

EPA (Environmental Protection Agency). 1999a. *Estimating Radiogenic Cancer Risks. Addendum: Uncertainty Analysis.* EPA Report 402-R-99-003, Washington, DC: U.S. EPA.

EPA (Environmental Protection Agency). 1999b. *Cancer Risk Coefficients for Environmental Exposure to Radionuclides.* EPA Report 402-R-99-001, Washington, DC: U.S. EPA.

EPA (Environmental Protection Agency). 2003. *EPA Assessment of Risks from Radon in Homes*. EPA Report 402-R-03-003, Washington, DC: U.S. EPA.

Everitt BS. 1995. *The Cambridge Dictionary of Statistics in the Medical Sciences*. Cambridge University Press: NY.

Fritsch FN, RE Carlson. 1980. Monotone piecewise cubic interpolation. SIAM J Numer Anal **17:** 238-246.

Furukawa K, DL Preston, S Lonn, S Funamoto, S Yonehara, T Matsuo *et al.* 2010. Radiation and smoking effects on lung cancer incidence among atomic bomb survivors. Radiat Res **174:** 72-82.

Gelman A, JB Carlin, HS Stern, DB Rubin. 2003. *Bayesian Data Analysis*. Chapman and Hall: NY.

Gilbert ES. 1991. Chapter 3: Late somatic effects. In: S Abrahamson, MA Bender, BB Boecker *et al*. *Health Effects Models for Nuclear Power Plant Accident Consequence Analysis. Modifications of Models Resulting from Recent Reports on Health Effects of Ionizing Radiation, Low LET Radiation, Part II: Scientific Bases for Health Effects Models.* NUREG/CR-4214, Rev. 1, Part II, Addendum 1, LMF-132. U.S. Nuclear Regulatory Commission: Washington, DC.

Gilbert ES, NA Koshurnikova, ME Sokolnikov, VF Khokhryakov, S Miller, DL Preston *et al*. 2000. Liver cancers in Mayak workers. Radiat Res **154:** 246-252.

Gilbert ES, NA Koshurnikova, ME Sokolnikov, NS Shilnikova, DL Preston, E Ron *et al*. 2004. Lung cancer in Mayak workers. Radiat Res **162:** 505-516.

Goodhead DT. 2006. Energy deposition stochastics and track structure: What about the target? Radiat Prot Dosim **122:** 3-15.

Grogan HA, WK Sinclair, PG Voillequé. 2001. Risks of fatal cancer from inhalation of ^{239,240}plutonium by humans: a combined four-method approach with uncertainty evaluation. Health Phys **80:** 447-461.

Hahn FF, BA Muggenburg, RA Guilmette, BB Boecker. 1999. Comparative stochastic effects of inhaled alpha- and beta-particle-emitting radionuclides in beagle dogs. Radiat Res **152:** S19-S22.

Hahn FF, B Scott, DL Lundgren. 2010. Comparative stochastic effects of alpha, beta or X-irradiation of the lung of rats. Health Phys **99:** 363-366.

Harrison JD, CR Muirhead. 2003. Quantitative comparisons of induction in humans by internally deposited radionuclides and external radiation. Int J Radiat Biol **79:**1-13.

Hatch M, E Ron, A Bouville, L Zablotska, G Howe. 2005. The Chernobyl disaster: Cancer following the accident at the Chernobyl Nuclear Power Plant. Epidemiol Rev **27:** 56-66.

Hawkins MM, LMK Wilson, HS Burton, MHN Potok, DL Winter, HB Marsden, MA Stovall. 1996. Radiotherapy, alkylating agents, and risk of bone cancer after childhood cancer. JNCI **88:** 270-278.

Hildreth NG, RE Shore, PM Dvoretsky. 1989. The risk of breast cancer after irradiation of the thymus in infancy. N Engl J Med **321:** 1281-1284.

Howe GR, J McLaughlin. 1996. Breast cancer mortality between 1950 and 1987 after exposure to fractionated moderate-dose-rate ionizing radiation in the Canadian fluoroscopy cohort study and a comparison with breast cancer mortality in the atomic bomb survivors study. Radiat Res **145:** 694-707.

HPA (Health Protection Agency) (UK). 2007. *Review of Risks from Tritium*. Report of the Independent Advisory Group on Ionising Radiation. Available at: www.hpa.org.uk/publications/2007/tritium_advice/RCE_Advice_ontritium.pdf

Humphreys ER, KR Isaacs, TA Raine, J Saunders, VA Stones, DL Wood. 1993. Myeloid leukemia and osteosarcoma in CBA/H mice given ^{224}Ra. Int J Radiat Biol **64:** 231-235.

Hwang S-L, J-S Hwang, Y-T Yang, WA Hsieh, T-C Chang, H-R Guo *et al*. 2008. Estimates of relative risks for cancers in a population after prolonged low-dose-rate radiation exposure: A follow-up assessment from 1983 to 2005. Radiat Res **170:** 143-148.

ICRP (International Commission on Radiological Protection). 1991. *The Biological Basis for Dose Limitation in the Skin.* ICRP Publication 59. Ann ICRP **22**(2).

ICRP (International Commission on Radiological Protection). 1993. *Age-dependent Doses to Members of the Public from Intake of Radionuclides: Part 2. Ingestion Dose Coefficients.* ICRP Publication 67. Ann ICRP **23**(3/4).

ICRP (International Commission on Radiological Protection). 2000. *Pregnancy and Medical Radiation.* ICRP Publication 84. Ann ICRP **30**(1).

ICRP (International Commission on Radiological Protection). 2003. *Relative Biological Effectiveness (RBE), Quality Factor (Q), and Radiation Weighting Factor (w_R).* ICRP Publication 92. Ann ICRP **33**(4).

ICRP (International Commission on Radiological Protection). 2006. *Human Alimentary Tract model for Radiological Protection.* ICRP Publication 100. Ann ICRP **36** (1-2).

ICRP (International Commission on Radiological Protection). 2007. The 2007 *Recommendations of the International Commission of Radiological Protection.* ICRP Publication 103. Ann ICRP **37**(2-4).

Ishikawa Y, JAH Humphreys, CG Collier, ND Priest, Y Kato, T Mori, R Machinami. 1999. Revised organ partition of thorium-232 in thorotrast patients. Radiat Res **152:** S102-S106.

Jacob P, W Rühm, L Walsh, M Blettner, G Hammer, H Zeeb. 2009. Is cancer risk of radiation workers larger than expected? Occup Environ Med **66:** 789-796.

James AC, A Birchall, G Akabani. 2004. Comparative dosimetry of BEIR VI revisited. Radiat Prot Dosimetry **108:** 3-26.

Kadhim MA, DA MacDonald, DT Goodhead, SA Lorimore, SJ Marsden, EG Wright. 1992. Transmission of chromosomal instability after plutonium alpha-particle irradiation. Nature **355:** 738-740.

Kadhim MA, SR Moore, EH Goodwin. 2004. Interrelationships amongst radiation-induced genomic instability, bystander effects, and the adaptive response. Mutat Res **568:** 21-32.

Karagas MR, ER Greenberg, SK Spencer, TA Stukel, LA Mott. 1999. The New Hampshire Skin Cancer Study Group. Increase in incidence rates of basal cell and squamous cell skin cancer in New Hampshire, USA. Int J Cancer **81:** 555-559.

Kaul DC, SD Egbert, WA Woolson. 2005. Chapter 13: DS02 uncertainty analysis, pp. 921-926 in: *Reassessment of the Atomic Bomb Radiation Dosimetry for Hiroshima and Nagasaki: Dosimetry System 2002. Volume 2.* RW Young and GW Kerr, eds. Hiroshima: Radiation Effects Research Foundation.

Kesminiene A, A-S Evrard, VK Ivanov, IV Malakhova, J Kurtinaitis, A Stengrevics *et al.* 2008. Risk of hematological malignancies among Chernobyl liquidators. Radiat Res **170:** 721-735.

Kocher DC, AI Apostoaei, FO Hoffman. 2005. Radiation effectiveness factors for use in calculating probability of causation of radiogenic cancers. Health Phys **89:**3-32.

Kocher DC, AI Apostoaei, RW Henshaw, FO Hoffman, MK Schubauer-Berigan, DO Stancescu *et al*. 2008. Interactive Radioepidemiological Program (IREP): A Web-based tool for estimating probability of causation/assigned share of radiogenic cancers. Health Phys **95:** 119-147.

Koshurnikova NA, ES Gilbert, M Sokolnikov, VF Khokhryakov, S Miller, DL Preston *et al.* 2000. Bone cancers in Mayak workers. Radiat Res **154:** 237-245.

Krestinina LY, DL Preston, EV Ostroumova, MO Degteva, E Ron, OV Vyushkova *et al*. 2005. Protracted radiation exposure and cancer mortality in the Techa River Cohort. Radiat Res **164:** 602-611.

Krestinina LY, DL Preston, FG Davis, S Epifanova, E Ostroumova E Ron, A Akleyev. 2010. Leukemia incidence among people exposed to chronic radiation from the contaminated Techa River, 1953-2005. Radiat Environ Biophys **49:** 195-201.

Krewski D, JH Lubin, JM Zielinski, M Alavanja, VS Catalan, RW Field *et al*. 2005. Residential radon and the risk of lung cancer: A combined analysis of 7 North American case-control studies. Epidemiol **16:** 137-145.

Land CE. 1980. Estimating cancer risks from low doses of ionizing radiation. Science **209:** 1197-1203.

Land CE, WK Sinclair. 1991. The relative contributions of different organ sites to the total cancer mortality associated with low-dose radiation exposure. In: *Risks Associated with Ionising Radiations,* Annals of the ICRP **22 (1)**.

Larson MG. 1984. Covariate analysis of competing-risks data with log-linear models. Biometrics **40**: 459-469.

Leenhouts HP, MJP Brugmans, M Andersson, HH Storm. 2002. A reanalysis of liver cancer incidence in Danish patients administered Thorotrast using a two-mutation carcinogenesis model. Radiat Res **158:** 597-606.

Lehnert BE, EH Goodwin, A Deshpande. 1997. Extracellular factor(s) following exposure to alpha particles can cause sister chromatid exchanges in normal human cells. Cancer Res **57:** 2164-2171.

Lewis EB. 1963. Leukemia, multiple myeloma, and aplastic anemia in American radiologists. Science **142:** 1492-1494.

Lewis KG, MA Weinstock. 2004. Nonmelanoma skin cancer mortality (1988-2000). The Rhode Island follow-back study. Arch Dermatol **140:** 837-842.

Little JB, H Nagasawa, T Pfenning, H Vetrovs. 1997. Radiation-induced genomic instability: delayed mutagenic and cytogenetic effects of X-rays and α-particles. Radiat Res **148:** 299-307.

Little MP. 2002. Absence of evidence for differences in the dose-response for cancer and non-cancer endpoints by acute injury status in the Japanese atomic-bomb survivors. Int J Radiat Biol **78:** 1001-1010.

Little MP, DG Hoel, J Molitor, JD Boice Jr., R Wakeford, CR Muirhead. 2008. New models for evaluation of radiation-induced lifetime cancer risk and its uncertainty employed in the UNSCEAR 2006 report. Radiat Res **169:** 660-676.

Little MP, EJ Tawn, I Tzoulaki, R Wakeford, G Hildebrandt, F Paris *et al*. 2008b. A systematic review of epidemiological associations between low and moderate doses of ionizing radiation and late cardiovascular effects and their possible mechanisms. Radiat Res **169:** 99-109.

Lloyd EL, D Hodges. 1971. Quantitative characterization of bone. A computer analysis of microradiographs. Clin Orthop Relat Res **78:** 230-250.

Löbrich M, N Rief, M Kühne, M Heckmann, J Fleckenstein, C Rübe, M Uder. 2005. *In vivo* formation and repair of DNA double-strand breaks after computed tomography examinations. PNAS **102:** 8984-8989.

Loucas BD, R Eberle, SM Bailey, MN Cornforth. 2004. Influence of dose rate on the induction of simple and complex chromosome exchanges by gamma rays. Radiat Res **162:** 339-349.

Lubin J, E Ron (1998). Excess relative risk and excess absolute risk estimates for pooled analysis of thyroid cancer following exposure to external radiation, memorandum to Jack Schull, Chair, NRC Committee on Exposure of the American People to I-131 from Nevada Atomic-Bomb Tests: Implications for Public Health (National Cancer Institute, Rockville, Maryland).

Lubin J, DW Schafer, E Ron, M Stovall, RJ Carroll. 2004. A reanalysis of thyroid neoplasms in the Israeli tinea capitis study accounting for dose uncertainties. Radiat Res **61:** 359-368.

Lunn DJ, A Thomas, N Best, D Spiegelhalter. 2000. WinBUGS – a Bayesian modeling framework: concepts, structure, and extensibility. Stat Comput **10:** 325-337.

Lyng FM, CB Seymour, C Mothersill. 2000. Production of a signal by irradiated cells which leads to a response in unirradiated cells characteristic of initiation of apoptosis. Brit J Cancer **83:** 1223-1230.

Marková E, N Schultz, IY Belyaev. 2007. Kinetics and dose-response of residual 53BP1/γ-H2AX foci: Co-localization, relationship with DSB repair and clonogenic survival. Internat J Radiat Biol **83:** 319-329.

Marples B, MC Joiner. 1993. The response of Chinese hamster V79 cells to low radiation doses: Evidence of enhanced sensitivity of the whole cell population. Radiat Res **133:** 41-51.

Mays CW, MP Finkel. 1980. RBE of α-particles vs. β-particles in bone sarcoma induction. Proc. IRPA **5:** 401-405.

Mays CW, H Speiss. 1972. Bone sarcoma incidence vs. alpha particle dose, pp. 409-430 in: *Radiobiology of Plutonium*, BJ Stover and WSS Jee, eds. Salt Lake City: The J.W. Press.

Mays CW, RE Rowland, AF Stehney. 1985. Cancer risk from lifetime intake of Ra and U isotopes. Health Phys **48:** 635-647.

Mitchell SA, G Randers-Pehrson, DJ Brenner, EJ Hall. 2004. The bystander response in C3H 10T½ cells: the influence of cell-to-cell contact. Radiat Res **161:** 397-401.

Mole RH. 1990. Childhood cancer after prenatal exposure to diagnostic X-ray examinations in Britain. Br J Cancer **62:** 152-168.

Monson RR, B MacMahon. 1984. Prenatal X-ray exposure and cancer in children, pp. 197-206 in: *Radiation Carcinogenesis: Epidemiology and Biological Significance,* JD Boice, Jr. and JF Fraumeni, Jr., eds., New York: Raven Press.

Morgan WF, JP Day, MI Kaplan, EM McGhee, CL Limoli. 1996. Genomic instability induced by ionizing radiation. Radiat Res **146:** 247-258.

Mothersill C, CB Seymour. 1998. Cell-cell contact during gamma irradiation is not required to induce a bystander effect in normal human keratinocytes: evidence for release during irradiation of a signal controlling survival into the medium. Radiat Res **149:** 256-262.

Muirhead CR, JA O'Hagan, RGE Haylock, MA Phillipson, T Wilcock GLC Berridge, W Zhang. 2009. Mortality and cancer incidence following occupational radiation exposure: third analysis of the National Registry for Radiation Workers. Br J Cancer **100:** 206-212.

Nair RR, B Rajan, S Akiba, P Jayalekshmi, MK Nair, P Gangadharan *et al.* 2009. Background radiation and cancer incidence in Kerala, India–Karanagappally cohort study. Health Phys **96:** 55-66.

NAS (National Academy of Sciences). 1988. *Health Effects of Radon and Other Internally Deposited Alpha-Emitters (BEIR IV)*. Washington, DC: National Academy Press.

NAS (National Academy of Sciences). 1990. *Health Effects of Exposure to Low Levels of Ionizing Radiation. (BEIR V)*. Washington, DC: National Academy Press.

NAS (National Academy of Sciences). 1999. *Health Effects of Exposure to Radon. BEIR VI*. Washington, DC: National Academy Press.

NAS (National Academy of Sciences). 2006. *Health Risks from Exposure to Low Levels of Ionizing Radiation. BEIR VII Phase 2*. Washington, DC: National Academy Press.

NCHS (National Center for Health Statistics). 2004. *Bridged-Race Population Estimates, United States, 1990 - 2004, by Age Groups*. Compiled from the April 1, 2000 resident population developed by the Bureau of the Census in collaboration with the NCHS – accessed from the CDC WONDER On-line Database on June 3, 2006.

NCI (National Cancer Institute) 2011. *Fast Stats: An Interactive Tool for Access to SEER Cancer Statistics.* Surveillance Research Program, National Cancer Institute. http://seer.cancer.gov/faststats. (Accessed on 1-4-2011)

NCI (National Cancer Institute) 2005. *DevCan: Probability of Developing or Dying of Cancer Software, Version 6.4.1*; Statistical Research and Applications Branch, National Cancer Institute. http://srab.cancer.gov/devcan (Accessed on 5-6-2010)

NCRP (National Council on Radiation Protection and Measurements). 1980. *Influence of Dose and Its Distribution in Time on Dose-Response Relationships for Low-LET Radiations. NCRP Report No. 64.* Bethesda, MD: National Council on Radiation Protection and Measurements.

NCRP (National Council on Radiation Protection and Measurements). 1985. *Induction of Thyroid Cancer by Ionizing Radiation. NCRP Report No. 80.* Bethesda, MD: National Council on Radiation Protection and Measurements.

NCRP (National Council on Radiation Protection and Measurements). 1990. *The Relative Effectiveness of Radiations of Different Quality. NCRP Report No. 104.* Bethesda, MD: National Council on Radiation Protection and Measurements.

NCRP (National Council on Radiation Protection and Measurements). 2001. *Evaluation of the Linear-Nonthreshold Dose-Response Model for Ionizing Radiation. NCRP Report No. 136*. Bethesda, MD: National Council on Radiation Protection and Measurements.

NCRP (National Council on Radiation Protection and Measurements). 2008. *Risk to Thyroid from Ionizing Radiation. NCRP Report No. 159*. Bethesda, MD: National Council on Radiation Protection and Measurements.

Nekolla EA, M Kreisheimer, AM Kellerer, M Kuse-Isingschulte, W Gőssner, H Speiss. 2000. Induction of malignant bone cancers in radium-224 patients: risk estimates based on improved dosimetry. Radiat Res **153:** 93-103.

Nikjoo H, DT Goodhead. 1991. Track structure analysis illustrating the prominent role of low-energy electrons in radiobiological effects of low-LET radiations. Phys Med Biol **36:** 229-238.

Nikjoo H, S Uehara, WE Wilson, M Hoshi, DT Goodhead. 1998. Track structure in radiation biology: theory and applications. Int J Radiat Biol **73:** 355-364.

Nikjoo H, L Lindborg. 2010. RBE of low energy electrons and photons. Phys Med Biol **55:** R65-R109.

NIOSH (National Institute for Occupational Safety and Health). 2002. *NIOSH-Interactive RadioEpidemiological Program (NIOSH-IREP), Technical Documentation*. Cincinnati, OH: National Institute for Occupational Safety and Health. Accessed 6/2006 at: http://www.cdc.gov/niosh/ocas/pfs/irep/irepfnl.pdf.

Ostroumova E, B Gagnière, D Laurier, N Gudkova, L Krestinina, P Verger *et al*. 2006. Risk analysis of leukemia incidence among people living along the Techa river: a nested case-control study. J Radiol Prot **26:** 17-32.

Pawel D, D Preston, D Pierce, J Cologne. 2008. Improved estimates of cancer site-specific risks for A-bomb survivors. Radiat Res **169:** 87-98.

Pierce DA, GB Sharp, K Mabuchi. 2003. Joint effects of radiation and smoking on lung cancer risk among atomic bomb survivors. Radiat Res **159**: 511-520.

Pierce DA, M Vaeth, Y Shimizu. 2007. Selection bias in cancer risk estimation from A-bomb survivors. Radiat Res **167:** 735-741.

Pierce DA, M Vaeth, JB Cologne. 2008. Allowance for random dose estimation errors in atomic bomb survivor studies: a revision. Radiat Res **170:** 118-126.

Portess DI, G Bauer, MA Hill, P O'Neill. 2007. Low-dose irradiation of nontransformed cells stimulates the selective removal of precancerous cells via intercellular induction of apoptosis. Cancer Res **67:** 1246-1253.

Pottern LM, MM Kaplan, PR Larsen, JE Silva, RJ Koenig, JH Lubin *et al*. 1990. Thyroid nodularity after irradiation for lymphoid hyperplasia: A comparison of questionnaire and clinical findings. J Clin Epidemiol **43:** 449-460.

Preston DL, JH Lubin, DA Pierce, ME McConney. 1993. *Epicure Users Guide.* Hirosoft International Corporation, Seattle, WA, 1993.

Preston DL, E Ron, S Yonehara, T Kobuke, H Fujii, M Kishikawa *et al*. 2002a. Tumors of the nervous system and pituitary gland associated with atomic bomb radiation exposure. J Natl Cancer Inst **94:** 1555-1563.

Preston DL, A Mattsson, E Holmberg, R Shore, NG Hildreth, JD Boice Jr. 2002b. Radiation effects on breast cancer risk: a pooled analysis of eight cohorts. Radiat Res **158**: 220-235.

Preston DL, DA Pierce, Y Shimizu, HM Cullings, S Fujita, S Funamoto, K Kodama. 2004. Effects of recent changes in atomic bomb survivor dosimetry on cancer mortality risk estimates. Radiat Res **162:** 377-389.

Preston DL, E Ron, S Tokuoka, S Funamoto, N Nishi, M Soda, K Mabuchi, K Kodama. 2007. Solid cancer incidence in atomic bomb survivors: 1958-1998. Radiat Res **168:** 1-64.

Preston DL, H Cullings, A Suyama, S Funamoto, N Nishi, M Soda *et al.* 2008. Solid cancer incidence in atomic bomb survivors exposed in utero or as young children. JNCI: **100**: 428-436.

Priest ND, DG Hoel, PN Brooks. 2006. Relative toxicity of chronic irradiation by 45Ca beta particles and 242Cm alpha particles with respect to the production of lung tumors in CBA/Ca mice. Radiat Res **166:** 782-793.

Puskin JS. 2008. What can epidemiology tell us about risks at low doses? Radiat Res **169:** 122-124.

Raabe O, SA Book, NJ Parks. 1983. Lifetime bone cancer dose-response relationships in beagles and people from skeletal burdens of ^{226}Ra and ^{90}Sr. Health Phys. **44:** 33-48.

Ramsey ML. 2006. *Basal Cell Carcinoma*. Accessed at eMedicine website: www.emedicine.com/ derm/topic47.htm, last updated May 9, 2006.

Redpath JL, RJ Antoniono. 1998. Induction of an adaptive response against spon-taneous neoplastic transformation *in vitro* by low-dose gamma radiation. Radiat Res **149:** 517-520.

Richardson D, H Sugiyama, N Nishi, R Sakata, Y Shimizu, E Grant *et al*. 2009. Ionizing radiation and leukemia mortality among Japanese atomic bomb survivors: 1950-2000. Radiat Res **172:** 368-382.

Ries LAG, D Harkins, M Krapcho, A Mariotto, BA Miller, L Clegg *et al*. (eds). 2006. *SEER Cancer Statistics Review, 1975-2003*. National Cancer Institute. Bethesda, MD, http://seer.cancer.gov/csr/1975_2003/ based on November 2005 SEER data submission, posted to the SEER website, 2006.

Ries LAG, JL Young, GE Keel, MP Eisner, YD Lin, M-J Horner (editors). *SEER Survival Monograph: Cancer Survival Among Adults: U.S. SEER Program, 1988-2001, Patient and Tumor Characteristics*. National Cancer Institute, SEER Program, NIH Pub. No. 07-6215, Bethesda, MD, 2007.

Ries LAG, D Melbert, M Krapcho, DG Stinchcomb, N Howlader, MJ Horner *et al.* (editors). *SEER Cancer Statistics Review, 1975-2005*. National Cancer Institute.

Bethesda, MD, http://seer.cancer.gov/csr/1975_2005/, based on November 2007 SEER data submission, posted to the SEER website, 2008.

Roesch WC. 1987. Radiation Effects Research Foundation and the National Academy of Sciences (U.S.). *US-Japan Joint Reassessment of Atomic Bomb Radiation Dosimetry in Hiroshima and Nagasaki*. Minami-ku, Hiroshima: Radiation Effects Research Foundation.

Romanenko AY, SC Finch, M Hatch, JH Lubin, VG Bebeshko, DA Bazyka *et al.* 2008. The Ukrainian-American study of leukemia and related disorders among the Chornobyl cleanup workers from Ukraine: III. Radiation risks. Radiat Res **170:** 711-720.

Ron E, B Modan, JD Boice Jr., E Alfandary, M Stovall, A Chetrit, L Katz. 1988. Tumors of the brain and nervous system after radiotherapy in childhood. NEJM **319:** 1033-1039.

Ron E, B Modan, D Preston, E Alfandary, M Stovall, JD Boice Jr. 1989. Thyroid neoplasia following low-dose radiation in childhood. Radiat Res **120:** 516-531.

Ron E, B Modan, D Preston, E Alfandary, M Stovall, JD Boice. 1991. Radiation-induced skin carcinomas of the head and neck. Radiat Res **125:** 318-325.

Ron E, JH Lubin, RE Shore, K Mabuchi, B Modan, L Pottern *et al.* 1995. Thyroid cancer after exposure to external radiation: a pooled analysis of seven studies. Radiat Res **141:** 259-277.

Ron E, B Modan, DL Preston, E Alfandary, M Stovall, JD Boice. 1989. Thyroid neoplasia following low-dose radiation in childhood. Radiat Res **120:** 516-531.

Ron E, DL Preston, M Kishikawa, T Kobuke, M Iseki, S Tokuoka *et al*. 1998. Skin tumor risk among atomic-bomb survivors in Japan. Cancer Causes and Control **9**, 393-401.

Rossi HH, AM Kellerer. 1986. The dose rate dependence of oncogenic trans-formation by neutrons may be due to variation of response during the cell cycle (Letter to the Editor). Int J Radiat Biol **47:** 731-734.

Rothkamm K, M Löbrich. 2003. Evidence for a lack of DNA double-strand break repair in human cells exposed to very low x-ray doses. PNAS **100:** 5057-5062.

Sasaki MS, T Nomura, Y Ejima, H Utsumi, S Endo, I Saito *et al.* 2008. Experimental derivation of relative biological effectiveness of A-bomb neutrons in Hiroshima and Nagasaki and implications for risk assessment. Radiat Res **170:** 101-117.

Schneider AB, E Ron, J Lubin, M Stovall, TC Gierlowski. 1993. Dose-response relationships for radiation-induced thyroid cancer and thyroid nodules: Evidence for the prolonged effects of radiation on the thyroid. J Clin Endocrinol Metab **77:** 362-369.

(SEER 2009a). Surveillance, Epidemiology, and End Results (SEER) Program (www.seer.cancer.gov) *SEER*Stat Database: Incidence - SEER 13 Regs Research Data, Nov 2009 Sub (1992-2007) <Katrina/Rita Population Adjustment> - Linked To County Attributes - Total U.S., 1969-2007 Counties.* National Cancer Institute, DCCPS, Surveillance Research Program, Cancer Statistics Branch, released April 2010, based on the November 2009 submission.

(SEER 2009b). Surveillance, Epidemiology, and End Results (SEER) Program (www.seer.cancer.gov) *SEER*Stat Database: Incidence - SEER 17 Regs Research Data + Hurricane Katrina Impacted Louisiana Cases, Nov 2009 Sub (2000-2007) < Katrina/Rita Population Adjustment> - Linked To County Attributes - Total U.S., 1969-2007 Counties*. National Cancer Institute, DCCPS, Surveillance Research Program, Cancer Statistics Branch, released April 2010, based on the November 2009 submission.

SEER (2010). Surveillance, Epidemiology, and End Results (SEER) Program (www.seer.cancer.gov) SEER*Stat Database: Mortality - All COD, Aggregated With State, Total U.S. (1969-2007) <Katrina/Rita Population Adjustment>, National Cancer Institute, DCCPS, Surveillance Research Program, Cancer Statistics Branch, released June 2010. Underlying mortality data provided by NCHS (www.cdc.gov/nchs).

Shilnikova NS, DL Preston, E Ron, ES Gilbert, EK Vassilenko, SA Romanov *et al*. 2003. Cancer mortality risk among workers at the Mayak Nuclear Complex. Radiat. Res. **159:** 787-798.

Shore RE. 1990. Overview of radiation-induced skin cancer in humans. Int J Radiat Biol **57:**809-827.

Shore RE. 2001. Radiation-induced skin cancer in humans. Med Pediat Oncol **36:** 549-554.

Shore RE, N Hildreth, E Woodard, P Dvoretsky. 1986. Breast cancer among women given x-ray therapy for acute postpartum mastitis. J Natl Cancer Inst **77:** 689-696.

Shore RE, N Hildreth, P Dvoretsky, E Andresen, M Moscson, B Pasternak. 1993. Thyroid cancer among persons given x-ray treatment in infancy for an enlarged thymus gland. Am J Epidemiol **137:**1068-1080.

Shore RE, M Moseson, X Xue, Y Tse, N Harley, BS Pasternack. 2002. Skin cancer after X-ray treatment for scalp ringworm. Radiat Res **157:** 410-418.

Smith PG, R Doll. 1981. Mortality from cancer and all causes among British radiologists. Br J Radiol **49:** 187-194.

Sokolnikov ME, ES Gilbert, DL Preston, NS Shilnikova, VV Khokhryakov, EK Vasilenko, NA Koshurnikova. 2008. Lung, liver, and bone cancer mortality in Mayak workers. Int J Cancer **123:** 905-911.

Stewart A, J Webb, D Hewitt. 1958. A survey of childhood malignancies. Br Med J **1:** 1495-1508.

Tapio S, V Jacob. 2007. Radioadaptive response revisited. Radiat Environ Biophys **46:** 1-12.

Thompson DE, K Mabuchi, E Ron, M Soda, S Tokunaga, S Ochikubo *et al*. 1994. Cancer incidence in atomic bomb survivors. Part II: Solid tumors, 1958-1987. Radiat Res **137 (Suppl.):** S17-S67.

Tronko MD, GR Howe, TI Bogdanova, AC Bouville, OV Epstein, AB Brill *et al.* 2006. A cohort study of thyroid cancer and other thyroid diseases after the Chornobyl accident: thyroid cancer in Ukraine detected during first screening. JNCI **98:** 897-903.

Tubiana M, A Aurengo, D Averbeck, A Bonnin, B Le Guen, R Masse *et al*. 2005. *Dose-Effect Relationships and the Estimation of the Carcinogenic Effects of Low Doses of Ionizing Radiation*. Paris: Academy of Medicine (Paris) and Academy of Science. Joint Report No. 2.

Tucker MA, GJ D'Angelo, JD Boice Jr, LC Strong, FP Li, M Stovall *et al*. 1987. Bone sarcomas linked to radiotherapy and chemotherapy in children. N Engl J Med **317:** 588-593.

Ullrich RL, RJ Preston. 1987. Myeloid leukemia in male RFM mice following irradiation with fission spectrum neutrons or gamma-rays. Radiat Res **109:**165-170.

UNSCEAR (United Nations Scientific Committee on the Effects of Atomic Radiation). 1993. *UNSCEAR 1993 Report to the General Assembly with Scientific Annexes*. New York: United Nations.

UNSCEAR (United Nations Scientific Committee on the Effects of Atomic Radiation). 2000a. *UNSCEAR 2000 Report to the General Assembly with Scientific Annexes. Volume I: Sources*. New York: United Nations.

UNSCEAR (United Nations Scientific Committee on the Effects of Atomic Radiation). 2000b. *UNSCEAR 2000 Report to the General Assembly with Scientific Annexes. Volume II: Effects*. New York: United Nations.

UNSCEAR (United Nations Scientific Committee on the Effects of Atomic Radiation). 2008. *UNSCEAR 2006 Report to the General Assembly with Scientific Annexes*. *Volume I*. *Effects of Ionizing Radiation.* New York: United Nations.

Van Kaick G, A Dalheimer, S Hornik, A Kaul, D Liebermann, H Luhrs *et al*. 1999. The German Thorotrast study: recent results and assessment of risks. Radiat Res **152:** S64-S71.

Vu BL, F de Vathaire, A Shamsaldin, MM Hawkins, E Grimaud, C Hardiman *et al*. 1998. Radiation dose, chemotherapy and risk of osteosarcoma after solid tumours during childhood. Int J Cancer **77:** 370-377.

Wang J-X, JD Boice Jr, B-X Li, J-Y Zhang, JF Fraumeni Jr. 1988. Cancer among medical diagnostic x-ray workers in China. J Natl Cancer Inst **80:** 344-350.

Weinstock MA. 1994. Epidemiologic investigation of nonmelanoma skin cancer mortality: the Rhode Island follow-back study. J Invest Dermatol **102:**65-95.

Wick RR, EA Nekolla, W Gőssner, AM Kellerer. 1999. Late effects in ankylosing spondylitis patients treated with ^{224}Ra. Radiat Res **152:** S8-S11.

Wick RR, EA Nekolla, M Gaubitz, TL Schulte. 2008. Increased risk of myeloid leukaemia in patients with ankylosing spondylitis following treatment with radium-224. Rheumatology **47:** 855-859.

Wood SN. 2006. *Generalized Additive Models: An Introduction with R*. Chapman and Hall: New York.

Young RW, H Hasai. 2005. Executive Summary, pp. 8-41 in: *Reassessment of the Atomic Bomb Radiation Dosimetry for Hiroshima and Nagasaki: Dosimetry System 2002. Volume 1.* RW Young and GW Kerr, eds. Hiroshima: Radiation Effects Research Foundation.

GLOSSARY

Absorbed dose: The energy deposited by ionizing radiation per unit mass of tissue irradiated. It can be expressed in units of gray (Gy) or milligray (mGy) where 1 Gy = 1000 mGy.

Adaptive response: A reduced response to radiation induced by a prior dose.

Alpha particle (α-particle): A particle consisting of 2 protons and 2 neutrons emitted from a decay of certain heavy atomic nuclei; a type of high-LET radiation.

Apoptosis: Programmed cell death.

BCC: Basal cell carcinoma.

Baseline cancer rate: The cancer mortality or incidence rate in a population in the absence of the specific exposure being studied.

Bayesian: A statistical approach in which probability reflects the state of knowledge about a variable, often incorporating subjective judgment.

BEIR VII: A National Research Council Report, *Health Risks from Exposure to Low Levels of Ionizing Radiation. BEIR VII. Phase 2.*

Beta particle (β-particle): An electron emitted from a decay of an atomic nucleus; a type of low-LET radiation.

Bystander effect: A change in a cell due to irradiation of a nearby cell.

Confidence interval (CI): A range of values calculated from sample observations that are believed, with a particular probability to contain the true parameter value. Upper and lower values of a CI are called confidence limits. A 90% CI implies that if the estimation process were repeated many times, about 90% of the intervals would contain the true value. The 90% probability refers to the properties of the interval and not the parameter itself.

Confounder: In an epidemiological study, a factor that is associated with both the exposure and outcome of interest and thereby distorts or masks the true effect of the exposure.

Credible interval: In Bayesian statistics, credible intervals are used instead of confidence intervals to describe a range of parameter values which contain the true value with a particular probability. A 90% credible interval is an interval which contains the quantity of interest with posterior probability of 90%.

Dose and dose-rate effectiveness factor (DDREF): A factor used to account for an apparent decrease in the effectiveness of low-LET radiation in causing a biological end-point (*e.g.*, cancer) at low doses and dose rates compared with observations made at high, acutely delivered doses.

Dose effectiveness factor (DEF): A factor estimated from the LQ model to account for a decrease in the effectiveness of low-LET radiation in causing a biological end-point (*e.g.*, cancer) at low doses compared with that at high acute doses.

Dose equivalent: A weighted sum of absorbed doses of different types of radiation, measured in units of sieverts (Sv). The ICRP recommended values for the weighting factors w_r are: 1.0 for photons and electrons, 10 for fission neutrons, and 20 for α-particles. Thus, for low-LET radiation, the dose equivalent in Sv is numerically equal to the absorbed dose in Gy, whereas for α-particles an absorbed dose of 1 Gy corresponds to 20 Sv.

Dose rate effectiveness factor (DREF): A factor used to account for an apparent decrease in the effectiveness of low-LET radiation in causing a biological end-point (*e.g.*, cancer) at low dose rates compared with high dose rates.

Double strand break (DSB): DNA damage in which a break extends over both strands of the double helix.

Electron volt (eV): The customary unit of energy for all *ionizing radiations*: 1 eV is equivalent to the energy gained by an electron passing through a potential difference of 1 volt. 1 keV = 1000 eV; 1 MeV = 1,000,000 eV.

EPA: U.S. Environmental Protection Agency.

Excess absolute risk (EAR): The rate of disease in an exposed population minus that in an unexposed population. Also termed “attributable risk.”

Excess relative risk (ERR): The fractional increase in the rate of disease in an exposed population compared to that in an unexposed population. The ERR is equal to the RR-1.

Gamma rays (γ-rays or gamma radiation): Photons of nuclear origin similar to X- rays but usually of higher energy. A type of low-LET radiation.

Genomic instability: An enhanced rate of spontaneous genetic change in a cell population.

Geometric mean (GM): The GM of a set of positive numbers is the exponential of the arithmetic mean of their logarithms.

Geometric standard deviation (GSD): The GSD of a lognormal distribution is the exponential of the standard deviation of the associated normal distribution.

Gray (Gy): Unit of absorbed dose (1 Gy = 1 joule/kg).

High-LET radiation: Radiation, such as neutrons or α-particles, producing ionizations densely spaced on a molecular scale (*e.g.*, LET > 10 keV/μm).

HPA: Health Protection Agency of the United Kingdom.

ICRP: International Commission on Radiological Protection. An independent international organization providing recommendations and guidance on radiation protection.

Ionizing radiation: Any radiation capable of removing electrons from atoms or molecules as it passes through matter, thereby producing ions.

kVp (kV): Kilovolt potential – refers to the potential difference between the electrodes of an X-ray tube. For example, the output of a 200 kVp X-ray tube will consist of photons with a range of energies up to 200 keV.

LET: Average amount of energy lost per unit track length of an ionizing charged particle.

Life Span Study (LSS): RERF's long term epidemiological study of health effects in the Hiroshima and Nagasaki atomic bomb survivors.

Life table: A table showing the number of persons who, of a given number born or living at a specified age, live to attain successively higher ages, together with the number who die in each interval.

Lifetime attributable risk (LAR): The LAR approximates the probability that an individual will develop (die from) cancer associated with an exposure. It includes incident cases (deaths) that would have occurred later in time without the exposure.

Likelihood: In statistics, this refers to the probability of a set of observations given values for a set of parameters.

Linear no-threshold (LNT) model: Dose-response for which any dose greater than zero has a positive probability of producing an effect. The probability is calculated from the slope of a linear (L) model or from the limiting slope, as the dose approaches zero, of a linear-quadratic (LQ) model.

Linear (L) model: A model in which the probability of an effect (*e.g.*, cancer) is expressed as being proportional to the dose.

Linear-quadratic (LQ) model: A model in which the probability of an effect (*e.g.*, cancer) is expressed as the sum of two terms – one proportional to the dose, the other to the square of the dose. In the limit of low doses and low dose rates, the quadratic term can be ignored.

Low-LET radiation: Radiation, such as X-rays, γ-rays or electrons, producing sparse ionizing events on a molecular scale (*e.g.*, LET < 10 keV/μm).

Lognormal distribution: A distribution in which the logarithm of a randomly distributed quantity has a normal distribution.

Mortality (rate): the frequency at which people die from a specific cause (*e.g.*, lung cancer), often expressed as the number of deaths per 100,000 population per year.

NCRP: National Council on Radiation Protection and Measurements. A Council commissioned to formulate and disseminate information, guidance, and recommendations on radiation protection and measurements.

NIOSH: National Institute for Occupational Safety and Health.

Orthovoltage X-rays: X-rays produced by generators in the 200-500 kV range. Orthovoltage X-ray sources of about 200-250 kV have been extensively used as irradiators in radiobiology.

Photon: A quantum of electromagnetic energy. Energetic photons in the form of X-rays or γ-rays can ionize atoms or molecules in a medium upon which they are incident.

Posterior probability distribution: In Bayesian inference, posterior distributions are probability distributions that incorporate all that is known about a set of random quantities or parameter values, after obtaining information from empirical data. The posterior distribution for a parameter value is proportional to the product of the prior distribution and the likelihood.

Prior probability distribution: In Bayesian inference, prior distributions are probability distributions summarizing information about a set of parameters that is known or assumed, prior to obtaining further information from empirical data.

Radiation effectiveness factor (REF): A quantity comparing the cancer causing potency in humans of a specified type of radiation relative to some standard.

Radiation Effects Research Foundation (RERF): A joint Japan-U.S. research organization, based in Hiroshima and Nagasaki, for studying the health effects of radiation on the atomic bomb survivors.

Radiation risk: The increased probability of a cancer (or cancer death) due to a given dose of radiation.

Relative biological effectiveness (RBE): The relative effectiveness of a given type of radiation in producing a specified biological effect compared to some reference radiation. For purposes of this document, the reference radiation is generally taken to be low dose γ-rays.

RBE_M: The maximal limiting value of the RBE for a high-LET radiation attained in the limit of low doses.

Relative risk (RR): The rate of disease in an exposed population divided by that in an unexposed population.

Relative survival: Net survival measure representing cancer survival in the absence of other causes of death.

Risk coefficient: The increase in the annual incidence or mortality rate per unit dose: (1) absolute risk coefficient is the increase in the incidence or mortality rate per unit dose; (2) relative risk coefficient is the fractional increase above the baseline incidence or mortality rate per unit dose.

SCC: Squamous cell carcinoma.

SEER: Surveillance, Epidemiology, and End Results. A data base of cancer statistics collected from registries throughout the U.S.

Sievert (Sv): Unit of dose equivalent. In the BEIR VII analysis of the A-bomb survivor data, the dose equivalent was calculated from the absorbed γ-ray and neutron doses, assuming a radiation weighting factor of 10 for neutrons.

Stationary population: A hypothetical population in which the relative number of people of a given age and gender is proportional to the probability of surviving to that age.

Uncertainty: A term used to describe the lack of precision and accuracy of a given estimate.

Uncertainty distribution: A mathematical expression defining the relative probabilities of different values for an estimated quantity.

Uncertainty factor: A random factor by which an estimate or projection deviates from its "true" value due to a specific source of uncertainty such as DDREF or risk transport.

UNSCEAR: United Nations Scientific Committee on the Effects of Atomic Radiation. A UN committee that publishes reports on sources and effects of ionizing radiation.

WLM: Working level months, a measure of radon decay product exposure.

X radiation or X-rays: Energetic photons usually produced by bombarding a metallic target with fast electrons in a high vacuum. The potential (kVp) difference between the target (cathode) and the collecting plate (anode) limits the maximum energy of X-rays produced. “Orthovoltage” X-rays of 200-250 kVp have been commonly used as a source of photons for experiments in radiobiology. Diagnostic X-rays employed in medicine are typically in the 50-150 kVp range, except for mammography, where the typical voltage is about 30 kVp.

EPA Radiogenic Cancer Risk Models and Projections for the U.S. Population, April 2011, 402-R-11-001

ERRATA

The EPA has made several corrections in this report, summarized in the table below. This errata sheet corrects a misinterpretation of a publication by Nekolla *et al.* (2000), in addition to correcting additional typographical errors and unclear word choices. The original text of this report was not altered; users of this document are encouraged to reference the corrections in the table below for the respective text locations in the report.

Text Location	Current Text, Corrected Text, and Reason for Correction
Section 5.1.2, Pg. 111, Para. 2	**Current Text:** Second, Nekolla *et al.* adopted the ratio of 9 for endosteal to skeletal dose published by Speiss and Mays; we employ the updated estimate of 7.5. The effect of this change is to increase the coefficient α in the model above by a factor of 1.2 (= 9 / 7.5). **Corrected Text:** *Delete* **Reason for Correction:** The linear coefficient, α, measuring the unit increase in excess relative risk per Gy for bone cancer, had been multiplied by a skeletal-to-endosteal adjustment factor of 1.2 in error. This multiplicative factor was applied based on an incorrect assumption that the dose estimates used by Nekolla *et al.* (2000) were obtained by converting the mean skeletal dose reported in Spiess and Mays (1970) to a bone surface dose. Rather, Nekolla *et al.* (2000) relied on the revised dosimetry by Henricks *et al.* (1995) which did not merit this correction factor. Future revisions to the EPA bone risk model will address this error as well as more recent changes in how the target tissue of relevance for radiogenic bone cancer is defined. **References:** 1. Nekolla EA, Kreisheimer M, Kellerer AM, et al. Induction of Malignant Bone Tumors in Radium-224 Patients: Risk Estimates Based on the Improved Dosimetry. Radiat Res 2000;153:93–103. 2. Spiess H & Mays CW. Bone Cancers Induced by 224Ra (Th X) in Children and Adults. Health Phys 1970;19(6):713–729. 3. Henrichs K, Bogner L, Nekolla D, et al. Extended dosimetry for studies with Radium-224 patients. In *Health Effects of Internally Deposited Radionuclides: Emphasis on Radium and Thorium* (van Kaick G, Karaoglou A, and Keller AM, Eds.), pp. 33–38. World Scientific, Singapore, 1995.

Text Location	Current Text, Corrected Text, and Reason for Correction
Section 4.3, Pg. 77, Para. 2, Line 5	**Current Text:** At γ near -0.5, radiogenic risk would be almost 3 times as large at age 0 as at age 30 **Corrected Text:** At γ near -0.5, radiogenic risk would be almost <u>5</u> times as large at age 0 as at age 30 **Reason for Correction:** Typographical error
Section 4.5, Pg. 99, Para. 1, Lines 5-9	**Current Text:** The mean of the uncertainty distribution for female bladder cancer is greater than the EPA estimate because it "averages" observed risks for prostate cancer with the larger observed risks for other cancer sites. **Corrected Text:** The mean of the uncertainty distribution for female bladder cancer is <u>smaller</u> than the EPA estimate because it "averages" observed risks for <u>bladder</u> cancer with the <u>smaller</u> observed risks for other cancer sites. **Reason for Correction:** Incorrect word choice
Section 3.4, Pg. 33, Table 3-6	**Current Text:** [1]From NCRP (2009) **Corrected Text:** [1]From NCRP (<u>2008</u>) **Reason for Correction:** Typographical error